THE PHOTOPHYSICS OF LUMINESCENT BANDING IN REEF CORALS

Fiona Jane Wild

Thesis presented for the degree of Doctor of Philosophy

The University of Edinburgh

1999

Abstract

Under ultraviolet light, massive coral skeletons reveal a series of luminescent bands that can be categorised as "bright" (yellow/green) and "dull" (blue). In some corals, the laying down of bright luminescent bands coincides with increased rainfall and a subsequent increase in levels of terrestrial run-off into the surrounding marine environment. Hence, the bright luminescence has been attributed to the incorporation of terrestrially-derived humic material into the coral skeleton. Corals were then proposed as a valuable tool for retrospective environmental analysis. However, the relationship does not hold for all corals. In some areas, bright bands are laid down during the dry season, and can even be found in reefs that are never subject to terrestrial inundation. Hence, the nature and significance of the banding phenomenon is not well understood. This work elucidates the photophysical processes that are responsible for the appearance of bright and dull bands. Excitation-emission-matrix (EEM) spectroscopy, in combination with optical fibre beam delivery, has been used to investigate the luminescence properties of intact coral skeletons. Samples from Papua New Guinea (subject to terrestrial inundation) and Oman (not subject to terrestrial inundation) have been investigated and compared.

It has been shown that luminescent banding can be recorded directly from the surface of the coral, without the need for extraction of the component luminophores. Using 3D EEM spectroscopy, the luminescence properties of the bright and dull bands have been reproducibly characterised. Using optical fibre beam delivery, spatial resolution of the banding pattern has been achieved. The variations in intensity of luminescence along the coral core have been recorded with excellent reproducibility.

The bright and dull bands observed in all samples contain similar groups of luminophores. The relative intensity of luminescence from each group varies between bands and between samples from different locations. Samples from

locations with no terrestrial input exhibit similar luminescence characteristics as those that are regularly inundated with terrestrial run-off. This suggests that luminescent banding is not due solely to the incorporation of terrestrial matter into the coral skeleton. Studies have suggested that the banding pattern is also related to structural variations in the skeleton.

It has been established that corals exhibit phosphorescence. The difference in phosphorescence intensity between bright and dull bands is substantially greater than the difference in total luminescence intensity. Hence, phosphorescence is an important indicator of the banding pattern and may prove to be a more valuable tool than luminescence in unravelling the environmental records stored in coral skeletons.

Declaration

I hereby declare that this thesis has been composed by me, and the work presented in this thesis is my own, unless otherwise stated.

Fiona Jane Wild
January 1999

Acknowledgements

During the last three years, I have been fortunate enough to receive help from many sources, both here at the University of Edinburgh and during my time in Australia.

My supervisor, Dr. Anita Jones, has been fantastic, right from the start to the very end of my PhD. She provided me with the space to go ahead and try things, and the ability to support me with fresh ideas and words of wisdom. Not only that, but she is the most fantastic chef and has great taste in cars. Many thanks are also due to Sandy Tudhope in the Department of Geology, for providing me with coral samples and stories of all the beautiful places he'd been diving, thus inspiring me to go to the Great Barrier Reef for six months!

Life at university wouldn't have been nearly so much fun without the endless cups of tea and daft chat in the office with Mark, Ron, Pete and Ian. I shall never forget the numerous Tuesday nights at The Golden Rule, where no matter who else turned up, the hardcore could always be relied upon to remember who invented the teabag. Keith and Car were, and still are, the best listeners (and gossips) and helped me get through all the black bits. Carol and Adrian are the best flatmates, letting me pick at their food when I couldn't be bothered to cook my own. There are so many other people who, probably without even knowing it, said or did just the right thing at the right time.

In Australia, Dave Barnes was a great source of ideas and inspiration. I had the most fantastic time out there, and am eternally grateful to Shan, Kay and Margaret for making me feel like I was at home on the other side of the world.

Dedication

This thesis is dedicated to my mum and dad. They have always been there for me, and given me support for all the things I wanted to do. I simply couldn't have done it without them.

Courses and Conferences Attended

Courses

Introduction to Computing
Keyboard Skills
Word for Windows (Beginners and Intermediate)
Excel
Reference Manager

Beginner's German
Excited States
Advanced Spectroscopic and Dynamic Techniques

Departmental Colloquia

Conferences

Royal Society "Highlights of UK Chemistry Research", London, 1997
Ames Symposium, Edinburgh, 1997
Materials Forum, Edinburgh, 1997
Physical Section Meetings, Firbush Point Field Centre, 1996-1998
Insight into Management, Durham, 1997
Climates of the Past (CLIP) Conference, Townsville, 1997
AIMS Science Conference, Townsville, 1997

Contents

Figures

Tables

Equations

1 Chapter One: Introduction

In recent years, global environmental awareness has risen to the forefront of both political and social agendas. Variations in environmental conditions due to natural phenomena and those attributed to anthropogenic influences have highlighted the need for reliable environmental records.

Environmental information can come from a wide variety of sources. Over the last hundred years, detailed instrumental records have provided a wealth of information. These records have been used to understand the processes giving rise to the ozone hole, linking CFC emissions with the reduction in atmospheric ozone. Records of CO_2 emissions have helped us to understand the greenhouse effect. However, environmental records have been stored since time began. Rocks, fossils, sediments, trees, ice cores and coral reefs all possess information of the changing environment. Our challenge is to unlock this information.

1.1 Utilising natural resources as an environmental proxy

Unlike direct measurements, natural resources act as proxy records. By their very nature, proxy records provide an imperfect history of past conditions, but by combining and comparing many different records, we can start to piece together the jigsaw puzzle of past climate variations. All proxy recorders have certain features in common:

1) they preserve information about past environmental conditions in a manner which allows the record to be reliably dated year to year;
2) the information can be recovered and interpreted as environmental variation;

3) the reliability of records can be tested and cross-checked, allowing development of principles and procedures for routine recovery of environmental information.

Trees provide the most obvious example of an environmental recorder. In temperate and sub-polar regions, trees produce rings as they undergo their annual growth cycle. A ring marks the boundary between the slowing down and stopping of growth as winter approaches, and the onset of new, rapid growth in the following spring. Tree rings are therefore a measure of the quality of the growing season. Tree rings may be obtained from dead but well-preserved trees and tree stumps, as well as living trees. By determining the ^{14}C content of tree rings, in conjunction with accurate dating, the extent of solar activity can be estimated. More recent trees act as markers of net release of carbon from the burning of fossil fuels, soil organic matter decay and deforestation.

In the polar regions, ice cores can provide a record of changing atmospheric conditions. Each year, snow falls on glaciers and ice caps, thaws in the sun, recrystallizes and subsequently consolidates. As it freezes, bubbles of gas are trapped in the ice. These bubbles can be extracted and analysed for various gases such as carbon dioxide, oxygen and methane. The oxygen isotope ratio ($^{18}O/^{16}O$) provides information on temperature variation. Measurements of ice accumulation with time provide information about the amount of precipitation The longest continuous ice core ever drilled covers 160,000 years, providing a wealth of knowledge of climates past.

The tropics comprise nearly half the Earth's surface; they are the primary "heat engine" driving global climate and are the source of short term climate variations such as the El Niño-Southern Oscillation. However, ice cores can tell us nothing of climatic variability in tropical regions. Even trees in tropical regions do not provide reliable environmental records, as the winter temperatures do not fall low enough to

inhibit growth. So, what natural resource can we use as an environmental proxy? In tropical oceans, coral reefs can offer us a complex and unique environmental record.

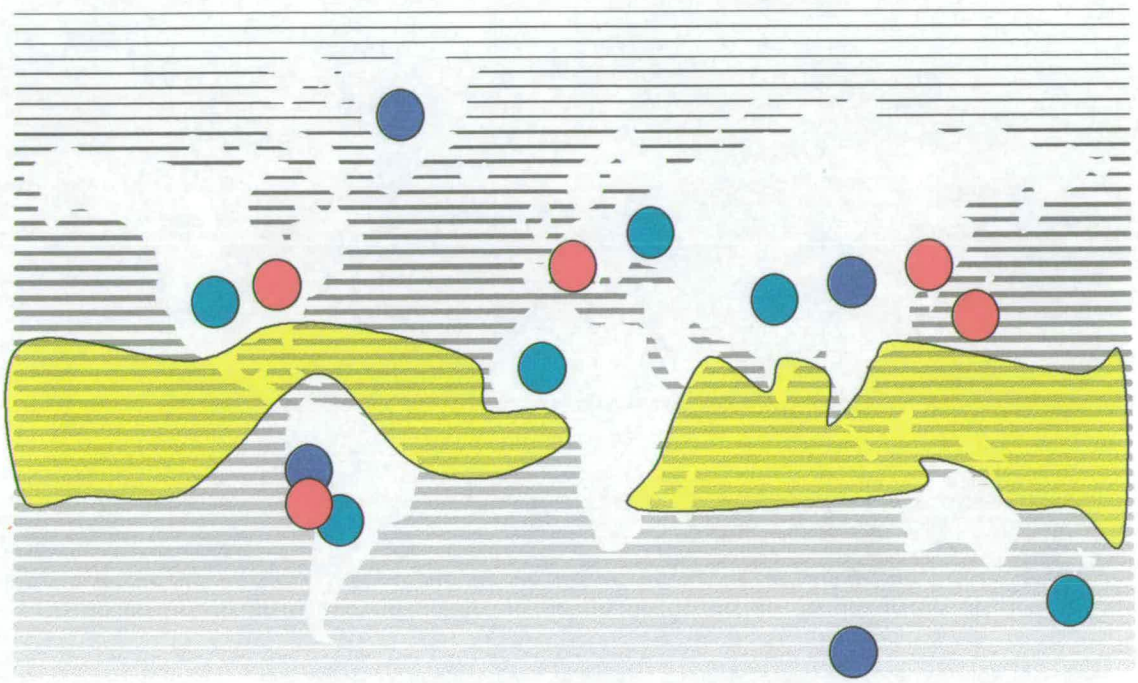

Figure 1.1: World map showing locations for which major proxy climate records have been reconstructed. Red circles indicate documentary records; blue circles indicate ice core records and green circles indicate tree ring records. The yellow shaded area shows the tropical ocean region where coral reefs are found. After Barnes and Lough, 1996.

1.2 An introduction to coral reefs

Hard corals (Scleractinia) have a highly complex superstructure, consisting of individual units of living tissue or polyps that secrete a calcareous skeleton. The polyp consists of a smooth cylindrical column with a mouth and tentacles. Coral polyps are carnivorous, trapping zooplankton with their tentacles and transporting it to the mouth. Contained within the walls of the polyp are large numbers of symbiotic algae known as zooxanthellae. These small plants have a very important role, removing excess metabolic waste from the polyp and promoting growth of the skeleton. The polyp produces a super-saturated solution of calcium carbonate, which calcifies into crystals. The zooxanthellae remove carbon dioxide during photosynthesis, thus aiding the calcification process.

There are many different types of hard corals, but most studies of coral skeletons as environmental records have focused on the genus *Porites*. *Porites* is a massive hard coral. "Massive" describes the shape of the coral colony in that all the dimensions are approximately the same. Other hard corals can be branched or plate like.

Massive corals are particularly useful proxy environmental recorders because:

1) their skeletons are formed continuously and large colonies represent growth over several hundred years;
2) their growth rate is rapid (typically 5-20 mm/yr) allowing sub-annual (seasonal) analyses;
3) once the skeleton is laid down, it is effectively protected from external variation.

Porites grows from the northern to the southern limits of reef development and from oceanic sites far from land to highly turbid, inshore environments. The coral colony, or *bommie*, can grow to several metres high. The polyps are approximately 1mm in diameter and occupy only the outer regions of the skeleton, forming a band at and

below the surface of the coral mass. The walls between the polyps are not solid. The vertical walls separating the individual polyps are perforated and each polyp is joined to its nearest neighbours, giving an interconnected colony or *perforate* coral. Since the polyps are joined, the coral skeleton is laid down in horizontal sections across the entire colony, giving a relatively even skeletal structure. Once the polyp dies, the space it occupied becomes a pore space in the coral skeleton. The skeleton is thus made up of a series of horizontal and vertical sections, separated by pore space.
Just as tree growth is affected by changing environmental conditions, so too the surrounding environment affects the growth of corals. The variations in physical and chemical composition of coral skeletons could offer a more diverse range of environmental information than any other proxy recorder.

1.3 Environmental variations in coral skeletons

1.3.1 Seasonal variations in density

In 1972, Knutson *et al.* observed that when slices of massive coral were X-rayed, the skeleton exhibited a series of light and dark regions, corresponding to regions of high and low density respectively. The corals studied originated from Bikini Atoll and Eniwetak, sites of atmospheric testing of nuclear weapons in the period 1948-1958. The corals had incorporated radioactive species (^{90}Sr) into their skeletons which coincided with the biennial test series. Comparing the autoradiographs from the skeletons and the X-ray images, Knutson *et al.* found that a pair of density bands corresponded to one year's growth.

Annual density banding has been confirmed in massive corals from a variety of locations using a variety of techniques. However, the cause of the density variations has not been established. The intra-annual timing of the density banding varies from sample to sample and from location to location, suggesting that many factors may

control the fluctuations in skeletal density. Since the skeletal deposition rate of corals is enhanced by the presence of photosynthetic zooxanthellae, some authors have suggested that seasonal variations in light intensity may control the density variations (Knutson *et al.,* 1972; Buddemeier and Kinzie, 1975; Wellington and Glynn, 1983). Other authors have suggested seawater temperature as the controlling factor (Dodge and Vaisnys, 1975; Weber *et al.,* 1975; Hudson *et al.*, 1976; Dodge and Lang, 1983). Certainly, there is a temperature optimum for coral skeletal growth and the rate of calcification and skeletal growth are decreased as the temperature fluctuates above and below the optimum (Clausen and Roth, 1975; Houck *et al.*, 1977). As there are so many environmental factors that vary on an annual basis, it is very difficult to attribute the density banding pattern to just one variation (Barnes and Devereux, 1988). Since the environmental causes of density banding could not be readily identified, work shifted focus to chemical variations within the skeletons.

1.3.2 Chemical tracers

Trace materials in corals provide three distinct types of record (Taylor *et al.*, 1995);

1) inclusions due to long term environmental variations over several years or decades;
2) inclusions that have a continuous annual variation;
3) inclusions due to occasional or pulse events.

1.3.2.1 Long term Environmental Variations

Coral skeletons have been used to study a number of long term environmental variations. In 1978, Nozaki *et al.* interpreted changes in ^{13}C and ^{14}C levels in corals as records of burning of fossil fuels. Increases in levels of phosphorus and lead in skeletons have been attributed to increasing levels of chemical and industrial pollution (Dodge and Gilbert, 1984). Changes in levels of ^{14}C have been used to follow the history of nuclear fallout and the circulation and exchange processes

between the atmosphere and the oceans (Druffel and Linick, 1978). As previously mentioned, the ten year atmospheric testing of nuclear weapons at Bikini Atoll (Knutson *et al.* 1972) was instrumental in estimating annual growth rates and establishing the annual nature of the density banding pattern.

1.3.2.2 Monitoring Continuous Environmental Variations

Since coral skeletons grow continuously and rapidly, variations in materials associated with the laying down of the skeleton can be studied from multiple samples within a year's growth. Within the carbonate structure of the skeleton, the relative concentrations of the stable isotopes of oxygen and carbon have been utilised to give records of seawater temperature, salinity and light intensity (Tudhope, 1994; Gagan *et al*, 1994). Levels of strontium also vary with seawater temperature, and provide a second source of environmental record (Goreau, 1977; McCulloch *et al*, 1994).

1.3.2.3 Pulse Events

With the ability to take multiple samples from within a year's growth, occasional or pulse events can be studied. Barium, cadmium, copper, magnesium, manganese and uranium concentrations have been studied in relation to El-Niño and the associated changes in the trade winds and oceanic circulation (Taylor *et al.* 1995). The oxygen isotope ratio has been used to identify monsoonal flood events and the carbon isotope ratio to date coral spawning events (Gagan *et al.*, 1994).

Another feature of coral skeletons that holds information about variations in environmental conditions is the phenomenon of fluorescent banding. It is with this phenomenon that the work presented in this thesis is concerned.

1.4 Luminescent banding in coral skeletons

Under ultraviolet light, massive corals exhibit a series of bright and dull bands. This phenomenon is shown in Figure 1.2.

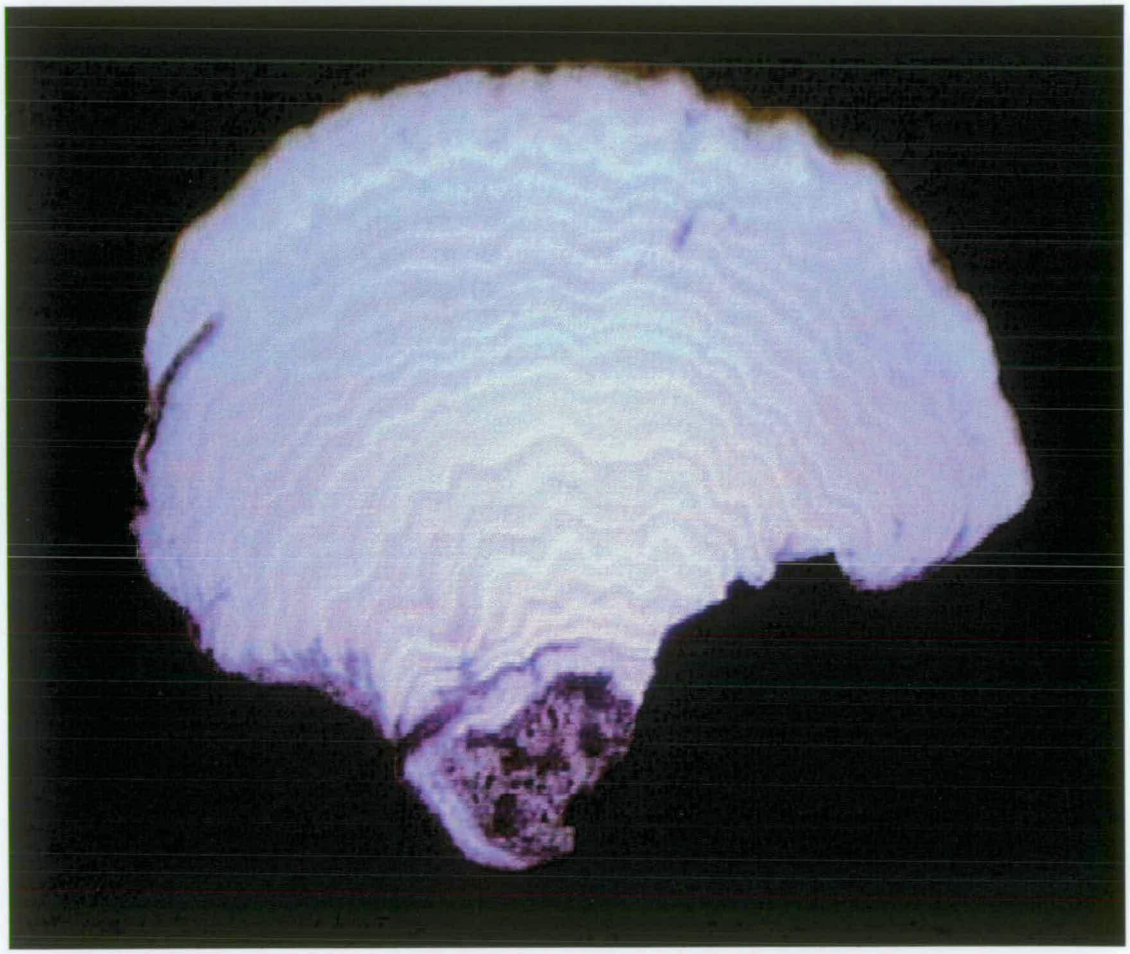

Figure 1.2: A 5mm thick slice of coral from Stephen's Reef, Great Barrier Reef, Australia, illuminated under uv light. The growing edge of the coral is at the top of the image. The yellow banded regions of the skeleton are termed bright bands, and the adjacent purple/blue regions are termed dull bands.

Fluorescent banding[1] in massive coral skeletons was first observed in 1984 by Peter Isdale from the Australian Institute of Marine Science (Isdale, 1984). He illuminated slices of *Porites* from Pandora Reef, Great Barrier Reef (GBR), Australia under longwave uv light. The bright (yellow/green) and dull (blue) bands were clearly visible in inshore samples (within 20km of the shore) but were not detected in mid- and outer shelf reefs.

By comparing the occurrence of the fluorescent lines with the density banding pattern seen in X-radiographs, Isdale was able to provide a temporal analysis of the fluorescent bands laid down over the 114 years of the sample. The coral exhibited a pair of bands for each year of growth. The bright bands coincided with regions of high density skeleton and the dull bands coincided with regions of low density skeleton. On the Great Barrier Reef, the highest skeletal density of massive corals is deposited in summer. The interdependence between the deposition of fluorescence material in the coral skeleton and the outflow of the Burdekin River was quantified by cross-correlating the cube of the fluorescence intensity with Burdekin River flow, giving a maximum square cross-correlation of 0.80 (95% confidence level = 0.69-0.87, n=62) for zero time lag. However, a correlation between the absolute fluorescence intensity (i.e. not the *cubed* intensity) and the river outflow was not recorded.

Isdale postulated that the chromophores giving rise to the yellow/green bands were derived from terrestrial sources. The fluorescent banding pattern in scleractinian corals could then provide a powerful tool for hindcasting the volume and periodicity of terrestrial run-off into the nearshore environment.

---

[1] Prior to this work, the banding pattern observed in massive corals was termed "fluorescent", as it was believed to derive solely from short-lived fluorophores. In this work, it has been established that the banding pattern is due to both fluorescence and phosphorescence emission. Consequently, the banding pattern observed in massive corals is now correctly termed "luminescent".

1.4.1 Introducing terrestrially-derived species into the marine environment

During the monsoon season, the levels of dissolved organic matter in rivers increase. Humic material is derived from detritus found in soils, freshwater, seawater and their associated sediments (Libes, 1992). Humic material can be subdivided according to molecular weight and solubility, but for the purposes of this work, the collective name will cover all subgroups.

1.4.1.1 Humic Material

The structure of humic material is not well understood. On a macromolecular level, it has a complex three-dimensional coiled structure and consists of the low molecular weight residues of biopolymers (500 - >250,000 amu; Hedges, 1988). These residues are very varied, but include a high proportion of aromatics, carboxylic acids and amines. The composition of terrestrial and marine humic material is linked to their surrounding environments. Terrestrial humic material has a higher proportion of lignin-derived residues, increased acidity and aromaticity. Marine humic material is richer in aliphatics, nitrogen and sulphur. Humic material can therefore be used as an effective biotracer.

Humic substances make up 60-70% of the total organic carbon (TOC) found in soils and 40-60% of the dissolved organic carbon (DOC) found in natural waters (Mobed *et al*, 1996). Natural waters impart a blue fluorescence (Kalle, 1949) which has been attributed to a fluorescent fraction of the DOC. This fluorescent fraction can account for more than 90% of DOC (Mantoura and Riley, 1975). Since humic substances are an important fraction of both marine and terrestrial organic carbon contents, there has been great interest in their luminescence characteristics.

1.4.1.1.1 Luminescence properties of humic material

Both marine and terrestrial humic substances are highly fluorescent, yielding broad emission spectra with wavelength and intensity dependent on the nature and origin of

the humic material (Senesi *et al*, 1991). Since humic material is very complex in structure and consists of many individual fluorescing species, most previous work concentrating on single line excitation and emission spectra has been inconclusive in determining specific characteristics of humic material from different locations.

In general, terrestrially-derived humic material exhibits longer wavelength excitation and emission maxima (excitation wavelength/emission wavelength at 230-260, 320-350/420-450nm) than humic material of marine origin (Senesi *et al*, 1991; Mobed *et al*, 1996; Coble, 1996). The shorter wavelength excitation and emission observed in marine DOC (275/300-340nm) has been attributed to increased levels of protein-like fluorophores (Coble *et al*, 1993; De Souza Sierra *et al*, 1994). Matthews (1996) identified four characteristic humic peaks in samples from marine (coral extracts, seawater, solid coral) and terrestrial (commercial humic material) sources at 280/350, 310/430, 340/450 and 390/490nm. The terrestrial samples also exhibited a longer wavelength peak at 460/540nm.

The dissolved organic matter is carried from the land to rivers and eventually reaches the sea. Hence, a massive volume of terrestrially-derived organic matter is introduced into the marine environment. The Burdekin River, with its mouth lying 135km south of Pandora Reef, drains 130,000km^2 of the adjacent landmass. The vast majority (>90%) of run-off from the Burdekin occurs between January and March during the monsoon season. The riverine input is thus an occasional, or pulse event.

1.4.2 Characterising the chromophores responsible for fluorescent banding

Boto and Isdale (1985) set about characterising the chromophores giving rise to the banding pattern. Dissolution of the coral samples in dilute hydrochloric acid gave broad excitation and emission fluorescence peaks typical of humic material, with a maximum excitation peak at 360nm and a maximum emission recorded between 440-460nm. Hot alkaline extraction of crushed coral, using 0.1M sodium hydroxide,

gave spectra of a similar nature, suggesting the existence in the skeleton of organic acid functional groups. Addition of excess Fe^{3+} to acid and alkali-extracted solutions resulted in a red-shifted emission spectrum with a 30% reduction in fluorescence intensity. This is consistent with the formation of a humic- Fe^{3+} complex and quenching of humic compounds by Fe^{3+}. They found the maximum differences in the emission spectra of the "banded" and the "background" regions occurred at 480-530nm, corresponding to the visual appearance of the yellow/green bright bands. However, they attributed this difference to increased levels of low molecular weight fulvic acids (soluble at pH1) in the bright bands. This is inconsistent with previous studies that show that the low molecular weight fraction of humic material (fulvic acids) have maximum emission intensities at shorter wavelengths than those observed (Mobed *et al,* 1996).

1.4.3 Utilising the fluorescent banding pattern as an environmental proxy

Following Boto and Isdale's work, there was great enthusiasm for unravelling the records stored in the fluorescent bands of coral skeletons. Kotwicki and Isdale (1991) correlated fluorescent bands from Pandora Reef, GBR, with occasional inflow to Lake Eyre, a huge dry lake in the centre of Australia. The correlation was good between coral fluorescence and Burdekin river discharge, with 73% of the variance in river flow explained by the coral fluorescence record for the period 1952-1980. However, it was less robust between fluorescence and Lake Eyre inflow, with only 41% of the variance in flow explained by the fluorescence record. Smith *et al.*(1989) used a coral core from Florida Bay to hindcast freshwater flow from the Everglades. Again, the correlation was poor, with only 57.2% of the variance in flow explained by the fluorescence record. These results suggest that, although the coral fluorescence is an indicator of river run-off, there are other factors present that will affect the occurrence and intensity of coral fluorescence.

In 1989, Scoffin *et al.* studied corals from Papua New Guinea (PNG) and Indonesia. At Motupore, PNG, the fluorescent bands in corals >2km from stream mouths

exhibited strong fluorescence, the bright bands coinciding with periods of increased rainfall in the Port Moresby area. The bright fluorescent bands coincided with regions of low density skeleton. Corals lying closer to stream mouths exhibited strong yellow fluorescence throughout their skeletons, and broad and diffuse banding. This suggests that, despite low freshwater run-off during dry seasons, there are sufficient organic compounds that cause fluorescence in coral skeletons to swamp seasonal effects. In the corals from Pulau Seribu, Indonesia, fluorescent bands were found in corals >5km from the mainland, with similar banding patterns in reefs separated by up to 25km. However, there was no direct relationship between Jakarta monthly rainfall records and the pattern of fluorescent banding. Again, the fluorescent bands coincided with regions of low density skeleton.

In Isdale's first investigation, the regions of bright fluorescence corresponded to peak run-off and high density regions of the skeleton. The relationship between run-off, high density skeleton and fluorescent banding no longer applied to the samples studied by Scoffin *et al.*. Variations and inconsistencies in the fluorescent banding patterns led Scoffin to propose that there may be more than one source of input of organic species to the reefs studied at Pulau Seribu. He proposed four explanations:

1) the seasonal freshwater plume may be fragmented by marine currents;
2) the freshwater plume from individual rivers may affect different reefs;
3) the reefs may be affected by localised freshwater run-off from the nearby vegetated reef islands;
4) there may be re-suspension of sea bed sediments, containing previously deposited terrestrial organics, by turbulent waters which follow a pattern unrelated to rainfall.

Klein *et al.*(1990) studied corals from the Red Sea and observed that low density bands were laid down in summer. These living corals exhibited no fluorescent banding pattern. However, fossil corals showed the yellow/green and blue bands

associated with the incorporation of humic material into the coral skeletons. Klein interpreted this observation as evidence that the climate of the Sinai desert region close to the reefs had previously been very much wetter, including seasonal rainfall events.

Susic *et al.*(1991) observed faint fluorescent banding in offshore corals of the GBR, where previously it had been stated that fluorescence was limited to corals within 20km of the shore (Isdale, 1984). In 1992, Scoffin *et al.* found that for corals from Phuket, South Thailand, regions of yellow/green fluorescence coincided with the dry season. Tudhope *et al.*(1996) observed fluorescent bands in corals from the Gulf of Oman. The adjacent Arabian landmass is very arid, with no permanent rivers and very little terrestrial vegetation. In these conditions, it seems unlikely that the fluorescence is due to the uptake of terrestrial humic material. Tudhope attributed the fluorescent bands to marine humic material, perhaps resulting from plankton blooms.

From the literature, it seems that there is no reliable relationship between fluorescent banding and terrestrial run-off. The relationship holds for corals from the GBR and PNG, but fails for those from South Thailand, Indonesia and Oman.

Consequently, the use of coral banding as a direct record of terrestrial run-off, and therefore continental rainfall, seems unwise. It would appear that there is not simply one environmental factor that affects the deposition and intensity of the banding pattern. In order to fully understand the records stored within the bands, it is necessary to understand the nature of the luminescent material and the factors that might influence luminescence intensity giving rise to fluorescent banding.

1.5 Aims of the Present Work

The aims of the work presented here are:

- to elucidate the luminescence processes which are responsible for the appearance of bright and dull bands in coral skeleton;
- to enable the factors that give rise to the banding phenomenon to be determined and;
- to thereby assess the potential of luminescent banding as an environmental proxy.

Extraction of humic material from solid samples, for example, soil, sediments and coral skeletons, requires the presence of a strong base e.g. sodium hydroxide or pyrophosphate. This can result in a number of molecular alterations, including base hydrolysis of esters and incorporation of oxygen into the humic structure. Previous work (Matthews *et al*, 1996) has been unable to identify differences between extracts from bright and dull bands, suggesting that during extraction, the features of the luminophores and the coral skeleton that lead to the observation of banding are lost.

The initial objective of this investigation was to reproducibly record the luminescence characteristics of coral skeletons directly from intact coral samples. Matthews *et al* introduced the use of 3D excitation-emission matrix (EEM) spectroscopy as a means to studying the luminescence *in situ*, although the results were not reproducible. The 3D matrix allows the study of the luminescence intensity of the sample across a range of excitation and emission wavelengths, thus taking account of the complex system of luminophores present in humic material.

Using the 3D EEM technique, the precise differences in the luminescent emissions of the different bands can be qualitatively and quantitatively compared, in terms of both the spectroscopic structure and the intensity of luminescence. Once it was established that the technique was reproducible, it could be applied to samples of coral from different geographical locations, in order to compare their luminescence characteristics and any variations in component species that could be attributed to changing environmental conditions.

The next objective was to extend the investigation to study the spatial variation of luminescence along the coral skeleton, rather than the localised emission from a single point on the coral surface. This involved designing and implementing a new experimental technique using optical fibre probes for excitation and emission beam delivery.

As the study progressed, it became apparent that the emission from the skeleton could not be attributed solely to short-lived fluorescence. This gave rise to a third objective: to investigate the long-lived phosphorescence emission in detail, by developing a technique to temporally resolve the luminescence and determine the contribution of phosphorescence to the observed banding pattern.

1.6 Overview of Thesis

This thesis has been subdivided into eight chapters, detailing work carried out during the period of my PhD. Chapter One gives a broad introduction to the area of study and the motivation for this work. Chapter Two describes the photophysical principles of luminescence, from an introduction to electronic transitions in a simple atom to the complicated inter-relationships taking place in a multi-component system. Chapter Three describes the experimental techniques utilised and developed

throughout this investigation. Chapter Four presents the results of primary studies of the luminescence characteristics of solid coral using 3D excitation-emission matrix spectroscopy. Chapter Five presents the results of experiments that allow spatial resolution of the luminescence signal from the coral surface, and gives a more detailed insight into the banding pattern. Chapter Six presents the first investigation of the phosphorescence characteristics of modern corals. Chapter Seven presents results obtained at The Australian Institute of Marine Science and The University of Sydney, Australia, studying the structural properties of coral skeletons and their relationship to the luminescence banding pattern. Chapter Eight completes this work, with an overview of the conclusions that can be drawn from the investigation.

1.7 Bibliography

Barnes, D.J. and Devereux, M.J., 1988. Variations in skeletal architecture associated with density banding in the hard coral Porites. Journal of Experimental Marine Biology and Ecology, 121: pp. 37-54.

Barnes, D.J. and Lough, J.M., 1996. Coral skeletons: storage and recovery of environmental information. Global Change Biology, 2: pp. 569-582.

Boto, K. and Isdale, P., 1985. Fluorescent bands in massive corals result from terrestrial fulvic acid inputs to nearshore zone. Nature, 315: pp. 396-398.

Buddemeier, R.W. and Kinzie, R.A., 1975. The chromometric reliability of contemporary corals: p. 135-147. Growth rhythms and the history of the earth's rotation. John Wiley & Sons, Inc. London.

Clausen, C.D. and Roth, A.A., 1975. Effect of temperature and temperature adaption on calcification rate in the hermatypic coral *Pocillopora damicornis*. Marine Biology, 33: pp. 93-100.

Coble, P.G., 1996. Characterization of marine and terrestrial DOM in seawater using excitation emission matrix spectroscopy. Marine Chemistry, 51: pp. 325-346.

Coble, P.G., Schultz, C.A., and Mopper, K., 1993. Fluorescence contouring analysis of DOC intercalibration experiment samples - a comparison of techniques. Marine Chemistry, 41: pp. 173-178.

De Souza Sierra, M.M., Donard, O.F.X., Lamotte, M., Belin, C., and Ewald, M. , 1994. Fluorescence spectroscopy of coastal and marine waters. Marine Chemistry, 47: pp. 127-144.

Dodge, R.E. and Gilbert, T.R., 1984. Chronology of lead pollution contained in banded coral skeletons. Marine Biology, 82: pp. 9-13.

Dodge, R.E. and Lang, J.C., 1983. Environmental correlates of hermatypic coral (*Monastrea annularis*) growth on the East Flower Gardens Bank, northwest Gulf of Mexico. Limnology and Oceanography, 28: pp. 228-240.

Dodge, R.E. and Vaisnys, J.R., 1975. Hermatypic coral growth banding; an environmental recorder. Nature, 258: pp. 706-708.

Druffel, E.M. and Linick, T.W., 1978. Radiocarbon in annual coral rings of Florida. Geophysics Results Letters, 5: pp. 913-916.

Gagan, M.K., Chivas, A.R., and Isdale, P.J., 1994. High-resolution isotopic records from corals using ocean temperature and mass-spawning chronometers. Earth And Planetary Science Letters, 121: pp. 549-558.

Goreau, T.J., 1977. Coral skeletal chemistry: physiological and environmental regulation of stable isotopes and trace metals in *Monastrea annularis*. Proceedings of the Royal Society of London, Series B, 196: pp. 291-316.

Hedges, J.I., 1988. Humic substances and their role in the environment: pp. 45-58. Edited by Frimmel, F.H. and Christmann, R.F. John Wiley & Sons, Inc. London.

Houck, J.E., Buddemeier, R.W., Smith, S.V. and Jokiel, P.L., 1977. The response of the coral growth rate and skeletal strontium content to light intensity and water temperature. Proceedings of the Third International Coral Reef Symposium, 2. Rosensteil School of Marine and Atmospheric Sciences, Miami, Florida: pp. 455-461.

Hudson, J.H., Shinn, E.A., Halley, R.B. and Lidz, B., 1976. Sclerochronology: a tool for interpreting past environments. Geology, 4: pp. 361-364.

Isdale, P., 1984. Fluorescent bands in massive corals record centuries of coastal rainfall. Nature, 310: pp. 578-579.

Kalle, K., 1949. Fluoreszenz und Gelbstoff im Bottnischen und Finnischen Meerbusen. Dtsch. Hydrogr. Z., 2: pp. 117-124.

Klein, R., Loya, Y., Gvirtzman, G., Isdale, P.J., and Susic, M., 1990. Seasonal rainfall in the sinai desert during the late quaternary inferred from fluorescent bands in fossil corals. Nature, 345: pp. 145-147.

Knutson, R.A., Buddemeier, R.W., and Smith, S.V, 1972. Coral chronologies: seasonal growth bands in reef corals. Science, 177: pp. 270-272.

Kotwicki, V. and Isdale, P., 1991. Hydrology of Lake Eyre, Australia - El-Niño link. Palaeogeography, Palaeoclimatology and Palaeoecology, 84: pp. 87-98.

Libes, S. 1992, The Production and Destruction of Organic Compounds: p. 407-413. An Introduction to Marine Biogeochemistry. John Wiley & Sons, Inc. London.

Mantoura, R.F.C. and Riley, J.P., 1975. The Analytical Concentration of Humic Substances from Natural Waters. Analytica Chimica Acta, 76: pp. 97-106.

Matthews, B.J.H., Jones, A.C., Theodorou, N.K., and Tudhope, A.W., 1996. Excitation-Emission-Matrix Fluorescence Spectroscopy Applied to Humic Acid Bands in Coral Reefs. Marine Chemistry, 55: pp. 317-332.

McCulloch, M.T., Gagan, M.K., Mortimer, G.E., Chivas, A.R. and Isdale, P.J., 1994. A high resolution Sr/Ca and $\delta^{18}O$ coral record from the Great Barrier Reef, Australia and the 1982-1983 El-Niño. Geochimica Cosmochimica Acta, 58: pp. 2747-2754.

Mobed, J.M., Hemmingsen, S.L., Autry, J.L., and McGown, L.B., 1996. Fluorescence Characterization of IHSS Humic Substances: Total Luminescence Spectra with Absorption Correction. Environmental Science and Technology, 30: pp. 3061-3065.

Nozaki, Y., Rye, D.M., Turekian, K.K. and Dodge, R.E., 1978. A 200 year record of carbon-13 and carbon-14 variations in a Bermuda coral. Geophysics Results Letters, 5: pp. 825-828.

Scoffin, T.P., Tudhope, A.W., Brown, B.E., Chansang, H., and Cheeney, R.F., 1992. Patterns and possible environmental controls of skeletogenesis of *Porites lutea*, South Thailand. Coral Reefs, 11: pp. 1-11.

Scoffin, T.P., Tudhope, A.W., and Brown, B.E., 1989. Fluorescent and skeletal density banding in *Porites lutea* from Papua New Guinea and Indonesia. Coral Reefs, 7: pp. 169-178.

Senesi, N., Miano, T.M., Provenzano, M.R., and Brunetti, G., 1991. Characterization, differentiation, and classification of humic substances by fluorescence spectroscopy. Soil Science, 152: pp. 259-271.

Smith, T.J., Hudson, J.H., Robblee, M.B., Powell, G.V.N., and Isdale, P.J., 1989. Fresh-water flow from the Everglades to Florida Bay - a historical reconstruction based on fluorescent banding in the coral *Solenastrea bournoni*. Bulletin Of Marine Science, 44: pp. 274-282.

Susic, M., Boto, K., and Isdale, P., 1991. Fluorescent humic-acid bands in coral skeletons originate from terrestrial runoff. Marine Chemistry, 33: pp. 91-104.

Taylor, R.B., Barnes, D.J., and Lough, J.M., 1995. On the inclusion of trace materials into massive coral skeletons. 1. Materials occurring in the environment in short pulses. Journal of Experimental Marine Biology and Ecology, 185: pp. 255-278.

Tudhope, A.W., 1994. Extracting high-resolution climatic records from coral skeletons. Geoscientist, 4: pp. 17-20.

Tudhope, A.W., Lea, D.W., Shimmield, G.B., Chilcott, C.P., and Head, S., 1996. Monsoon climate and Arabian Sea coastal upwelling recorded in massive corals from southern Oman. Palaios, 11: pp. 347-361.

Weber, J.N, White, E.W. and Weber, P.H., 1975. Collection of density banding in reef coral skeletons with environmental parameters: the basis for interpretation of chronological records preserved in the coralla of corals. Paleobiology, 1: pp. 137-149.

Wellington, G.M. and Glynn, P.W., 1983. Environmental Influences on Skeletal Banding in Eastern Pacific (Panama) Corals. Coral Reefs, 1: pp. 215-222.

2 Chapter Two: The Photophysics of Luminescence

2.1 Introduction

In order to be able to correctly interpret the luminescence emission from a molecule or group of molecules, it is important to understand the processes leading to the emission and the inter-relationships between them. This chapter discusses the photophysical principles of luminescence, from a relatively simple system describing a single emitting molecule, to a more complicated system involving a number of luminescing species.

2.2 Electronic Excitation Processes in Molecular Systems

Light is a form of energy that can be considered to have wave-like and particle-like properties (wave particle duality). Light is electromagnetic radiation; its wave-like properties arise from the transverse oscillation of electric and magnetic fields in planes perpendicular to each other and to the direction of propagation of the light. The frequency or wavelength of these oscillations determines the colour of the light. Light also behaves as though it consists of a stream of particles, or photons. Each of these photons has a fixed energy that depends on the frequency (or wavelength) of radiation. The fixed energy of a photon is called a quantum and can be defined by the equation;

$$E = h\upsilon$$

where h is Planck's constant and υ is the photon frequency.

2.2.1 Electronic energy levels in a simple hydrogen atom

Electrons also exhibit wave-particle duality. In any molecule, the constituent electrons occupy certain, well-defined energy levels, or electronic states. Since the wave-motion has to be stationary, only a limited set of waveforms is allowed. The waveforms can be represented by three-dimensional regions of high charge density called orbitals. The orbital defines the region in space where the electron is likely to be found. For the simplest system, the hydrogen atom, only one electron is present. The lowest energy orbital (1s) is spherical with a high charge density around the positive nucleus. The next higher energy level corresponds to the 2s orbital. This is another spherical orbital but higher in energy due to the greater average distance between the electron and nucleus and the resulting decrease in electrostatic attraction. Next are the three 2p orbitals, all of equal energy and similar dumbbell shape, but lying perpendicular to each other. Despite the fact that the electron will normally be occupying the lowest energy orbital, the higher energy orbitals still exist and can be populated through absorption of electromagnetic radiation and promotion of the electron.

2.2.2 Electronic energy levels in a molecule

In comparison with the simplest hydrogen atom, molecules have many electrons occupying many orbitals. These molecular orbitals are centred around many nuclei. To simplify the calculation of the relative energy levels of the multi-electron system, two assumptions are made. Firstly, each pair of electrons is essentially localised near just two nuclei. Secondly, the shapes of these localised molecular orbitals and their disposition to each other are related in a simple way to the shapes and disposition of atomic orbitals in the component atoms.

The simplest molecule to consider is H_2. The electrons group around a two-centre positive interior and the component s and p orbitals become stretched along the molecular axis to form σ and π molecular orbitals. Quantum mechanics shows that

the combination of two atomic orbitals gives two molecular orbitals, one bonding and one anti-bonding. Where electrons in a bonding orbital tend to hold the atoms together, electrons in an anti-bonding orbital tend to force the atoms apart. The anti-bonding orbitals are denoted σ^* and π^*. In addition to the bonding and anti-bonding orbitals are the non-bonding orbitals. Electrons in these orbitals neither weaken nor strengthen the bonding between atoms.

In a complex molecule with many different functional groups (or reactive sites), such as humic acid, there are very many electronic transitions that can occur. Molecules with aromatic character are more likely to exhibit luminescence. The functional group of a molecule that determines its ability to exhibit luminescence is known as the luminophore.

An aromatic molecule contains one or more benzene rings. The benzene ring has a unique electronic orbital arrangement. It consists of six carbon atoms and six hydrogen atoms. Each carbon atom is bonded to two other carbon atoms and a hydrogen atom. The carbon atomic orbitals (2s; $2p_x$ and $2p_y$) hybridise to form sp^2 atomic orbitals. These overlap to form 3 σ molecular orbitals. However, there is a third p orbital (p_z) associated with each carbon atom, perpendicular to those involved in the σ bonding. The p_z orbitals overlap to form a π molecular orbital. This π orbital lies above and below the plane of the benzene ring. Since the π orbital is not limited to two neighbouring atoms, it is said to be **delocalised**. In benzene, 24 of the 30 electrons are involved in σ bonds, and the remaining six partially occupy the π orbital. Hence, in the ground state, the highest occupied molecular orbital (HOMO) is a delocalised π bonding orbital. Other cyclic molecules are termed aromatic if their HOMO is a delocalised π bonding orbital. Excitation of a constituent electron leads to population of the lowest unoccupied molecular orbital (LUMO). This will tend to be a π^* anti-bonding orbital. This transition is termed π to π^*.

Some molecules such as heterocyclics contain a lone pair of electrons associated with an oxygen or nitrogen atom in a p type atomic orbital. An electron from a lone pair can also be excited to a π^* orbital of a benzene ring. This transition is termed n to π^*.

π to π^* and n to π^* transitions tend to be separated by energies corresponding to the ultraviolet, visible and infrared regions of the electromagnetic spectrum. Consequently, if a molecule absorbs a photon corresponding to the defined energy difference of these states, it is likely that an electron will be promoted into the higher energy level. This results in the production of an excited state.

2.2.3 Singlet and Triplet States

Electrons can be considered to possess "spin" or spin angular momentum that can take up one of two orientations in the presence of an applied magnetic field. The spin quantum number, s of each of these orientations is +/-½. The orientation determines the sign of the spin quantum number. Electrons with opposing spins are said to be paired; electrons with similar spins are said to be unpaired. The total spin angular momentum of a molecule is represented by the total spin quantum number, S or vector sum of each individual electron quantum number. The spin multiplicity, (2S + 1), gives the number of states expected in the presence of an applied magnetic field. Hence, for a molecule with all electrons paired, the total spin quantum number, S is zero (+½ – ½). The spin multiplicity, 2S + 1, is therefore 1. This is termed a singlet state, S_n. For a molecule with two unpaired electrons, the total spin quantum number is 1 (½+ ½). The spin multiplicity is therefore 3. This is termed a triplet state, T_n.

Transitions between states of different multiplicities are forbidden by the spin selection rule. Hence, the S_0 to S_1 transition is spin-allowed but the S_0 to T_1 transition is spin –forbidden. This makes intuitive sense, as one would expect that the most probable transition is the one that requires the least perturbation of the molecule.

Although selection rules show in principle which transitions may or may not be possible, forbidden transitions are often seen, although they tend to be considerably weaker than allowed transitions.

Spin-forbidden transitions can occur by means of spin-orbit coupling. Interactions between spin angular momentum and orbital angular momentum mean that S, the total spin quantum number, is no longer valid and selection rules based on it fail. Spin-orbit coupling tends to give singlet states more triplet character and vice versa, thus blurring the distinction between the different multiplicities. Systems with heavy atoms are more likely to exhibit spin-orbit coupling as it is dependent on the fourth power of the atomic number of the component atoms. Spin-orbit coupling is also much more likely in large molecular systems where there may be considerable overlap between the energies of states of different multiplicities.

A generalised state diagram showing the relationship of singlet and triplet states is shown in Figure 2.1;

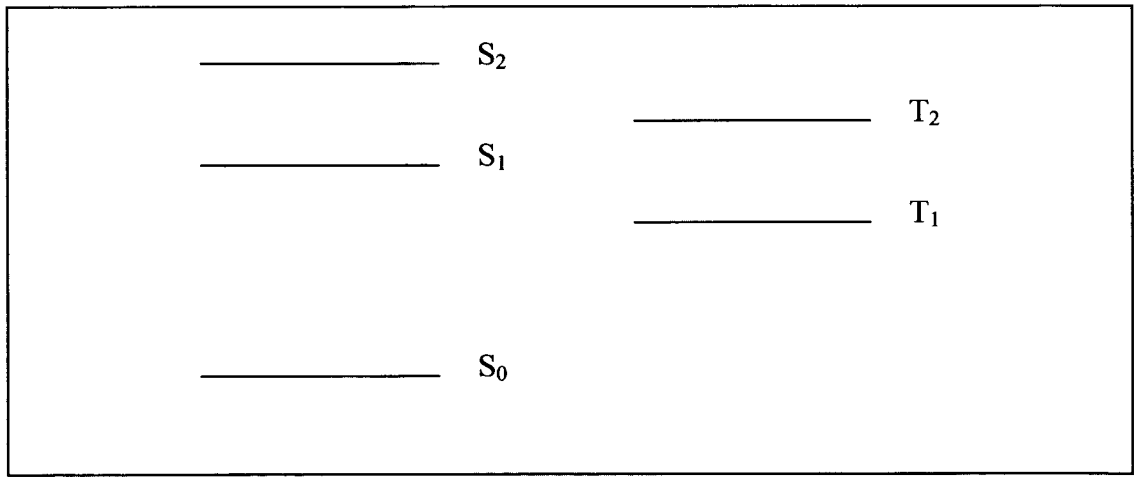

Figure 2.1: State diagram showing the relative energy levels of singlet and triplet states. The horizontal lines represent the zero point energy levels of the different states

Triplet states have lower energy than the corresponding singlet states. This is expressed by Hund's rule of maximum multiplicity. Electrons with parallel spins tend to stay well apart and hence repel each other less, lowering the overall energy of the system.

2.2.4 Vibronic Transitions

Associated with each electronic energy level are vibrational energy levels. As with the electronic energy levels, these vibrational energy levels are quantised. On absorption of a photon, an electron is excited to an upper state before the nuclei have had a chance to respond to the new electronic structure. This is the Franck-Condon principle. The excited state may be produced with some additional vibrational excitation; this is known as a vibronic state. The Franck-Condon factor is a parameter derived from the mathematical expression of the Franck Condon principle and indicates which vibronic transitions will be intense and which will be weak. It can be expressed qualitatively as follows. For a molecule in which the nuclear geometries of the ground and the excited states are very similar, the low vibrational levels of the first excited state are most likely to be populated on optical excitation. For a molecule in which the nuclear geometries of the ground and excited states are very different, higher vibrational levels are favoured. The absorption spectrum of a simple molecule shows a series of peaks corresponding to the vibronic transitions, with the transition of greatest probability having the greatest intensity.

For polyatomic molecules, the situation is more complex as there are many overlapping vibronic transitions. Hence, the absorption profile tends to be broad. Since the overall shape of the absorption profile is still controlled by the Franck-Condon principle, it is called the Franck-Condon envelope. The Franck-Condon principle also applies to emission spectra in the same way, with broad emission profiles for polyatomic molecules.

2.3 *De-excitation Processes*

If an electronically excited molecule does not undergo some kind of chemical reaction (fragmentation or rearrangement), it must lose its excitation energy in some other way, since the excited state is unstable with respect to the ground state. De-excitation can occur by emission of radiation, non-radiative processes or quenching processes. The favoured de-excitation pathway depends on the type of molecule and the nature of the electronic states involved. However, in most systems, several types of de-excitation occur in competition.

Radiative and non-radiative transitions are illustrated in Figure 2.2

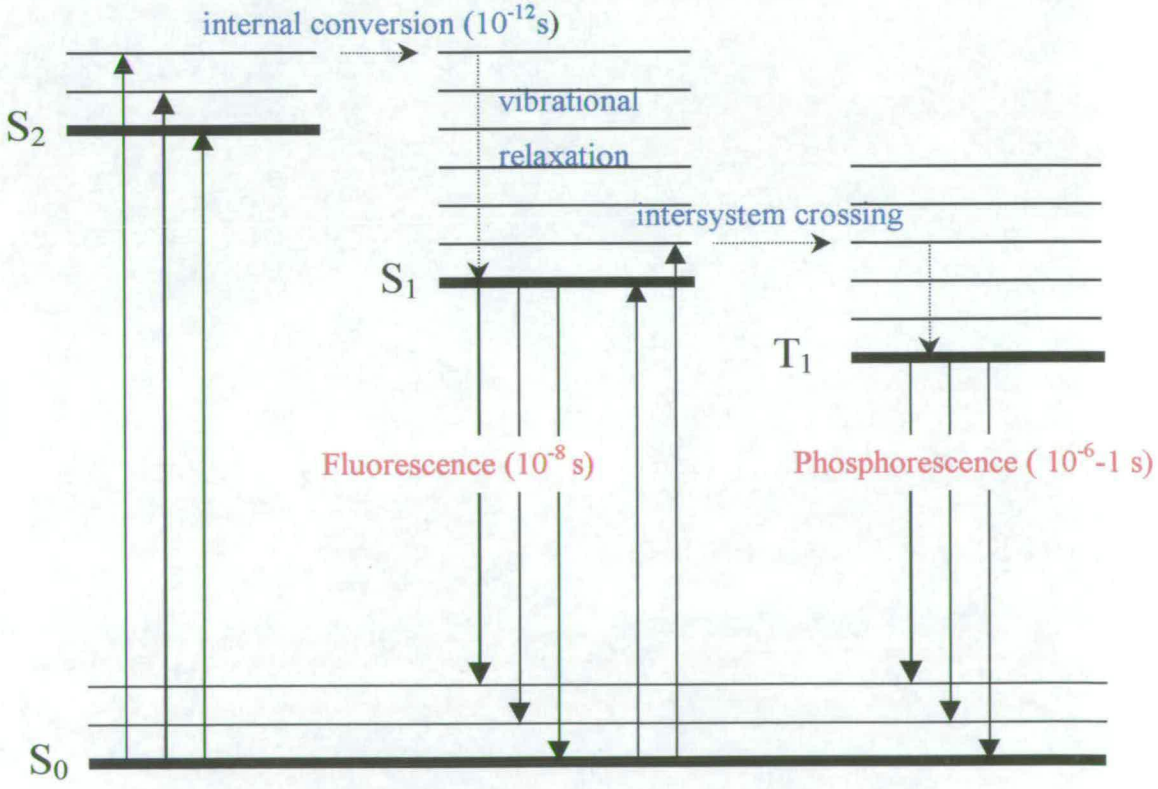

Figure 2.2: Jablonskii diagram showing electronic and vibrational energy levels and associated transitions. Solid lines denote radiative transitions. Dashed lines denote non-radiative transitions.

2.3.1 Radiative Processes

Radiative emission or **luminescence** involves the loss of excitation energy as electromagnetic radiation. For aromatic molecular systems, this emission lies in the visible or ultraviolet regions of the electromagnetic spectrum. Luminescence can be further categorised by the spin multiplicities of the excited and lower energy levels. If the transition giving rise to emission occurs between states of the same multiplicity, the emission process is termed **fluorescence**. If the transition giving rise to emission occurs between states of different multiplicities, the emission process is termed **phosphorescence**.

2.3.1.1 Fluorescence

Fluorescence is the radiative emission from an excited state of the same spin multiplicity as the lower state in the transition. Since the transition is spin-allowed, fluorescence occurs on very short timescales, usually in the region of 10^{-8}s.

2.3.1.2 Phosphorescence

Phosphorescence is the radiative emission from an excited state of different spin multiplicity than the lower state in the transition. Due to spin-orbit coupling, spin-forbidden transitions may become weakly allowed. Hence, phosphorescence occurs on a much longer timescale than fluorescence and is much less intense. Typically, phosphorescent emissions can have lifetimes of between 10^{-6}s and seconds. As the triplet state lies at lower energy than the corresponding singlet state, the $T_1 \rightarrow S_0$ transition leads to emission of lower energy (longer wavelength) radiation than fluorescence.

2.3.1.3 Excitation and Emission Spectra

There are two different types of spectrum that can be useful in studying luminescence phenomena; the excitation spectrum and the emission spectrum. An excitation spectrum is obtained by measuring the intensity of emission as the

excitation wavelength is altered. The emission spectrum is obtained by measuring the emission intensity as a function of wavelength for excitation at a fixed wavelength.

The nature of a fluorescence emission spectrum depends on whether the sample is excited in the gas phase or the condensed phase. Consider a sample of atoms or simple molecules in the gas phase at low pressure. Excitation with monochromatic light, corresponding to the transition from the ground state, S_0 to the first excited state, S_1, results in a series of fluorescence bands (Stokes lines). These correspond to transitions from the excited vibronic state to the vibrational levels of the ground state. At higher pressures, collisions between molecules reduce the probability of fluorescence from vibrational levels of the excited state. For a solution or solid phase sample containing only a single type of emitting molecule, the emission spectrum is independent of the excitation wavelength. The fluorescence corresponds to transitions from the low vibrational levels of the first excited state to the ground state (see non-radiative processes later). The transition between the lowest vibrational level of the first excited state and the lowest vibrational level of the ground state (the 0-0 band) is the most intense for many organic molecules. Hence, the maxima of intensity both in absorption and in fluorescent emission correspond to the same transition. This suggests that the upper and lower electronic states of such molecules must be of a similar shape and size, and it is likely that the vibrational spacings will be the same in both states. Thus, the absorption and emission spectra are often almost mirror images of each other. In solution, the absorption and emission spectra are offset, with the emission spectra lying at lower energy (longer wavelength). This shift is due to differing interactions between the ground and excited states of the molecule with the surrounding solvent molecules. Figure 2.3 shows the mirror image relationship between excitation and fluorescence spectra for a sample of 5-methoxyindole monomer in ethanol at 77K.

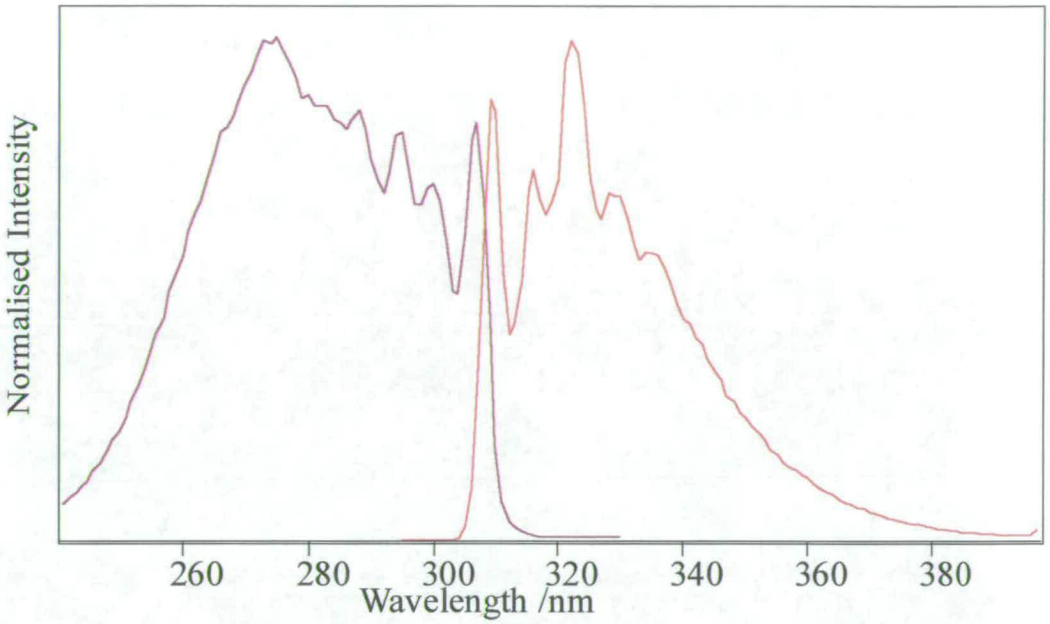

Figure 2.3: Excitation (purple) and fluorescence (red) spectra of 5-methoxyindole monomer in ethanol at 77K.

Just as with fluorescence, there is often a mirror image relationship between absorption and phosphorescence spectra. In large organic molecules, the vibrational spacings are nearly identical in all three lowest energy states (S_1, S_0, T_1). Since the T_1 state is of lower energy than S_1, the long-lived phosphorescent emission is of longer wavelength than the short-lived fluorescent emission. Figure 2.4 shows the relationship between fluorescence and phosphorescence spectra for a sample of 5-cyanoindole trimer in ethanol at 77K, exciting at 320nm. The phosphorescence spectrum is offset to longer wavelengths than the fluorescence spectrum.

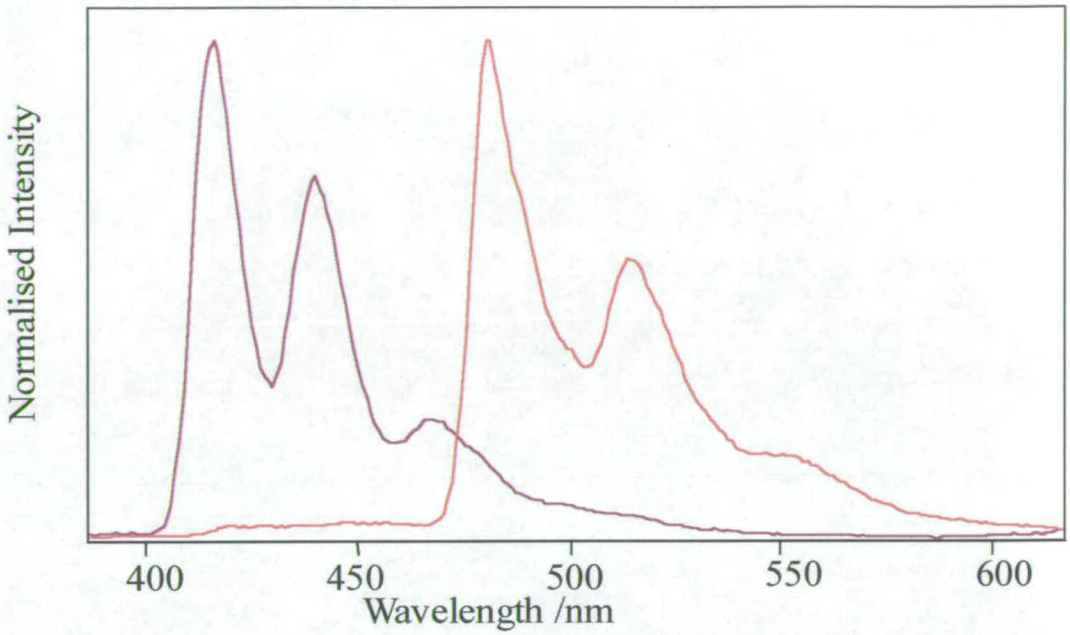

Figure 2.4: Fluorescence (purple) and phosphorescence (red) spectra of 5-cyanoindole trimer in ethanol at 77K, exciting at 320nm.

2.3.2 Non-radiative Processes

Non-radiative transitions describe intramolecular (between quantum states of an individual molecule) and intermolecular processes that lead to conversion from one state to another without the emission of radiation. If radiative transitions are imagined to be "vertical" transitions on the Jablonskii diagram, then intramolecular non-radiative transitions are "horizontal". In an intramolecular non-radiative transition, energy is conserved, but electronic energy is converted to vibrational energy.

2.3.2.1 Internal Conversion

Absorption of electromagnetic radiation can excite an electron to a higher electronic state than the first electronic exited state. For example, the electron may be excited to the second electronically excited state, S_2. The intramolecular transfer of population from one electronic state e.g. S_2 to another of the same multiplicity e.g. S_1 is called internal conversion (see Figure 2.2). Since internal conversion occurs to an isoenergetic level of S_1, the S_1 state formed will possess a considerable amount of vibrational excitation. The electronic energy of the system is decreased whilst the vibronic energy remains constant.

2.3.2.2 Intersystem Crossing

The intramolecular transfer of population between states of different multiplicities is called intersystem crossing. It can provide a route to the T_1 state via the optical excitation of S_1, as shown in Figure 2.2. Since the triplet state lies at lower energy than the corresponding singlet state, the horizontal transition produces a vibrationally excited T_1 state.

2.3.2.3 Vibrational Relaxation

Vibrational relaxation is an intermolecular process by which a vibrationally excited molecule loses energy to its surroundings as heat. The vibrationally excited molecule collides with other surrounding molecules and transfers its energy, allowing it to return to the low vibrational levels (those which are thermally populated) of that particular state. The efficiency of vibrational relaxation depends on the phase of the excited sample. At low gas pressures, emission and vibrational relaxation compete, giving rise to emission observed from higher vibronic levels of the excited state. At higher gas pressures, at which the collision rate greatly exceeds the rate of emission, vibrational relaxation is essentially complete and no fluorescence is observed from higher vibronic levels. Vibrational relaxation is extremely probable in solution and in solids, the molecules are so close together that fluorescence from vibrationally

excited levels is never observed. Hence, under these conditions, phosphorescence and fluorescence always occur from only the thermally populated vibrational levels (only the few lowest vibrational levels at room temperature) of the T_1 and S_1 states, respectively.

2.3.3 Quenching Processes

Quenching involves the intermolecular transfer of electronic excitation energy from one molecule to another. The acceptor molecule, which receives excitation from the donor, then participates in processes open to it as an electronically excited species. Quenching competes with emission, so that the presence or addition of a quenching species reduces the intensity of fluorescence of phosphorescence.

2.3.3.1 Electronic Energy Transfer

An important mechanism responsible for the quenching of molecular emission involves the transfer of excitation energy from the excited molecule, M, to a quencher molecule, Q, in a bimolecular process. This process is summarised below:

$$M^* + Q \rightarrow M + Q^*$$

In this reaction, excitation energy provided initially to M via the absorption of a photon appears in Q with a subsequent reduction in the concentration of excited M molecules and hence a reduction in the total emission from M*. For this type of mechanism to occur, the excited energy level of Q* must be lower than (or equal to) that of M*. There are two distinct types of energy transfer processes; radiative energy transfer and non-radiative energy transfer.

2.3.3.1.1 Radiative Energy Transfer

Radiative energy transfer involves the emission of a photon from the initially excited molecule M* and its reabsorption by the molecule Q. It is summarised below;

$$M^* \rightarrow M + h\nu \qquad\qquad Q + h\nu \rightarrow Q^*$$

For this process to occur, the emission spectrum of M* must overlap with the absorption spectrum of Q. Since the photon emitted by M* is absorbed by Q in the same way as direct excitation of Q, radiative energy transfer is subject to the same principles as direct excitation processes. Consequently, radiative energy transfer to singlet states is far more likely than the spin-forbidden excitation to triplet states.

2.3.3.1.2 Non-radiative Energy Transfer

Non-radiative energy transfer involves the transfer of excitation energy without the emission of a photon. It requires the presence of a specific interaction between M* and Q. There are two types of energy transfer to consider; long-range Coulombic (Forster) and short-range electron-exchange.

Long-range energy transfer occurs as a result of Coulombic (predominantly dipole-dipole) interactions between donor and acceptor over large intermolecular separations up to the order of 10nm. The dipole-dipole interactions cause perturbations of the electronic structures of the energy donor and acceptor. As M* and Q approach, the M* dipole (excited electron) interacts with the Q dipole (an unexcited electron in the HOMO of Q). The resulting dipole-dipole interaction can cause the electron in the HOMO of Q to oscillate violently. This leads to excitation of the electron into the LUMO, and a corresponding de-excitation of the excited electron on M. The end result of this interaction is that M* has become de-excited and has returned to the ground electronic state with a simultaneous excitation of Q to Q*. Energy has been transferred from M* to Q despite the fact that the two species

have not come into close contact, and no electrons have been transferred between them.

Short-range energy transfer requires much closer contact between M* and Q. The excited electron on M* transfers into the LUMO of Q, with a simultaneous transfer of an electron from the HOMO of Q into the corresponding orbital on M. For the transfer to take place, M* and Q must be sufficiently close (<2nm) that there is overlap of the electron orbitals involved.

Energy transfer processes result in the migration of excitation energy from chromophores of high excitation energy to chromophores of lower excitation energy. Hence, the observed emission shows a subsequent shift to longer wavelength. These processes are particularly important in multi-chromophoric systems such as humic acid, where there are numerous chromophores with overlapping excitation and emission spectra

2.3.3.2 Collisional Deactivation

Collisional deactivation describes energy transfer between the excited molecule, M* and an acceptor molecule, A, in which the excitation spectrum is not relevant. The process is summarised below;

$$M^* + A \rightarrow M + A$$

The electronic excitation of M* usually becomes degraded to vibrational, translational and sometimes rotational energy in A. Collisional deactivation is especially important in solution phase where collisions between excited molecules and solvent molecules are frequent. At low pressures in the gas phase, collisions may not be competitive with emission or energy transfer. In solids, collisions may be hindered by the rigidity of the structure.

2.3.3.3 Quenching of Phosphorescence

Since phosphorescence is due to a "weakly allowed" spin-forbidden transition, it occurs on a much longer timescale to fluorescence. Hence, phosphorescence emission is particularly prone to bimolecular quenching. Collisional deactivation of the triplet competes effectively with radiation, and visible phosphorescence is not normally observed unless the collisional deactivation rate is sufficiently reduced e.g. by studying the molecules in a more rigid media, such as at low temperatures or in a solid matrix. It is also extremely important to ensure high purity solvents are used when studying phosphorescence. Impurities can be luminescent, swamping the phosphorescence emission, or can act as efficient quenchers. Molecular oxygen is one of the most effective quenchers of phosphorescence. It has a triplet ground state and can interact with a triplet excited molecule leading to quenching via electron-exchange energy transfer;

$$^3M^* + {}^3Q \rightarrow {}^1M + {}^1Q^*$$

2.4 Excited State Decay Kinetics

Radiative emission is a spontaneous process i.e. the excited molecule loses its energy of its own accord in the absence of an electromagnetic field.

$$M^* \rightarrow M + h\nu$$

However, this is not a full description of the system, as there are other processes taking place in competition with direct fluorescence (or phosphorescence) emission. These processes can be summarised as;

$^1M^* \rightarrow {}^1M$	internal conversion
$^1M^* \rightarrow {}^3M^*$	intersystem crossing
$^1M^* + Q \rightarrow {}^1M + Q^*$	quenching

In real systems where these other processes compete effectively with emission, the measured lifetime will be reduced in comparison with the natural radiative lifetime and the intensity of fluorescence (or phosphorescence) will be reduced.

Excited state decay is a random process and depends only on the concentration of the excited species. Consequently, it follows first order decay kinetics;

$$-\frac{d}{dt}[M^*] = k\,[M^*]$$

where k is the rate coefficient and can be considered as the sum of the rate coefficients for emission (E), internal conversion (IC), intersystem crossing (ISC) and quenching (Q);

$$k = k_E + k_{IC} + k_{ISC} + k_Q$$

Integration of the rate equation gives us;

$$[M^*] = [M^*]_0\, e^{-kt}$$

Hence, the concentration of M* decays exponentially to zero from some initial concentration $[M^*]_0$ at t = 0. The decay of intensity of luminescent emission is

characterised quantitatively by the fluorescence or phosphorescence lifetime, τ. This is the time taken for intensity to decay to 1/e of its initial intensity immediately after the exciting radiation is cut off. The fluorescence (phosphorescence) lifetime is defined as the reciprocal of the rate coefficient;

$$\tau = 1/k$$

Since k has the units of a first order rate coefficient (s^{-1}), the lifetime has units of s.

2.5 Multi-Chromophore Systems

For a system consisting of a single type of emitting molecule, the emission spectrum is independent of the excitation wavelength as discussed in section 2.3.1.3. In a multi-chromophoric system where there is no energy transfer, the emission is characteristic only of optically-excited molecules. Consequently, it may be possible to selectively excite a particular chromophore or group of chromophores. In a multi-chromophoric system with energy transfer, the situation becomes much more complex, as the emission can be directly (optically) or indirectly (*via* energy transfer) excited. To fully define the system, we must consider the excitation, emission and intensity characteristics at any given wavelength. This gives rise to the Excitation-Emission Matrix (EEM).

2.5.1 The Excitation-Emission Matrix (EEM)

An EEM is constructed from individual excitation or emission spectra, which are collated to give a matrix. Within an EEM, each matrix element is the luminescence intensity at a particular combination of excitation and emission wavelengths. A typical EEM of humic material is shown in Figure 2.5. The humic material was

dissolved in water to a concentration of 100ppm. The data are represented as a contour plot with excitation wavelength, emission wavelength and intensity as the three variables. The excitation wavelength is plotted on the y-axis and the emission wavelength is plotted on the x-axis. The contours link points of equal intensity. The sharp edge to the plot, running from bottom left to top right, indicates first-order Rayleigh-Tyndall scattering that occurs when the excitation wavelength is equal to the emission wavelength. If not removed from the plot, this would swamp the luminescence signal. Second-order Rayleigh-Tyndall scattering occurs when the emission wavelength is twice that of the excitation wavelength. This series of intense peaks has also been removed from the plot for clarity.

The EEM is composed of several component peaks in which the wavelength of maximum emission increases with excitation wavelength, indicating the contribution of many individual emitting species to the luminescence signal. This contrasts with the EEM of a single-emitting molecule, in which the wavelength of maximum emission is independent of excitation wavelength.

The central region of the EEM has two obvious peaks, at 270nm excitation and 470nm emission (written as 270/470nm) and 350/470nm. Other less intense peaks appear as "shoulders" on the central peaks, distorting them from a concentric shape. There is a prominent shoulder at 450/500nm, and another smaller shoulder at 370/520nm. The individual excitation spectra collated to give the matrix EEM show these shoulders as composite peaks. Figure 2.6 shows three of the individual excitation spectra used to create the EEM;

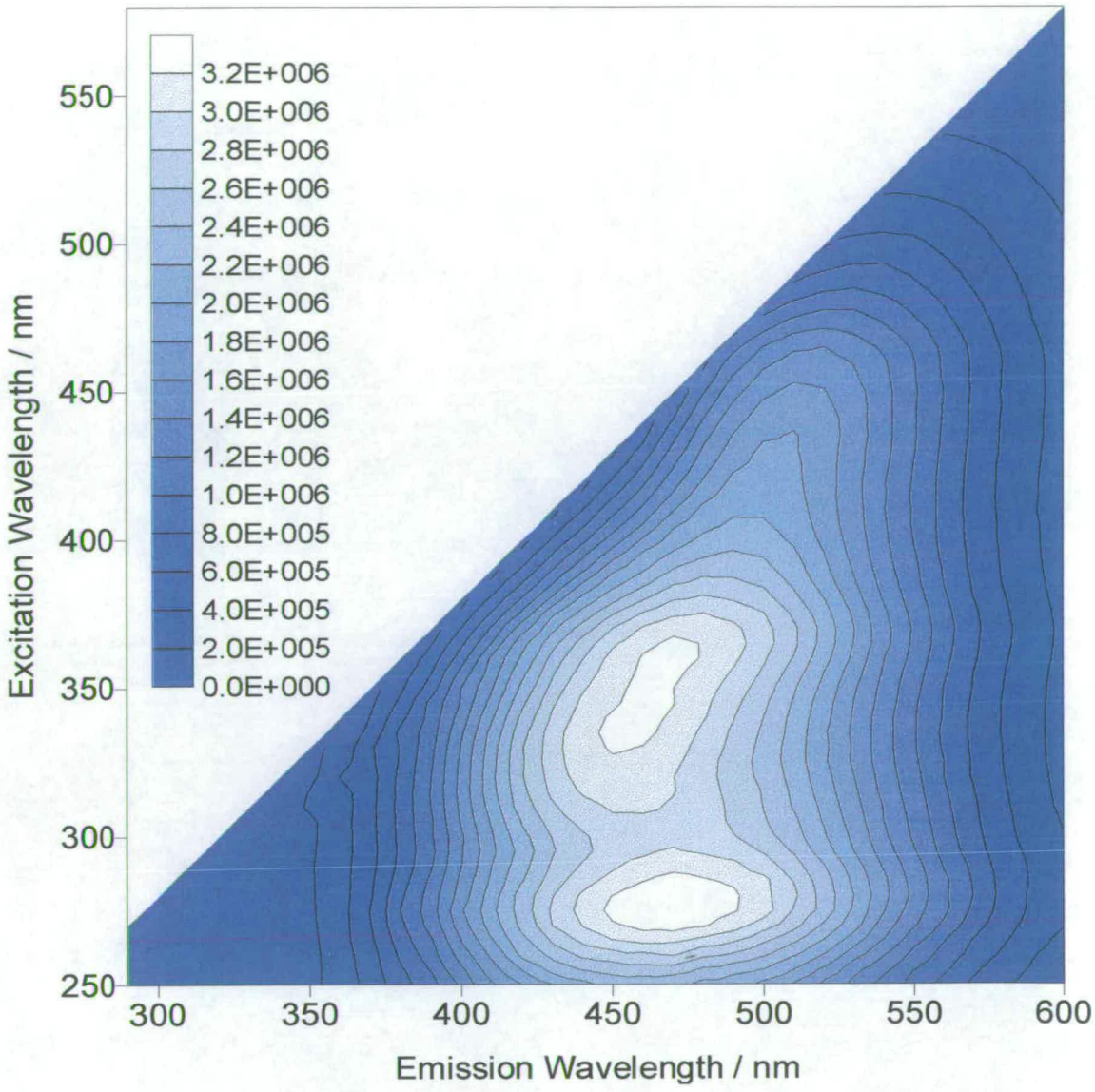

Figure 2.5: EEM of humic acid solution (100ppm) at room temperature. The contours link points of equal intensity between zero and 3.2 x 10^6 cps at 2 x 10^5 cps intervals.

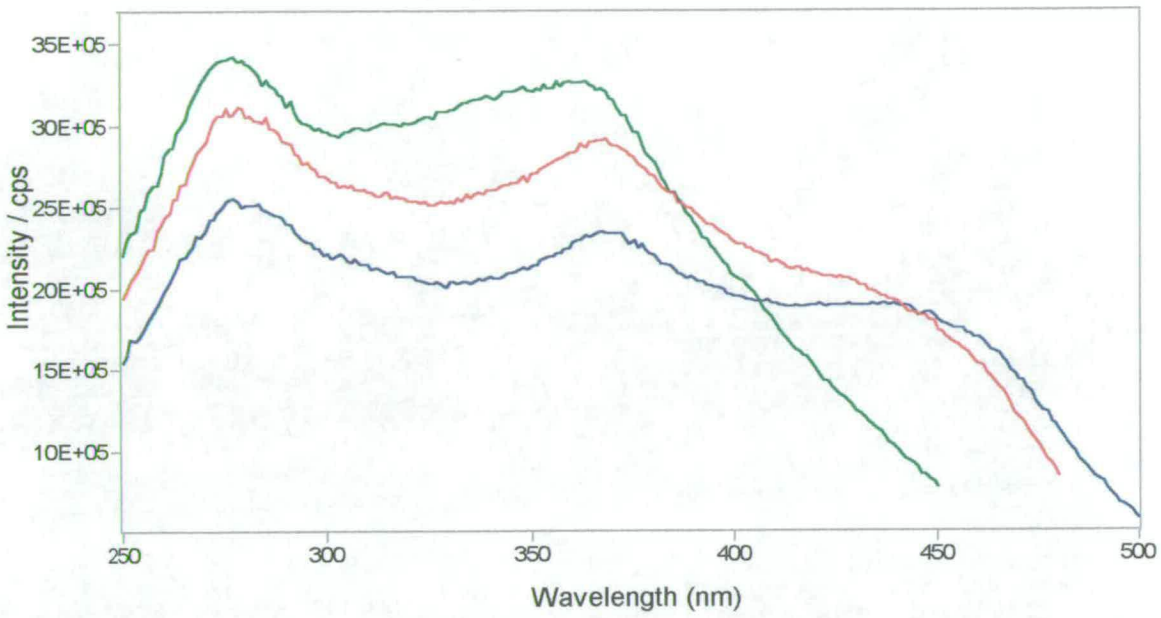

Figure 2.6: Excitation spectra of humic acid in 100ppm solution. The green scan corresponds to 470nm emission, the red scan to 500nm emission and the blue scan to 520nm emission.

The three scans show the inter-relationship between excitation and emission wavelength in a complex multi-chromophoric system. At 470nm emission (green scan), there are two excitation peaks, at 270 and 350nm. At 500nm emission (red scan), another excitation peak becomes evident at 450nm. At 520nm emission (blue scan), the 450nm peak is much more evident. All these peaks are identified in the EEM, but with only single wavelength spectra, much of the information about component peaks would be lost.

Weber (1961) developed the EEM as a method for analysis of a fluorescent sample containing multiple components. The first study of multiple-component fluorescence in the natural environment using the EEM was made by Coble *et al.* (1990). She

utilised the three-dimensional matrix to study DOM in the Black Sea and suggested that this technique could be used to distinguish between different types and sources of DOM in natural waters. Investigations of freshwater and seawater samples showed distinct differences in fluorescence properties of DOM from marine and terrestrial sources (Coble, 1994). Hence, the EEM can provide a "fingerprint" image of the total fluorescence in an environmental sample.

2.6 Bibliography

Papers cited in text:

Coble, P.G., Green, S.A., Blough, N.V., and Gagosian, R.B., 1990. Characterization of dissolved organic-matter in the black-sea by fluorescence spectroscopy. Nature, 348: pp. 432-435.

Coble, P.G., 1994. Distribution and characterization of marine and terrestrial humic substances in seawater as determined by excitation-emission matrix spectroscopy. Abstracts of Papers of The American Chemical Society, 207: pp. 122-GEOC.

Weber, G., 1961. Enumeration of components in complex systems by fluorescence spectrophotometry. Nature, 190: pp. 27-29.

General texts and papers referred to:

Boto, K. and Isdale, P., 1985. Fluorescent bands in massive corals result from terrestrial fulvic acid inputs to nearshore zone. Nature, 315: pp. 396-398.

Bowen, E. J., 1968. Luminescence in Chemistry. D. Van Nostrand Co. Ltd: London.

Christian, G. D., Callis, J. B., and Davidson, E. R. 1981, Array Detectors and EEM's in Multicomponent Analysis: pp. 136-165. Modern Fluorescence Spectroscopy. Plenum Press: New York.

Coble, P.G., 1991. Characterization of dissolved organic-matter using total fluorescence spectroscopy. Abstracts of Papers of the American Chemical Society, 201: pp. 12-GEOC.

Dunlap, W.C. and Susic, M., 1985. Determination of pteridines and flavins in seawater by reverse-phase, high-performance liquid-chromatography with fluorometric detection. Marine Chemistry, 17: pp. 185-198.

Fu, T. and Pocklington, R., 1983. Quantitative adsorption of organic-matter from seawater on solid matrices. Marine Chemistry, 13: pp. 255-264.

Gentien, P., 1981. Fluorescent Metabolites in Coral Reefs off Townsville, Queensland. Australian Journal of Marine and Freshwater Research, 32: pp. 975-980.

Gilbert, A. and Baggott, J., 1991, Essentials of Molecular Photochemistry. Blackwell Scientific Publications: Oxford.

Isdale, P., 1984. Fluorescent bands in massive corals record centuries of coastal rainfall. Nature, 310: pp. 578-579.

Mantoura, R.F.C. and Riley, J.P., 1975. The Analytical Concentration of Humic Substances from Natural Waters. Analytica Chimica Acta, 76: pp. 97-106.

Matthews, B.J.H., Jones, A.C., Theodorou, N.K., and Tudhope, A.W., 1996. Excitation-Emission-Matrix Fluorescence Spectroscopy Applied to Humic Acid Bands in Coral Reefs. Marine Chemistry, 55: pp. 317-332.

Miano, T.M., Sposito, G., and Martin, J.P., 1988. Fluorescence Spectroscopy of Humic Substances. Soil Science Society of America , 52: pp. 1016-1019.

Morrison, R. T. and Boyd, R. N., 1987. Organic Chemistry. Allyn and Bacon: Boston.

Theodorou, N. K., 1995. The enigmatic properties of fluorescent banding in massive corals of the species *Porites lutea* from Phuket, Thailand. The University of Edinburgh. PhD.

Wayne, C. E. and Wayne, R. P., 1996. Photochemistry. Oxford University Press: Oxford.

3 Chapter Three: Experimental

3.1 Introduction

The study of luminescent banding in coral skeletons can be split into two areas; that involving extraction of the constituent luminophores giving rise to the banding pattern, and the study of the banding pattern *in situ*. Since this work is concerned with the study of the banding pattern *in situ*, this section will discuss previous experimental work in this area only.

Initial work to study the luminescence banding phenomenon carried out by Isdale (1984) concentrated on recording the variations in fluorescence intensity from the coral surface. The coral skeleton was illuminated with longwave uv light and stepped in 0.5mm increments past the tip of an optical fibre using a milling machine bed. Fluorescence in the skeleton was measured with the optical fibre connected to the emission monochromator of a spectrofluorimeter. The *cube* of the fluorescence intensity was correlated to the outflow of the nearby Burdekin River, suggesting there may be interdependence between the two phenomena.

Following this initial investigation, Isdale and Boto (1985) modified the experimental set-up to include excitation at 360nm from a 150W mercury arc lamp via a quartz optical fibre focused into a 3mm spot on the coral surface. This allowed preliminary emission spectra to be recorded, highlighting the broad emission with a maximum at 440-460nm, indicative of the presence of humic acids. Smith *et al.* (1989) used the same experimental technique to record the variations in fluorescence in coral samples from Florida Bay. They detected emission at 460nm, considering it to be the wavelength that gave the best enhancement of terrestrial over marine fluorescence signals. The variations were then compared to the freshwater flow from the Everglades.

Work carried out by Jones (1990) re-iterated the limitations of the method pioneered by Isdale. In order to compare fluorescence intensity and other environmental variations, it was necessary to remove the "background fluorescence" by subtraction of the lowest recorded fluorescence intensity from each measurement. Each measurement was cubed to allow for "the inability of the equipment to measure the fluorescence observed by eye". The fluorescence intensity along the length of the coral core was translated to a time scale by aligning the peak fluorescence recorded each year with the peak monthly streamflow volume and linearly interpolating the timescale between the peaks.

Milne and Swart (1994) used a low power, sealed plasma cartridge pulsed N_2 laser as the excitation source at 337nm. The pulses were coupled to a fused silica optical fibre via a fused silica lens mounted on a fibre coupler. Emission was detected at 460nm using linearly arranged collection fibres within the same optical fibre. By stepping the coral skeleton underneath the fixed optical fibre, the luminescence variation from the surface was recorded. However, the results show little definition between bright and dull regions of the skeleton. Milne and Swart attributed this limited resolution to a high "background" signal and the heterogeneity of the coral structure.

Matthews *et al.* (1996) studied the fluorescence directly from the coral surface by fixing the coral sample in the sample chamber of a fluorimeter and aligning the excitation beam within a band. The intensity of the fluorescence was very dependent on the geometry of the sample relative to the excitation and emission monochromators, and meant that there could be no quantitative comparison between the bright and dull bands.

The present investigation uses several different experimental approaches to the study of the luminescent banding pattern in order to optimise and reproducibly record the

intensity variation and allow quantitative comparisons between regions of bright and dull luminescence.

This chapter gives detailed descriptions of the samples used in this investigation, their geographical location and environment. The methods of luminescence data acquisition, manipulation and presentation are included, from initial measurements to adaptations of the basic experiment, allowing for both spatial and temporal resolution. The techniques used to study the skeletal structure of coral skeletons are described (confocal fluorescence microscopy and scanning electron microscopy) including the method of dating coral skeletons by means of skeletal density variations.

3.2 Samples

Investigations were carried out on samples from a variety of geographical locations that are prone to different environmental conditions. In all cases, corals of the genus *Porites* were used due to its longevity, rapid growth rate and apparent reliability in paleoenvironmental reconstruction.

3.2.1 Laing Island, Papua New Guinea (PNG)

All cores from Laing Island Reef were collected by Tudhope and co-workers (Tudhope *et al.*, 1995). Laing Island Reef is situated on the Bismark Sea coast of PNG (4° 9'S; 144° 53'E). The coastal rainfall averages about 3,000 mm/year with a dry season from June to September. The reef lies close to the mouths of two large rivers, the Sepik River (50km distant) and the Ramu River (25km distant). These rivers drain 300,000km^2 of land. For six months of the year, the currents wash the river output away from the reef, but for the next six months, the output washes past Laing Island Reef. Using staining techniques (Tudhope *et al.*, 1995) it has been

ascertained that the bright bands are deposited during the wet season and the dull bands during the dry season. Samples from Laing Island Reef can be considered to be seasonally influenced by coastal run-off.

3.2.2 Madang Lagoon, PNG

All cores from Madang Lagoon Reef PNG (5° 13'S; 145° 49'E) were collected by Tudhope and co-workers (Tudhope *et al.*, 1995). Strong tidal and wind-driven currents flush the lagoon, which ensures no stagnation of water. The lagoon has an area of 46km^2 with a terrestrial catchment area of 240km^2. For each year of growth, there are two bright bands and two dull bands laid down in the skeleton (Tudhope *et al.*, 1995). There is a correlation between periods of increased rainfall and bands of bright luminescence. Samples from Madang Lagoon Reef can be considered to be seasonally-influenced by coastal run-off.

3.2.3 Wadi Ayn region, Gulf of Oman

Samples from Wadi Ayn in the Gulf of Oman (17°N; 55°E) were collected by Tudhope and co-workers (Tudhope *et al.*, 1996). This sampling site is prone to ocean and coastal upwelling but can be considered to be free from terrestrial input, as it is not subject to sub-annual inundation from coastal run-off.

The coral samples are cored or cut from the large coral mass, or *bommie* using a hand-held corer or specially adapted underwater drill. After collection, the brown polyp tissue layer located in the first 5 – 10mm of the top surface was removed with bleach and then the whole sample thoroughly cleaned with water before analysis. For the purposes of analysis, samples were cut into slices around 5mm thick and 20mm by 50mm in area. A sample piece of coral from Laing Island, illuminated under uv light, is shown in Figure 3.1.

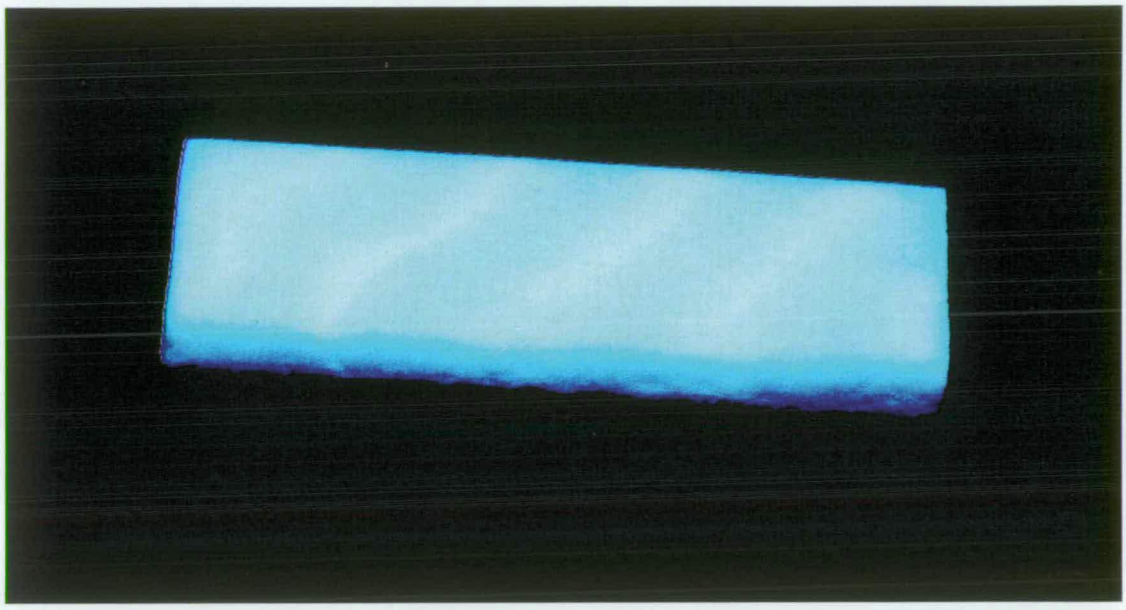

Figure 3.1: Sample of Laing coral illuminated under uv light at 365nm. The coral piece is approximately 20mm by 50mm in area and 5mm thick.

3.3 Recording luminescence spectra and creating an EEM

3.3.1 Operational Overview

The luminescence measurements were carried out using a Jobin Yvon Spex Fluoromax fluorimeter and associated Datamax control and data processing software. The excitation source is a 150W continuous ozone-free xenon lamp. Illumination from the lamp is collected by an elliptical mirror and directed towards the excitation slit of the excitation monochromator. The excitation and emission monochromators have a groove density of 1200 grooves/mm and are blazed at 330nm and 500nm respectively. The photomultiplier detector (PMT) operates in the photon-counting mode and is sensitive between 200 and 900nm with saturation at 4 x 10^6 cps. The

coral sample was fixed in a commercially available solid sample holder in the sample chamber. The sample was fixed at 45° relative to both the incident radiation and the detection system. This proved to be the optimum angle for the maximum signal to scattered light ratio. The system layout is shown in Figure 3.2.

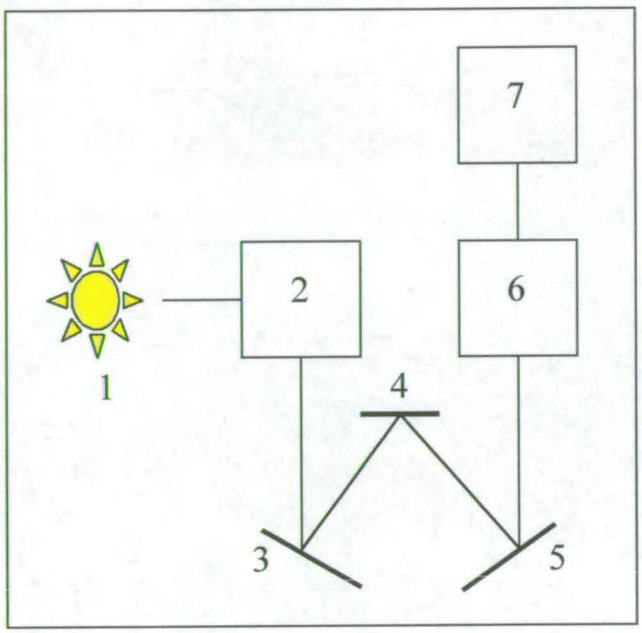

Key to Figure 3.2:

1	Xenon Lamp
2	Excitation Monochromator
3	Coupling Optics
4	Sample
5	Coupling Optics
6	Emission Monochromator
7	Photomultiplier Tube

Figure 3.2: System Layout.

3.3.2 Data Collection

The excitation beam was focused on to the coral surface, giving an illuminated area of approximately 1mm wide by 5mm high. Since individual bright and dull luminescent bands are each a few millimetres wide (the coral extends 10 – 20mm annually) the excitation beam could be located within a bright or dull band on the coral surface. Data acquisition was performed using 1.5nm bandwidths for both the excitation and emission monochromators and a 1s integration time. The wavelength increment was set at 1nm. Consequent excitation spectra were collected between 250

and 580nm, with a fixed emission wavelength at 20nm greater than the maximum excitation wavelength to avoid first order Rayleigh-Tyndall (RT) scattering. Running each subsequent scan with a 5nm reduction in maximum excitation wavelength led to collection of 63 scans per sample.

3.3.3 Producing an EEM

The raw data consisted of 63 individual excitation spectra recorded at different emission wavelengths between 600nm and 290nm. When the emission wavelength corresponded to twice the excitation wavelength e.g. for an excitation spectrum recorded at 600nm emission and scanning the excitation at 300nm, second order Rayleigh-Tyndall scattering appeared as a very intense and sharp peak. These peaks were deleted from each individual scan after collection using the "Zap" function of the Datamax software. The excitation spectra were corrected for the wavelength-dependent response of the PMT by multiplying by factors provided by the manufacturer corresponding to the recorded emission wavelength. The spectra were also corrected for the lamp intensity distribution as a function of wavelength by ratioing the luminescence signal to a reference signal (approximately 8% of the incident light). This correction could be made during data collection by setting the signals to S/R in the experimental set-up of the Datamax software.

Once the individual excitation spectra had been corrected, they were exported as a sequence of ASCII files from Datamax into Origin v3.5. Origin is a technical graphics and data analysis package. Each excitation spectrum was imported as a series of intensities as a function of excitation wavelength at a given emission wavelength. Once all 63 had been imported into the same spreadsheet, the maximum and minimum values of excitation and emission wavelengths were set and the spreadsheet was converted to a matrix. This matrix had 63 columns (emission wavelengths) and 330 rows (excitation wavelengths). The matrix was then exported as a complete unit into Surfer v6.0, another graphics package with more advanced mapping capabilities. The matrix was then converted to a 3D contour plot, using the

gridding and mapping functions. The data was gridded using a quadrant search and minimum search elipse (10 or below).

3.4 Adaptations of the basic experiment

3.4.1 Spatially-resolved luminescence measurements

In order to produce spatially resolved measurements of luminescence, it was necessary to modify the initial experimental set-up. Figure 3.3 shows the modified experimental set-up.

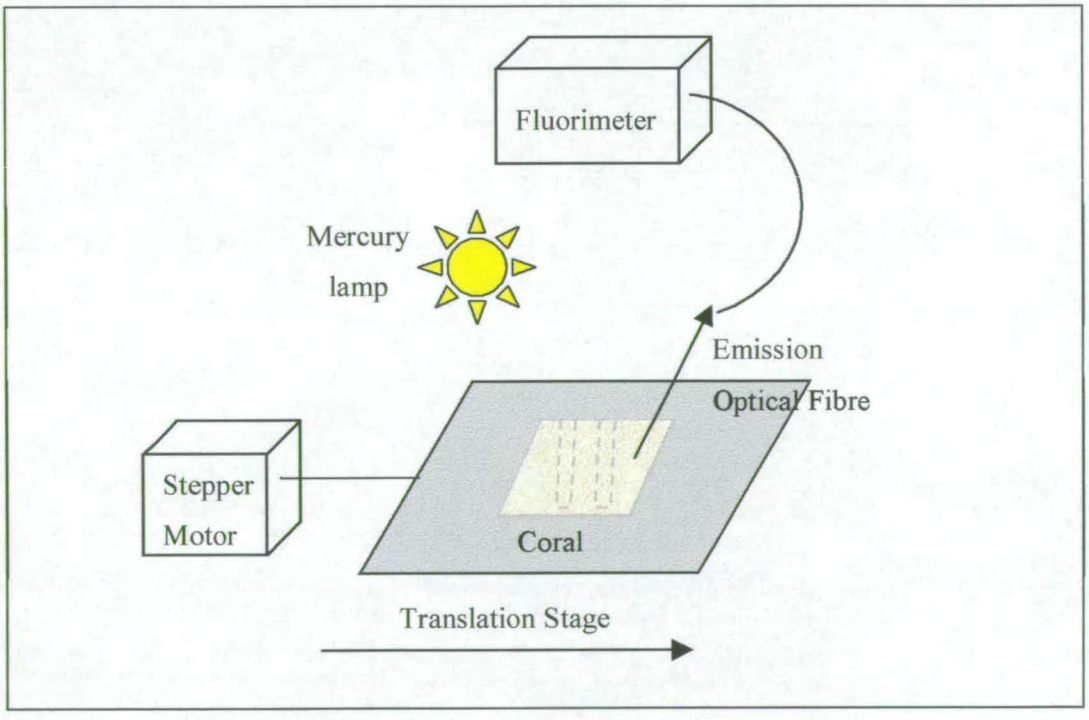

Figure 3.3: Experimental set-up for spatially resolved measurements of luminescence using the Mercury lamp excitation source

The coral sample was mounted outside the fluorimeter on a precision linear translation stage (Ealing 22-2067; large linear stage, manual drive, 100mm travel, drum micrometer). The stage was driven incrementally by a stepper motor. The sample was illuminated using a mercury lamp (Fisons LCG-100-100Q; longwave (UV-A) and shortwave (UV-C) with 4W LW tube, 4W SW tube and filter assembly) at 365nm positioned directly above the translation stage in a metal lamp stand. Luminescent emission was collected using a glass optical fibre bundle (L.O.T. Oriel; 400 – 1300nm transmittance) interfaced to the emission monochromator within the Spex Fluoromax fluorimeter. Data were recorded using the associated Datamax software. The sample was passed beneath the fibre bundles at a fixed velocity of 6 x 10^{-5} ms^{-1}. The experiment was set in Time Base Acquisition mode in the Datamax software. A scan of the variation in luminescence intensity as a function of lateral position was achieved.

3.4.2 Using an excitation optical fibre

In order to record the variations in luminescence intensity with excitation wavelength, the mercury lamp was replaced with an excitation optical fibre, as shown in Figure 3.4.

The excitation beam was delivered from the excitation monochromator of the Spex Fluoromax fluorimeter to the sample in a fused silica optical fibre bundle (L.O.T. Oriel standard grade; transmittance from 250 – 1100nm). The excitation optical fibre terminated approximately 2mm above the surface of the coral. The positions of the fibres were optimised to produce and record the most intense emission from the coral surface, found to be when the bundles were positioned at 90° to each other and 45° to the vertical. The bundles were then clamped in place for the duration of the experiment.

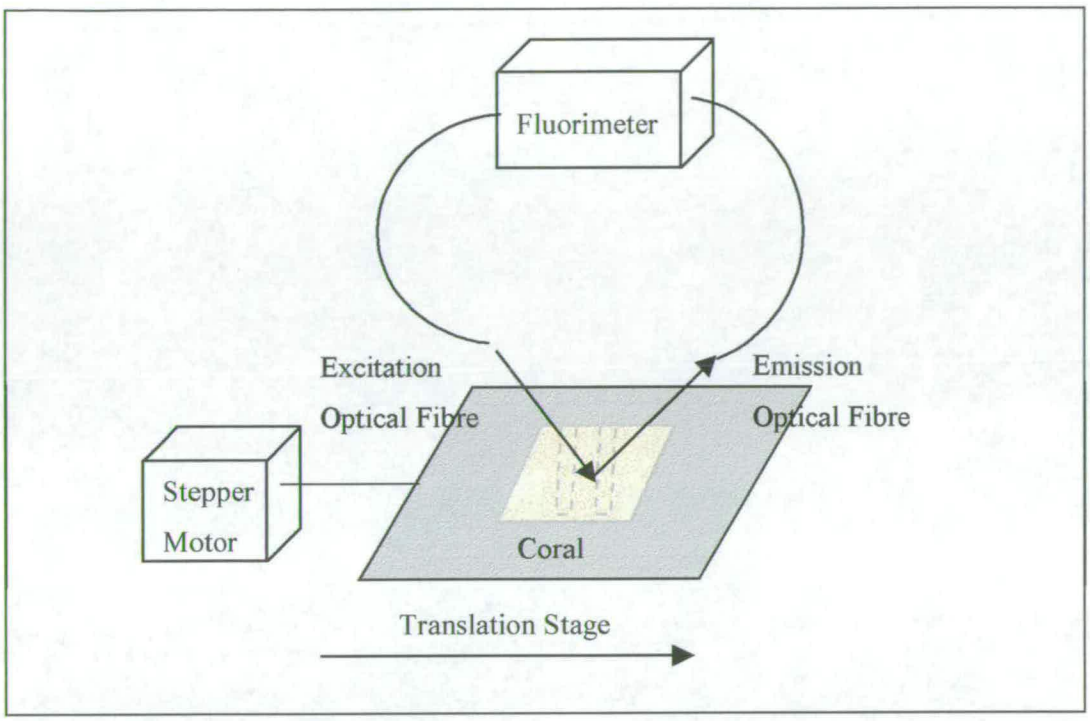

Figure 3.4: Experimental apparatus for varying excitation wavelength when measuring spatially resolved luminescence

By positioning the sample to correspond to a bright band intensity peak or dull band intensity trough, the points of greatest intensity difference could be probed. At these points, EEM of the luminescence intensity were recorded. Excitation spectra were collected between 300 and 630nm, with emission wavelengths set at 20nm greater than the maximum excitation wavelength for each scan. The minimum emission wavelength used was limited to 400nm by the transmittance of the glass optical fibre bundle. Both the excitation and emission bandwidths were set at 4nm. The integration time was 0.4s and the increment was 1nm.

3.4.3 Measuring Phosphorescent Decay

Initially, measurements were carried out using the Spex Fluoromax fluorimeter with DM3000 software. The coral sample was fixed in the solid sample holder and the excitation source focused on to a particular band as described in section 3.3.2. After approximately two seconds, the excitation source was cut off using the excitation shutter in manual control mode. The shutter closing time is in the region of 100ms. The decaying emission signal was recorded as a function of time over 10s at 0.01s increments.

The total luminescence of the coral is made up of short-lived fluorescence and long-lived phosphorescence. By closing the shutter in the excitation beam, the short-lived fluorescence signal is cut off but the long-lived phosphorescence persists and the decay of its intensity with time can be measured. This phosphorescence decay can be fitted to an exponential function, which gives information on the triplet state lifetimes of the emitting species. By extrapolation (see Chapter Six, Section 6.3.1), an estimate of the fractional contribution of phosphorescence to the total luminescence of the system can be obtained. Since the shutter has a closing speed of 100ms, only long-lived components with phosphorescence persisting for greater than 100ms can be considered. This method does not take into account short-lived phosphorescing species and is thus an underestimation of the total phosphorescence of the system.

3.4.4 Spatially-resolved measurements of phosphorescence spectra

In order to be able to record phosphorescence spectra and consider the contribution of short-lived phosphorescing species to the overall luminescence of the system, it was necessary to modify the experimental set-up. Using electronic shutters, the delay between excitation and detection of emission could be varied, and hence the luminescence of the system could be time-resolved.

The excitation shutter of the fluorimeter was removed and replaced with an electronic shutter (L.O.T. Oriel model 76994). A similar shutter was fixed in front of the emission monochromator. The shutters were connected to a pair of electronic shutter controllers (L.O.T. Oriel model 76995). A digital delay/pulse generator (Stanford Research Systems model DG 535) externally controlled the sequence of opening and closing of the shutters. Figure 3.5 shows the sequence of events in the shutter operation.

Initially, both shutters are closed, until the delay generator signals the excitation shutter to open. At this point, the excitation beam illuminates the sample and luminescence is emitted. The delay generator then signals the excitation shutter to close, and illumination ceases. After a preset delay time, the emission shutter opens, and any emission from the sample is detected at the photomultiplier tube. The delay generator then signals the emission shutter to close and the cycle starts again.

The delay between the closing of the excitation shutter and the opening of the emission shutter (or detection window) allows the type of luminescence recorded to be controlled. Since fluorescence decays in less than 1 μs, the opening of the excitation and emission shutters must overlap in order to detect fluorescence. To record the total luminescence (fluorescence + phosphorescence) of a sample, the delay between the closing of the excitation shutter and the opening of the emission shutter ($t_5 - t_3$) was reduced to –10ms. This led to the overlapping opening of the two shutters, and hence all the short-lived fluorescence emission and longer-lived phosphorescence could be collected. To preclude fluorescence detection, the delay ($t_5 - t_3$) was increased to at least 20ms. After this time, only phosphorescing species could be detected. To compare the maximum emission wavelength due to phosphorophores of different phosphorescence lifetimes, the delay was increased incrementally up to a maximum of 2 seconds.

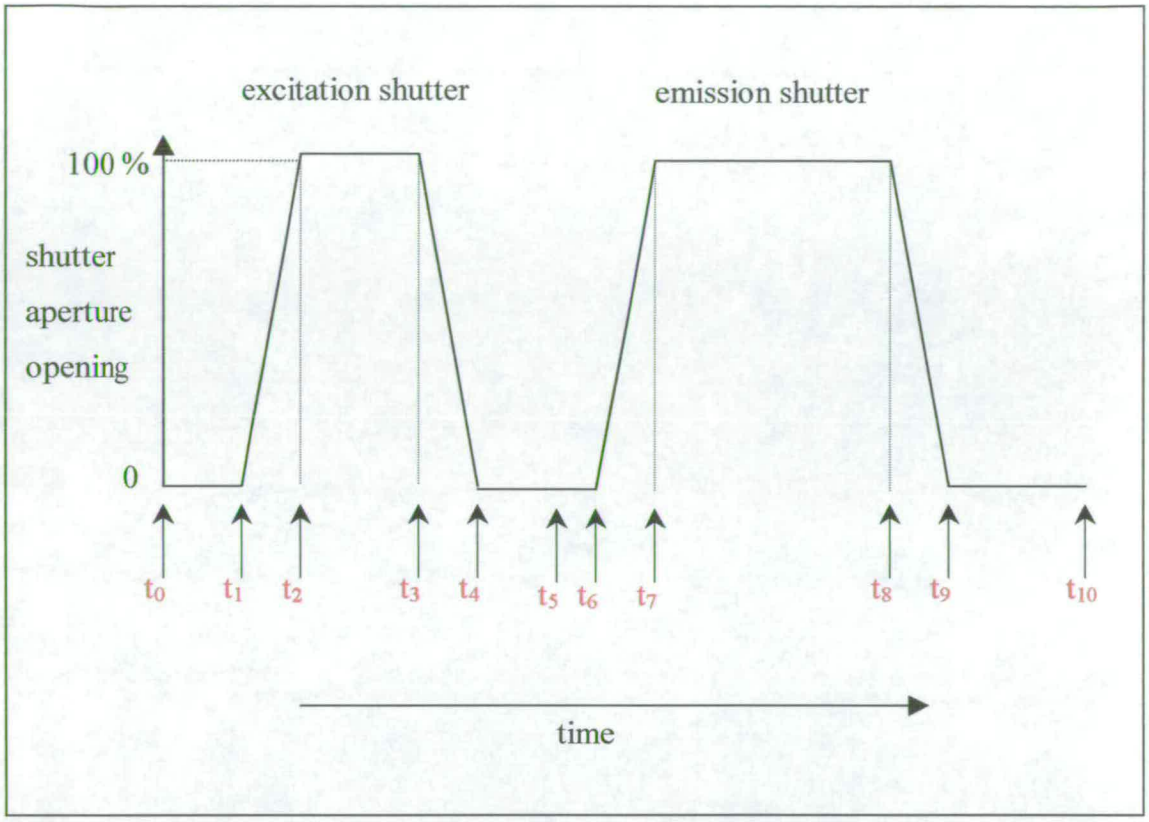

For a typical set-up to detect phosphorescence emission with a 15ms ($t_3 - t_0$) excitation pulse, 20ms ($t_5 - t_3$) delay and 100ms ($t_8 - t_5$) emission detection, the shutter sequence is as follows:

t_0	open signal from delay generator to excitation shutter
$t_1 = t_0 + 3$ ms	shutter starts to open
$t_2 = t_1 + 3$ ms	shutter fully open
$t_3 = t_2 + 9$ ms	close signal from delay generator to excitation shutter
$t_4 = t_3 + 4.2$ ms	shutter fully closed
$t_5 = t_4 + 15.8$ ms	open signal from delay generator to emission shutter
$t_6 = t_5 + 3$ ms	shutter starts to open
$t_7 = t_6 + 3$ ms	shutter fully open
$t_8 = t_7 + 94$ ms	close signal from delay generator to emission shutter
$t_9 = t_8 + 4.2$ ms	shutter fully closed
$t_{10} = t_9 + 60$ms	cycle starts again

Figure 3.5: Shutter operation as controlled by the delay generator

The experimental set up to measure spatially-resolved phosphorescence is shown in Figure 3.6.

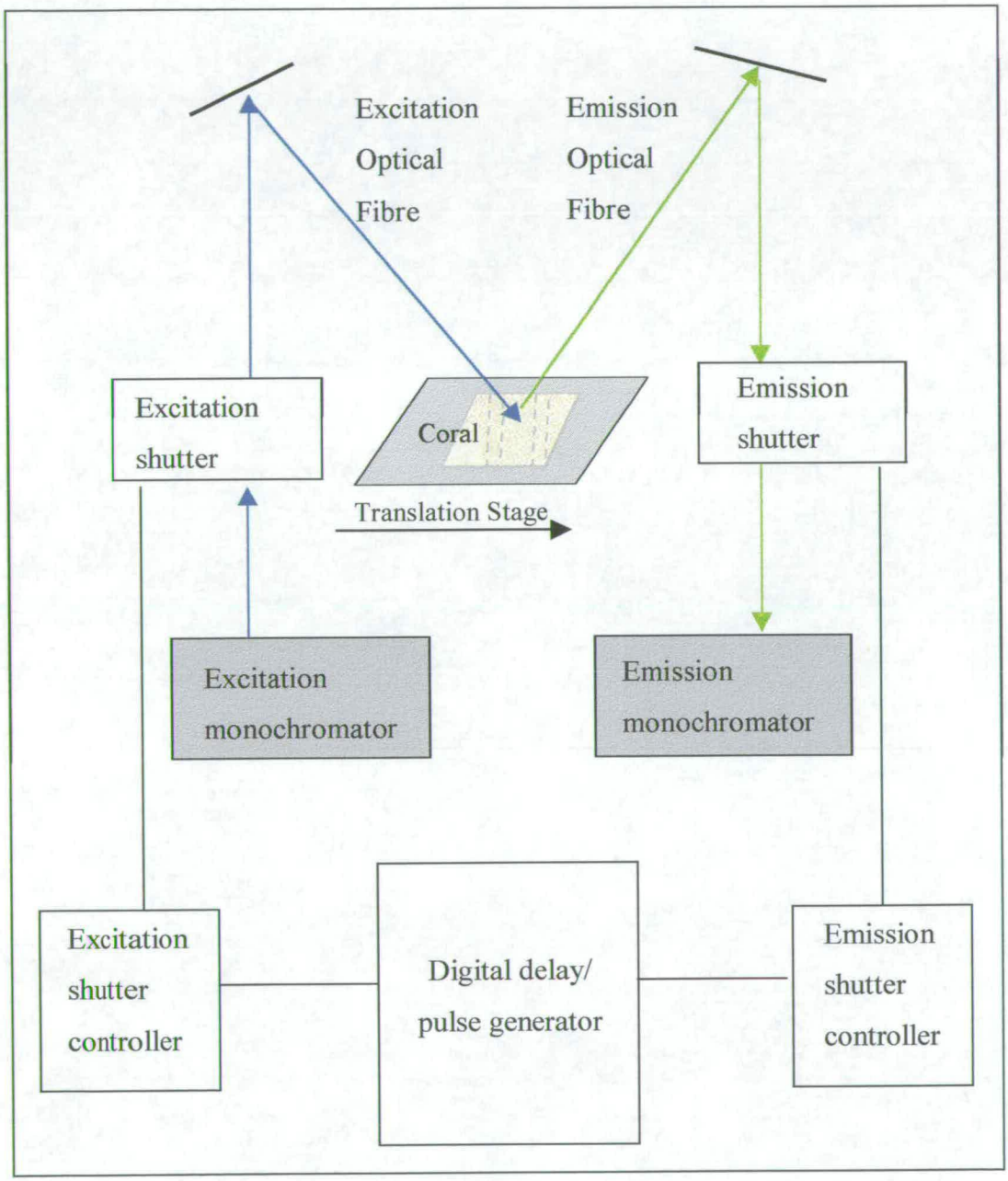

Figure 3.6: Experimental Set-up to measure spatially resolved phosphorescence

Initially, to record the banding pattern, the coral was stepped incrementally beneath the optical fibres and the lateral variations in emission intensity recorded at various excitation/emission wavelength combinations. The delay between closing of the excitation shutter and opening of the emission shutter was set at –10ms to include both fluorescence and phosphorescence emission. The procedure was then repeated for a delay of 20ms to exclude fluorescence emission and detect phosphorescence emission only. The experimental data was collected using Timebase Acquisition in the Datamax software. The integration time was 0.5s and the increment 1s.

The excitation and emission bandwidths were increased in comparison to previous measurements to allow for the reduced intensity of phosphorescence emission (relative to total luminescence). The excitation bandwidth was 10nm and the emission bandwidth was 20nm. The delay generator was internally triggered at a frequency of 40Hz.

To record the phosphorescence spectrum of a bright band, the point of maximum emission of the band was located using the translation stage, and an emission spectrum collected using Emission Acquisition. The sample was excited at 360nm and the emission scanned between 380 and 650nm at various delay settings. The increment was set at 1nm and the integration time at 1s. The excitation and emission bandwidths were both 10nm. This was then repeated for the minimum emission intensity of a dull band.

3.4.5 Recording a Phosphorescence EEM

Using the translation stage and excitation and emission optical fibres previously described (Section 3.4.2), the sample could be probed at the peak of bright band luminescence intensity or the trough of dull band intensity and the phosphorescence EEM recorded at this point.

To record a phosphorescence EEM, excitation spectra were recorded between 280 and 580nm, with emission wavelengths set at 20nm greater than the maximum excitation wavelength for each scan. The minimum emission wavelength used was limited to 400nm by the transmittance of the glass optical fibre bundle. The excitation and emission bandwidths were increased to allow for the reduced intensity of the phosphorescence signal. The excitation bandwidth was 10nm and the emission bandwidth was 20nm. The increment was set at 1nm and the integration time at 0.5s. The digital delay generator trigger frequency was set at 40Hz. The excitation pulse ($t_3 - t_0$) was set at 15ms, the delay ($t_5 - t_3$) at 20ms (to exclude fluorescence emission) and the emission detection window ($t_8 - t_5$) at 50ms. The delay ($t_5 - t_3$) was then increased to 100ms and the integration time to 0.8ms, and the experiment repeated. Following the collection of 19 component spectra, the data were manipulated as previously described in section 3.3.2. The optical fibres were then positioned at the point of minimum emission intensity of the adjacent dull band and the procedure repeated.

3.5 Structural studies of coral skeletons

3.5.1 Density banding

Massive colonies of *Porites* were collected from the Great Barrier Reef (GBR), Australia. Colonies from the GBR were collected from six reefs (Figure 3.7; Table 3-I).

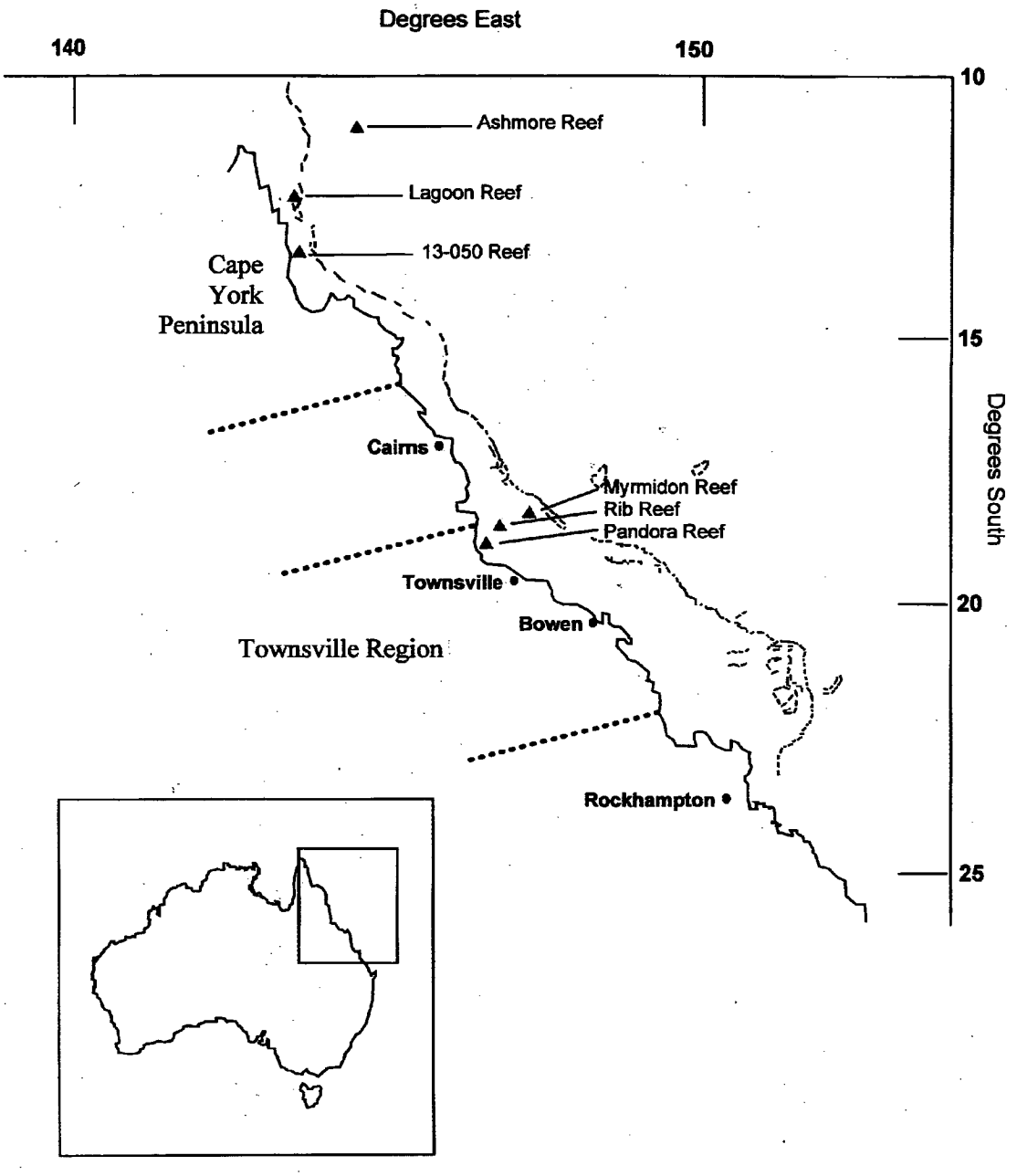

Figure 3.7: Map of the Great Barrier Reef and surrounding area.

Reef	Latitude	Longitude	Collected	Distance from coast (km)	Type
Ashmore	10.25S	144.50E	Dec 89	176	Offshore
Lagoon	12.38S	143.73E	Jul 90	42	Offshore
13-050	13.33S	143.95E	Jul 90	40	Offshore
Myrmidon	18.27S	147.38E	Nov 87	110	Offshore
Rib	18.48S	146.88E	Nov 87	56	Midshelf
Pandora	18.80S	146.43E	Nov 87	16	Inshore

Table 3-1: Collection sites and dates for colonies of massive Porites from the GBR. Latitude and longitude are in decimal notation.

Slices, 6 – 7mm thick, were sawn from a central growth axis of each colony. At least ten slices from each reef were used in the investigation. As well as the slices from the GBR, samples from the Wadi Ayn region of the Gulf of Oman (described in section 3.1.3) were also included in this investigation.

Luminescent bands were displayed in the coral slices using a 7W ultraviolet (UV) light. Outlines of the bands were drawn on transparent acetate film. The banding pattern was recorded for both sides of each slice. Images of coral slices were recorded using a Sony CCD/RGB colour video camera with a Fujinon-tv zoom lens and Fujinon close-up lens CL11052. The camera system was linked to a 486 IBM-compatible PC and the images stored on the hard drive.

Density variations in coral skeletal slices were recorded by X-radiography (see Barnes *et al.*, 1989) and gamma densitometry (Chalker and Barnes, 1990). X-radiographs give good contrast between regions of low density (darker) and high-density (lighter) skeleton. Outlines of density bands were traced onto acetate film

placed on the X-radiograph. The density banding pattern was dated by assuming that the outermost high density band corresponded to the summer immediately before the coral was collected (see Lough and Barnes, 1992). By overlaying the acetate film of density variations with the acetate film of luminescent bands, the year corresponding to the laying down of the luminescent bands could be estimated.

3.5.2 Confocal Fluorescence Spectroscopy

All experiments were carried out on a BioRad MRC 600 Confocal Fluorescence Microscope at the Electron Microscope Unit, University of Sydney using COMOS (Confocal Microscope Operating System). Coral samples from Laing Island, Papua New Guinea, were freshly sawn, washed with deionised water and dried for 24 hours before analysis. The samples were then mounted on the microscope stage. The bright and dull regions were identified using a 10x Zeiss Epiplan- NEOFLUAR lens in a Zeiss Axiophot Fluorescence Microscope, and exciting at 365nm. In the confocal mode, the excitation wavelength was determined using a BHS (lowpass) filter giving excitation at 488nm. All emission at wavelengths longer than 510nm could be detected. The microscope focused the excitation and emission at a single point and collected the fluorescence image as a series of planes through the coral sample, from the surface to approximately 200 μm. Each plane was recorded at 5μm intervals, giving rise to around 50 individual sets of data for each sample studied. Intense fluorescence was denoted by pink regions, and weak fluorescence by blue regions. Each 3D image was converted to a .tif file and imported to the Confocal Assistant software. In Confocal Assistant, the individual planes were added together to give a 3D image of the skeleton and the distribution of fluorescence within it. The image was then exported into Adobe Photoshop v4.0 for presentation.

3.5.3 Scanning Electron Microscopy

All work was carried out on a Phillips XL30 Scanning Electron Microscope (SEM) operating at 10kV at the Electron Microscope Unit, University of Sydney. The bright and dull regions of the freshly cut coral samples were identified under a handheld uv light and marked using carbon paint (ProSci Tech). The samples were then sputtered in a thin layer of gold before analysis under the SEM. The samples were magnified to study the same regions analysed using the confocal fluorescence microscope. In this way, the two sets of images could be directly compared. The samples were magnified between 50 and 100 times, covering an area approximately 1mm^2. The images were printed out on videograph paper directly from the SEM screen.

3.6 Bibliography

Barnes, D.J., Lough, J.M., and Tobin, B.J., 1989. Density measurements and the interpretation of X-radiographic images of slices of skeleton from the colonial hard coral Porites. Journal of Experimental Marine Biology And Ecology, 131: pp. 45-60.

Boto, K. and Isdale, P., 1985. Fluorescent bands in massive corals result from terrestrial fulvic acid inputs to nearshore zone. Nature, 315: pp. 396-398.

Chalker, B.E. and Barnes, D.J., 1990. Gamma densitometry for the measurement of skeletal density. Coral Reefs, 9: pp. 11-23.

Isdale, P., 1984. Fluorescent bands in massive corals record centuries of coastal rainfall. Nature, 310: pp. 578-579.

Jones, G., 1990, Environmental assessment of a coral core to record phosphorus and trace element pollution in Cleveland Bay- preliminary investigations: Townsville/Thuringowa Water Board: Townsville City Council, Queensland 4810.

Lough, J.M. and Barnes, D.J., 1992. Comparisons of skeletal density variations in Porites from the central Great Barrier Reef. Journal of Experimental Marine Biology and Ecology, 155: pp. 1-25.

Matthews, B.J.H., Jones, A.C., Theodorou, N.K., and Tudhope, A.W., 1996. Excitation-Emission-Matrix Fluorescence Spectroscopy Applied to Humic Acid Bands in Coral Reefs. Marine Chemistry, 55: pp. 317-332.

Milne, P.J. and Swart, P.K., 1994. Fiber-optic-based sensing of banded luminescence in corals. Applied Spectroscopy, 48: pp. 1282-1284.

Smith, T.J., Hudson, J.H., Robblee, M.B., Powell, G.V.N., and Isdale, P.J., 1989. Fresh-water flow from the everglades to Florida bay - a historical reconstruction based on fluorescent banding in the coral solenastrea- bournoni. Bulletin Of Marine Science, 44: pp. 274-282.

Tudhope, A.W., Lea, D.W., Shimmield, G.B., Chilcott, C.P., and Head, S., 1996. Monsoon climate and Arabian sea coastal upwelling recorded in massive corals from southern Oman. Palaios, 11: pp. 347-361.

Tudhope, A.W., Shimmield, G.B., Chilcott, C.P., Jebb, M., Fallick, A.E., and Dalgleish, A.N., 1995. Recent changes in climate in the far western equatorial Pacific and their relationship to the Southern Oscillation; oxygen isotope records from massive corals, Papua New Guinea. Earth and Planetary Science Letters, 136: pp. 575-590.

4 Chapter Four: EEMs of Coral Luminescence

4.1 Introduction

The luminescence of solid coral is due to the presence of a number of emitting (fluorescing and phosphorescing) species. The excitation spectrum is dependent on the emission wavelength, and the emission spectrum is dependent on the excitation wavelength, since at any one combination of emission and excitation wavelengths, any one of the component luminophores could be excited or emitting luminescence. To give a full description of the luminescence of a complex system, it is necessary to describe the intensity of luminescence across a range of excitation and emission wavelengths. The Excitation–Emission Matrix (EEM) describes the variations in excitation and emission intensity across a range of wavelengths by collating individual spectra together into a three-dimensional array.

Previous work using the EEM to describe the luminescence of coral has concentrated mainly on extracted solutions of the coral luminophores (Matthews, 1996). The coral extract EEM showed a number of component peaks giving rise to a diagonal ridge, in which the wavelength of maximum emission increased with excitation wavelength. The maximum intensity peak was identified at approximately 340nm excitation and 440nm emission. In addition to this prominent peak, there were several "shoulders", one at 280/350nm, attributed to the presence of protein-type luminescence, and another at 390/490nm. In any EEM, it is difficult to assign the peaks to one component luminophore and it is likely that each shoulder is also the composite of several contributory species. There were no apparent spectral differences between bright and dull band extracts, suggesting that there is no intrinsic difference in the nature of the luminescent material in the different bands. Matthews postulated that

the visual appearance of banding may be due to concentration effects of humic material or physical factors such as porosity of the coral skeleton.

It is important to remember that during the extraction, it is likely that the structure and functionality of the extracted species may be altered. In order to avoid this, the banding phenomenon must be studied *in situ*. Work on solid coral samples (Matthews, 1996) yielded similar results although comparative studies between bright and dull bands were not reliable due to the geometry of the excitation and emission optics. The main peak at 350/440nm was evident, although the peak at 390/490nm was considerably more intense than in the extract samples. This was attributed to increased energy transfer processes within the solid sample, leading to emission from lower energy luminophores. The EEM's were not extended to shorter wavelength combinations so there was no study of the protein-type luminescence at 280/350nm in the solid samples.

In this chapter, results are presented that show it is possible to obtain a reproducible three-dimensional excitation-emission matrix of the total luminescence of solid coral. The EEM's of solid samples from various locations (described in section 3.1) are presented, using the technique to obtain an EEM as described in section 3.2. For each coral sample from the different locations, EEMs were produced for both bright and dull bands. The reproducibility of the technique is demonstrated in the appendix.

4.2 EEMs of coral from Laing Island, Papua New Guinea

4.2.1 Introduction

Laing Island reef is an inshore reef, lying close to the mouths of two large rivers. A pair of bright and dull bands is laid down annually, with the bright band deposited during the wet season and the dull band during the dry season (Tudhope *et al.*, 1995).

The luminescent banding pattern is easily observable and distinct under ultraviolet light, with narrow bright bands appearing yellow/green and broad dull bands appearing blue/purple. No previous studies of luminescence characteristics have been carried out on samples from Laing Island Reef. Since Laing Island samples are subject to monsoonal rainfall and subsequent seasonal inundation by terrestrial run-off, the banding pattern can be attributed to the influence of seasonal variations. Using this premise, the banding pattern can be studied as an indicator of seasonal variations in environmental conditions.

4.2.2 Bright Band EEMs

The EEM of a bright band of Laing Island coral is shown in Figure 4.1. The x axis shows the emission wavelength, the y axis shows the excitation wavelength and the contours link points of equal intensity. Sections parallel to the y axis represent individual excitation spectra.

The dependence of the wavelength of maximum emission intensity (λ_{em}^{max}) on excitation wavelength and the wavelength of maximum excitation intensity (λ_{ex}^{max}) on emission wavelength is demonstrated by the diagonal shape of the central peak. Ridges extend at various angles to the excitation and emission axes, showing that EEM is the composite of a number of underlying peaks. This indicates the contribution of many individual emitting species to the total observable signal.

The EEM shown in Figure 4.1 describes the **luminescence** of a sample of coral from Laing Island, PNG. Luminescence consists of two distinct types of emission; fluorescence and phosphorescence (Chapter Two, section 2.3.1). It is demonstrated (Chapter Six, section 6.1) that the emission from coral skeletons is due to both fluorescence and phosphorescence.

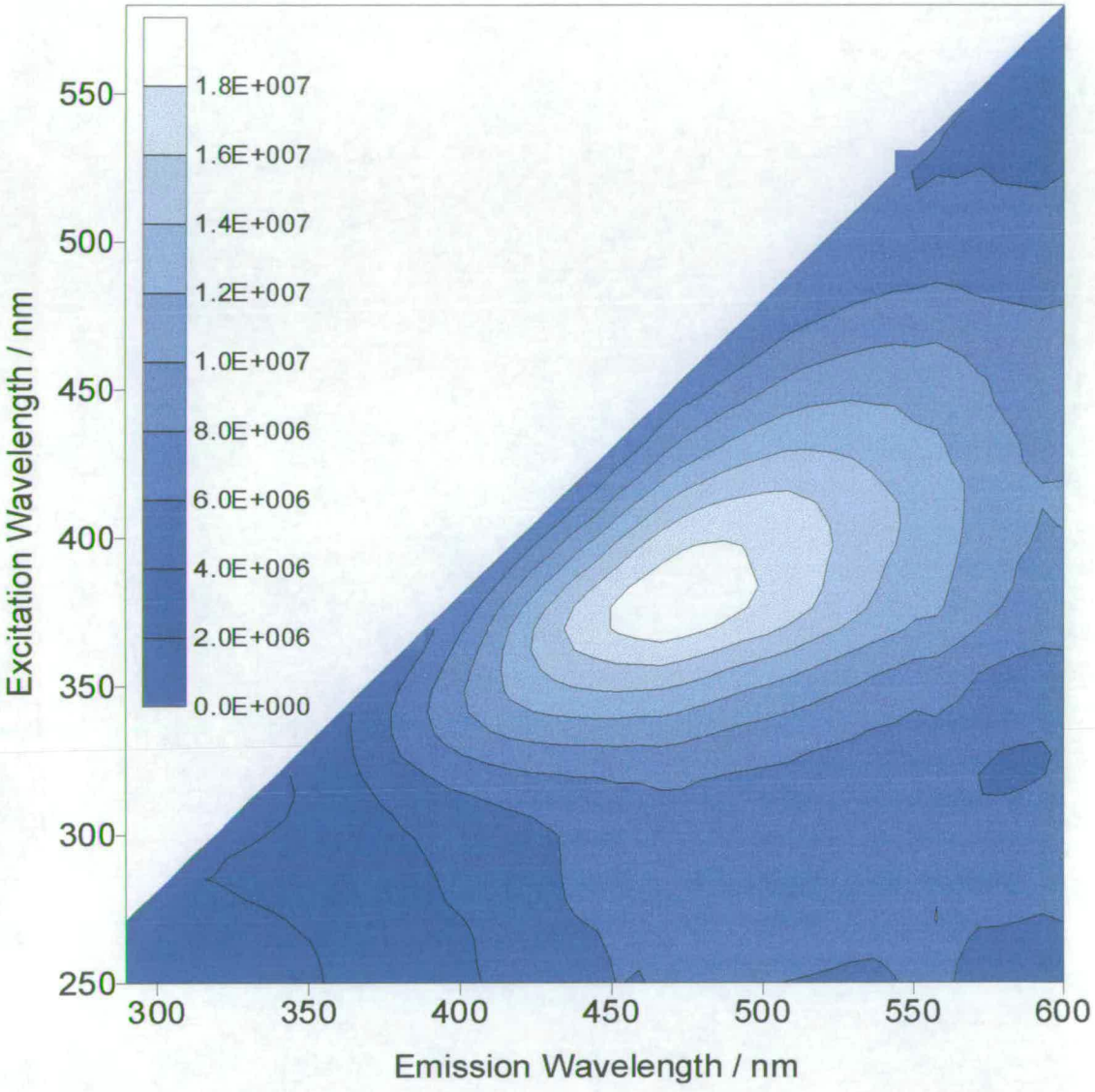

Figure 4.1: An Excitation-emission-matrix (EEM) of a bright band of solid coral. The sample originated from Laing Island, Papua New Guinea. The contours are plotted between zero and 1.8 x 10^7 cps at intervals of 2 x 10^6 cps.

Broad asymmetric features dominate the EEM with a peak at $\lambda_{ex}^{max}/\lambda_{em}^{max}$ 370/470nm. It is apparent in the EEM that quite well-defined peaks are present in the excitation dimension but the emission is very broad in comparison, extending over a wide spectral range. This anisotropy is the consequence of electronic energy transfer (section 2.3.3.1), together with the contribution of phosphorescence to the total luminescence intensity. As a result of energy transfer, excitation of a particular chromophore can result in luminescence from many other luminophores of lower excitation energy. The occurrence of phosphorescence as well as fluorescence further broadens the range of wavelengths over which emission occurs.

The positions of the component excitation peaks were estimated by fitting the individual excitation spectra to the sum of several Gaussian peaks, using the GRAMS/386 peak fitting program (CurveFit) which is incorporated in the Datamax software package. This program employs an iterative non-linear least squares curve fitting procedure based on the Marquardt algorithm.

The spectra were fitted in the wavenumber (cm^{-1}) domain as the wavenumber is linearly related to the amount of energy associated with a transition and hence it would be expected that single luminophores would have comparable peak widths. The component excitation peaks were constrained to have a full-width at half-maximum in the range 2000-4000 cm^{-1}, typical of a single absorbing luminophore.

At short emission wavelengths (320-350nm), the excitation spectra can be fitted by a single peak with λ_{ex}^{max} of 280nm, as illustrated in Figure 4.2.

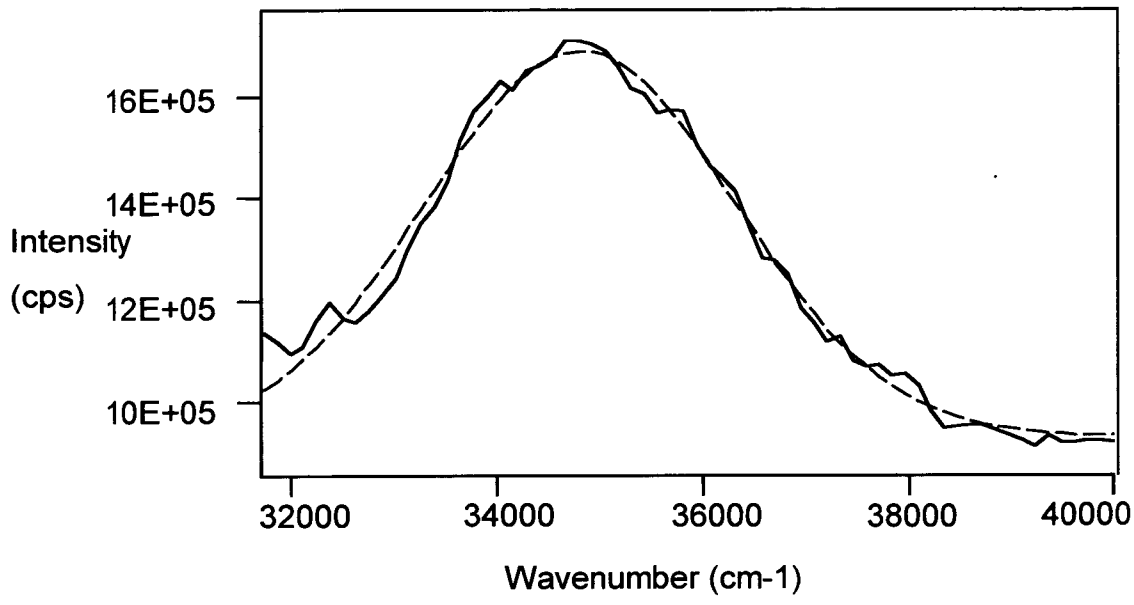

Figure 4.2: Excitation spectrum of coral from Laing Island, Papua New Guinea. The spectrum was recorded between 250 and 315nm excitation and at a fixed emission wavelength of 335nm. The excitation spectrum has been fitted to a Gaussian curve (dotted) with an excitation wavelength maximum of 280nm.

At longer emission wavelengths, up to five component peaks are required to fit the excitation spectra. For example, the excitation spectrum at an emission wavelength of 450nm can be fitted well by the sum of four component peaks, as shown in Figure 4.3.

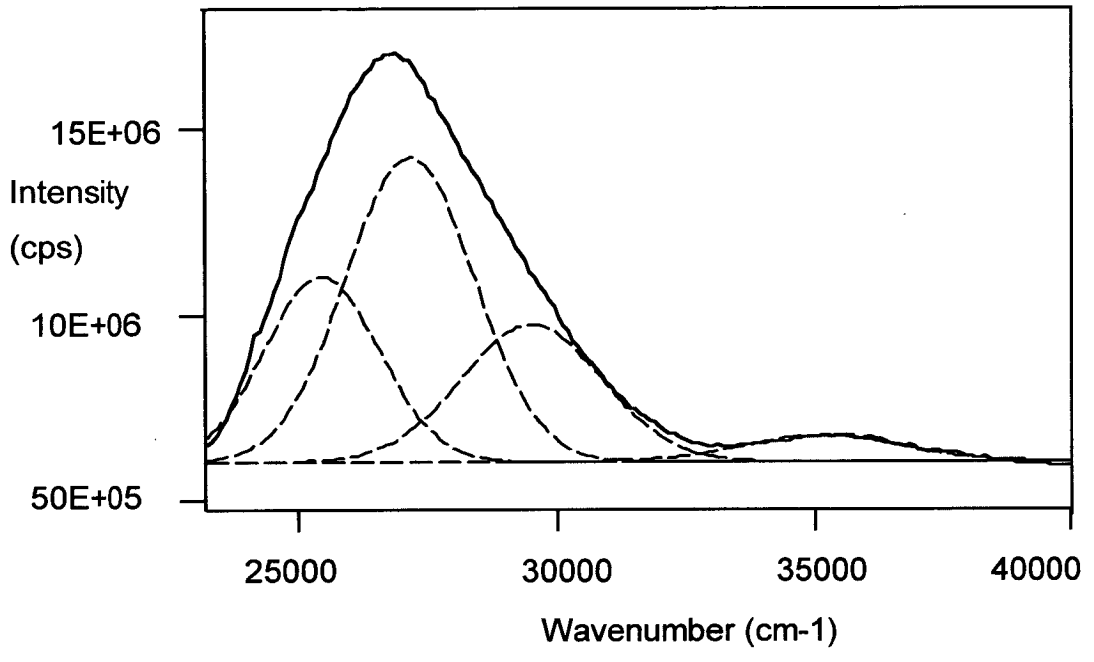

Figure 4.3: Excitation spectrum of coral from Laing Island, Papua New Guinea. The spectrum was recorded between 250 and 430nm excitation and at a fixed emission wavelength of 450nm. The excitation spectrum has been fitted to the sum of four Gaussian peaks (dotted).

The shortest wavelength (highest wavenumber) peak in this excitation spectrum corresponds to the 280nm peak of Figure 4.2. The broad peak at lower wavenumbers can be fitted by three Gaussian components with λ_{ex}^{max} of 340nm (29500cm^{-1}), 370nm (27000cm^{-1}) and 395nm (25500cm^{-1}). Using this procedure it was found that combinations of only six different component peaks could fit the excitation spectra over the range of emission wavelengths from 330 to 570nm. The λ_{ex}^{max} values and corresponding λ_{em}^{max} values are listed in table 4.1.

Excitation Wavelength / nm	280	340	370	390	420	450
Emission Wavelength / nm	450-600	450	470	485	505	530

Table 4-1: Excitation/emission peak positions estimated by Gaussian curve fitting for bright band regions of coral samples from Laing Island, Papua New Guinea.

This suggests that a minimum of six different chromophores (or families of closely related chromophores) is predominant in the excitation of luminescence over this spectral range. Although only six excitation peaks are identified here, it is likely that there are substantially more species contributing to the luminescence, with closely overlapping spectra. In this multichromophoric system, much of the emission may come from species that are excited indirectly via energy transfer, rather than by direct absorption of the excitation light. Thus the chromophores that are dominant in the excitation process may differ from and be fewer than those which are dominant in emission.

The peaks identified in the EEM of solid coral from Laing Island Reef are indicative of the presence of humic material. The positions of the excitation/emission peaks may be compared with those identified previously by Matthews (1996), in Thai corals. The first peak identified in this investigation has an excitation maximum at 280nm and corresponds to the amino acid tryptophan. Tryptophan is one of three luminescent, aromatic amino acids, also including phenyl alanine and tyrosine. However, the luminescence emission spectrum of aromatic amino acids arises predominantly from tryptophan. Phenyl alanine and tyrosine have higher excitation energies and the emission from these amino acids is transferred to tryptophan via electronic energy transfer. The presence of protein-type luminescence has been observed in EEM's of open ocean water (Coble *et al.*, 1993) and it has been suggested that it is due to planktonic activity in surface waters. Hence, the presence of protein-type luminescence indicates a source of marine luminophore.

The characteristic tryptophan excitation/emission peak in solution occurs at 280/350nm. The tryptophan peak has been identified in coral extracts, but preliminary studies by Matthews did not locate it in the solid coral EEM. Figure 4.1 shows a broad emission extending from 450nm to 600nm corresponding to excitation at 280nm. Due to energy transfer, absorption at 280nm may lead to emission from many different luminophores that have lower excitation energies than tryptophan. Tryptophan phosphorescence has a maximum emission intensity at 450nm (Strambini and Gonnelli, 1995). Hence, this observed emission could correspond to phosphorescence emission of tryptophan. In Chapter Six, the phosphorescence characteristics of solid coral are discussed in more detail.

The peak at 340/450nm corresponds to a peak identified in solid coral by Matthews at 350/440nm. Poryvkina et al. (1992) observed a peak at 350/450nm in EEMs of marine dissolved organic matter (DOM).

The peak identified at 370/470nm has not been isolated before, and may have been obscured by the 390/485nm peak identified coral samples and extract solutions by Matthews. Two further peaks are identified at 420/505nm and 450/530nm. Matthews identified a peak at 480/540nm in extracts of commercial humic acid from Fluka and Aldrich. Such low-energy peaks are known to be more typical of terrestrial (lignin-derived) humic acid luminescence.

4.2.3 Dull Band EEMs

The EEM of the immediately adjacent dull band on the same sample of coral from Laing Island Reef is shown in Figure 4.4.

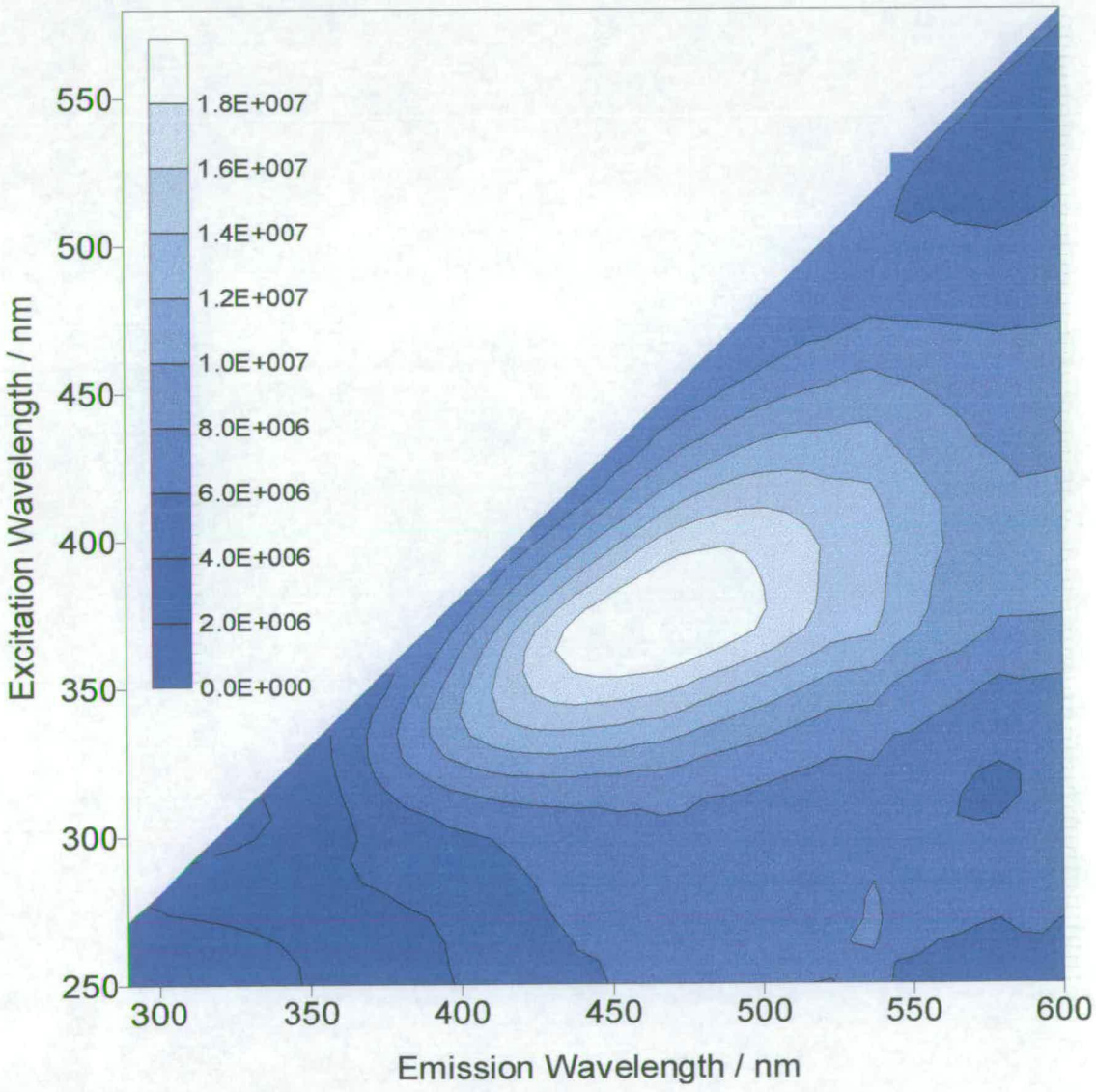

Figure 4.4: An excitation-emission-matrix (EEM) of a dull band of solid coral from Laing Island, Papua New Guinea. The contours are plotted between zero and 1.8 x 10^7 cps, at intervals of 2 x 10^6 cps.

The dull band EEM shows similar macroscopic features to the EEM of the adjacent bright band. The peak corresponding to maximum excitation and emission intensity is centred at 370/470nm and of similar intensity to the peak in the corresponding bright band. This similarity in absolute intensity at the excitation/emission maximum would appear surprising, since the dull bands appear less intense to the eye when viewed under ultraviolet light. However, as will be discussed in the next section (section 4.2.4), the relative intensity distribution gives a much more accurate description of the observable banding pattern.

There are obvious "shoulders" suggesting the presence of other component peaks at both longer and shorter wavelength combinations. Using Gaussian curve fitting, the dull band EEM showed the same six component peaks as the adjacent bright band EEM. This suggests that the component luminophores are the same (or very similar) in both bands.

By dividing the individual component spectra of the bright band EEM by the equivalent spectra of the dull band EEM, and collating the resulting spectra into a matrix, we obtain a ratio EEM. This provides insight into the relative intensity of the bright and dull bands across the wavelength range. In order to determine the absolute intensity difference of the constituent luminophores, we can construct a subtraction matrix. A subtraction matrix is acquired by subtracting a dull band EEM from the adjacent bright band EEM.

4.2.4 Ratio and subtraction EEMs

Figures 4.5 shows the resultant ratio EEM produced when the bright band EEM is divided by the dull band EEM. The ratio EEM shows the relative intensity variation with wavelength. A figure of one denotes an equal intensity in both bands. Regions of intensity greater than one have an increased intensity in the bright band. Regions of intensity less than one have an increased intensity in the dull band.

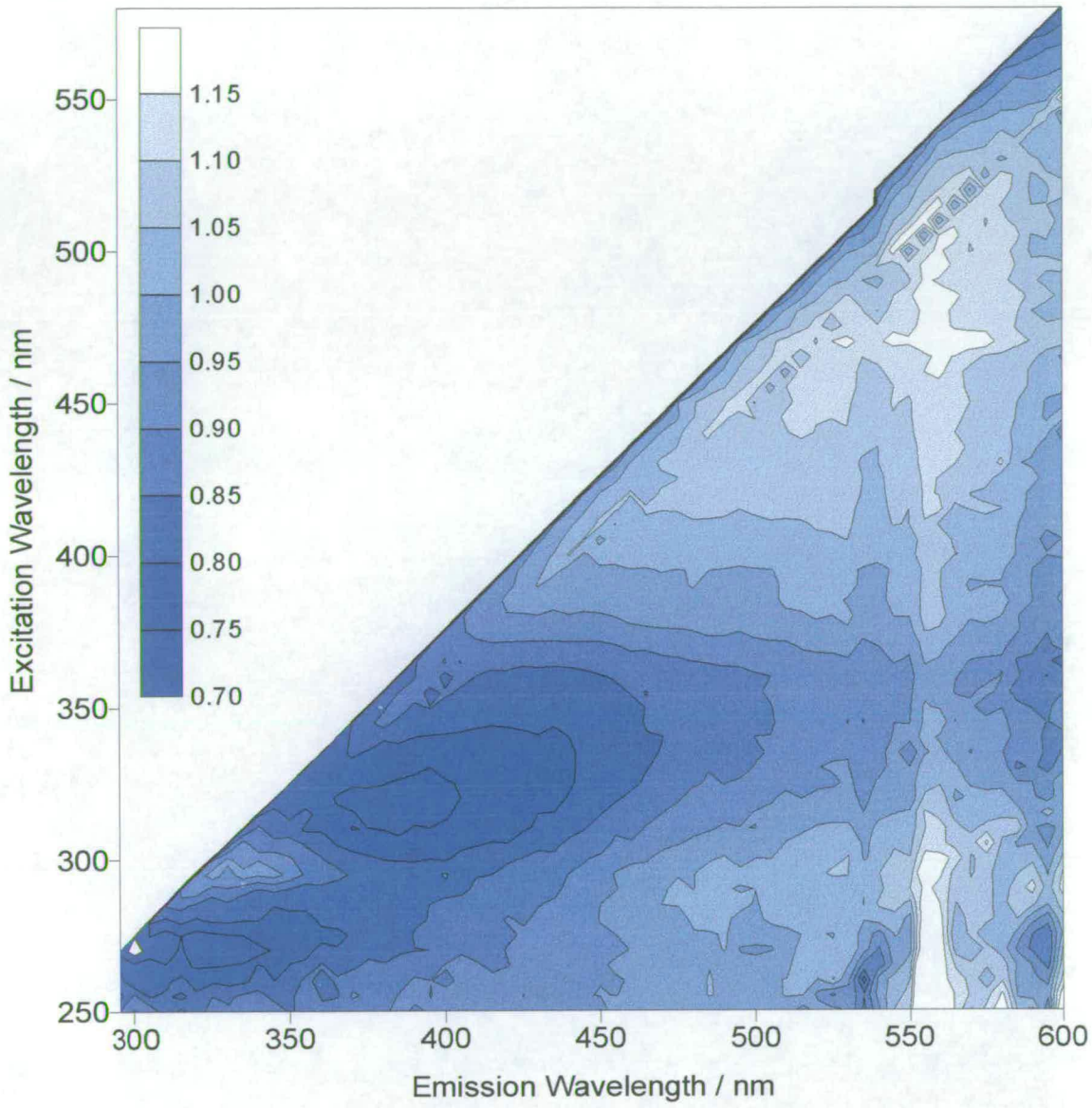

Figure 4.5: Ratio EEM of a sample of coral from Laing Island Reef, PNG. It is constructed by dividing the bright band EEM by the adjacent dull band EEM. The contours are marked between 0.7 and 1.15 at intervals of 0.05 units.

The subtraction matrix corresponding to (Figure 4.1 – Figure 4.4) is shown in Figure 4.6. The positive regions of the plot correspond to regions where the bright band luminescence is more intense than the dull band luminescence. Conversely, negative regions of the plot correspond to regions where the dull band luminescence is more intense than the adjacent bright band luminescence.

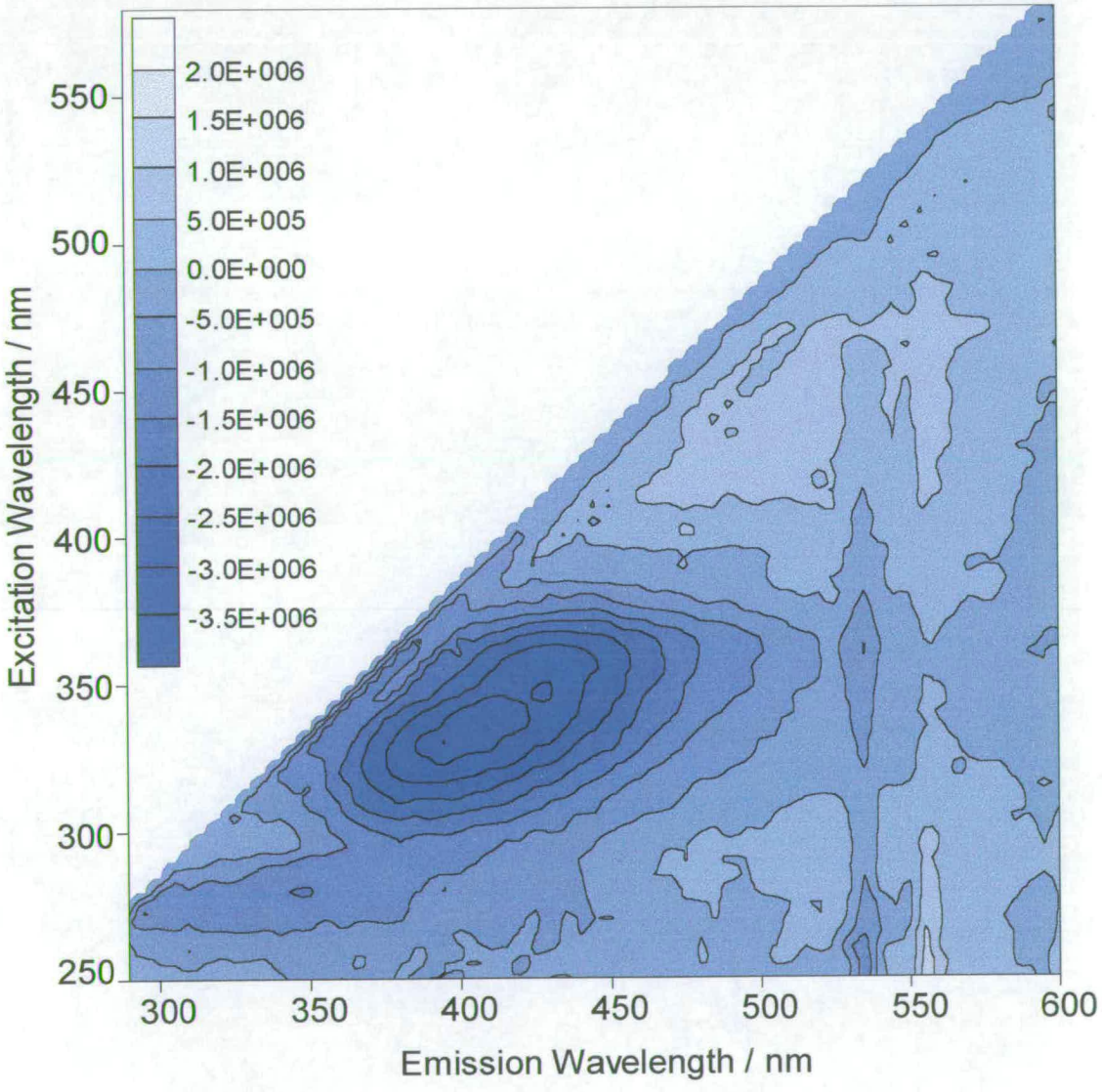

Figure 4.6: A subtraction excitation-emission-matrix (EEM) of solid coral from Laing Island, Papua New Guinea. The contours are plotted between – 4 x 10^6 and 2 x 10^6 cps, at intervals of 5 x 10^5 cps.

From the ratio and subtraction EEMs, it can be seen that the relative intensities of the bright and dull bands are not uniform across the studied wavelength region.

Between 250-350nm excitation and 300-470nm emission, the dull band shows an increased intensity (approximately 25% in the ratio EEM) in comparison to the adjacent bright band. The subtraction EEM has the same features as the ratio EEM, with the dull band showing an increased intensity at short excitation (250-350nm) and emission (300-500nm) wavelengths. This includes the region of emission due to protein-type luminescence. Since protein-type luminescence is due to marine planktonic input, it is likely that there would be less evidence of this in the bright bands if these are attributed to the uptake of terrestrial humic material during the monsoonal run-off.

At excitation wavelengths of 450-500nm and 300nm, and emission wavelengths of 500-600nm, the bright band shows increased intensity, with the bright band approximately 15% more intense than the adjacent dull band in the ratio EEM. The bright band is also more intense in the subtraction EEM at longer emission wavelengths (500-600nm).

There are a number of possible factors that might contribute to increased emission intensity at longer wavelengths. The bright bands may have a different luminophore composition than the adjacent dull band, with a higher concentration of luminophores emitting at longer wavelengths. The relative increase in low energy emission (500-600nm) may be due to increased levels of electronic energy transfer. Electronic energy transfer involves the transference of energy from high energy emitting species to lower energy absorbing and emitting species, so that absorption at short wavelengths may lead to indirect emission at long wavelengths. The lower energy emission in the bright bands may also be due to the contribution of longer wavelength phosphorescence emission.

It is important to note that the regions of greatest difference in intensity (Figures 4.5 and 4.6) do not correspond to the region of greatest luminescence intensity (Figures 4.1 and 4.4). At the main peak identified in Figures 4.1 and 4.4, corresponding to 370/470nm, the dull band has comparable intensity to the bright band, and is actually more intense at 340/450nm. Thus, the luminophores that give rise to the most intense emission in both the bright and dull bands (370/470nm) do not contribute to the banding pattern. However, in Figures 4.5 and 4.6, the bright band is significantly more intense than the adjacent dull band at 300/500-600nm and 450/450-550nm. This corresponds to emission in the yellow/green region of the electromagnetic spectrum, and corresponds with the visual appearance of the bright band when illuminated under uv light.

Hence, the ratio and subtraction EEMs give insight into the differences between the bright and dull band luminescence intensity that are not directly observable from the luminescence EEMs.

4.3 EEMs of coral from Madang Lagoon, Papua New Guinea

4.3.1 Introduction

Madang Lagoon Reef is an inshore reef, subject to seasonal inundation with terrestrial run-off from the nearby landmass. There are two pairs of bright and dull bands laid down each year with bright bands corresponding to the periods of increased run-off. The environmental conditions can be considered similar to those at Laing Island Reef. Under ultraviolet illumination, the banding pattern is less distinct than that observed in corals from Laing Island. The bright bands appear yellow/green and are broader and less well-defined than those from the Laing corals. The dull bands are broad and blue/purple.

4.3.2 Bright Band EEMs

An EEM of a bright band of coral from Madang Lagoon Reef is shown in Figure 4.7.

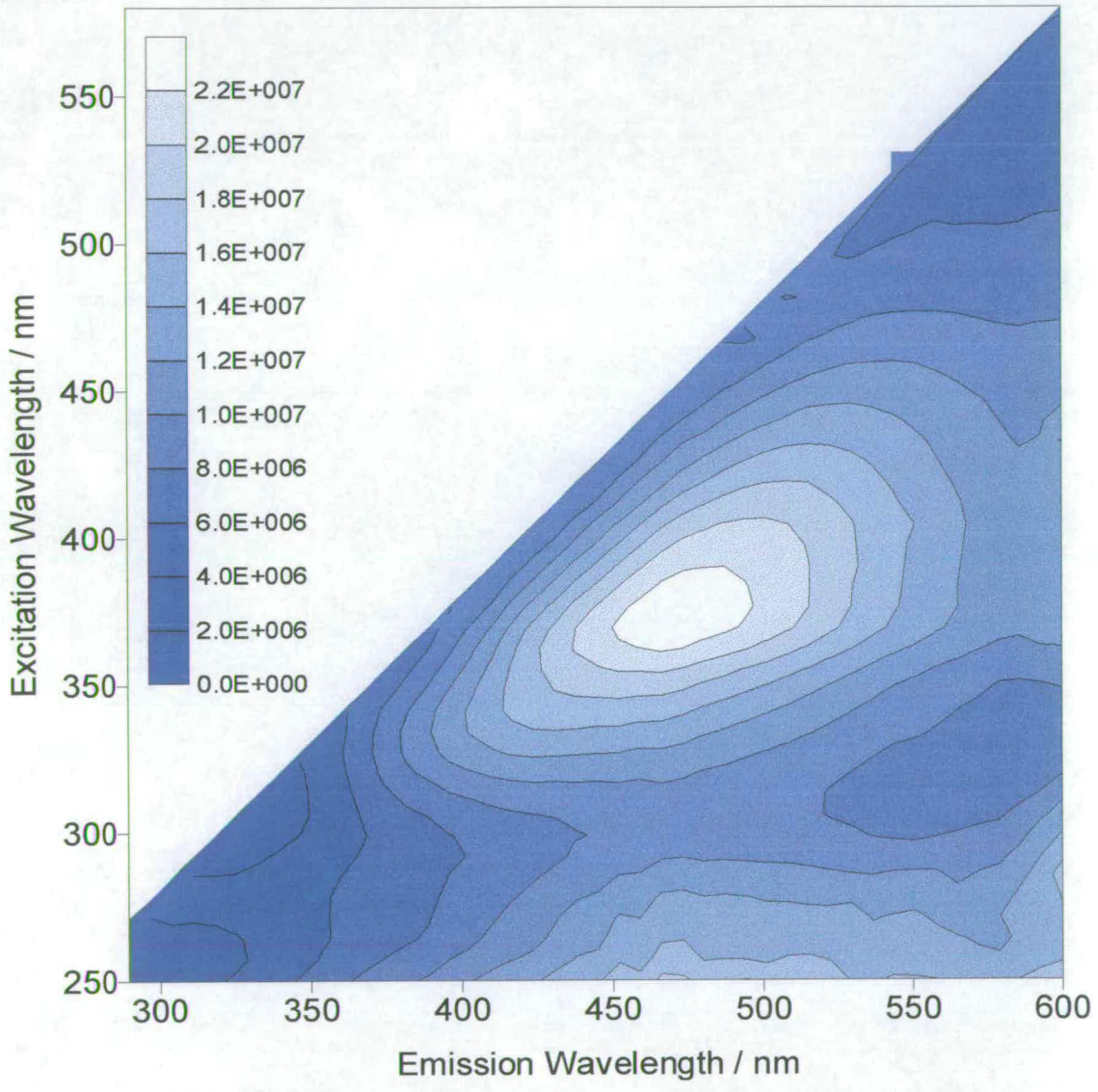

Figure 4.7: An excitation-emission-matrix (EEM) of a bright band of solid coral from Madang Lagoon Reef, Papua New Guinea. The contours are plotted between zero and 2.2 x 10^7 cps, at intervals of 2 x 10^6 cps.

The bright band EEM shows broad and asymmetric features similar to those in the EEM of Laing coral, indicating the presence of numerous emitting components. Using Gaussian curve fitting, the component peaks were determined. These are listed in Table 4.2:

Excitation Wavelength / nm	285	340	370	400	425	455
Emission Wavelength / nm	450-600	430	470	490	510	535

Table 4-2: Excitation/emission peak positions estimated by Gaussian curve fitting for bright band regions of coral samples from Madang Lagoon, Papua New Guinea.

These peaks are similar to peaks identified in the Laing Island sample. This suggests that the component luminophores are similar in both samples. The excitation peaks show less variation between samples of different origin than the emission peaks. It is likely that similar luminophores are dominant in absorption processes but there are variations in the luminophores contributing to emission. This behaviour demonstrates the important role of energy transfer in the excitation process in these systems, and may also be symptomatic of differences in the phosphorescence properties of different samples.

4.3.3 Dull Band EEMs

The adjacent dull band EEM is shown in Figure 4.8. This EEM has the same macroscopic features as the bright band EEM, and the same composite peaks.

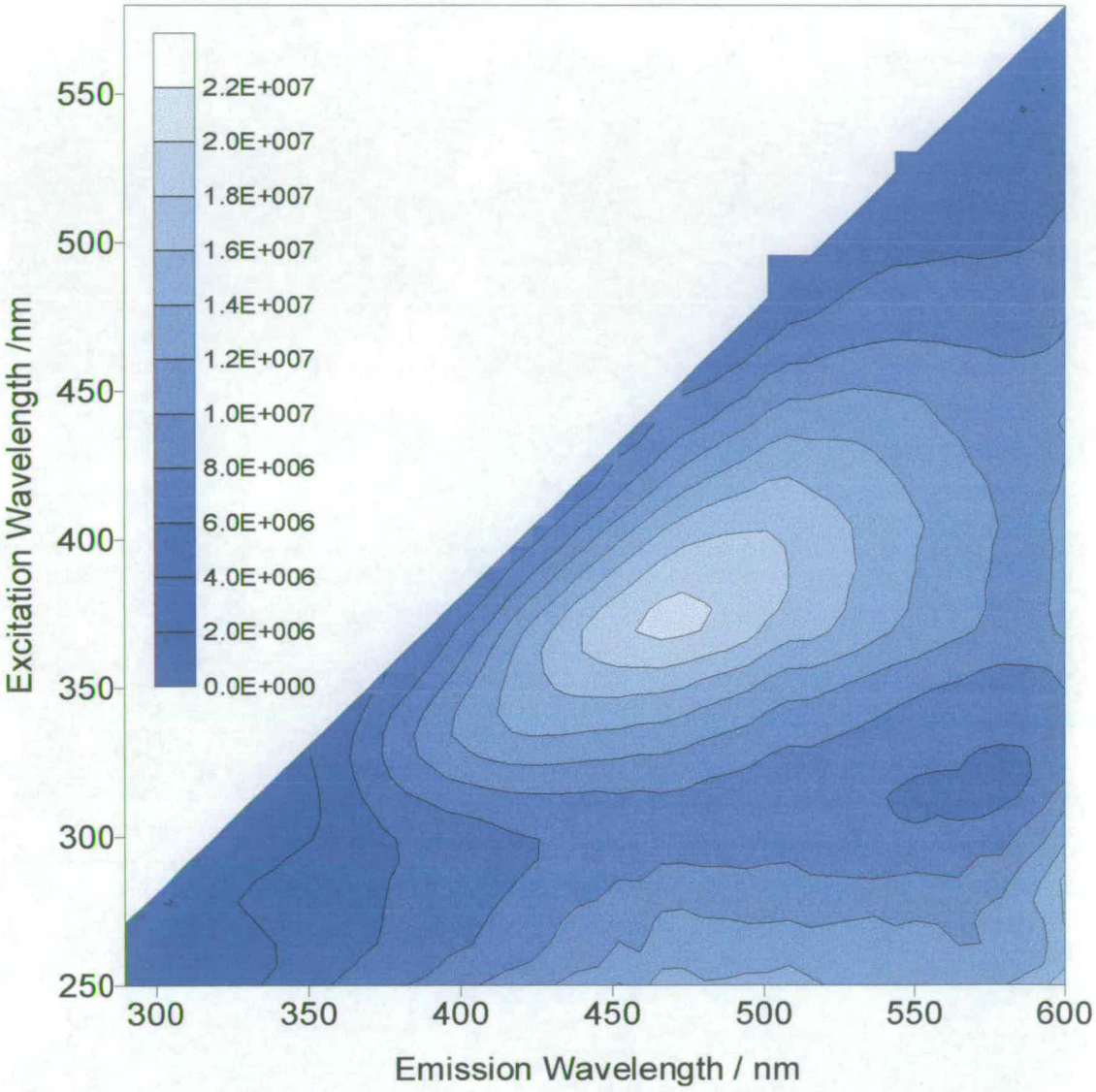

Figure 4.8: An excitation-emission-matrix (EEM) of a dull band of solid coral from Madang Lagoon, Papua New Guinea. The contours are plotted between zero and 2.2 x 10^7 cps at intervals of 2 x 10^6 cps.

4.3.4 Ratio and subtraction EEMs

The ratio EEM (bright band EEM divided by dull band EEM) for a sample of coral from Madang Lagoon Reef, PNG is shown in Figure 4.9:

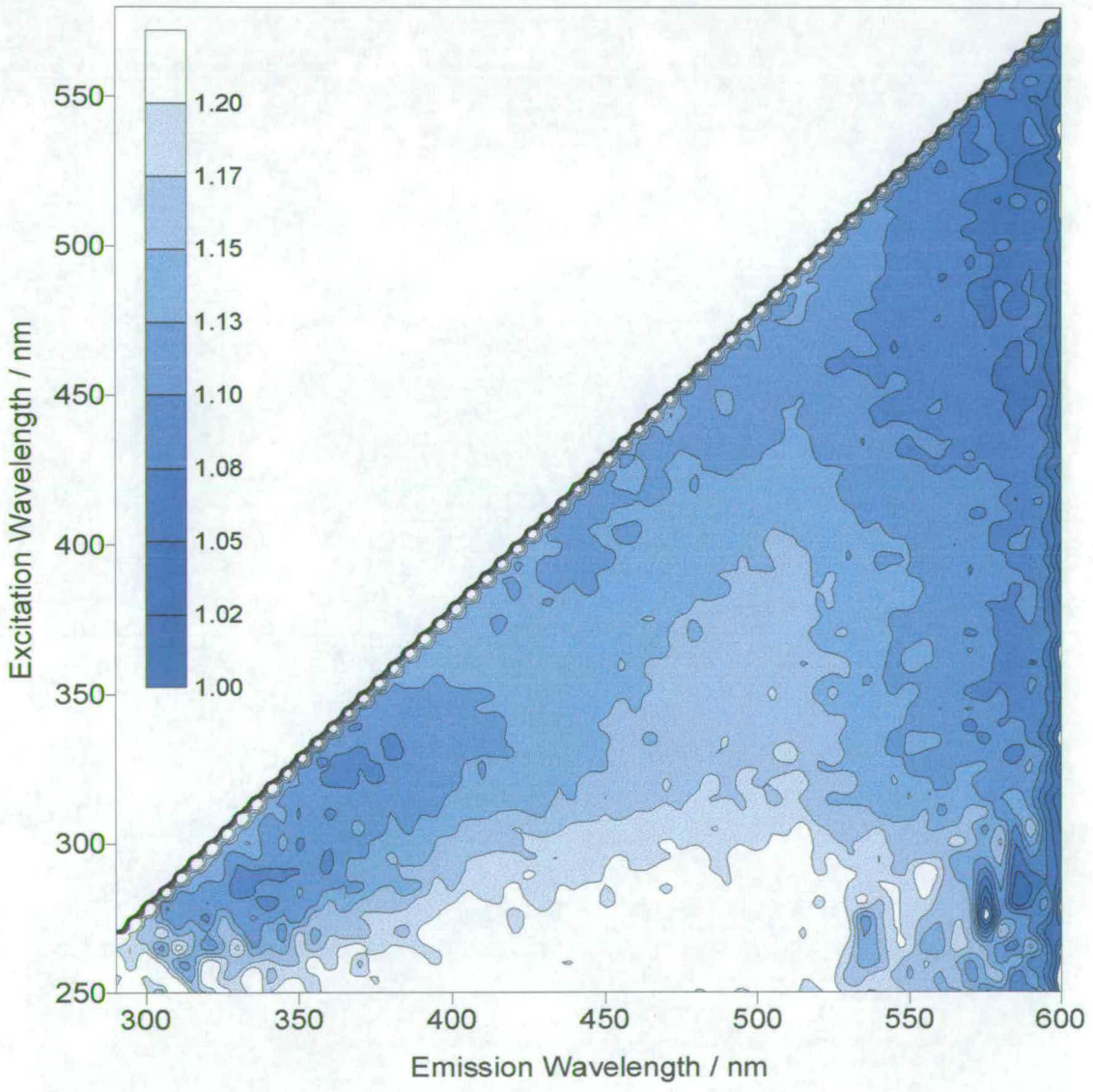

Figure 4.9: Ratio EEM for a sample of coral from Madang Lagoon Reef. The contours are shown from 1.00 to 1.20 at 0.025 unit intervals.

Figure 4.10 shows the subtraction EEM (bright band EEM minus dull band EEM) for a sample of coral from Madang Lagoon Reef, PNG.

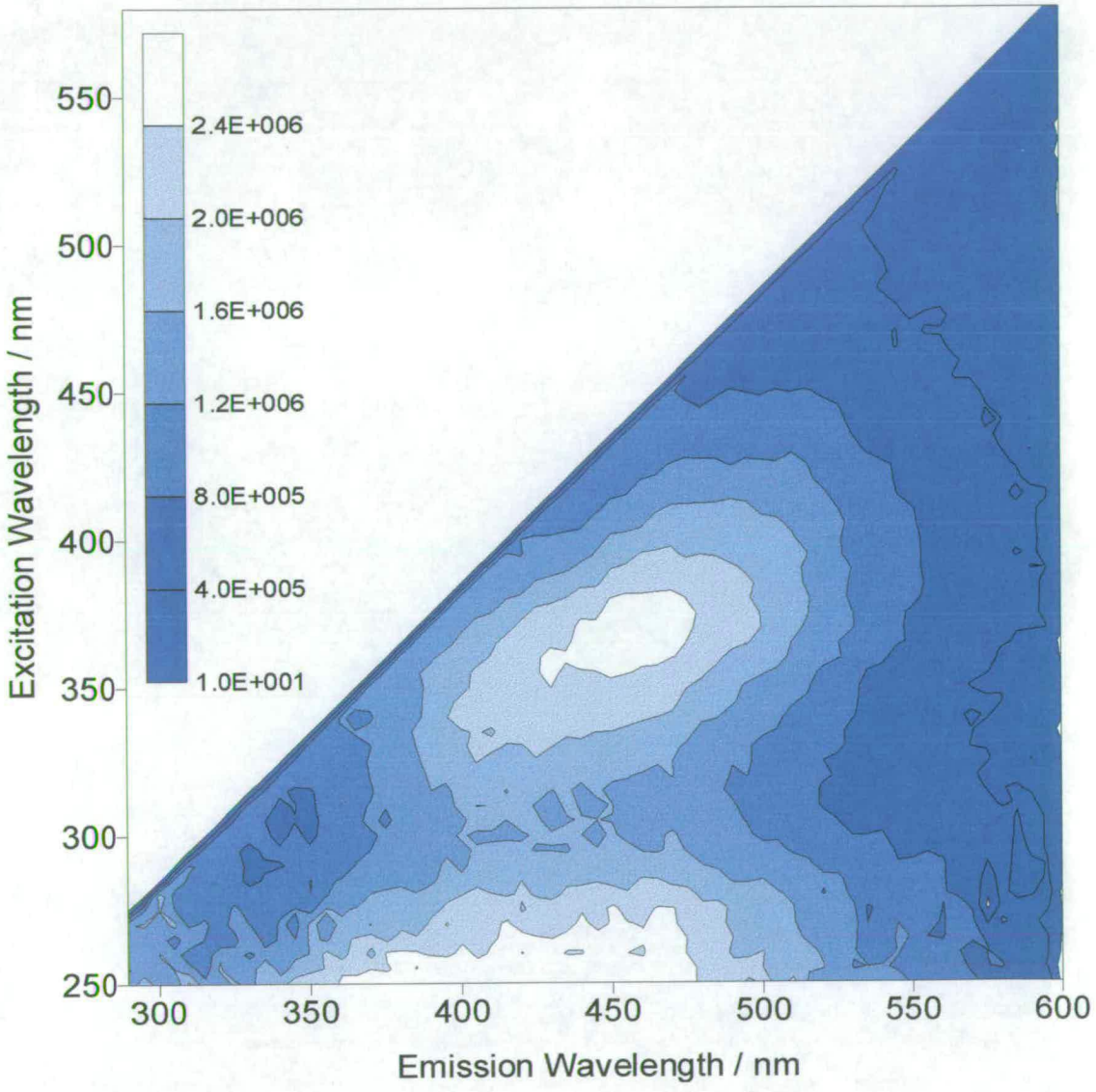

Figure 4.10: A subtraction excitation-emission-matrix (EEM) of solid coral from Madang Lagoon, Papua New Guinea. The contours are plotted between zero and 2.4 x 10^6 cps, at intervals of 4 x 10^5 cps.

The ratio of the bright band intensity to the dull band intensity is positive across the entire wavelength range studied. However, the relative intensity distribution is not uniform. The ratio of bright to dull band intensity varies between 1.00 and 1.20. The relative intensity increases as the excitation wavelength decreases. The ratio is a maximum for emission wavelengths between 400 and 500nm. There is a prominent shoulder at approximately 350/450-500nm. This corresponds to the main peak identified in the bright and dull band luminescence EEMs (Figures 4.7 and 4.8).

The bright band has increased luminescence intensity at all wavelengths within the subtraction matrix in comparison to the dull band i.e. there are no negative regions. The greatest difference in absolute intensity coincides with the main peak in the bright and dull band luminescence EEMs (Figures 4.7 and 4.8). Again, the diagonal peaks at the bottom right of the EEM are due to the subtraction of truncated second order Rayleigh Tyndall scattering peaks.

Both the corals from Laing Island and those from Madang Lagoon are subject to seasonal inundation by terrestrial sources. The luminescence EEMs show similar macroscopic features and are very similar in intensity for the bright and dull bands. However, the ratio and subtraction EEMs are quite different for the two geographical locations. This may be due to the different environmental conditions at Madang Lagoon, where the reefs are exposed to two peak freshwater flows each year, separated by only a few months. Since the two bright bands are very close together, it is difficult to know exactly where the bright bands end and where the central dull band begins. Consequently, without further resolution of the luminescence, it is possible that the ratio and subtraction EEMs presented here are not optimised to give an accurate comparison between the characteristics of the bright and dull bands.

4.4 EEMs of corals from Wadi Ayn, Oman

4.4.1 Introduction

Reefs in the Wadi Ayn region of the Gulf of Oman are considered to be free from terrestrial input from the surrounding landmass. There is so little precipitation in this region that there is little or no coastal run-off. Consequently, these reefs are subject to different environmental conditions from those found at Laing Island and Madang Lagoon Reefs, PNG. Under ultraviolet illumination, the banding pattern is quite indistinct, with diffuse bright and dull bands of similar width. The bright and dull bands are more difficult to distinguish than those seen in samples from Laing and Madang, although the bright bands appear slightly more yellow/green and the dull bands slightly more blue/purple.

4.4.2 Bright Band EEMs

The EEM for a bright band of Oman coral is shown in Figure 4.11. The bright band EEM shows broad and asymmetric features indicating the presence of numerous emitting components. Using Gaussian curve fitting, the component peaks were determined and are listed in Table 4-3:

Excitation Wavelength / nm	280	340	365	395	420	450
Emission Wavelength / nm	470-600	470	475	500	515	540

Table 4-3: Excitation/emission peak positions estimated by Gaussian curve fitting for bright band regions of coral samples from Wadi Ayn, Oman.

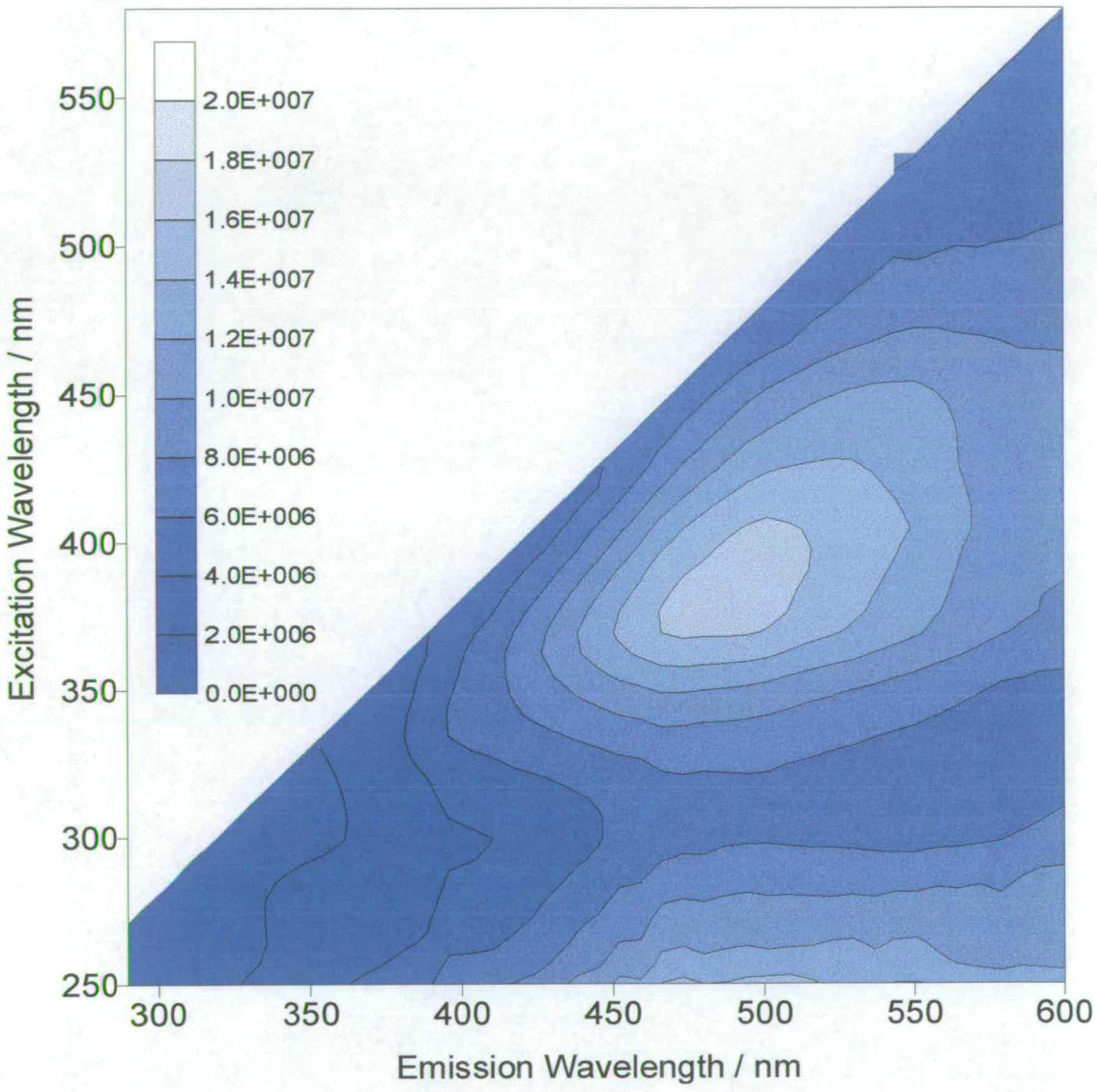

Figure 4.11: An EEM of a bright band of solid coral from Wadi Ayn, Oman. The contours are plotted between zero and 2.x 10^7 cps, at intervals of 2 x 10^6 cps.

These peaks correspond to the peaks identified in the Laing Island and Madang Lagoon samples, suggesting that the component luminophores are similar in all the samples studied. The excitation peaks show less variability between samples than the emission peaks. Again, this highlights the importance of energy transfer processes and the contribution of phosphorescence to the luminescence characteristics of solid coral from a variety of locations. Since the coral samples from Oman are not prone to inundation by terrestrial organic run-off, it seems unlikely that the component luminophores giving rise to the banding pattern can be terrestrially-derived. Consequently, they must come from some other source. As all samples from the three geographical locations show similar components, these must be found in both marine and terrestrial dissolved organic matter.

4.4.3 Dull Band EEMs

The adjacent dull band EEM is shown in Figure 4.12. This EEM has the same macroscopic features as the bright band EEM and the same composite peaks.

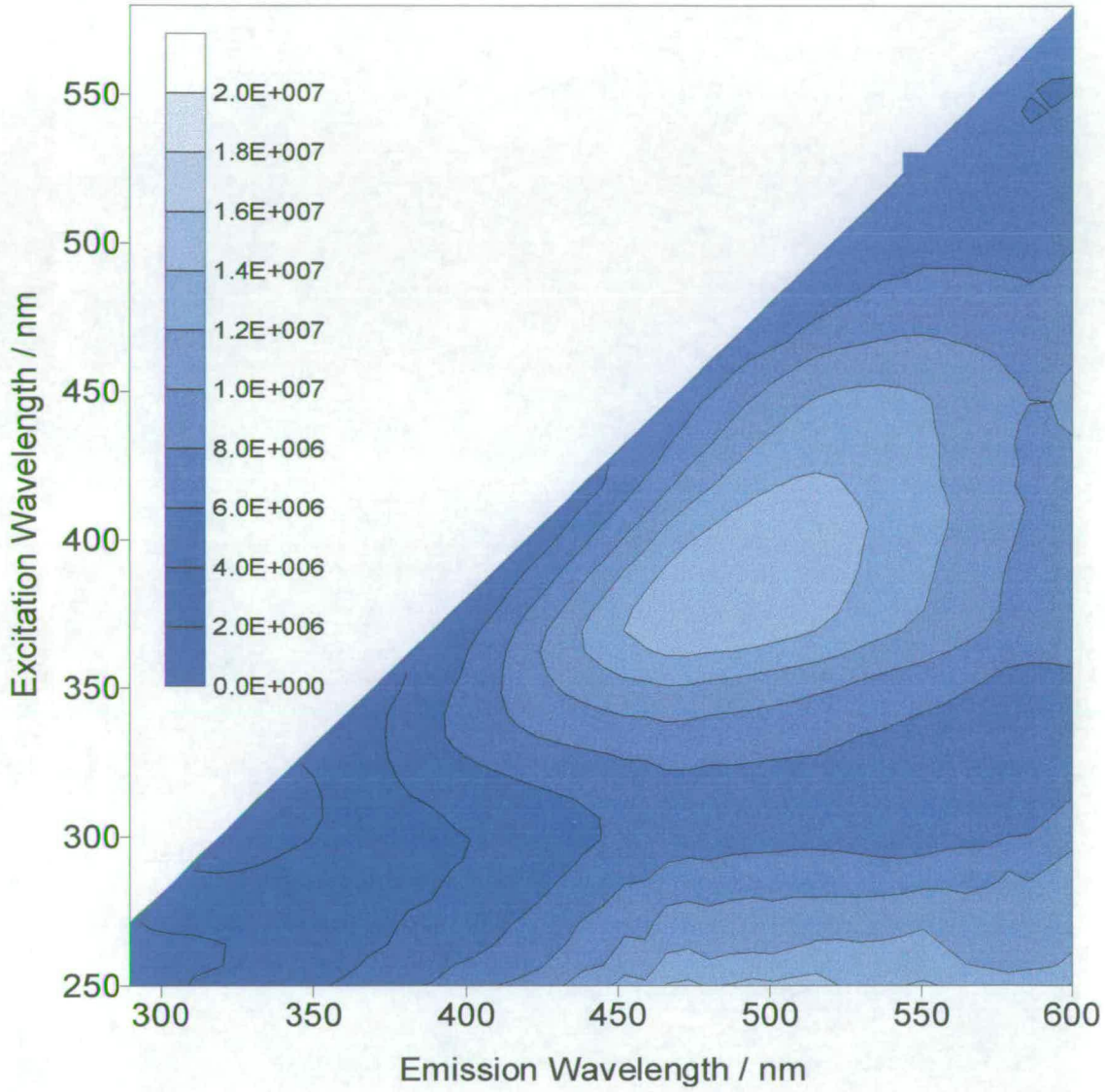

Figure 4.12: An excitation-emission-matrix (EEM) of a dull band of solid coral from Wadi Ayn, Oman. The contours are plotted between zero and 2.0 x 10^7 cps at intervals of 2 x 10^6 cps.

4.4.4 Ratio and subtraction EEMs

The ratio EEM for a sample for coral from Wadi Ayn is shown in Figure 4.13.

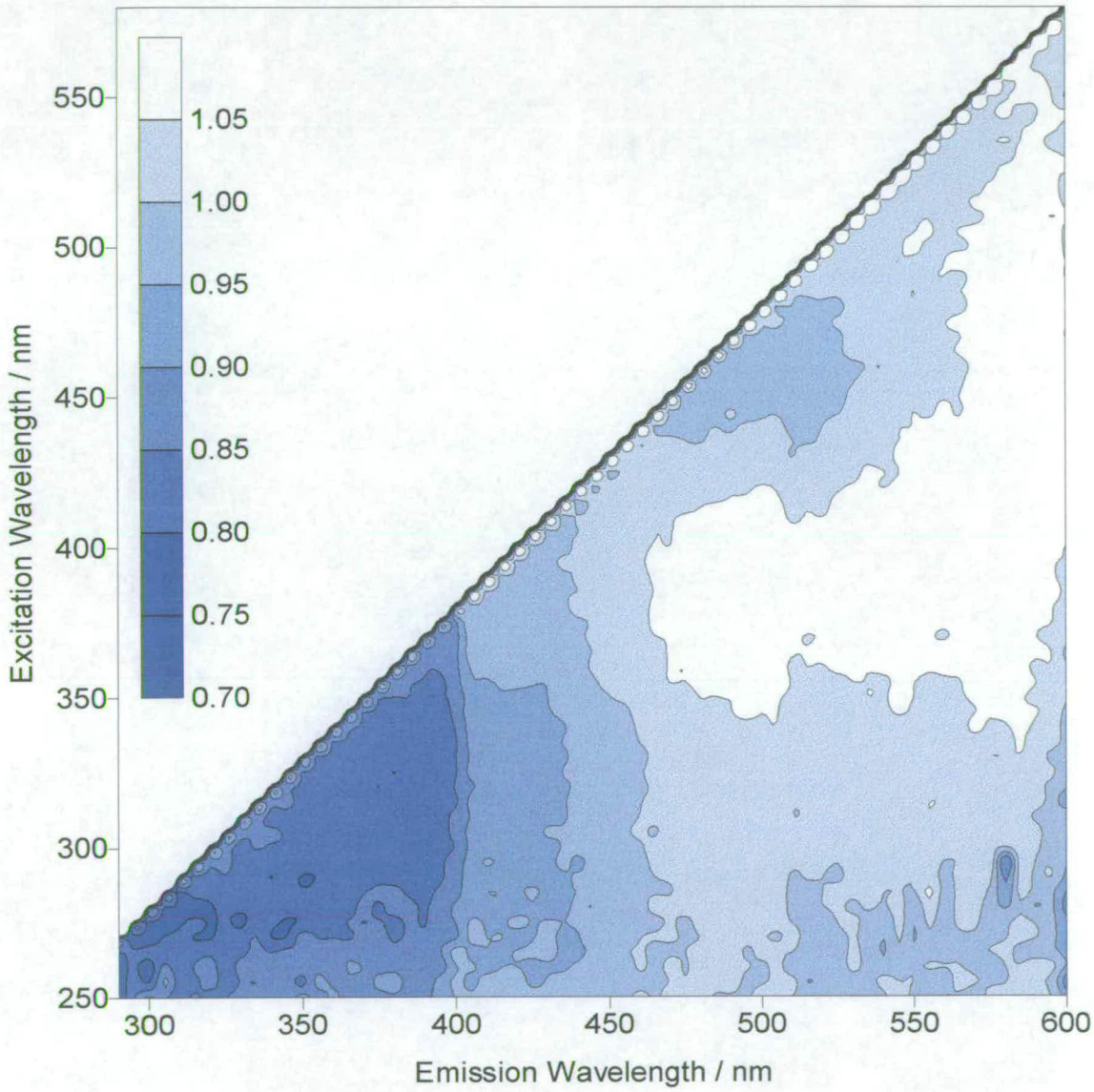

Figure 4.13: Ratio EEM of a sample of coral from Wadi Ayn, Oman. The contours are plotted between 0.7 and 1.10 at 0.05 unit intervals.

The subtraction EEM for a sample of coral from Wadi Ayn, Oman is shown in Figure 4.14.

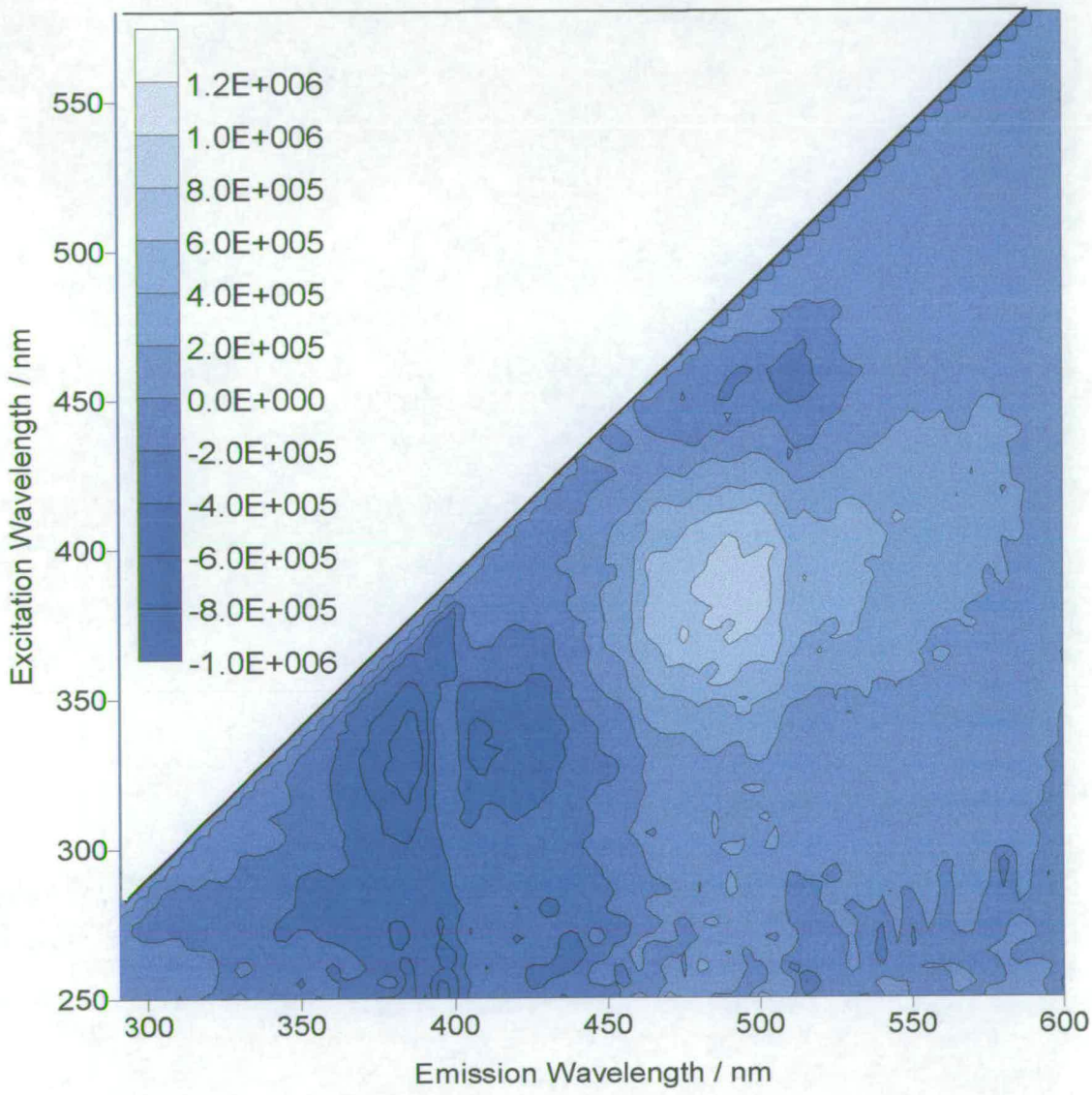

Figure 4.14: A subtraction EEM of bright and dull band samples from Wadi Ayn, Oman. The contours are plotted between -1×10^6 and 1.2×10^6 cps at intervals of 2×10^5 cps.

The ratio EEM shows the relative intensity distribution across the entire wavelength range. The bright band is relatively more intense at emission wavelengths greater than 450nm, with a maximum relative intensity (greater than 5% more intense than the adjacent dull band) at excitation wavelengths between 350 and 450nm. In contrast, the dull band is relatively more intense at shorter emission wavelengths. Below 350/400nm, the dull band is approximately 20% more intense than the neighbouring bright band. It is interesting to note that the maximum relative intensity difference between the bright and dull band of the sample of coral from Oman is approximately 5%, whereas that for Laing is 15% and for Madang, 20%. This corresponds with the observation that, visually, the bright and dull bands are much less easy to distinguish in the samples of coral from Oman.

In the subtraction EEM, the bright band has increased absolute intensity emission at wavelengths greater than 450nm and a maximum intensity difference at an excitation wavelength of 400nm. This peak extends out to longer emission wavelengths and broadens out at an emission wavelength of 600nm to longer excitation wavelengths. This may correspond to increased concentrations of luminophores at longer wavelengths (lower energy), increased electronic energy transfer or increased phosphorescence contribution in the bright bands. The dull band is more intense at shorter excitation and emission wavelengths. The minimum intensity in the subtraction EEM corresponds to excitation/emission wavelengths of 300-350/360-450nm. This corresponds to the region of luminescence emission attributed to protein-type luminophores. Hence, this suggests that there is a relative increase in the intensity or concentration of these protein-type species within the dull bands.

4.5 Conclusions

Using the technique of 3D excitation-emission-matrix spectroscopy, it is possible to reproducibly record the luminescence of solid coral directly from the surface of the skeleton, without the need for extraction of the component luminophores. The EEMs show that the luminescence is due to emission from many component species. The component peaks have been estimated using Gaussian curve-fitting. The same six peaks are evident in all bright and dull bands from the same samples, and in all samples from varying geographical locations. This suggests that the same component luminophores are present in all the samples studied. Since the samples from Oman are not subject to terrestrial inundation, it appears that the banding pattern cannot be attributed solely to the incorporation of terrestrial organics into the coral skeleton.

The estimated peaks can be grouped into two types of species: protein-type luminophores and humic-type luminophores. The protein-type luminophores are identified at short excitation and emission wavelengths (around 280/450nm), characteristic of the presence of tryptophan. Tryptophan has peak emission intensity at 280/350nm, but the longer emission wavelength observed in these studies can be attributed to electronic energy transfer from high energy emitting tryptophan to lower energy absorbing and emitting humic-type species. The humic-type species are identified at longer excitation and emission wavelengths: 340/430-470, 370/470, 390/485-500, 420/505-515 and 450/530-540. It is likely that this method of peak analysis underestimates the total number of component species, since the emission spectra of numerous species may overlap and cannot be individually resolved.

Ratio and subtraction EEMs allow us to spectroscopically analyse the differences between bright and dull band emission. The EEMs of bright and adjacent dull bands have similar macroscopic features, suggesting that they have similar component luminophores. However, the relative bright and dull band intensities are not uniform across the wavelength ranges studied here. In samples from Laing Island and Oman,

the dull bands show increased luminescence intensity at short wavelengths, characteristic of protein-type luminophores. Since the presence of tryptophan is characteristic of marine-derived organics, this would suggest that the laying down of the dull bands coincides with periods when the coral is exposed to marine organic matter. The bright bands show increased luminescence intensity at longer wavelengths, characteristic of humic-type luminophores. This could be due to various factors: an increased concentration of humic-type luminophores in the bright bands, increased electronic energy transfer to lower energy species, increased low energy phosphorescence emission or a combination of these effects. Chapter Six studies the contribution of phosphorescence to the banding pattern in more detail. Since the samples from Oman and Laing Island show such similarities in the ratio and subtraction EEMs, it implies that both are subject to similar conditions that affect the appearance of the banding pattern. It therefore seems unlikely that the concentration of terrestrial run-off is the major controlling factor in the laying down of the bright and dull bands. Samples from Madang are more difficult to interpret since the corals are subject to two annual inundations of freshwater and the bright bands are difficult to resolve. Hence the EEMs obtained may not be an accurate reflection of the banding pattern. This could be overcome by spatially resolving the emission using optical fibre probes.

There are some important limitations to consider when using this approach to study the luminescent banding *in situ*. When making comparisons of luminescence of bright and dull bands, it is essential to compare bands that are spatially and temporally close. The background signal is not constant but varies along the length of the coral core, and must be taken into account before any quantitative comparisons can be made. Within the sample chamber, it is difficult to carry out comparative, quantitative measurements between bright and dull bands as we cannot ensure reproducible excitation/collection geometry in moving the sample. Also, it is difficult to locate the excitation beam precisely at the maximum intensity of a bright band and the minimum intensity of a dull band. Consequently, further investigations into the

luminescence characteristics of bright and dull bands were carried out using an optical fibre probe.

4.6 Bibliography

Coble, P.G., Schultz, C.A., and Mopper, K., 1993. Fluorescence contouring analysis of DOC intercalibration experiment samples - a comparison of techniques. Marine Chemistry, 41: pp. 173-178.

Matthews, B.J.H., Jones, A.C., Theodorou, N.K., and Tudhope, A.W., 1996. Excitation-Emission-Matrix Fluorescence Spectroscopy Applied to Humic Acid Bands in Coral Reefs. Marine Chemistry, 55: pp. 317-332.

Poryvkina, L.V., Babichenko, S.M. and Lapimaa, J.J., 1992. Spectral variability of humus substance in marine ecosystems. Ambio, 21: pp. 465-467.

Strambini, G.B. and Gonnelli, M., 1995. Tryptophan phosphorescence in fluid solution. Journal of the American Chemical Society, 117: pp. 7646-7651.

Tudhope, A.W., Shimmield, G.B., Chilcott, C.P., Jebb, M., Fallick, A.E., and Dalgleish, A.N., 1995. Recent changes in climate in the far western equatorial Pacific and their relationship to the Southern Oscillation; oxygen isotope records from massive corals, Papua New Guinea. Earth and Planetary Science Letters, 136: pp. 575-590.

4.7 Appendix

This appendix contains further subtraction EEMs corresponding to the samples discussed in the chapter. The subtraction EEMs consist of a matrix of synchronous scans. A synchronous scan is recorded with the excitation and emission monochromators fixed at a particular wavelength interval, or offset. This is shown on the x axis. The y axis shows the excitation wavelength. At any particular point on the matrix, the emission wavelength corresponds to the excitation wavelength plus the offset.

Figure 4.15 shows the synchronous subtraction EEM for another pair of bright and dull bands from a sample of coral from Laing Island, Papua New Guinea (PNG). The maximum intensity difference between the bright and dull bands is found at 450nm excitation, and an offset of 50-100nm. This corresponds to an emission wavelength of 500-550nm. The subtraction scan shown in the chapter (Figure 4.6) shows the maximum intensity difference at 450/450-550nm. The minimum intensity difference is found at 350nm excitation and an offset of 20-100nm, corresponding to emission wavelengths of 370-450nm. Figure 4.6 shows the minimum intensity difference at 350/370-450nm.

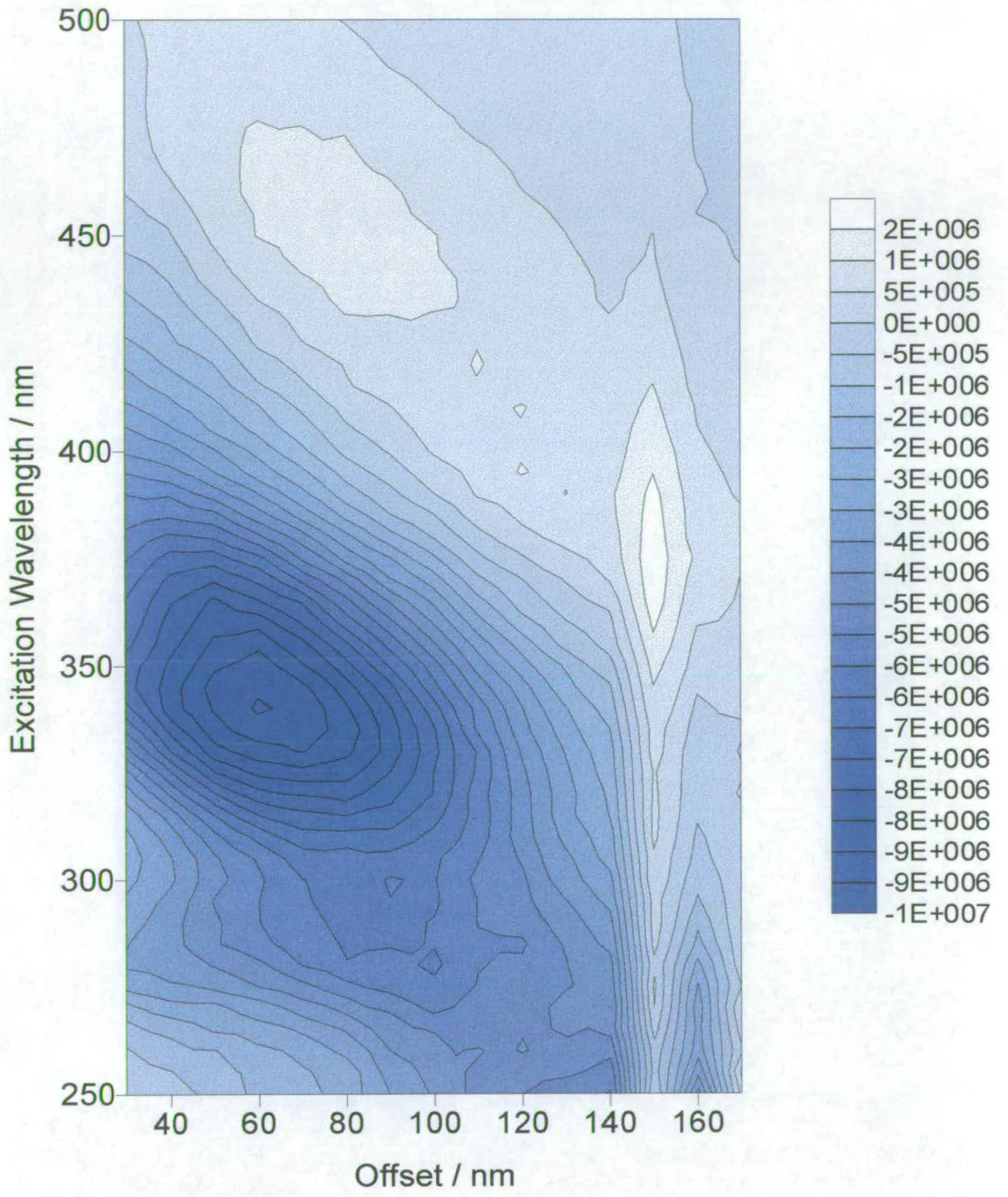

Figure 4.15: Synchronous subtraction scan of a pair of adjacent bright and dull bands of a sample of coral from Laing Island, PNG. The contours are plotted between -1×10^{-7} and 2×10^{6} at 5×10^{5} cps intervals.

Figure 4.16 shows the synchronous subtraction EEM for another pair of bright and dull bands from a sample of coral from Madang Lagoon, Papua New Guinea (PNG). The subtraction scan is positive at all wavelengths, implying that the bright band is more intense than the adjacent dull band at all wavelength combinations. This feature was also observed in the previous subtraction EEM (shown in the chapter) of another pair of bands from the same geographical location (Figure 4.10). The maximum intensity difference between the bright and dull bands is found at 330-370nm excitation, and an offset of 60-120nm. This corresponds to an emission wavelength of 390-490nm. The previous subtraction scan (Figure 4.10) shows the maximum intensity difference at 340-390/400-500nm. The minimum intensity difference is found at 300nm excitation and an offset of 40-80nm, corresponding to emission wavelengths of 340-380nm. Figure 4.10 shows the minimum intensity difference at 300/320-360nm.

Figure 4.17 shows the synchronous subtraction EEM for another pair of bright and dull bands from a sample of coral from Wadi Ayn, Oman The maximum intensity difference between the bright and dull bands is found at 360-400nm excitation, and an offset of 60-120nm. This corresponds to an emission wavelength of 420-520nm. The subtraction scan shown in the chapter (Figure 4.14) shows the maximum intensity difference at 350-420/450-550nm. The minimum intensity difference is found at 300-350nm excitation and an offset of 40-80nm, corresponding to emission wavelengths of 340-430nm. Figure 4.14 shows the minimum intensity difference at 300-350/350-430nm.

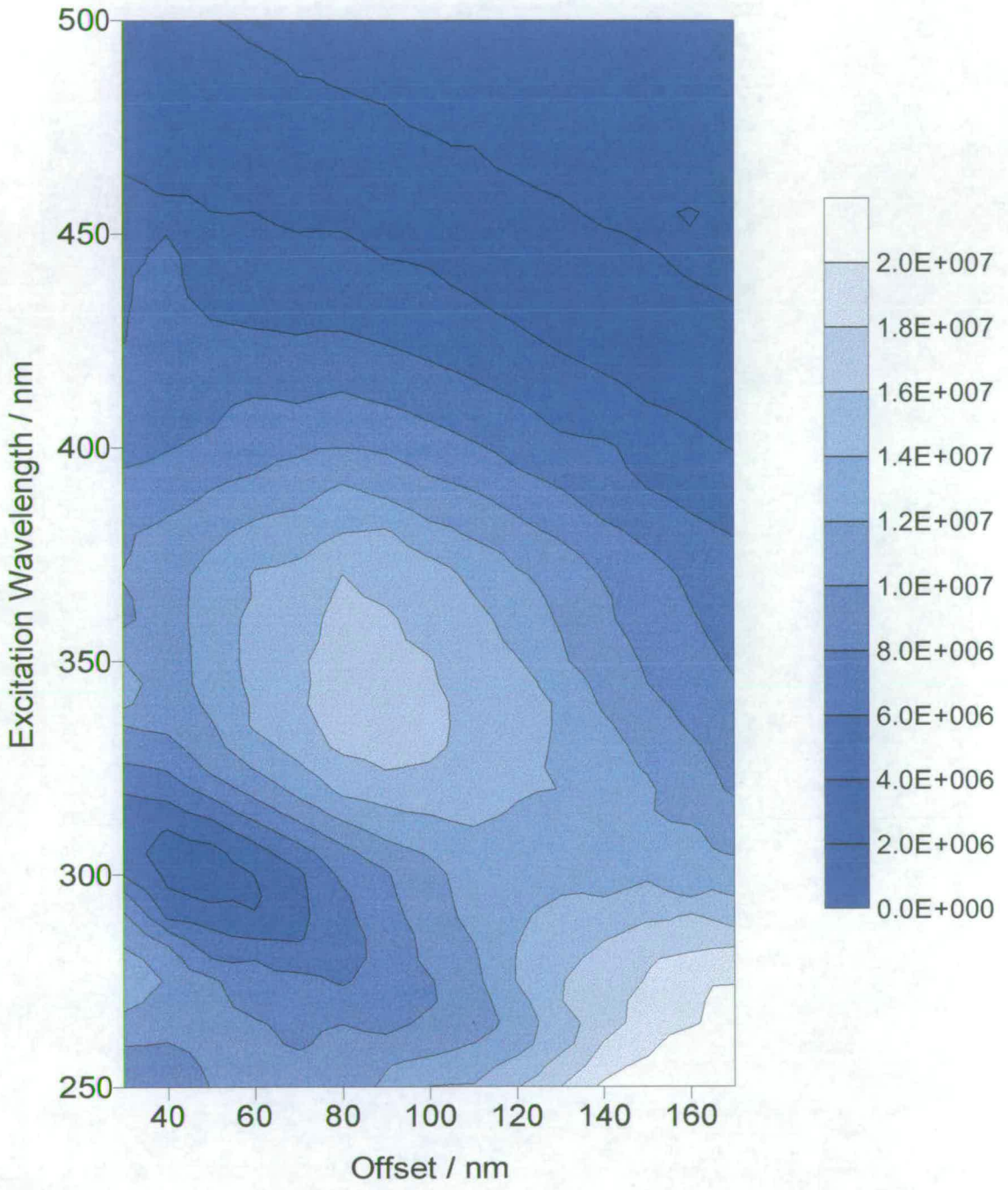

Figure 4.16: Synchronous subtraction scan of a pair of adjacent bright and dull bands of a sample of coral from Madang Lagoon, Papua New Guinea. The contours are plotted between zero and 2 x 10^7 at 2 x 10^6 cps intervals.

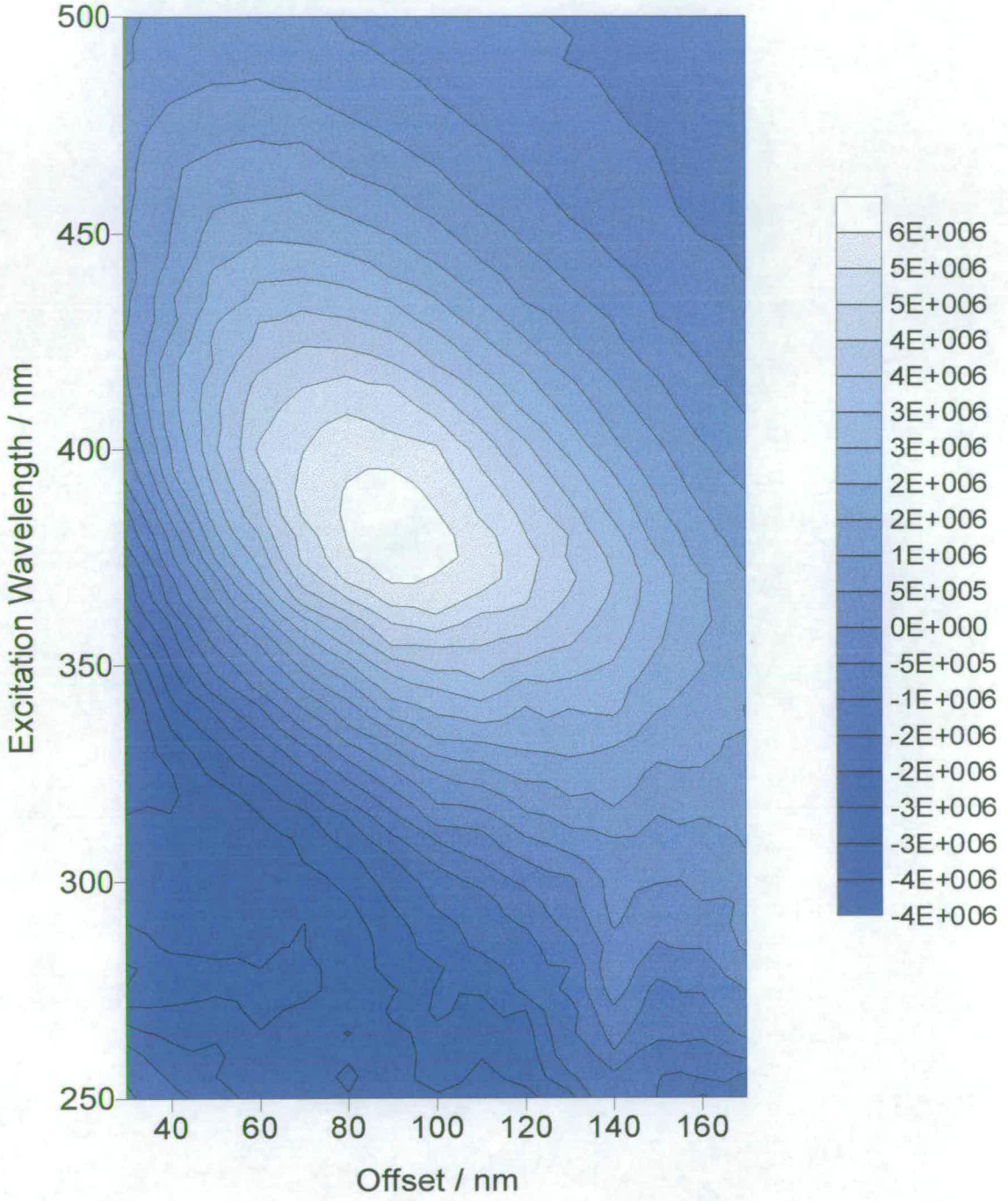

Figure 4.17: Synchronous subtraction scan of a pair of adjacent bright and dull bands of a sample of coral from Wadi Ayn, Oman. The contours are plotted between 4 x 10^{-6} and 6 x 10^{6} at 5 x 10^{5} cps intervals.

5 Chapter Five: Spatially-resolved Measurements of Luminescence

5.1 Introduction

The luminescence banding pattern of solid coral is clearly visible by eye when the sample is illuminated with uv light at 365nm. The skeleton exhibits regions of "bright" (yellow-green) luminescence and adjacent "dull" (blue) luminescence. It is thought that environmental factors such as seasonal rainfall and salinity control the appearance and characteristics of the banding pattern. Consequently, in order to understand the environmental significance of the bands, it is important to be able to quantify the luminescence intensity variations within the skeleton. The luminescence variations could offer an effective environmental proxy in regions where other records e.g. tree rings, ice cores, are not viable.

Previous work investigating the luminescence variations directly from the coral skeletal surface is limited. In 1984, Isdale correlated regions of bright luminescence in corals from the Great Barrier Reef with periods of increased rainfall and consequent terrestrial inputs to the nearshore zone. However, intensity measurements were cubed to improve the contrast between regions of bright and dull luminescence. Milne and Swart (1994) studied the luminescent banding in coral from the Caribbean using laser-induced fluorescence and a bifurcated optical fibre bundle. They excited the sample at 337nm and detected emission at 460nm. They found it difficult to isolate the "luminescence" signal (bright bands) from the background signal (dull bands) and were unable to resolve the banding pattern into a series of annual bright and dull bands.

In the present investigations, the coral sample was fixed to a precision linear translation stage and stepped incrementally beneath optical fibre bundles interfaced to the fluorescence spectrometer. Initial studies used a mercury lamp as the fixed wavelength (365nm) excitation source. Further studies utilised a fused silica optical fibre bundle to deliver the excitation beam from the fluorescence spectrometer, to give variable wavelength excitation. This method allowed precise positioning of the excitation and emission beams, and ensured reproducible excitation/collection geometry. Details of the experimental set-up are found in the Experimental Section (Chapter Three, Section 3.3.1).

5.2 Variations in Luminescence Intensity with Lateral Position on the Coral Surface

5.2.1 Using a Mercury lamp as the excitation source

Initially, investigations were carried out using a mercury lamp as the excitation source and collecting the emission via a fibre optic bundle, as described in Chapter Three, Section 3.4.1. The mercury lamp has a peak emission at 365nm. The banding pattern is clearly visible by eye when the mercury lamp illuminates the coral skeleton. Using this diffuse excitation source, it was possible to record variations in the luminescence intensity of the coral surface, corresponding to the banding pattern. This approach was used to study coral samples from a variety of geographical locations; Laing Island and Madang Lagoon, Papua New Guinea, and Wadi Ayn, Oman.

5.2.1.1 Laing Island samples

The variations in luminescence intensity with position on the coral surface of a sample from Laing Island, Papua New Guinea, exciting using the mercury lamp

(365nm) and detecting at 600nm are shown in Figure 5.1. The x axis shows the distance travelled along the coral sample, perpendicular to the banding pattern. The y axis shows the intensity of the luminescence emission. The rise and fall in intensity corresponds to bright and dull regions of the skeleton. It can be seen clearly that there are five bright bands in this region of the skeleton, flanked on each side by dull bands. To the eye, the first bright band appears approximately 3mm in width. The full width half maximum (FWHM) of the first peak in Figure 5.1 is 2mm. The second bright band appears wider, and the corresponding peak shows an increased FWHM of 2.5mm. The last three bands are visibly wider and more diffuse. In Figure 5.1, these are seen as broad peaks with a reduced intensity difference between the neighbouring bright and dull bands. The background luminescence varies with lateral position along the skeleton. In order to make meaningful quantitative measurements of the relative luminescence intensity of bands, it is necessary to consider this background variation. The steep drop-off in intensity at the right hand end of the scan corresponds to the edge of the sample.

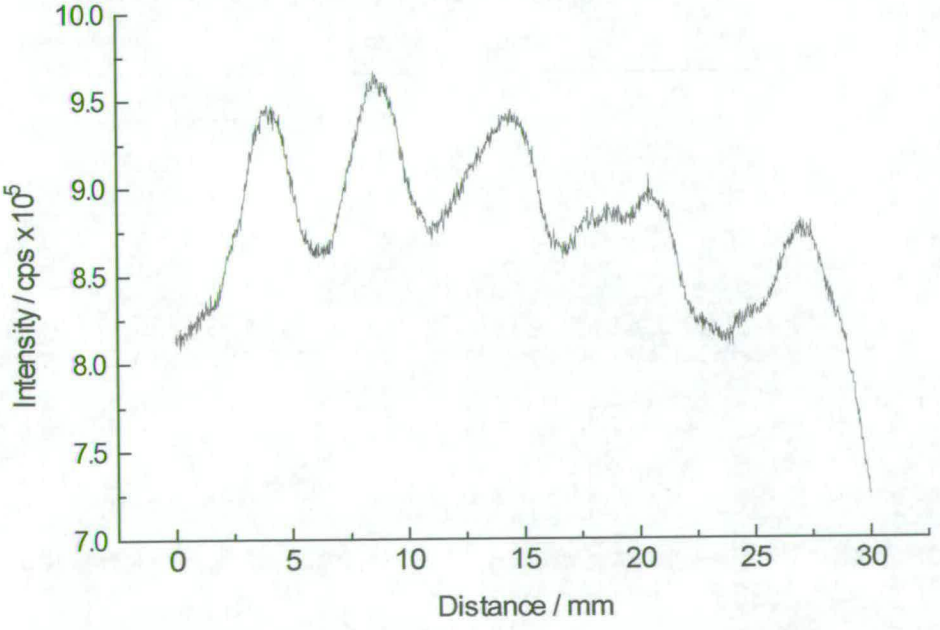

Figure 5.1 The intensity variation across the surface of a sample of solid coral from Laing Island, Papua New Guinea. The scan was recorded perpendicular to the banding pattern at excitation/ emission wavelengths of 365/600nm.

The second and third bright band peaks in Figure 5.1 are shown in more detail in Figure 5.2. At an emission wavelength of 600nm, the left-hand bright band is approximately 10% more intense than the central dull band. Figure 5.3 shows the variation in intensity when the scan is performed in the opposite direction to that in Figure 5.2. The shape and relative intensity of the peaks are identical in both scans, showing that the experimental method is highly reproducible. The same bright band (now appearing second in the scan from left to right) is 10% more intense than the neighbouring dull band. Hence the method produces reproducible intensity measurements of the variation in luminescence emission from the surface of solid coral.

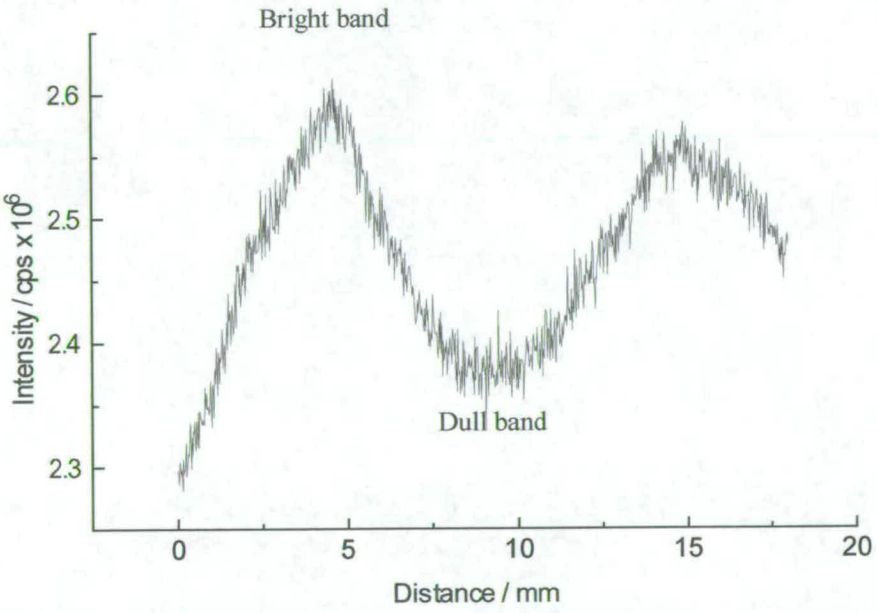

Figure 5.2: The intensity variation across the surface of a sample of coral from Laing Island, Papua New Guinea. The scan was recorded perpendicular to the direction of the banding pattern at excitation/emission wavelengths of 365/600nm.

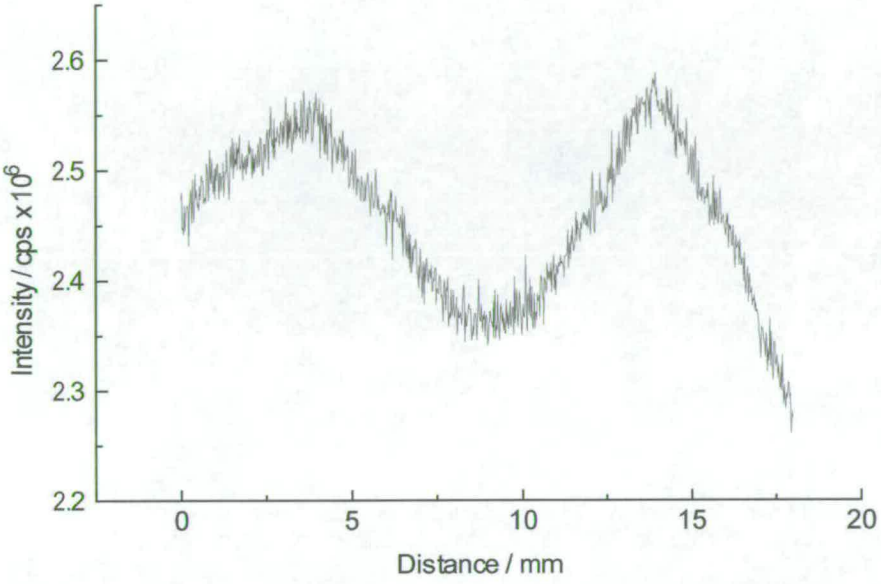

Figure 5.3: Intensity variation recorded by scanning in the opposite direction along the coral axis to Figure 5.2.

The difference in luminescence intensity between bright and dull bands is quantitatively only a few percent. Since the percentage difference between the regions of bright and dull luminescence is small, it is unsurprising that the absolute intensities recorded within the sample chamber were so similar for the dull and bright bands.

The ratio of the bright band intensity to the dull band intensity was a maximum between emission wavelengths of 550 and 650nm. This is consistent with earlier findings (Chapter Four, Figure 4.5) which showed the maximum bright band relative intensity around 550nm at this excitation wavelength (365nm). There is a smooth trend in the dependence of the ratio of bright:dull band intensity on the emission wavelength. This is illustrated in Figure 5.4.

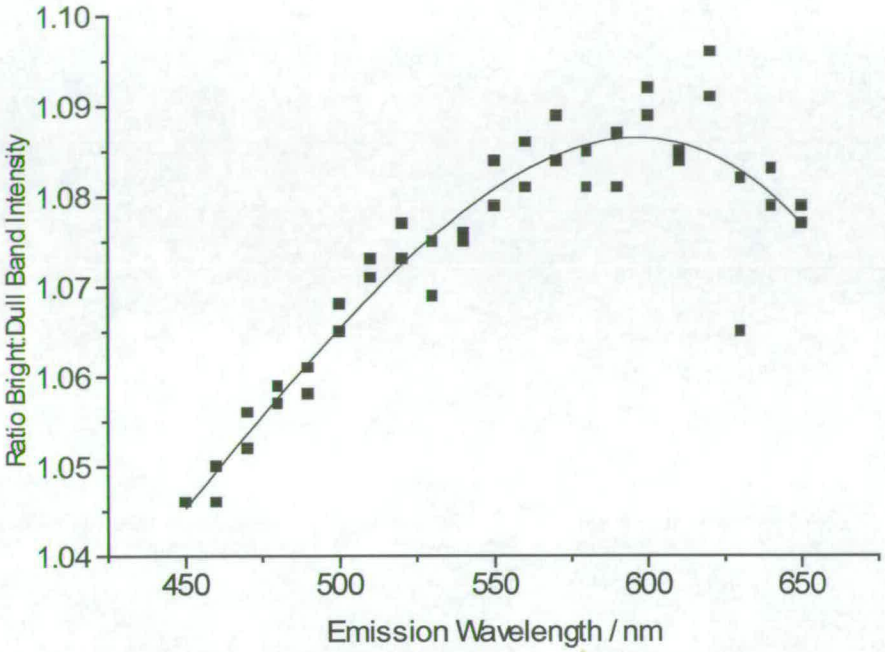

Figure 5.4: Ratio of bright:dull band luminescence intensity for a sample of coral from Laing Island, Papua New Guinea when excited at 365nm.

As the emission wavelength increases, the ratio of the bright:dull band intensity increases to a maximum at around 600nm. The ratio starts to decrease at longer wavelengths. Between 620 and 650nm, there is an increased error in the ratio since the absolute intensity is greatly reduced. The ratio EEM calculated from luminescence EEMs recorded within the sample chamber (Chapter Four, Figure 4.5) shows a reduced bright:dull intensity ratio in comparison with the ratio calculated here. For example, at 365/550nm, the ratio is between 1 and 1.05, whereas Figure 5.4 suggests that the ratio is 1.08. This can be attributed to the experimental technique of mounting the sample in the sample chamber. It is difficult to accurately position the excitation beam on a bright or dull band by eye, and hence this may lead to an underestimate of the bright: dull band intensity ratio.

Figure 5.5 shows the variation in the recorded banding pattern with emission wavelength. For all the scans highlighted, the excitation wavelength was fixed at 365nm. The red scan shows the banding with the emission fixed at 450nm, the blue scan shows banding at 500nm, the green scan shows banding at 550nm and the black scan shows the banding pattern at 600nm. The banding pattern does not look the same at all emission wavelengths. With the emission fixed at 450nm, the banding pattern is quite different from that observed at 500, 550 and 600nm, as the two bright band peaks are much less distinct. Emission at 500nm shows better distinction between the peaks, but the clearest representation is seen with the emission fixed at 550 or 600nm. This suggests that at shorter emission wavelengths, there may be increased "background" signal. This causes a relative increase in the dull band intensity, thus reducing the difference between the maximum intensity of the bright band and the minimum intensity of the neighbouring dull band.

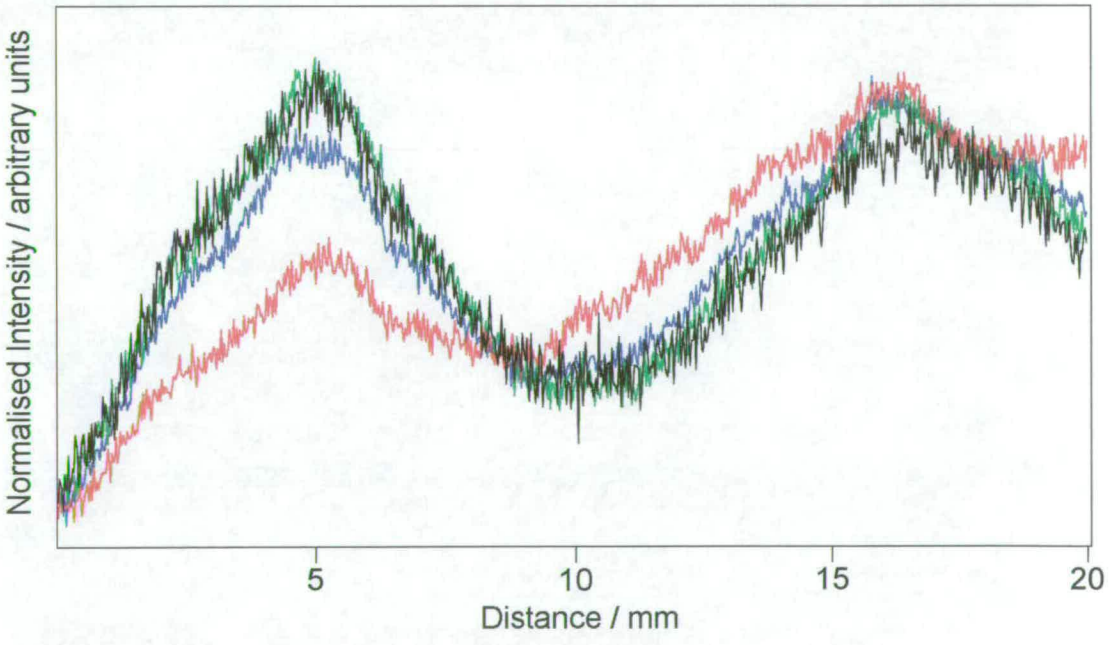

Figure 5.5: The variation in recorded intensity with varying emission wavelength with 365nm excitation. The red scan corresponds to 450nm emission, the blue to 500nm, the green to 550nm and the black to 600nm. The intensity has been normalised for clarity.

5.2.1.2 Madang Lagoon samples

The variations in luminescence intensity with lateral position on the coral surface for a sample of coral from Madang Lagoon, PNG, exciting at 365nm and detecting emission at 600nm are shown in Figure 5.6. The banding pattern is much less distinct than that seen in the samples of coral from Laing Island. To the eye, the bands appear broader and have less distinct boundaries between regions of bright and dull luminescence. The first bright band can be resolved into two component peaks and is 6% more intense than the neighbouring dull band (to the left of the bright band in Figure 5.6) at 600nm emission.

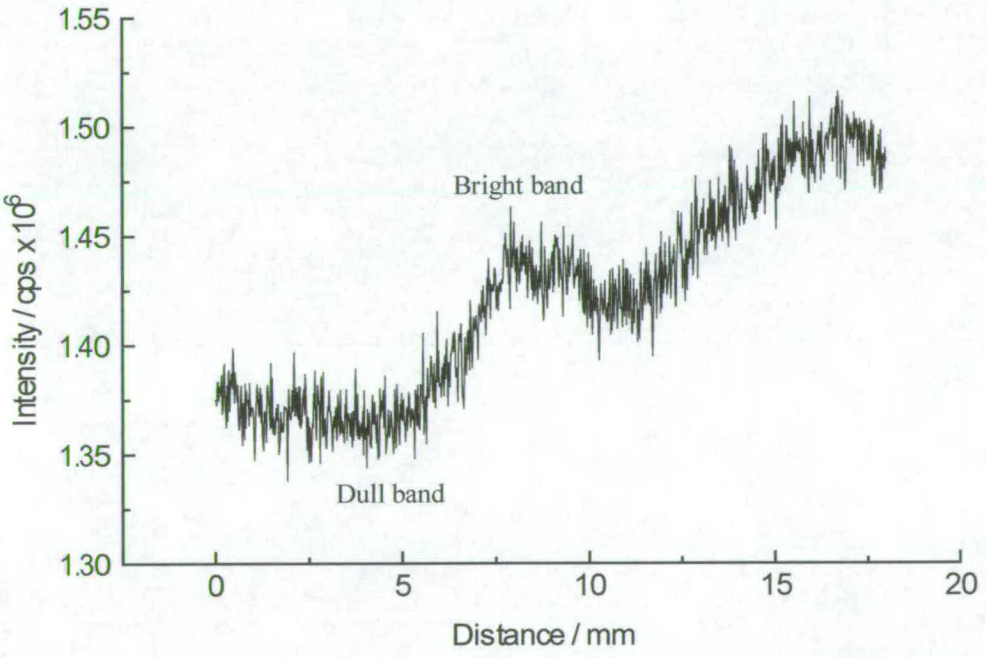

Figure 5.6: Variation in intensity of luminescence with lateral position for a sample of coral from Madang Lagoon, PNG, recorded at 365nm excitation and 600nm emission

The dependence of the ratio of the bright:dull band intensity on emission wavelength is shown in Figure 5.7.

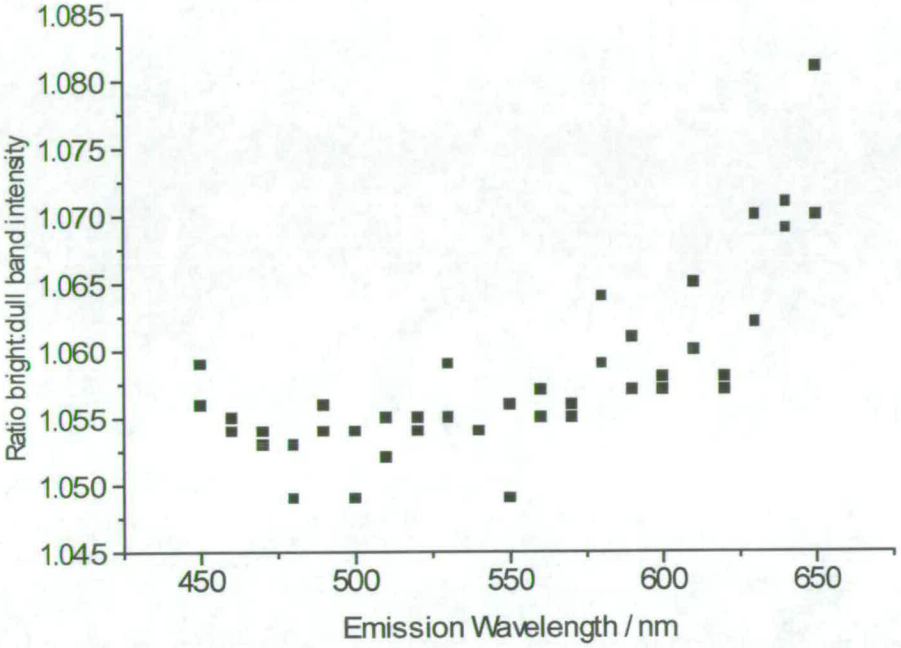

Figure 5.7: Ratio of bright:dull band luminescence intensity versus emission wavelength for samples of coral from Madang Lagoon, PNG. The sample was excited at 365nm.

The wavelength-dependence of the ratio of the intensities of the bright to dull bands is much less marked than that for the samples of coral from Laing Island, PNG. The ratio increases slightly with emission wavelength. Between 620 and 650nm, the absolute intensities are greatly reduced, so the error in the ratio is increased.

This result suggests that in the bright bands, the emission from the component luminophores is more intense across the whole wavelength range. The corresponding ratio EEM (Chapter Four, Figure 4.9) shows an increased intensity across the whole emission wavelength range (450 – 600nm), with no particular regions of localised difference between bright and dull bands.

5.2.1.3 Oman samples

The variation in intensity with lateral position on a sample of coral from Wadi Ayn, Oman, is shown in Figure 5.8. The bright and dull bands are very diffuse in these samples, and are often hard to visually distinguish. Hence, it is often difficult to judge where one band ends and another begins.

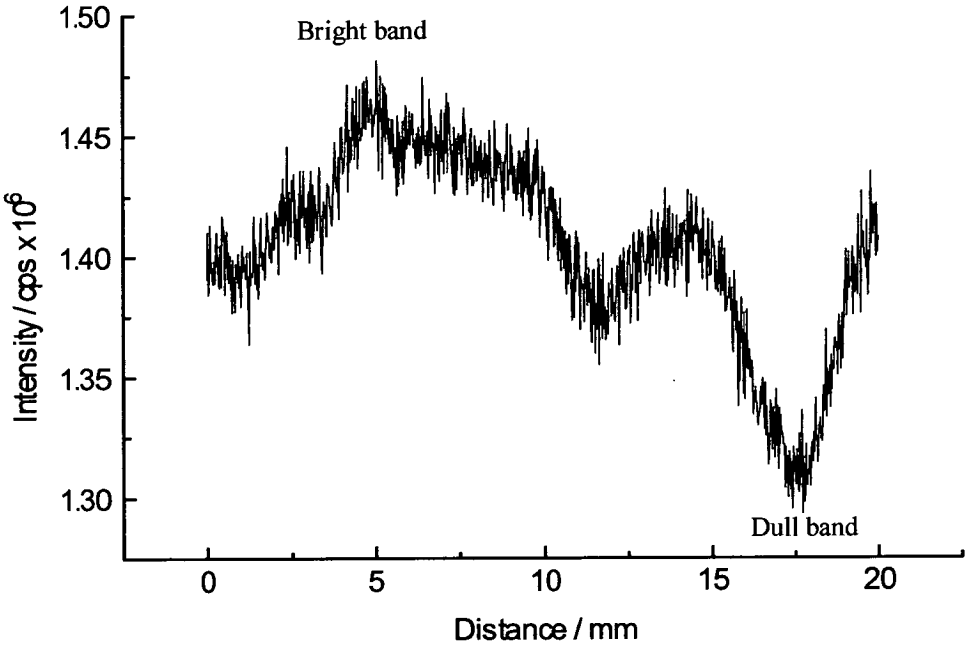

Figure 5.8: Variation in luminescence intensity with lateral position for sample of coral from Oman, exciting at 365nm and recording emission at 600nm.

At 600nm emission, the bright band was 12% more intense than the dull band. The bright:dull band intensity ratio shows a clear trend with emission wavelength. The variation in intensity difference between bright and dull bands as a function of wavelength is shown in Figure 5.9.

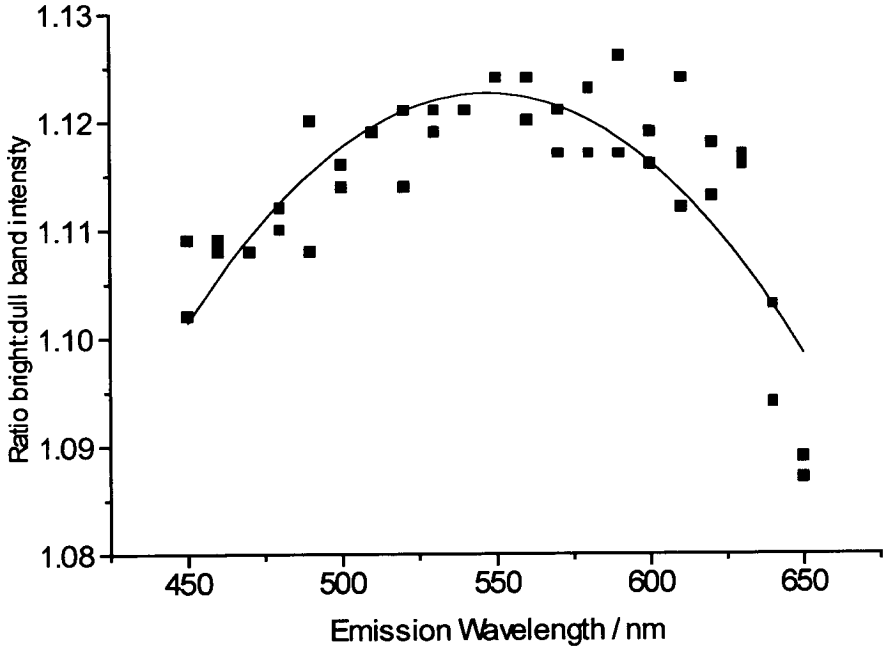

Figure 5.9: Ratio of bright:dull band luminescence intensity as a function of emission wavelength for a sample of coral from Oman. The sample was excited at 365nm.

As the emission wavelength increases so the ratio of bright:dull band luminescence intensity increases. The maximum intensity ratio corresponds to an emission wavelength of around 550nm. Beyond this wavelength, the ratio starts to decrease. The corresponding ratio EEM (Chapter Four, Figure 4.13) shows a maximum bright:dull intensity ratio between 500 and 550nm at this excitation wavelength (365nm).

5.2.2 The luminescence banding pattern in samples from different geographical locations

Samples from Laing Island, PNG show a distinct series of bright and dull bands when viewed under uv light at 365nm. When scanning across the length of a sample, the banding pattern can be reproducibly recorded. The relative width of the bands is consistent with the observed banding pattern under uv light. The samples are subject to annual inundation by freshwater laden with humic material.

Samples from Madang Island, PNG are subject to two annual inundations by freshwater, and as such are expected to show two bright bands and two dull bands annually. Resolving these sets of bands is difficult by eye, and tends to give the appearance of smeared regions of bright or dull luminescence. Scanning across the surface allows resolution of the broad and indistinct peaks into component peaks. This suggests that this technique can be used to resolve sub-annual variations in environmental conditions.

Samples from Oman have broad and diffuse bright and dull bands observable under uv light, and are not subject to any terrestrial organic input throughout the year. Scanning along the length of the coral core shows the broad banding pattern.

5.2.3 Trends in intensity variation with lateral position on the coral surface

For all samples studied, it was possible to record an intensity variation with lateral position on the coral surface without the need for manipulation of data.

The "background" luminescence (or luminescence of the dull regions of the skeleton) is not constant and varies with lateral position on the coral skeleton. Hence, there can

be no effective quantitative comparison of intensity between dull and bright bands unless this variation is considered. The background variation is least for neighbouring bright and dull bands. Consequently, the best quantitative comparisons can be drawn between adjacent bands.

The ratio of the bright:dull band intensities varies depending on the sample studied and the bright and dull points considered. However, the trend with emission wavelength is consistent for all samples from a similar geographical location. The bright:dull band intensity ratio of luminescence is dependent on emission wavelength. Corals from Laing Island show the greatest emission wavelength dependence of the samples studied, with a maximum difference between the intensity of luminescence of the bright and dull bands between 550 and 650nm emission. At 600nm, the bright band:dull band intensity ratio is 1.085. The corresponding ratio EEM (Chapter Four, Figure 4.5) shows a reduction in bright:dull band intensity. At 365/600nm, the ratio is less than 1.0. However, the wavelength-dependent trend of the ratio is consistent in both approaches.

Samples from Madang Island show little relationship between the ratio of the bright:dull band intensity and the emission wavelength. Between 450nm and 600nm, the ratio is approximately 1.055. The corresponding ratio EEM (Chapter Four, Figure 4.9) shows an increased bright:dull band intensity. At 365/450-600nm, the ratio is between 1.15 and 1.08. The ratio shows a gradual decrease as the emission wavelength increases between 450 and 600nm.

Samples from Oman show a maximum emission intensity difference between 500 and 600nm. At 550nm, the bright:dull band intensity ratio is 1.125. This ratio is high in comparison to the samples that are subject to terrestrial inundation. This suggests that the differences in luminescence intensity between the dull and bright bands seen in coral skeletons may be due to some factor other than the incorporation of humic acids into the skeleton as a result of terrestrial run-off. The corresponding ratio EEM

(Chapter Four, Figure 4.13) shows a decreased bright:dull band intensity. At 365/550nm, the ratio is 1.05. The trend in intensity ratio is consistent in both figures (Figures 5.9 and 4.13), with the maximum ratio between 500 and 600nm.

It is likely that the positioning of the excitation beam on the bands, carried out in the sample chamber, is relatively inaccurate in comparison to that using the optical fibre probes. Consequently, the ratio of bright:dull band intensity recorded in this chapter is a more reliable estimate.

Since the samples from Laing Island showed the greatest wavelength-dependence and had clear, distinct banding, these were used for all subsequent spatially-resolved measurements.

5.2.4 Using an excitation optical fibre as the excitation source

Figure 5.10 shows the intensity variation with lateral position recorded using an excitation optical fibre bundle as the method of beam delivery to the surface of a sample of coral from Laing Island (Chapter Three, Figure 3.4). This is the same sample as shown in Figure 5.1, but the variations in intensity with lateral position are recorded across a different section of the sample. The sample is excited at 365nm and the emission recorded at 500nm. There are clearly four bright bands identified with neighbouring dull bands. The overall intensity of the luminescence is reduced compared to that recorded using the mercury lamp. This is due to the decreased beam intensity and area of illumination of the excitation fibre optic in comparison to the mercury lamp. The trace corresponding to a scan in the opposite direction is shown in Figure 5.11. The method has excellent reproducibility.

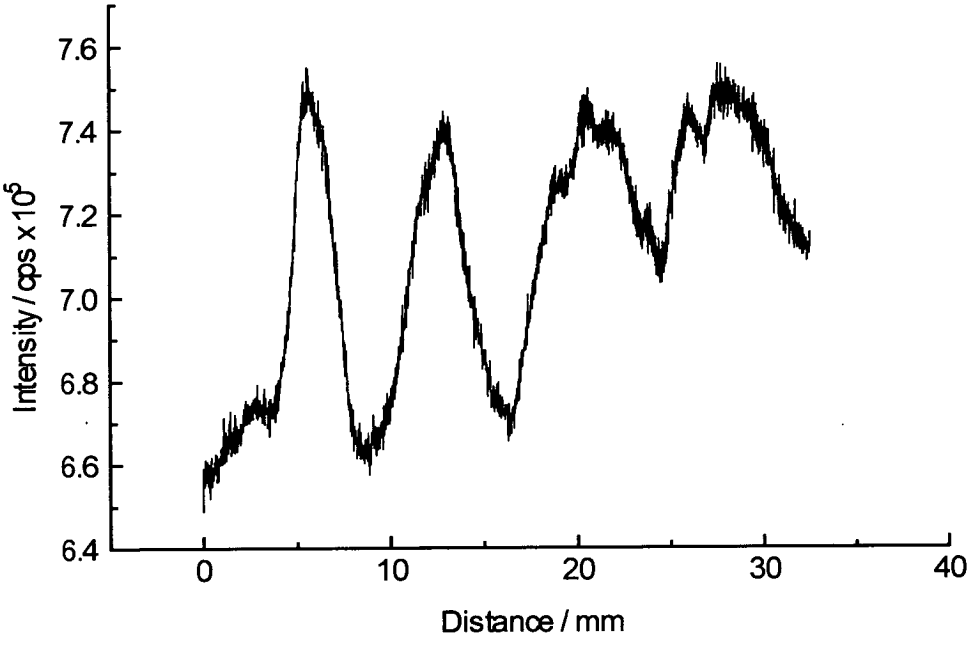

Figure 5.10: Intensity variation with lateral position at 365/500nm for a sample of coral from Laing Island, PNG. The excitation beam was delivered via a fused silica optical fibre bundle.

Within the bright and dull bands, there are reproducible variations in intensity of luminescence. This fine structure could hold a record of other environmental factors affecting the growth of the coral and incorporation of organics into the coral skeleton. In order to study these fine details it would be necessary to increase the spatial resolution of the technique, and compare these fluctuations with data available detailing short-term variations in the environment surrounding the coral mass.

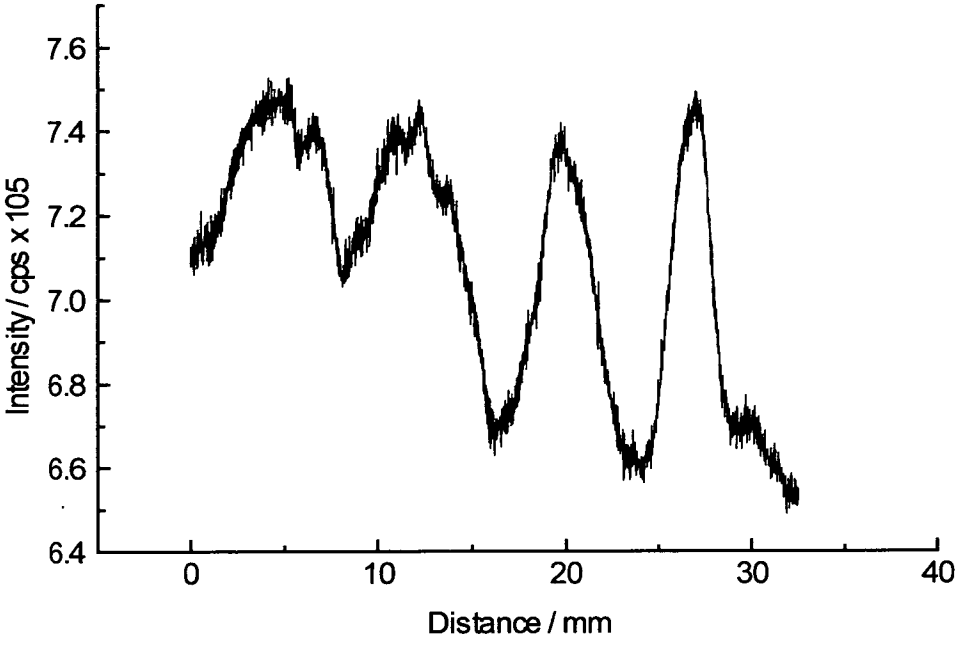

Figure 5.11: Intensity variation with lateral position for the same sample in the opposite direction to that shown in Figure 5.10.

Using the optical fibre bundle as the excitation source allows us to vary the excitation wavelength. By locating the excitation and emission optics at the position of peak intensity of a bright band or the minimum intensity of a dull band, we can ensure clear discrimination between the bright and dull bands. With the excitation and emission optics fixed, an EEM can be constructed.

5.3 Recording EEMs using excitation/emission optical fibre bundles

The variation in luminescence intensity with both excitation and emission wavelength could be studied using the arrangement described in Chapter 3, Section 3.4.2. The use of optical fibre probes and the translation stage allowed precise positioning of the excitation beam before recording the EEM of any particular band.

5.3.1 Bright Band EEMs

The EEM corresponding to the total luminescence of the peak of a bright band of coral from Laing Island, PNG is shown in Figure 5.12. The x axis shows the emission wavelength across the range 420 to 600nm. The minimum emission wavelength was limited to 420nm by the transmittance of the glass optical fibre. The y axis shows the excitation wavelength across the range 280 to 580nm. The excitation fibre is made of fused silica, which can transmit wavelengths down to 250nm.

The EEM shows a broad diagonal peak with several distinct shoulders. This suggests that there are a number of individual luminescing species giving rise to the signal. In comparison to the EEM recorded within the sample chamber of the spectrometer, which has been replotted over the same wavelength range and is shown in Figure 5.13, the EEM has more defined shoulders, particularly at 425/500nm. This peak corresponds to the 420/505 peak identified in curve-fitting the EEM recorded within the sample chamber. This suggests that using optical fibres for beam delivery and collection gives a more accurate and detailed representation of the luminescence of the system.

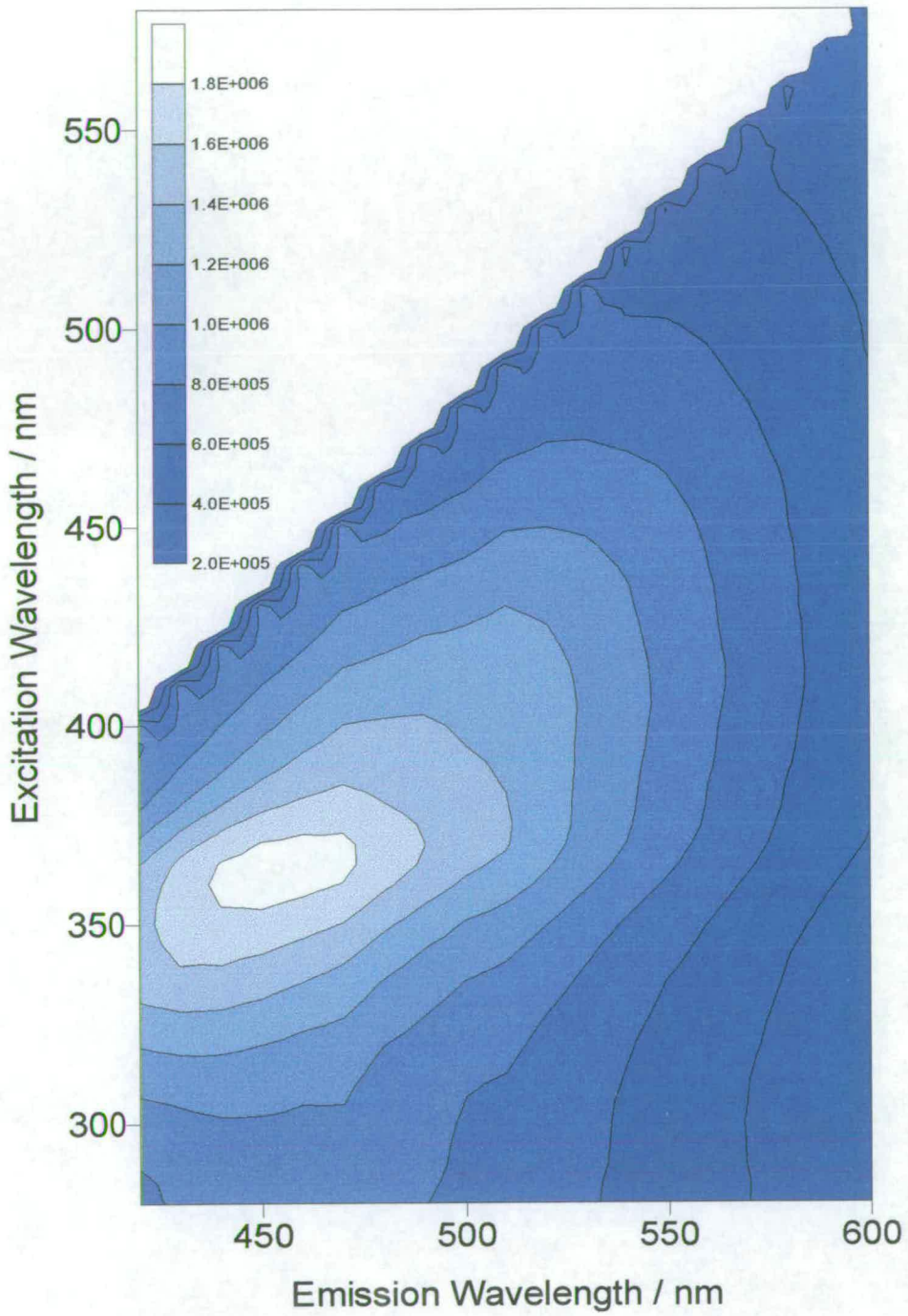

Figure 5.12: EEM of a bright band of solid coral from Laing Island, Papua New Guinea. The EEM was recorded using optical fibre bundles to deliver excitation and emission radiation. The contours are plotted between 2 x 10^5 and 1.8 x 10^6 cps, at intervals of 2 x 10^5 cps.

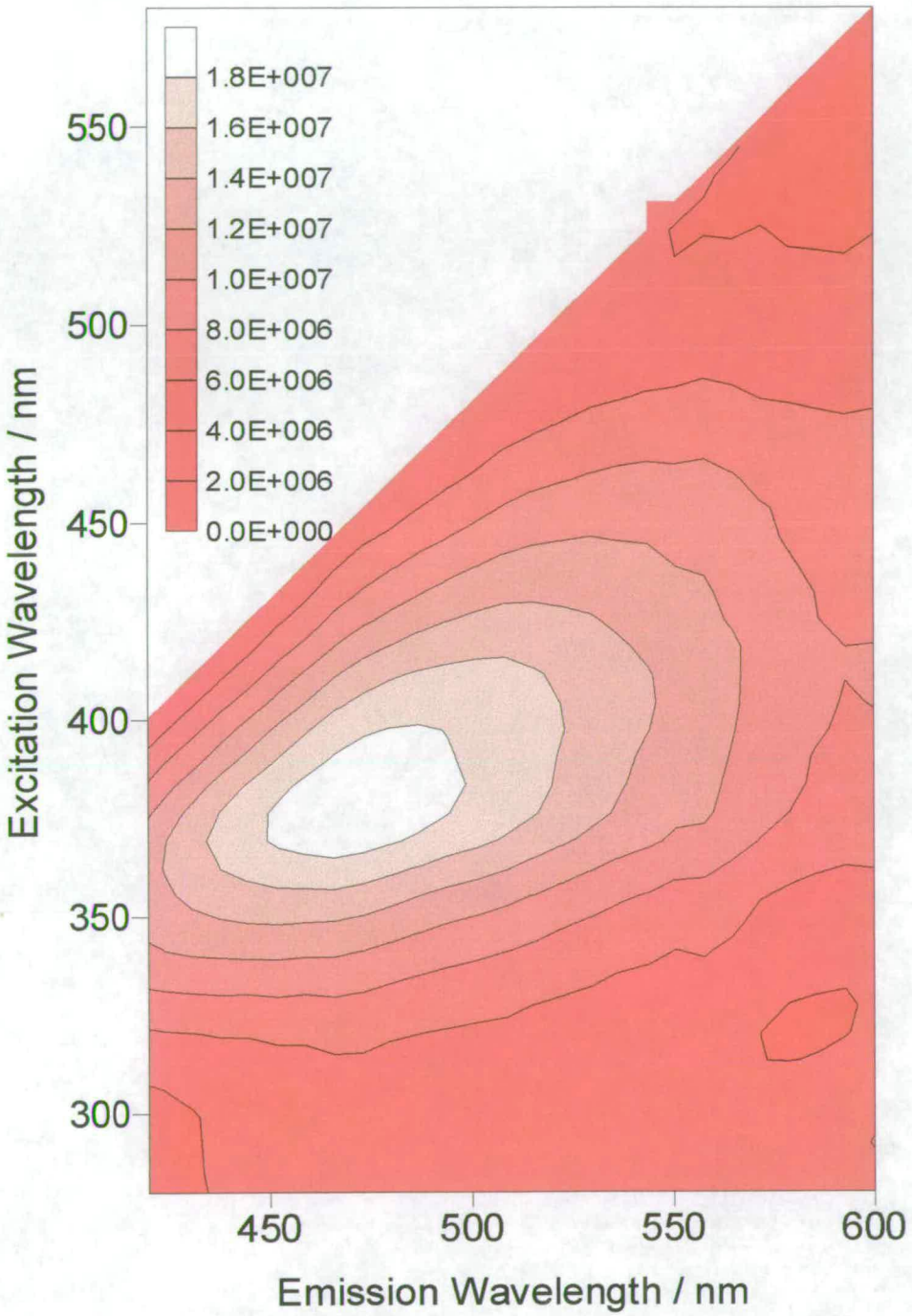

Figure 5.13: EEM of a bright band of solid coral from Laing Island, PNG, recorded in the sample chamber of the fluorimeter (as Chapter Four, Figure 4.1) shown over the same wavelength range as Figure 5.12. The contours are plotted between zero and 1.8×10^7 at 2×10^6 unit intervals.

The luminescence shows peak intensity at excitation/emission wavelengths 370/470nm. This corresponds to the peak intensity identified in the EEM recorded within the sample chamber of the spectrometer. In comparison with the EEM recorded within the sample chamber, the overall intensity of the recorded peak luminescence is reduced by a factor of 10, from 1.8×10^7 to 1.8×10^6 cps. This would be expected since the efficiency of the excitation and detection systems is reduced by the use of the fibre optic assembly.

The EEM of the bright band was reproducible for several positions on the same sample of coral and for other samples from Laing Island, PNG.

5.3.2 Dull Band EEMs

The EEM recorded at the minimum intensity of the adjacent dull band of coral from Laing Island, PNG, is shown in Figure 5.14.

The dull band EEM shows a reduction in intensity across the entire wavelength range in comparison with the adjacent bright band, which corresponds with the observed appearance of the banding pattern. The peak intensity is reduced from 1.8×10^6 to 1.6×10^6 cps. The dull band EEM recorded within the sample chamber, which has been replotted over the same wavelength range and is shown in Figure 5.15, has a comparable intensity to the adjacent bright band. This suggests that using the optical fibres for beam delivery and collection provides a more accurate description of the relative intensities of the dull and bright bands.

The peak intensity corresponds to the same excitation and emission wavelength combination as the bright band EEM at 370/470nm, and the EEM has the same macroscopic features. To compare the relative intensities of the dull and bright bands, the ratio EEM was constructed.

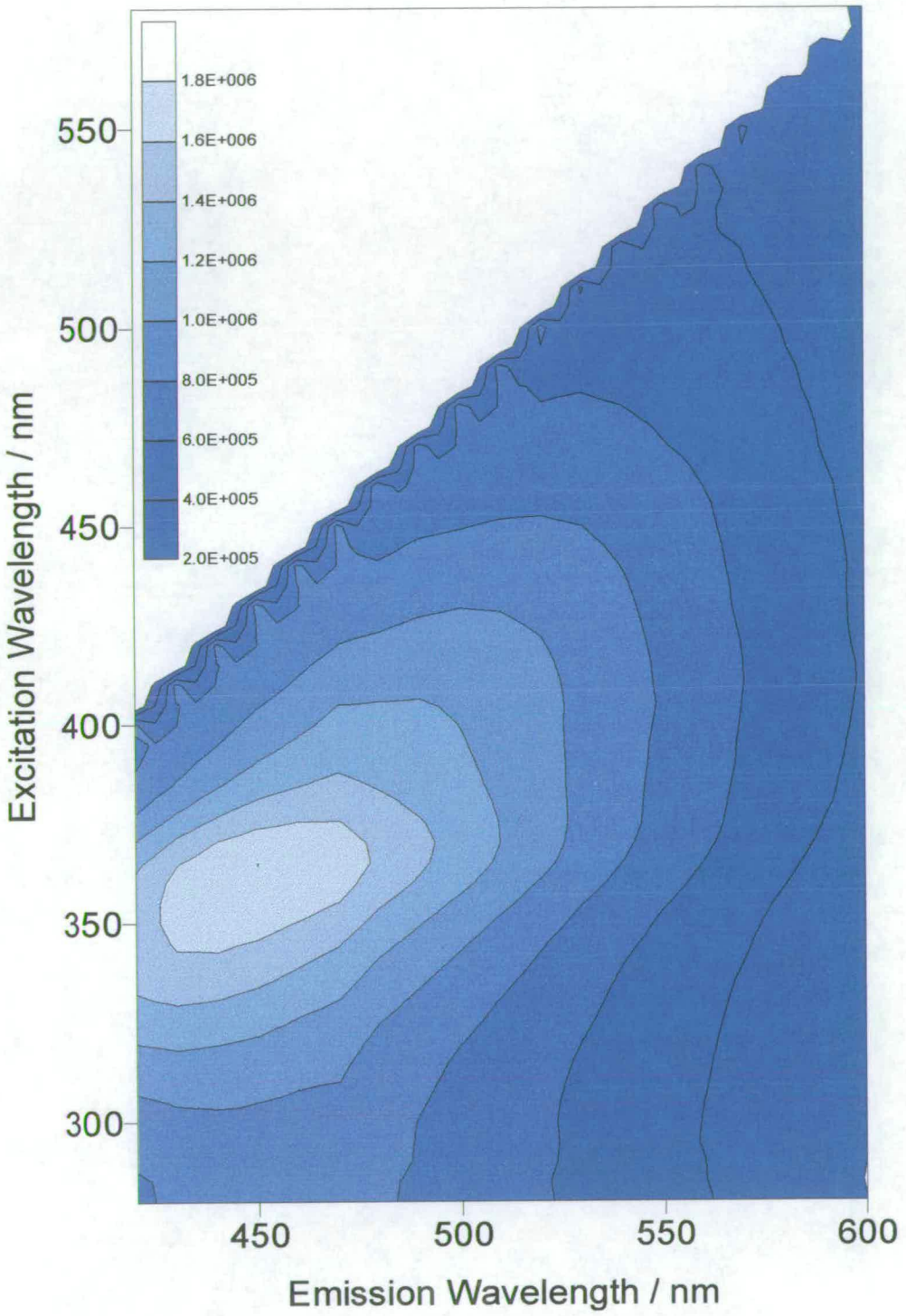

Figure 5.14: EEM of a dull band of solid coral from Laing Island, Papua New Guinea. The EEM was recorded using optical fibre bundles to deliver excitation and emission radiation. The contours are plotted between 2 x 10^5 and 1.8 x 10^6 cps, at intervals of 2 x 10^5 cps.

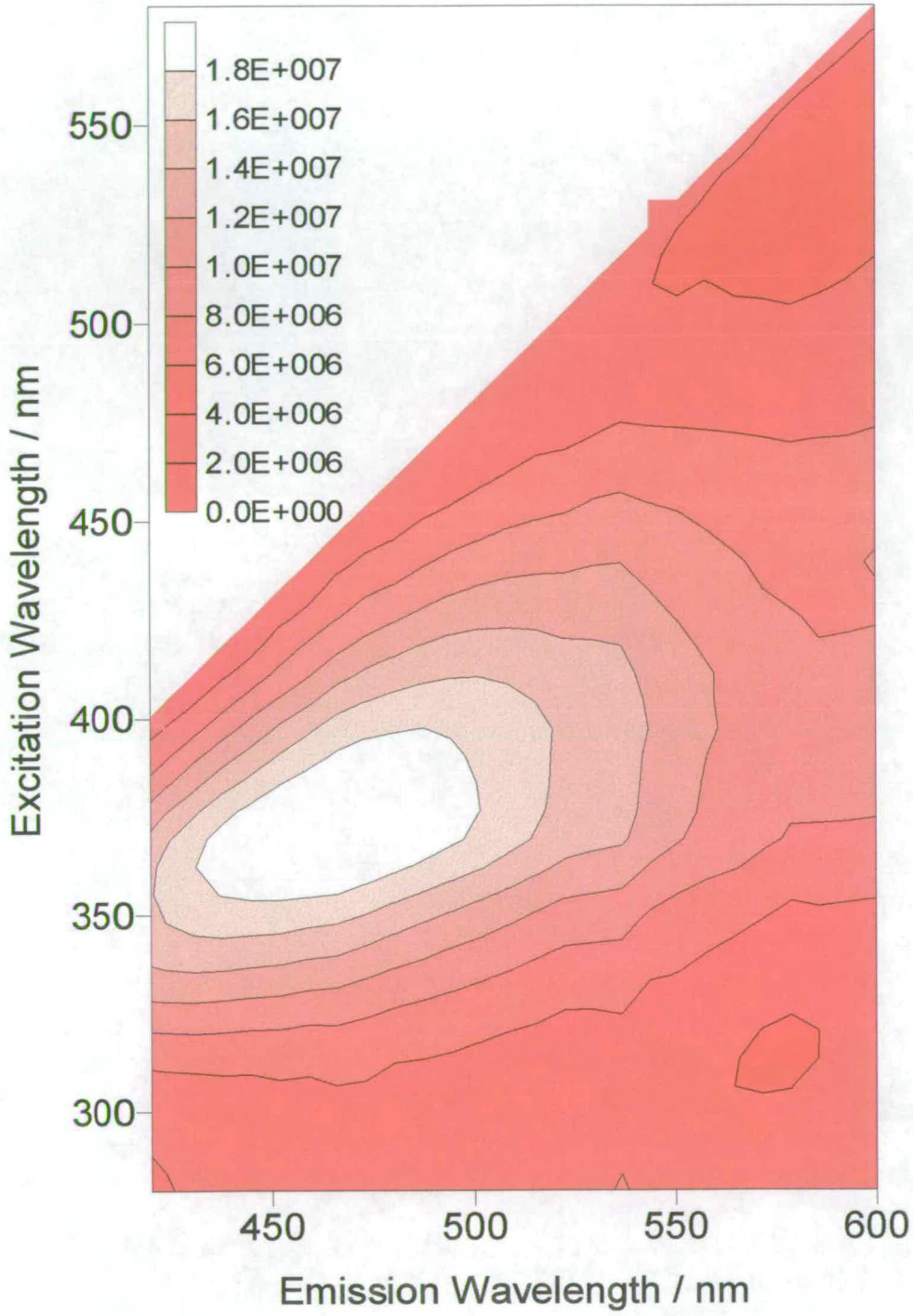

Figure 5.15: EEM of a dull band of solid coral from Laing Island, PNG, recorded in the sample chamber of the fluorimeter (as Chapter Four, Figure 4.4) shown over the same wavelength range as Figure 5.14. The contours are plotted between zero and 1.8 x 10^7 at 2 x 10^6 unit intervals.

5.3.3 Ratio EEMs

By dividing the bright band EEM (Figure 5.12) by the dull band EEM (Figure 5.14), the relative intensity variation with wavelength can be seen. The relative intensity distribution is shown in Figure 5.16. In this case, a figure of one denotes an equal intensity in both bands, with regions of intensity greater than one having an increased intensity in the bright band.

The relative intensity of the bright and dull bands is not uniform across the studied wavelength region. There is an increase in the relative emission intensity of the bright band between 500 and 600nm, with a peak ratio of 1.27 at 475/570nm. This regions is also apparent in the ratio EEM recorded within the sample chamber which has been replotted over the same wavelength range and is shown in Figure 5.17. This EEM shows a similar peak at 470/565nm with a ratio of 1.19.

In Figure 5.16, the relative intensity ratio varies between 0.95 and 1.20, with shorter excitation and emission wavelengths (around 300/400nm) showing the minimum ratio. This is also observed in the EEM recorded within the sample chamber, which has a minimum ratio of 0.73 at 320/390nm.

The relative intensity distribution shows that the presence of emitting species at longer emission wavelengths (lower energy) plays a significant role in characterising the banding pattern. This corresponds to green/yellow in the visible spectrum, and is seen as the characteristic colour of bright bands when illuminated under uv light. The eye is exceptionally sensitive to light in the region 500 - 650nm (Bergmans, 1960), and so any variation in the intensity of emission at these wavelengths will show an enhanced visual effect.

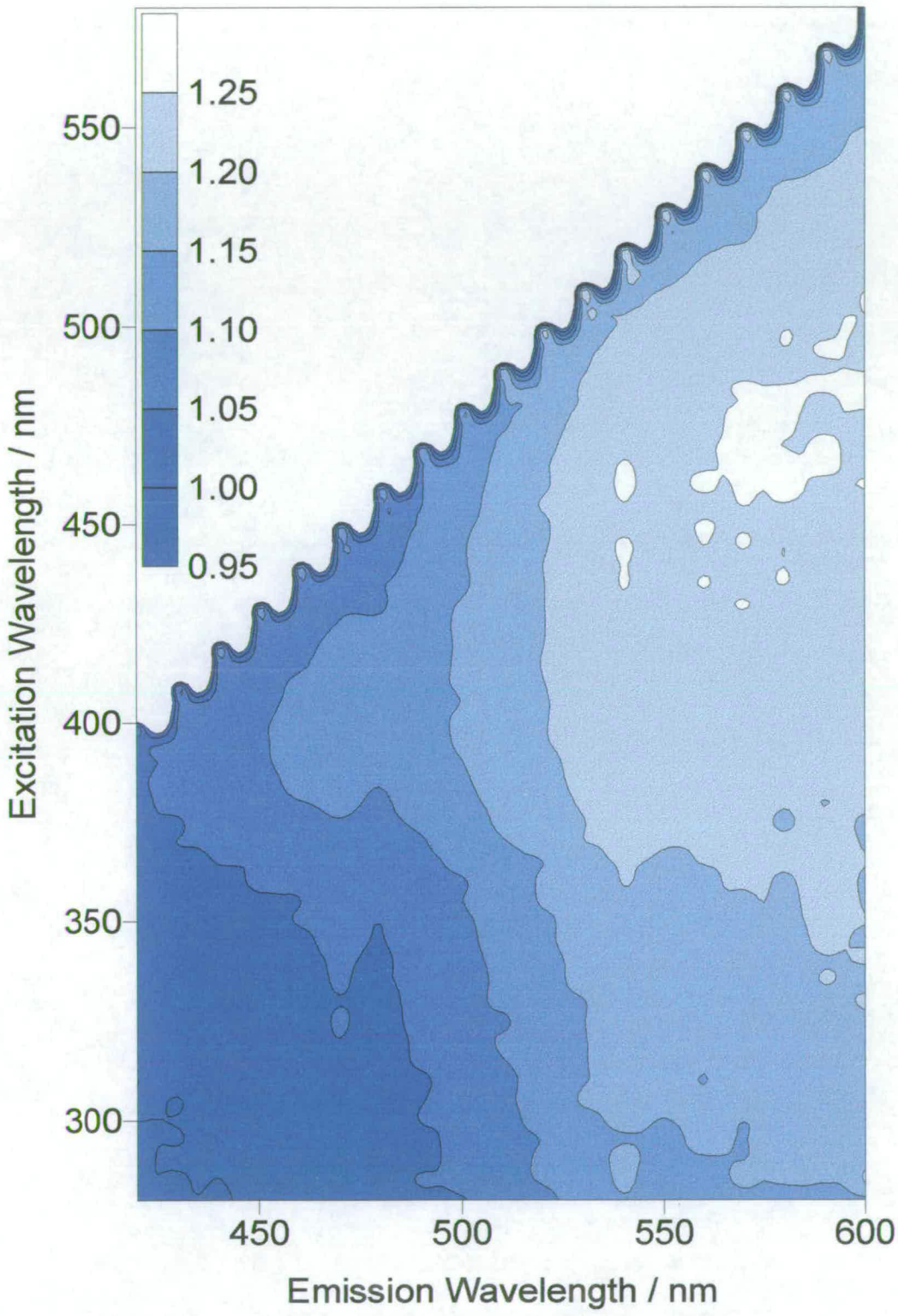

Figure 5.16: Ratio EEM for a sample of coral from Laing Island, PNG, using excitation and emission optical fibres. The contours are plotted between 0.95 and 1.25, at intervals of 0.05 units.

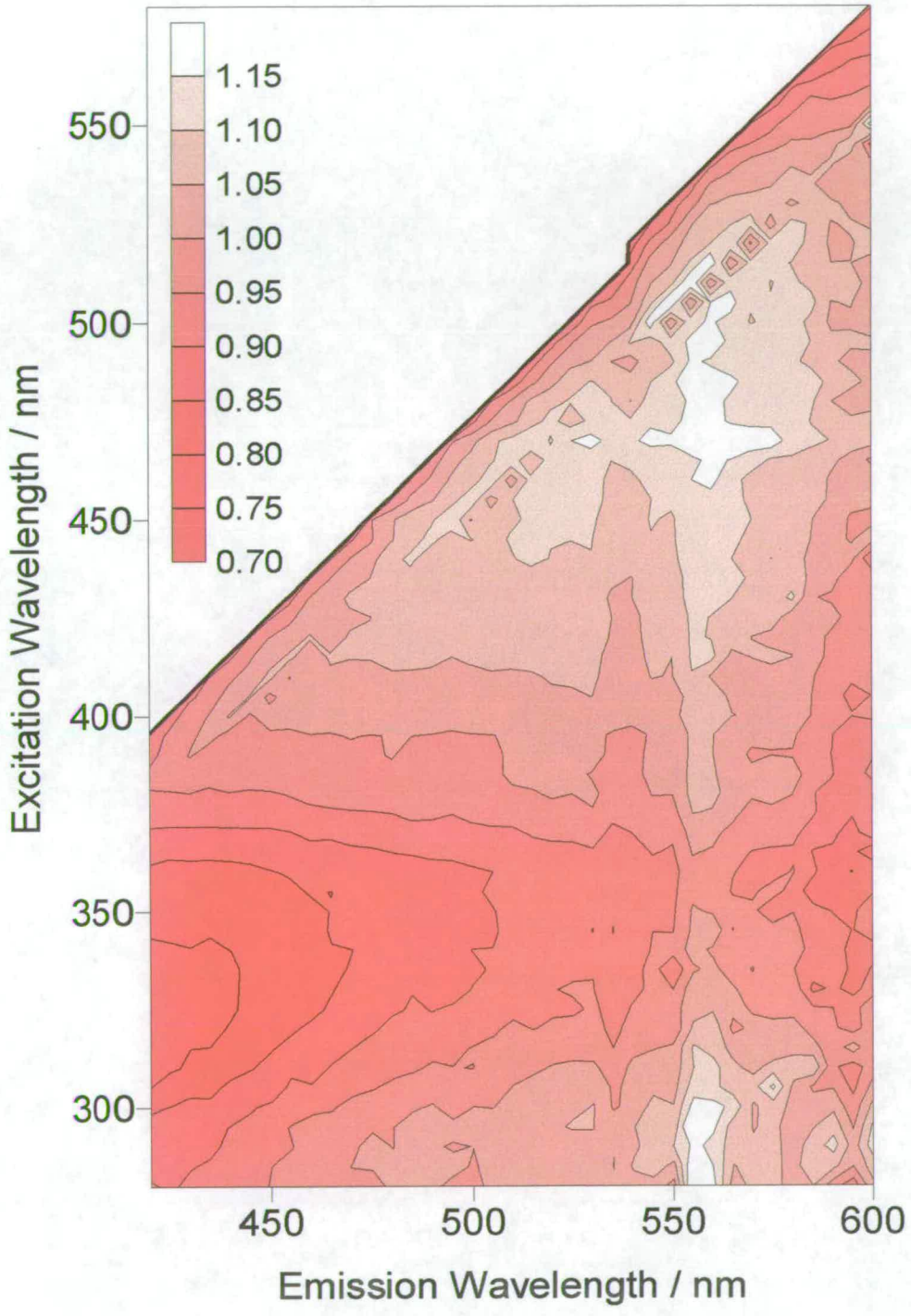

Figure 5.17: Ratio EEM for a sample of coral from Laing Island, PNG, recorded in the sample chamber of the fluorimeter (as Chapter Four, Figure 4.5) shown over the same wavelength range as Figure 5.16. The contours are plotted between 0.7 and 1.15 at 0.05 unit intervals.

There are several factors that may give rise to this enhanced emission at longer wavelengths in bright bands. There may be an increased concentration of lower-energy emitting luminophores, or an increased fluorescence or phosphorescence quantum yield for a particular luminophore that occurs in both bands. The environmental factors that affect the laying down of bright and dull bands may also cause variations in the skeletal structure of the coral. Fluorescence, and particularly phosphorescence will be affected by the architecture of the skeleton and the relative pore size of the bands.

5.3.4 Subtraction EEMs

The absolute intensity difference between the bright and dull bands is highlighted in the subtraction EEM, calculated by subtracting the dull band EEM from the bright band EEM. The subtraction EEM is shown in Figure 5.18.

The subtraction EEM shows a central peak at 400/510nm with two prominent shoulders at 370/480nm and 350/520nm. This EEM suggests that the main difference in absolute intensity between bright and dull bands occurs at longer excitation and emission wavelengths than the observed peak intensity of the individual bands at 370/470nm.

The subtraction EEM recorded within the sample chamber (Chapter Four, Figure 4.6), which has been replotted over the same wavelength range and is shown in Figure 5.19, shows a peak intensity difference at 400-450/500, which correlates well with the peak observed in this subtraction EEM. As the excitation and emission wavelengths decrease, the subtraction EEM shows negative intensity, as the dull band is more intense than the neighbouring bright band. A negative region is also seen in Figure 5.18, at the bottom left of the plot.

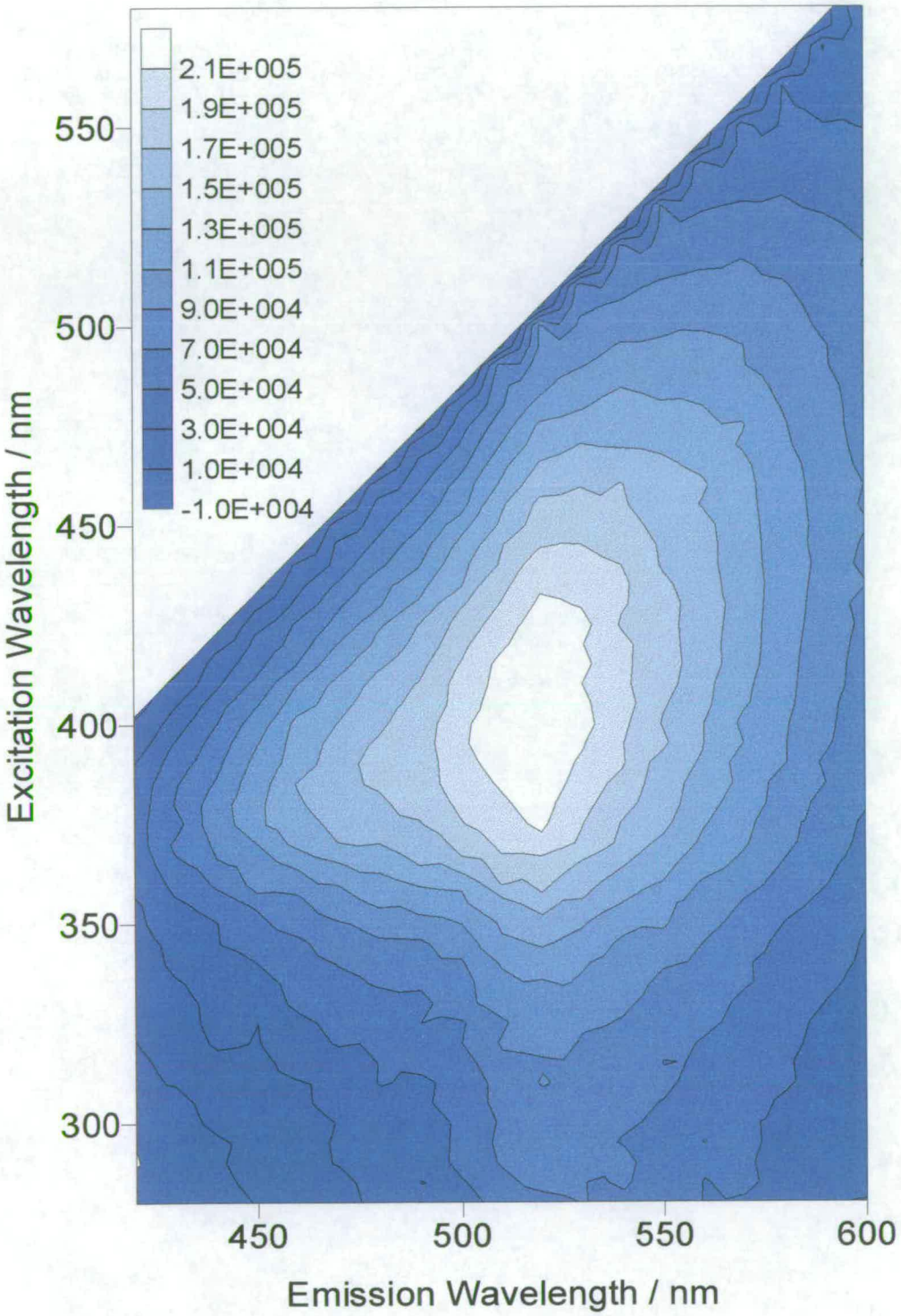

Figure 5.18: Subtraction EEM for a sample of coral from Laing Island, PNG, using excitation and emission optical fibres. The contours are plotted between – 1 x 10^4 and 2.2 x 10^5 at 2 x 10^4 cps intervals.

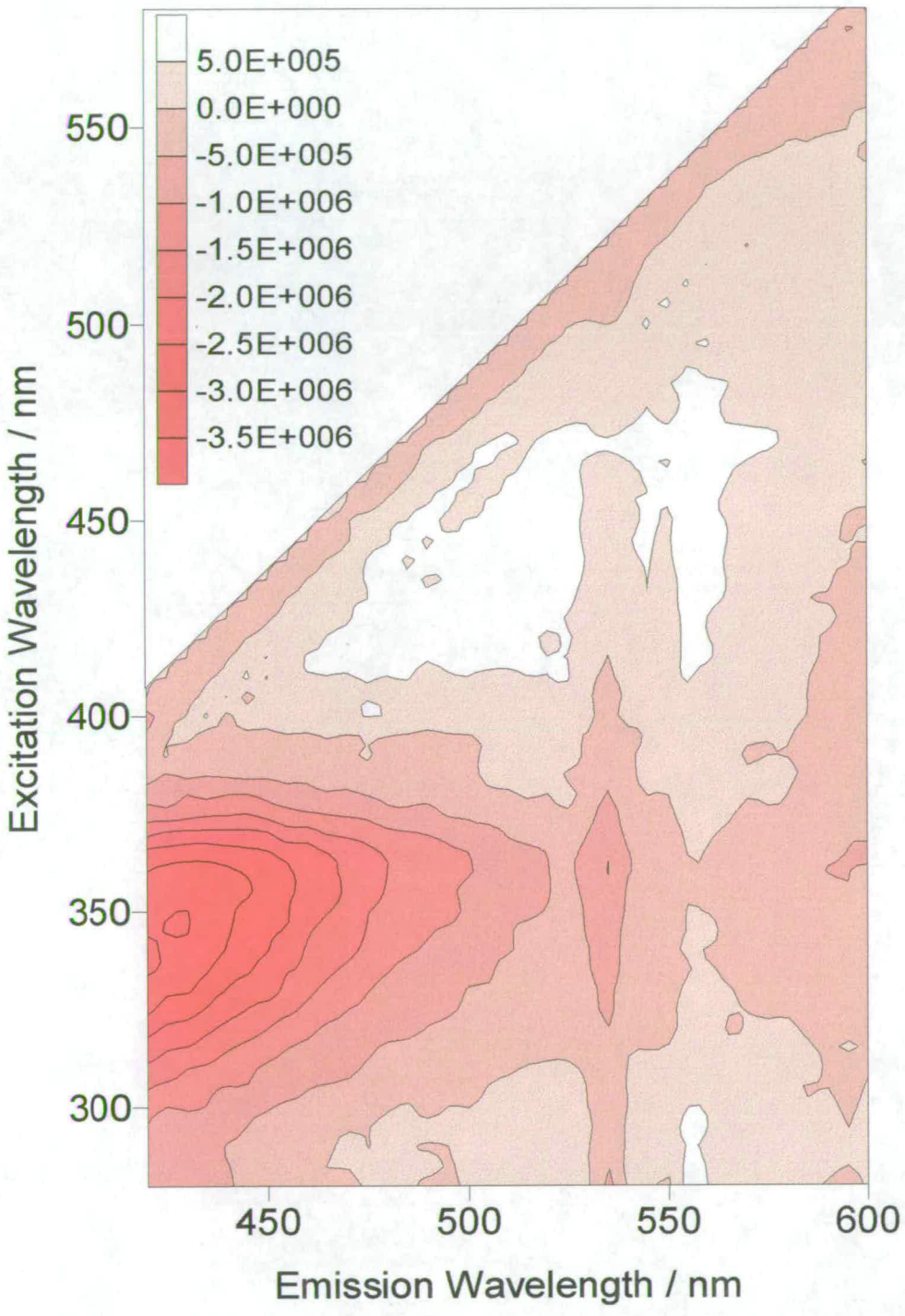

Figure 5.19: Subtraction EEM for a sample of coral from Laing Island, PNG, recorded in the sample chamber of the fluorimeter (as Chapter Four, Figure 4.6) shown over the same wavelength range as Figure 5.18. The contours are plotted between -3.5×10^6 and 5×10^5 in 5×10^5 unit intervals.

5.4 Conclusions

From the results presented in this chapter, it has been established that the banding pattern observed in coral skeletons when illuminated under uv light can be reproducibly recorded directly from the coral surface without the need for manipulation of the data. Previously, Isdale (1984) cubed the intensity in order to improve the contrast between the bright and dull band regions. Milne and Swart (1984) were unable to resolve the banding pattern into peaks and troughs. They excited the sample at 337nm and detected emission at 460nm. From the ratio EEM (Figure 5.16), the bright and dull bands are of equal intensity at the wavelengths used by Milne and Swart and therefore the banding pattern could not be reproducibly recorded. In the present investigation, both a mercury lamp source and an optical fibre probe provide adequate excitation intensity for the banding pattern to be resolved into a series of peaks and troughs, corresponding to the observed banding pattern.

The percentage difference in luminescence intensity between bright and dull bands is relatively small. For samples of coral from Laing Island, PNG, which show very obvious banding, the bright bands show a maximum increase in intensity of 25% compared to the neighbouring dull bands. As the excitation and emission wavelength increases, the relative intensity of the luminescence increases, to a maximum ratio at 450-500/550-600nm. This increase in long wavelength emission may be due to a number of factors including an increased concentration of low energy emitting luminophores in the bright bands, an increased quantum yield from luminophores present in both bands or an increased contribution from low energy phosphorophores. Results that are presented in Chapter Six show that the bright bands are indeed more phosphorescent than the dull bands.

Samples from other geographical locations also show a recordable banding pattern, including those from Oman, where the corals are not subject to terrestrial inundation.

In fact, these samples show a similar wavelength-dependent ratio of bright:dull band intensity to the samples from Laing Island, suggesting that the banding pattern cannot be due solely to the incorporation of terrestrially-derived organic matter. Samples from Madang show an inconsistent trend compared to the other samples. This may be due to the more complex nature of their banding, since they are subject to two inundations of freshwater each year, separated by only one month. Hence, the bright bands are actually made up of two peaks. Although there is some spatial resolution of these double peaks, it is likely that the signal is more convoluted and may lead to inaccurate comparisons between the bright and dull bands.

The experimental technique devised and implemented in this investigation allows spatial resolution of the banding pattern. Previous studies (Matthews *et al*, 1996) have been carried out with the coral sample fixed inside the sample chamber of the fluorimeter. Using this approach, it is very difficult to ascertain the peak intensity of a bright band and minimum intensity of a dull band, and hence comparisons between the two are subject to increased experimental error. Since the percentage difference between the luminescence of bright and dull bands is so minimal (20% maximum), the positioning of the excitation and emission optics is critical.

The dull band regions of the skeleton, or regions of "background" luminescence, are not constant along the coral core, but show a gradual increase or decrease as the sample is scanned. This suggests that there are features of the dull band luminescence that vary with, for example, age and varying environmental conditions. Further study into this shifting background may elucidate other factors that affect the banding pattern.

5.5 Bibliography

Bergmans, J., 1960. Seeing Colours. Philips Technical Library,

Isdale, P., 1984. Fluorescent bands in massive corals record centuries of coastal rainfall. Nature, 310: pp. 578-579.

Milne, P.J. and Swart, P.K., 1994. Fiber-optic-based sensing of banded luminescence in corals. Applied Spectroscopy, 48: pp. 1282-1284.

6 Chapter Six: Phosphorescence Measurements of Coral

6.1 Introduction

When a sample of coral is illuminated under uv light, the luminescent bands are clearly visible as alternating bright (yellow/green) and dull (blue) regions. If the uv light source is switched off, the banding pattern remains clearly visible to the eye for a few seconds. If the visible emission were due solely to fluorescing species within the sample, the emission would cease within microseconds of the removal of the exciting source. The prolonged emission suggests that the emission is also due to the presence of phosphorescing species. Phosphorescence can continue for seconds after the removal of the excitation source as it corresponds to electronic transitions that are spin-forbidden (Chapter Two, Section 2.3.1.2).

Phosphorescence in corals has been observed and documented previously. Klein *et al.* (1990) observed long-lived emission from fossil corals (250,000 – 108,000 years old) but did not observe any from modern corals (10,000 years and younger). They attributed the phosphorescence to the inclusion of inorganic species after the death of the corals.

All the samples we have studied, from a variety of geographical locations, exhibit long-lived phosphorescence emission. By discriminating against the short lifetime of fluorescence emission, the phosphorescence emission can be characterised. This was achieved by introducing a time delay between excitation of the sample and detection of emission that was greater than the lifetime of the fluorescing species. After this time, all emission can be considered long-lived and attributable to the phosphorescing species present in the sample.

6.2 Phosphorescence Decay

Using the experimental procedure previously described (Chapter Two, Section 3.3.2), it was possible to record phosphorescence from solid coral. A plot of luminescence intensity against time for a bright band of a sample of coral from Laing Island, Papua New Guinea is shown in Figure 6.1:

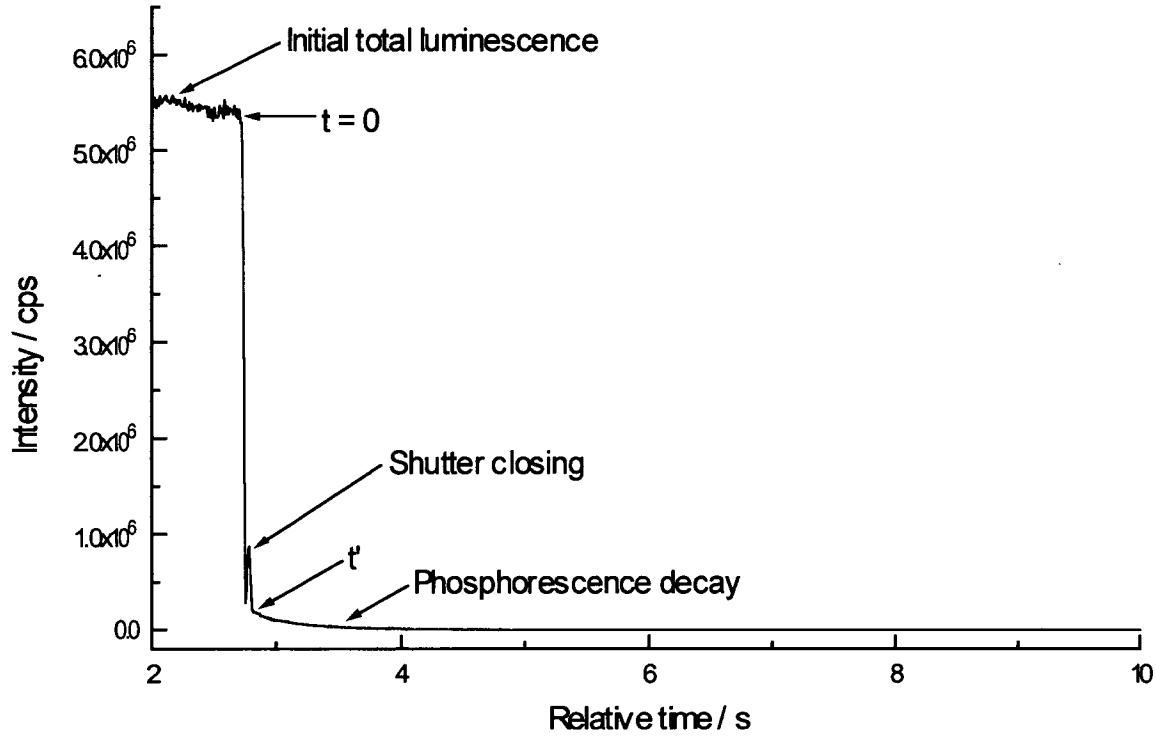

Figure 6.1: Intensity variation with time during an experiment to record phosphorescence decay, exciting at 300nm and detecting emission at 500nm. t = 0 is the time that the closing of the excitation shutter was initiated; t' is the time at which the shutter is closed.

The first portion of the plot shows the initial total luminescence (fluorescence and phosphorescence). Just before three seconds into the plot, the excitation shutter is closed and the intensity of the recorded emission falls dramatically. There is a slight increase in intensity as the shutter "bounces"; this can be seen as a small, sharp peak located at the base of the large drop in intensity. The delay between instigating the closing of the shutter and the shutter finally coming to rest is approximately 100ms. This corresponds to t' – (t = 0) as shown on the plot. From this point onwards, all emission due to fluorescence has ceased and the recorded emission is due solely to the emission from long-lived phosphorophores. This emission lasts for several seconds and is highlighted in Figure 6.2:

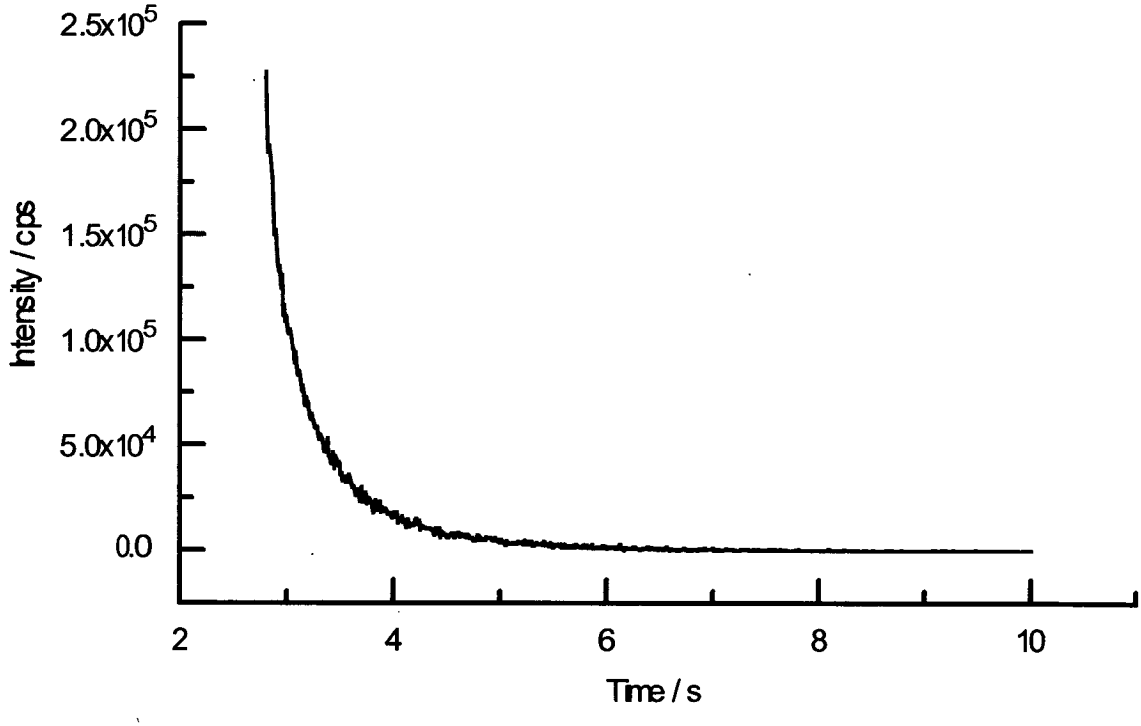

Figure 6.2: Phosphorescence decay of a bright band of solid coral from Laing Island, PNG, exciting at 300nm and detecting emission at 500nm.

By comparing the intensity of phosphorescence emission at time t = 100ms with the total luminescence intensity at time t = 0, at a particular excitation and emission wavelength, it was possible to obtain an idea of the wavelength-dependence of the phosphorescence intensity. The maximum phosphorescence intensity at t = 100ms (as a fraction of total luminescence intensity) for all excitation wavelengths investigated was recorded when exciting at 300nm and detecting emission at 500nm. The values were not extrapolated at this stage to estimate the contribution at time t=0 (see Section 6.3.1). The variation in phosphorescence contribution with emission wavelength for a bright band sample of coral from Laing Island, PNG, when excited at 300nm is shown in Table 6.1:

Emission Wavelength / nm	460	480	500	520	540
% Phosphorescence	3.2	4.1	4.6	4.2	3.7

Table 6-1: Estimate of % of total luminescence intensity due to phosphorescence at t = 100ms when exciting at 300nm and varying the emission wavelength.

The variation in phosphorescence intensity relative to total luminescence (at time t = 100ms) with excitation wavelength for a dull band of coral from Laing Island when detecting emission at 500nm is shown in Table 6.2:

Excitation Wavelength / nm	260	280	300	320	340
% Phosphorescence	1.2	2.3	2.5	2.1	1.2

Table 6-2: Estimate of % of total luminescence intensity due to phosphorescence at t = 100ms when varying the excitation wavelength and detecting emission at 500nm.

There was a phosphorescence contribution detected at all wavelength combinations investigated for all samples of coral from Laing Island. The excitation wavelengths ranged from 200 to 400nm and the emission wavelengths from 450 to 600nm. It was found that the maximum phosphorescence contribution to the total luminescence was observed when there was a 200nm offset between the excitation and emission wavelengths. This held for all samples studied from Laing Island, PNG. Both bright and dull bands showed the same wavelength-dependence of phosphorescence contribution, with a maximum contribution at 300/500nm. The detection of phosphorescence at such a wide range of wavelengths suggests that there are a number of phosphorescing species contributing to the observed signal.

6.3 Exponential fitting of the phosphorescence decay function

The phosphorescence decay observed in Figure 6.2 can be fitted to an exponential decay function. The decay was fitted from time t', 100ms after the shutter started to close. It was found that the decay could be well described by three exponential terms, but was less well fitted by one or two components. This is consistent with the existence of numerous phosphorescing species. There are expected to be more than three emitting species present, but this approximation gives an indication of the range of lifetimes present. Figure 6.3 shows a triple exponential decay function fitted to the phosphorescence signal from a bright band of solid coral from Laing Island.

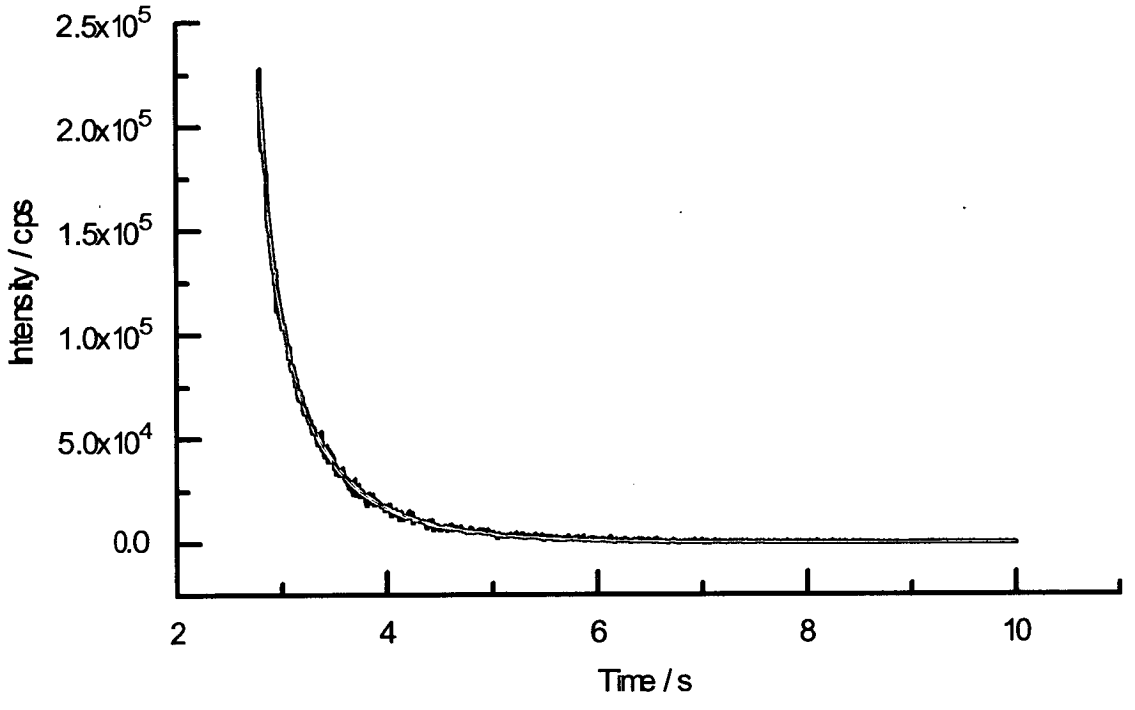

Figure 6.3: Triple exponential decay function fitted to the phosphorescence decay of a bright band of coral from Laing Island, PNG.

The decay can be described by the following triple exponential decay function:

$$I(t) = A_1 e^{(-(t-t')/\tau_1)} + A_2 e^{(-(t-t')/\tau_2)} + A_3 e^{(-(t-t')/\tau_3)}$$

Equation 6-1: Exponential decay fitting function

$I(t)$	Intensity of phosphorescence as a function of time after shutter closes (cps)
A_i	Pre-exponential factor for component i
$t = 0$	Time at which the closing of shutter was initiated
t'	Time at which the shutter closed NB. t' = 100 ms
τ_i	Lifetime of phosphorescent component i

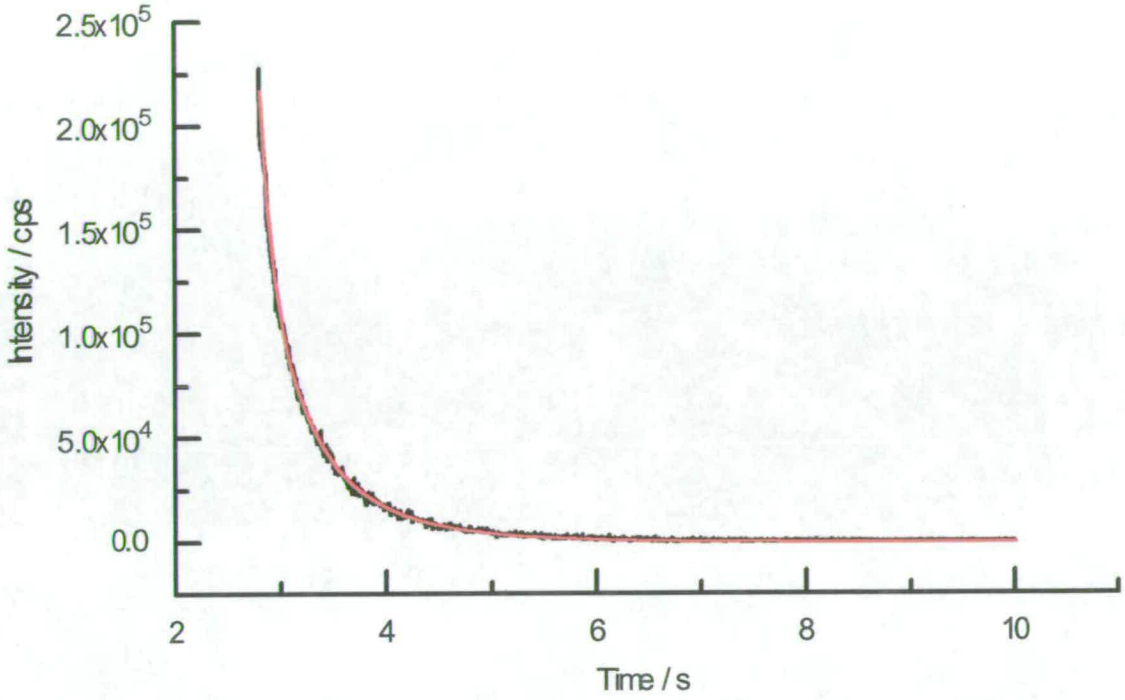

Figure 6.3: Triple exponential decay function fitted to the phosphorescence decay of a bright band of coral from Laing Island, PNG.

The decay can be described by the following triple exponential decay function:

$$I(t) = A_1 e^{(-(t-t')/\tau_1)} + A_2 e^{(-(t-t')/\tau_2)} + A_3 e^{(-(t-t')/\tau_3)}$$

Equation 6-1: Exponential decay fitting function

$I(t)$	Intensity of phosphorescence as a function of time after shutter closes (cps)
A_i	Pre-exponential factor for component i
$t = 0$	Time at which the closing of shutter was initiated
t'	Time at which the shutter closed NB. $t' = 100$ ms
τ_i	Lifetime of phosphorescent component i

For the decay shown in Figure 6.3, the fitted function values are as follows:

A_1	τ_1(s)	A_2	τ_2(s)	A_3	τ_3(s)
5.522×10^4	0.07	1.234×10^5	0.36	4.047×10^4	0.99

Table 6-3: Estimated values of A factors and lifetimes for triple exponential decay function for the phosphorescence of a bright band of coral from Laing Island, PNG.

The estimated lifetimes of the constituent phosphorophores are between 0.05s and 1s. Typically, τ_1 was 0.05s, τ_2 was 0.5s and τ_3 was 1.0s. In comparison, the short-lived constituent fluorophores found in samples of coral from Laing Island were found to have a fluorescence lifetime of approximately 10ns (Dr. A. C. Jones; private communication).

6.3.1 Extrapolating the decay function

In order to estimate the phosphorescence contribution to the total observable luminescence emission, it is necessary to consider the intensity of phosphorescence at the time at which the closing of the shutter was initiated. At this time the signal is a combination of fluorescence and phosphorescence. However, 100ms after this time, all fluorescence has ceased and the detectable emission is due solely to phosphorescence which persists for more than 100ms. Using the fitted values from the triple exponential decay function, the phosphorescence contribution to the total luminescence signal was calculated. The calculation for the bright band decay in Figure 6.3 is shown, for example, in Equation 6-2.

$$I(0) = A_1 e^{(-(0-t')/\tau 1)} + A_2 e^{(-(0-t')/\tau 2)} + A_3 e^{(-(0-t')/\tau 3)}$$
$$= 5.522 \times 10^4 \, e^{(0.1)/0.07386)} + 1.234 \times 10^5 \, e^{(0.1)/0.3626)}$$
$$+ 4.047 \times 10^4 \, e^{(0.1)/0.9878)}$$
$$= 213842 + 162588 + 44781$$
$$= 421211 \text{cps}$$

Equation 6-2: Calculating the phosphorescence intensity

The value obtained represents the extrapolated phosphorescence intensity at the time at which the closing of the shutter was initiated. Taking the mean value of the total luminescence intensity from the region highlighted in Figure 6.1 as 5441212cps, the phosphorescence contribution is calculated to be 7.7% for this bright band.

6.3.2 Phosphorescence contributions and the banding pattern

The phosphorescence decay of the adjacent dull band to that shown in Figure 6.2 is highlighted in Figure 6.4.

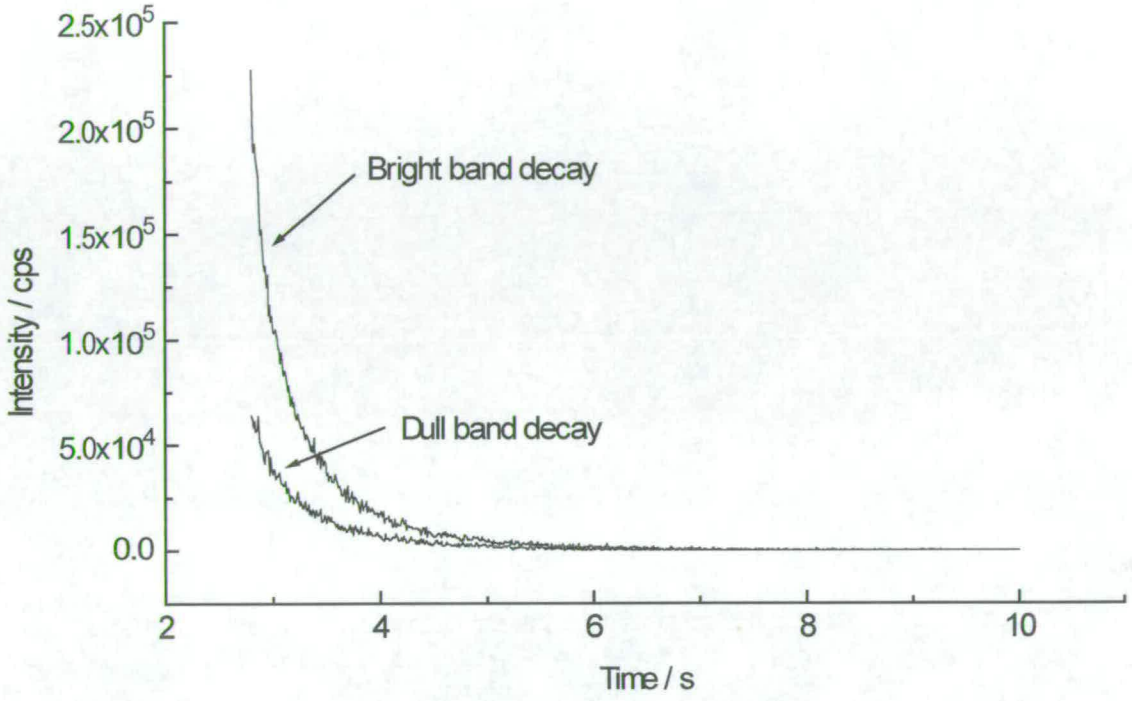

Figure 6.4: Comparison of phosphorescence decay for neighbouring bright and dull bands, exciting at 300nm and detecting emission at 500nm.

The dull band shows considerably less phosphorescence intensity than the adjacent bright band. The decay was fitted to a triple exponential function as shown in Figure 6.5. The estimated lifetimes of the constituent phosphorophores are between 0.1 and 1.5s. There is no significant difference between the estimated lifetimes of the phosphorophores in the bright or dull bands.

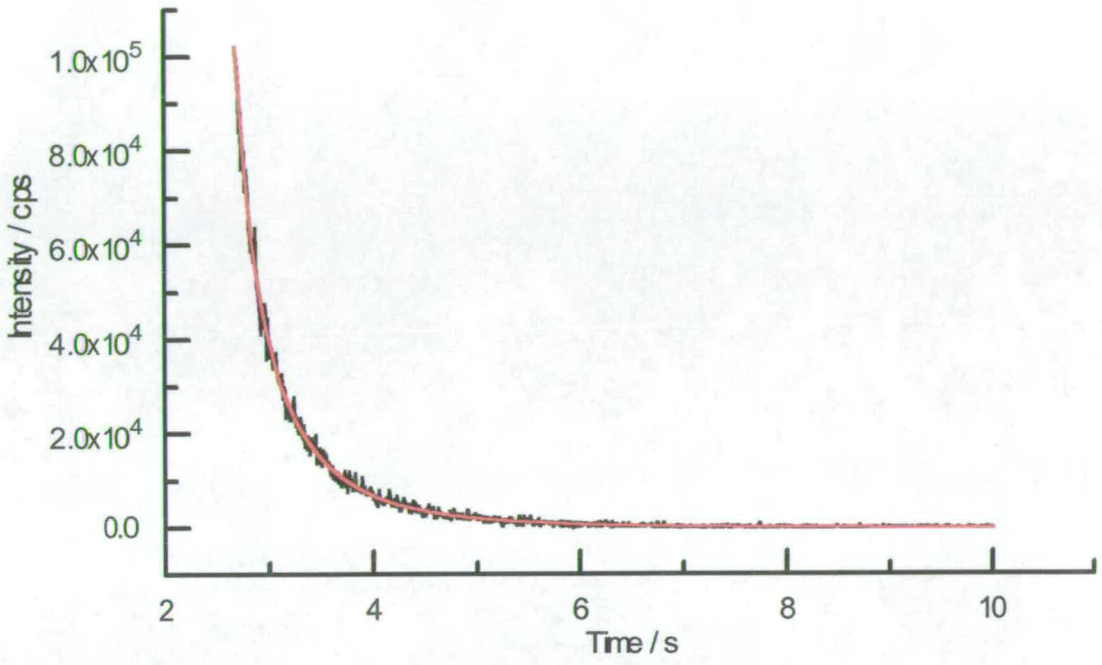

Figure 6.5: Triple exponential decay function fitted to the phosphorescence decay of a dull band of coral from Laing Island, PNG.

Extrapolating to the time at which the closing of the shutter was initiated and using the fitted values from the triple exponential decay function, the phosphorescence contribution to the total luminescence signal was calculated to be 3.5%, compared with 7.7% for the neighbouring bright band. There is a marked difference between the phosphorescence contributions of the dull and bright bands, with the bright bands having twice the contribution of the dull. Consequently, phosphorescence is an important indicator of the banding pattern.

It is important to consider adjacent bands since there can be a variation in the percentage contribution between bright bands from different regions of the skeleton, or from different samples from the same geographical location. Measurement of the

% phosphorescence contribution was carried out for 20 pairs of adjacent bright and dull bands and it was found that in all cases, the phosphorescence contribution to the total luminescence of the bright band is approximately twice that for the dull band. In comparison, the difference in total luminescence intensity between the bright and dull bands varied between -10% (where the dull band is actually more intensely luminescent than the neighbouring bright band) and +25%, depending on the excitation/emission wavelength combination (Chapter Five, Section 5.3.3).

6.4 Variations in phosphorescence with geographical location

6.4.1 Madang Lagoon, Papua New Guinea

Under uv light, the banding pattern is clearly visible in samples from Madang Lagoon, PNG. However, it is not as well defined as that observed in the samples from Laing Island. Samples from Madang Lagoon exhibit phosphorescence. When the light source is removed, the banding pattern can be seen to glow for a few seconds.

As with the samples from Laing Island, the phosphorescence intensity is dependent on the combination of excitation and emission wavelengths, suggesting that the signal is made up of a number of component phosphorophores. The phosphorescence decay (exciting at 300nm and detecting at 500nm), can be fitted well to a triple exponential decay function. By extrapolating the triple exponential decay function, the phosphorescence contribution to the total luminescence of the system can be estimated. It accounts for around 9% of the observable luminescence in the bright bands and around 7% in the dull bands. Thus, the difference between bright and dull bands is not as marked as that estimated for the samples from Laing Island. The total relative luminescence intensity varies between zero and +20%, depending on the excitation/emission wavelength combination (Chapter Four, Section 4.3.4).

6.4.2 Wadi Ayn, Oman

Under uv light, samples of coral from Wadi Ayn, Oman exhibit luminescent banding. However, the bright and dull bands are not as well-defined as those observed in the corals from PNG. The corals exhibit phosphorescence when the light source is removed, and appear to glow for a few seconds.

As with the samples from Laing Island and Madang Lagoon, the phosphorescence intensity varied with the combination of excitation and emission wavelengths, suggesting that the signal is due to a number of component phosphorophores. The phosphorescence decay (exciting at 300nm and detecting at 500nm) can be fitted well to a triple exponential decay function. By extrapolating the triple exponential decay function, the phosphorescence contribution to the total luminescence of the system can be estimated. The phosphorescence accounts for around 15% of the total observable luminescence in the bright bands and around 12% in the dull bands. Thus, the difference between the bright and the dull bands is reduced in comparison to the samples of coral from PNG. The relative total luminescence intensity between the bright and dull bands ranges from –30% to +5%, depending on the excitation/emission wavelength combination (Chapter Four, Section 4.4.4).

6.4.3 Limitations of this approach

It is likely that the measurements presented here underestimate the contribution of phosphorescence to the total luminescence of the system. As a result of the time taken for the shutter to close, any phosphorophores that decay in less than 100ms are neglected. The intensity of a phosphorophore decays to 1/e (where e = 2.718...) of its initial value in one lifetime, and thus to ~5% of its initial value in 3 lifetimes. For example, phosphorophores with lifetimes of less than 33ms will have decayed to less than 5% of their initial intensity in 100ms. In order to include the contribution of shorter-lived phosphorophores, we developed an improved experimental system with fast electronic shutters which allows a variable delay between the initiation of the

closing of the shutter and the detection of emission (Chapter Three, Section 3.4.4). Hence, we can study the contribution of phosphorophores of a range of lifetimes to the total luminescence signal.

6.5 Spatially-resolved Measurements of Phosphorescence Emission

To ensure a reproducible excitation and emission geometry and accurate location on bright and dull bands, measurements of phosphorescence emission were made using the excitation and emission optical fibres, as previously described in Chapter Five. The investigations were carried out on samples of coral from Laing Island, PNG to allow comparison with previous results.

6.5.1 Emission Spectra

Exciting at 360nm, the emission spectra (between 380 and 650nm) of a sample of coral from Laing Island, PNG were recorded with a delay time between the closing of the excitation shutter and the opening of the emission shutter of 20 and 100ms. The emission shutter was open for 100ms for both experiments. The resultant spectra are shown in Figure 6.6.

The emission spectrum of the total luminescence has a maximum intensity at 445nm. With a 20ms delay between the closing of the excitation shutter and the opening of the emission shutter, the maximum emission intensity peak has shifted to 520nm, shown by the red spectrum in Figure 6.6. With a 100ms delay, the peak emission intensity has broadened out to longer wavelengths. At this long delay time, the intensity of the signal is very low, and hence the signal to noise is reduced. At a delay of 500ms, the phosphorescence is still evident, although the peak is too broad to quantify a maximum intensity.

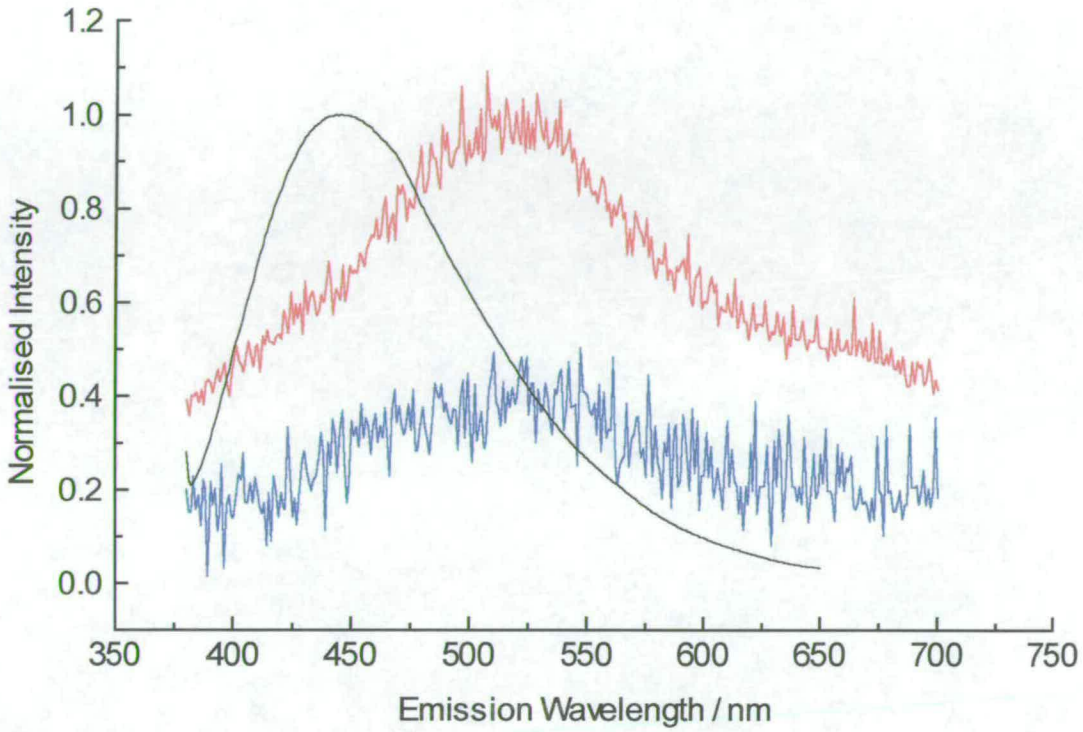

Figure 6.6: Emission spectra of a sample of coral from Laing Island, PNG, when excited at 360nm. The black line shows the total luminescence emission; the red line shows the emission with a 20ms delay between closing of the excitation shutter and opening of the emission shutter; and the blue line shows the emission with a 100ms delay. The intensities have been normalised to the maximum intensity emission of each spectrum and separated on the y axis for clarity.

This investigation reveals that phosphorescent emission occurs at longer wavelength (lower energy) than fluorescence emission. This is as expected, since phosphorescence corresponds to a transition between the triplet state and the ground state, with the triplet state at lower energy than the equivalent singlet state.

6.5.2 Variation in phosphorescence intensity with lateral position

Since the luminescence emission of solid coral is wavelength-dependent, experiments were carried out to determine the wavelength-dependent response of the phosphorescence emission. A sample of coral from Laing Island was scanned using the optical fibre excitation and emission probes at various excitation/emission wavelength combinations and with various delays between the closing of the excitation shutter and opening of the emission shutter. Figure 6.7 shows the scan recorded at 360/550nm with a 20ms delay and the emission shutter open for 100ms. There are four bands evident, corresponding to the four bright bands observed under uv light. Between the bright bands are dull regions of the skeleton.

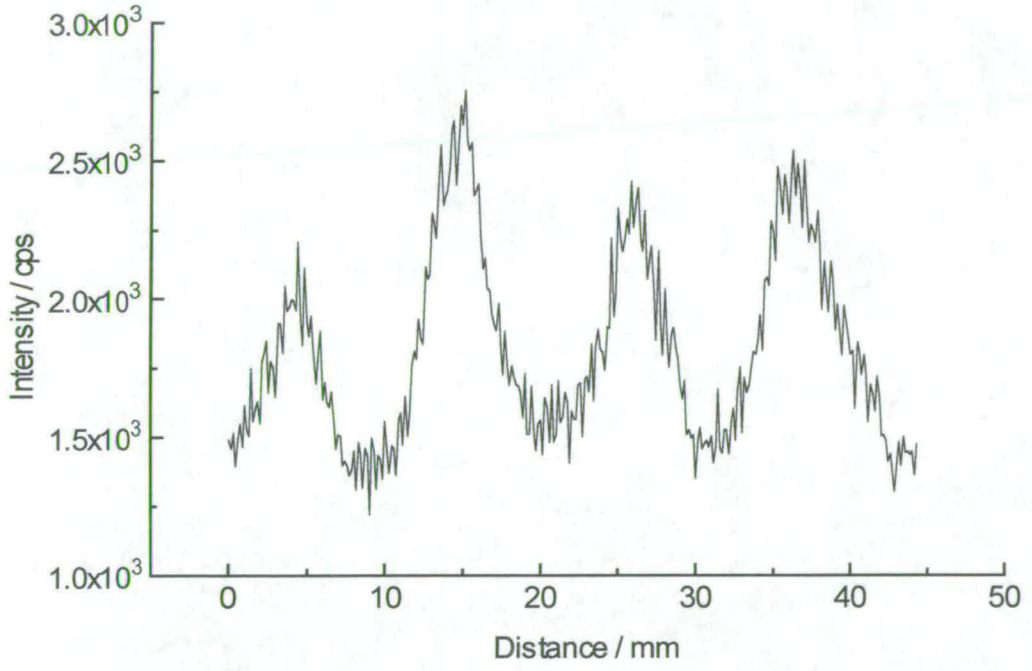

Figure 6.7: Scan across the surface of a sample of coral from Laing Island, PNG, exciting at 360nm and detecting the emission at 550nm. There is a 20ms delay between the closing of the excitation shutter and the opening of the emission shutter.

Figure 6.8 shows the scan recorded in the opposite direction.

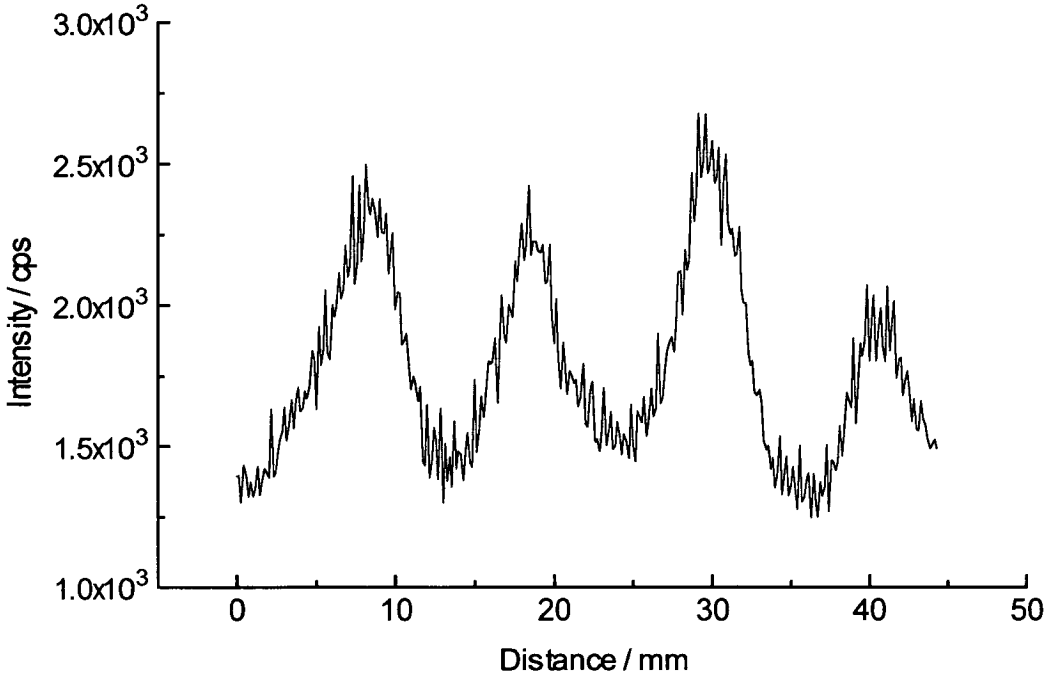

Figure 6.8: Scanning in the opposite direction to Figure 6.7.

Figure 6.9 shows the same region of the skeleton, scanned at 360/550nm with the excitation and emission shutters opened simultaneously and recorded in the same direction as Figure 6.7. This corresponds to a luminescence spectrum, since the excitation and emission shutters are open at the same time and all short-lived fluorescence is recorded.

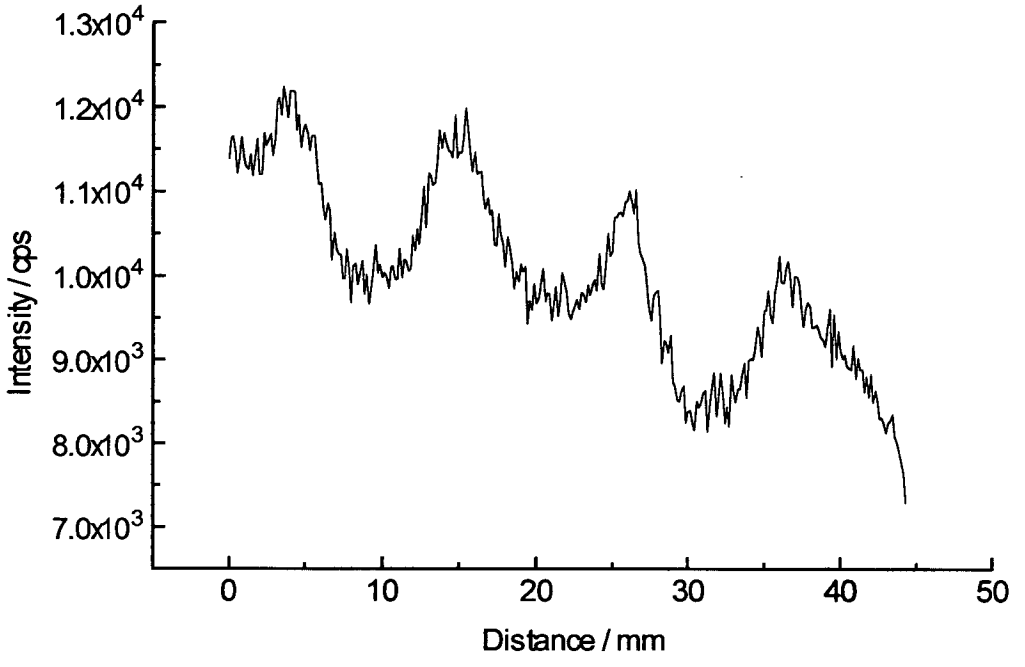

Figure 6.9: Scanning across the surface of a sample of coral from Laing Island, PNG at 360/550nm with the excitation and emission shutters open simultaneously to detect total luminescence.

The scan in the opposite direction is shown in Figure 6.10. Again, the scans show excellent reproducibility. There are evidently four bright bands, corresponding to the observed banding pattern, but in these spectra, the "background" intensity is not constant, but changes along the length of the sample. This is consistent with the previous measurements made in Chapter Five, which also showed a changing background luminescence. However, the phosphorescence scans do not show this changing background intensity at the same wavelength combination. Hence, the background phosphorescence emission is constant along the length of the sample.

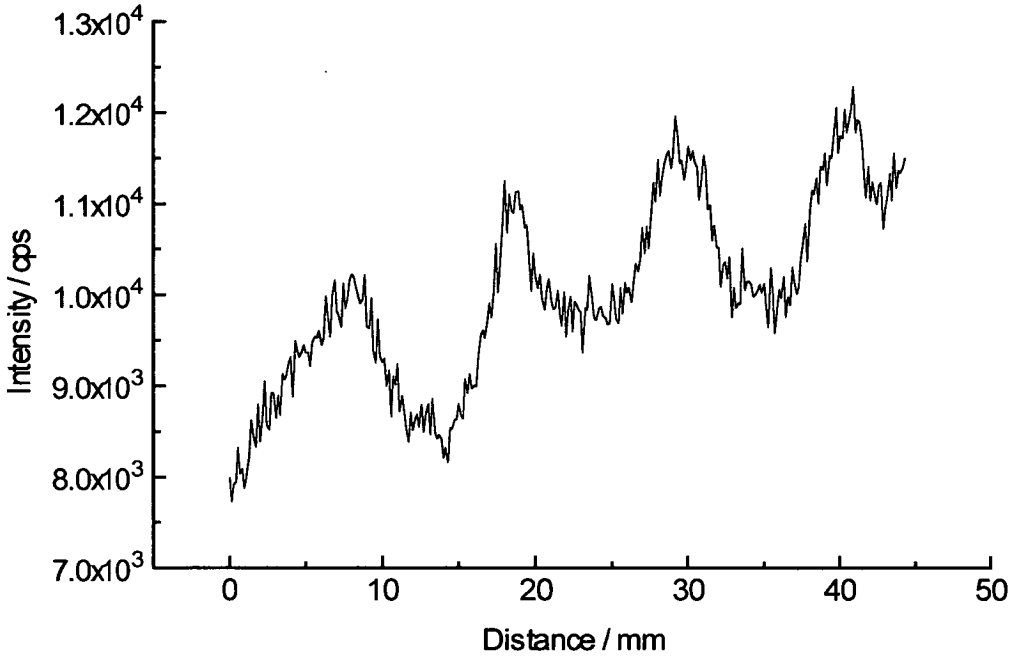

Figure 6.10: Scanning in the opposite direction to Figure 6.9.

Figure 6.11 shows the relative intensities of the phosphorescence scans at a variety of wavelength combinations (upper image) and the same scans with normalised intensities (lower image) in order to compare the relative structure of the scans at the various wavelength combinations.

It can be seen that the banding pattern is evident at all four wavelength combinations. The greatest difference in intensity between the bright and dull bands is observed in the red scan, corresponding to 360/550nm. This correlates with previous observations that the maximum intensity difference between bright and dull bands is observed when the offset between the excitation and emission wavelengths is approximately 200nm.

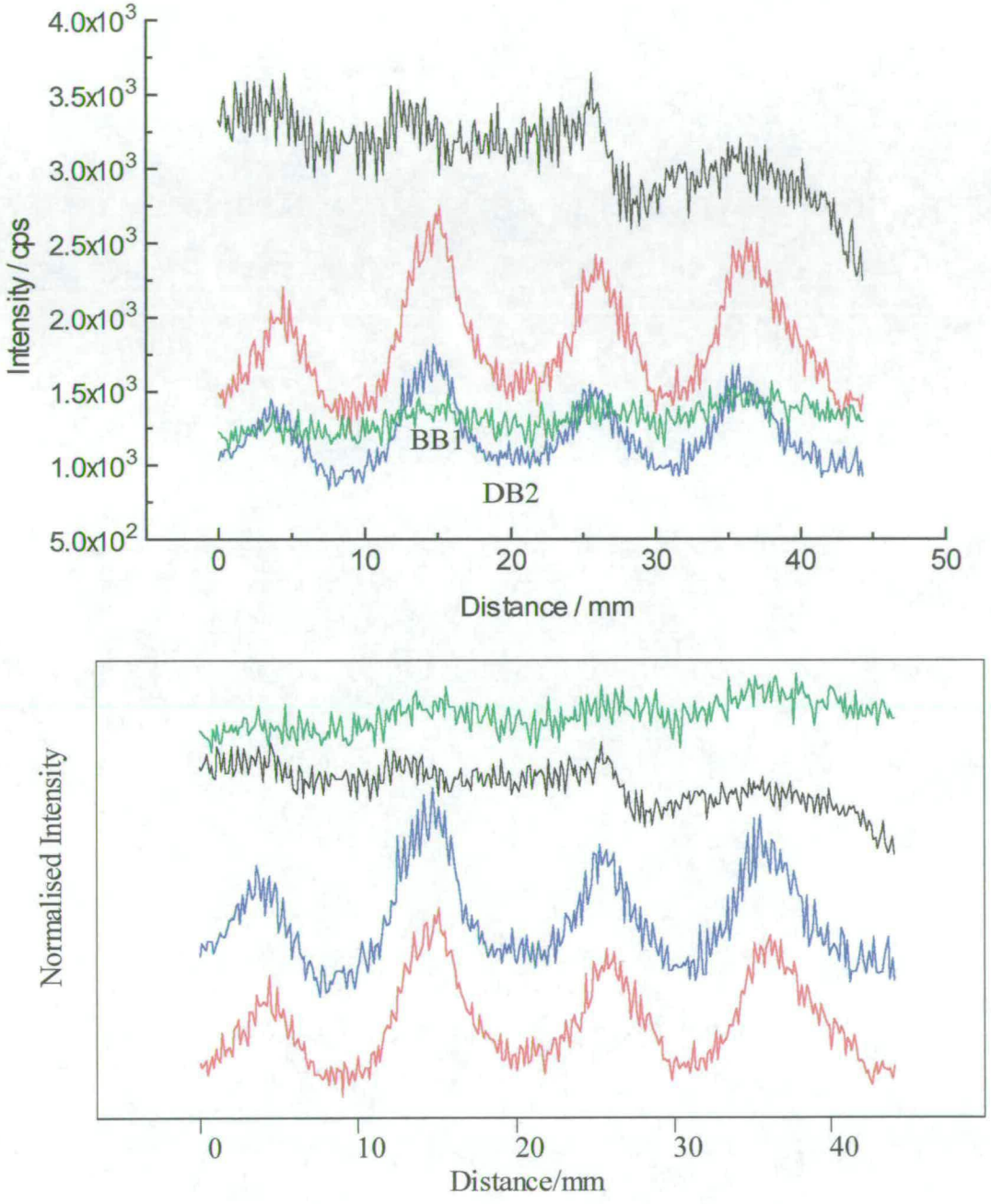

Figure 6.11: The upper plot shows the phosphorescence scans across a sample of coral from Laing Island, PNG at various excitation and emission wavelength combinations with a 15ms delay. The red scan corresponds to 360/550nm; the green to 360/650nm; the blue to 360/450nm and the black to 280/450nm. The lower plot shows the phosphorescence scans with normalised intensities.

The blue scan also shows good banding, corresponding to 360/450nm, but with reduced intensity. In both red and blue scans the background signal (between the bright band peaks) remains constant throughout the scan. At 360/650nm (green scan), there is still some intensity of phosphorescence emission, and the banding pattern is still evident, although it is much less well-defined. The black scan corresponds to 280/450nm, the region where tryptophan phosphoresces. There is more intense phosphorescence here although it follows the banding pattern less closely. This suggests that the origin of this phosphorescence may not be the same as that seen in the other scans and may not be affected by the same factors that cause the observed banding pattern.

At two different excitation wavelengths, 280 and 360nm, the 450nm emission gives two quite different phosphorescence traces (blue vs. black scans). This suggests that the emission is from two distinct species (or groups of species). This is consistent with the emission at 280/450nm being due to tryptophan phosphorescence, since tryptophan is not excited at 360nm.

The luminescence scans at the same wavelength combinations are shown in Figure 6.12. The upper plot shows the relative intensity of the luminescence scans and the lower plot shows the normalised intensities.

The blue scan, corresponding to a wavelength combination of 360/450nm, is by far the most intense. This correlates with previous results that show that the maximum luminescence intensity of both the bright and dull bands is found in this region. The red scan (360/550nm) is considerably less intense, but shows more distinct banding. At 650nm (green) the intensity of luminescence is very much weaker than the other scans. Both the red (360/550nm) and blue (360/450nm) scans show the four bright band peaks, but the "background" signal fluctuates across the scan, and there is a general decrease in background intensity from left to right.

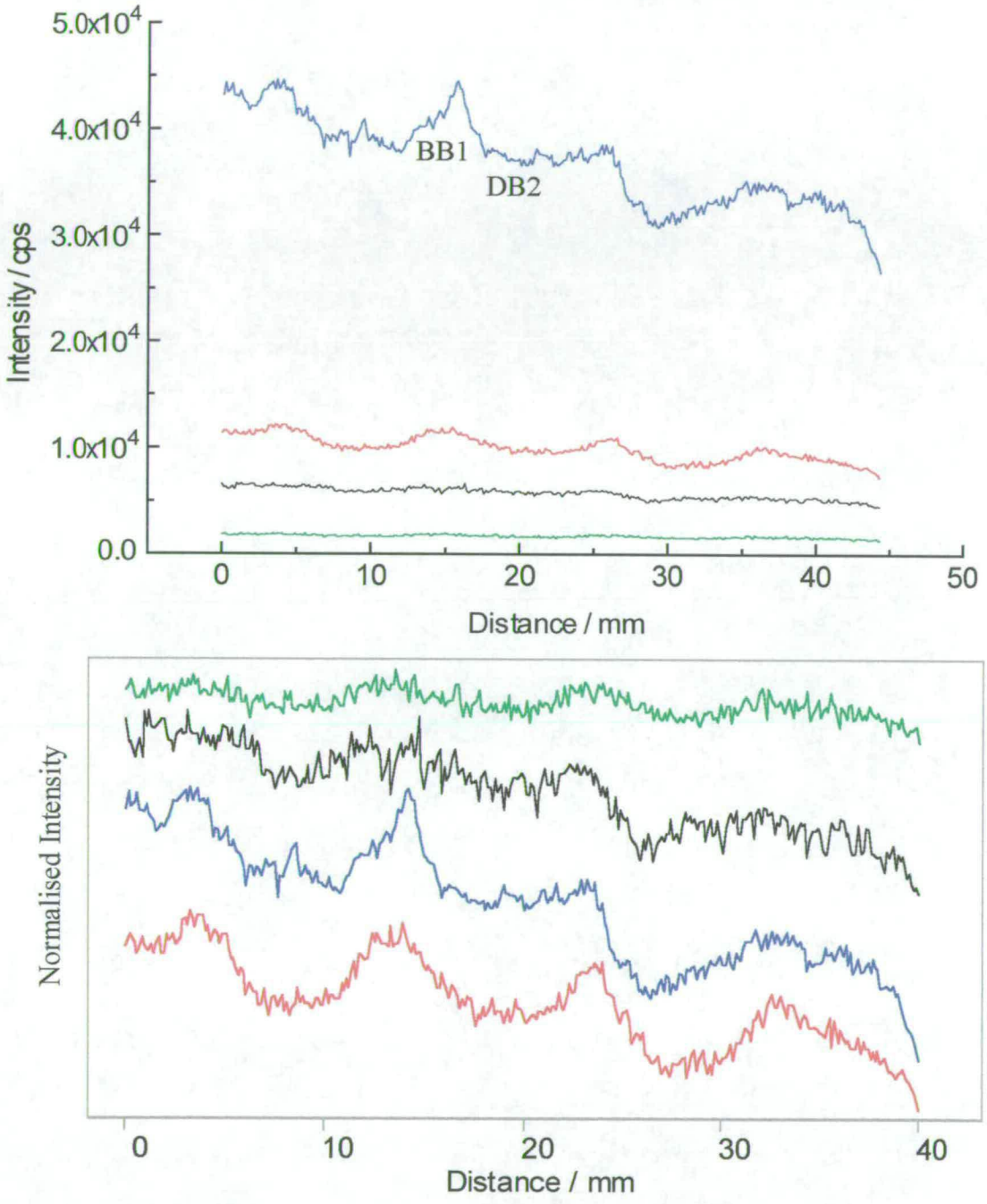

Figure 6.12: The upper plot shows the luminescence intensity scans across the surface of a sample of coral from Laing Island, PNG, at various excitation and emission wavelength combinations. The red scan corresponds to 360/550nm; the green to 360/650nm; the blue to 360/450nm and the black to 280/450nm. The lower plot shows the same scans with normalised intensities.

6.5.3 A comparison of luminescence and phosphorescence scans

As would be expected, the luminescence scans are considerably more intense than the phosphorescence scans. Fluorescence emission is due to the transition from the first excited singlet state to the ground state, and the transition is thus spin-allowed. Phosphorescence is due to the transition from the first excited triplet state to the ground state, and is spin-forbidden. It is therefore a much less likely transition to occur.

Table 6-4 shows the ratio of the bright to dull band luminescence and phosphorescence intensities (BB1:DB2), from Figures 6.11 and 6.12:

Excitation/Emission Wavelength / nm	BB1:DB2 Luminescence Intensity Ratio	BB1:DB2 Phosphorescence Intensity Ratio
280/450	1.09	1.08
360/450	1.20	1.63
360/550	1.22	1.74
360/650	1.17	1.13

Table 6-4: The relative phosphorescence and luminescence intensites of a bright (BB1) to a dull (DB2) band of coral from Laing Island, PNG.

The bright:dull band phosphorescence ratio is a maximum at 360/550nm, when the offset between the excitation and emission wavelengths is approximately 200nm. This corresponds to earlier findings (section 6.2, Tables 6-1 and 6-2).

At 280/450nm, the luminescence and phosphorescence ratios are very similar. This suggests that the intensity difference between the bands is due to phosphorescence at this combination of wavelengths. In Figure 6.12, the emission at 280/450nm shows a significant reduction in relative intensity compared to the other wavelength combinations, being the second lowest in intensity. However, in Figure 6.11, the phosphorescence emission at 280/450nm is the most intense. The phosphorescence and luminescence intensities at 280/450nm are of similar magnitude (3.5×10^3 vs. 5×10^3 cps), which suggests that the majority of the emission at this wavelength is due to phosphorescence alone. This emission can be attributed to directly excited tryptophan phosphorescence. Another point to note is that the luminescence and the phosphorescence scans have a very similar structure. This supports the observation that the majority of emission at 280/450nm is due to phosphorescence.

At 360/450nm (blue) and 360/550nm (red), the banding pattern is clearly visible in both the phosphorescence (Figure 6.11) and luminescence (Figure 6.12) scans. The varying background emission which is present in the luminescence scans is absent from the phosphorescence scans. Hence, at these wavelengths, the background emission can be attributed to fluorescence.

At 360/450nm, there is a much higher level of background fluorescence than at any other excitation/emission wavelength combination, as shown in Figure 6.12 by the blue scan. In the lower image, the banding pattern at 360/450nm is less distinct than that at 360/550nm. However, in Figure 6.11, the scan at 360/450nm shows the minimum phosphorescence intensity and very distinct banding. Hence, the luminescence at 360/450nm consists mainly of background fluorescence and the banding pattern is due mainly (or perhaps entirely if shorter lifetime phosphorophores were detected) to variations in phosphorescence intensity. The emission at 360/450nm corresponds to the peak of maximum intensity in the luminescence EEMs of bright and dull bands (Chapter Four). Hence, although this

emission is the most intense in terms of absolute intensity, it is mainly background fluorescence and makes little contribution to the banding pattern.

At 360/550nm, the most distinct banding is observed in both the phosphorescence and luminescence scans. This again suggests that phosphorescence may be the predominant contributor to luminescent banding. There is substantially less background fluorescence emitted at 360/550nm than at 360/450nm (Figure 6.12). This is consistent with phosphorescence being more significant at longer emission wavelengths.

There is enhanced contrast between bright and dull bands in the phosphorescence scans. The bright:dull band intensity ratios are greater than the equivalent luminescence ratios, and the scans show a constant background level. The luminescence scans show a varying background emission that is due to fluorescence. This appears to show a smooth variation across the samples studied and is not associated with the banding pattern. It could, therefore, be an indication of a variation in environmental conditions which does not show seasonal fluctuations. Since phosphorescence is not subject to this variation, it may enable quantitative measurements to be made and compared with other environmental factors to establish the origin of the banding pattern

6.6 Phosphorescence EEMs

By locating the maximum phosphorescence emission intensity of a bright band, or the minimum phosphorescence emission intensity of a dull band, a characteristic EEM can be produced. In order to time-resolve the phosphorescence emission from the coral sample, two EEMs were produced for each characteristic band; one

recorded with a 20ms delay, and one with a 100ms delay. This allows comparison of the phosphorescence emission at two different time windows.

6.6.1 Bright Band EEMs

The phosphorescence EEM of a bright band of coral from Laing Island, PNG, recorded with a 20ms delay between the closing of the excitation shutter and the opening of the emission shutter is shown in Figure 6.13. The emission shutter was opened for 100ms. The bright band EEM shows the emission wavelength from 420nm to 600nm (limited by the transmittance of the glass emission optical fibre) and the excitation wavelength from 280nm to 580nm. The bright band phosphorescence EEM shows a broad peak, suggesting that it is composed of several component phosphorophores. There is a maximum peak intensity at approximately 300nm excitation and 510nm emission. In contrast, the equivalent bright band luminescence EEM (described in Chapter Five) shows a peak intensity at 370/470nm. The peak phosphorescence emission is therefore at longer wavelength (lower energy) than the corresponding luminescence emission. This is expected since the transition from triplet state to ground state is less energetic than the transition from singlet state to ground state. The peak excitation intensity is at shorter wavelengths than that observed in the corresponding luminescence EEM. This indicates that the component luminophores giving rise to the maximum phosphorescence are different to those giving rise to the maximum fluorescence. There is a prominent shoulder at 280/450nm corresponding to the phosphorescence of tryptophan.

Figure 6.14 shows the EEM of the bright band with a 100ms delay. In comparison with the EEM recorded with a 20ms delay, the intensity of maximum phosphorescence is greatly reduced. The peak intensity corresponds to 300/520nm, suggesting that the emission is predominantly due to the same phosphorophores as those observed with a 20ms delay. The small shift to longer emission wavelengths may be due to a greater contribution from longer-lived phosphorophores.

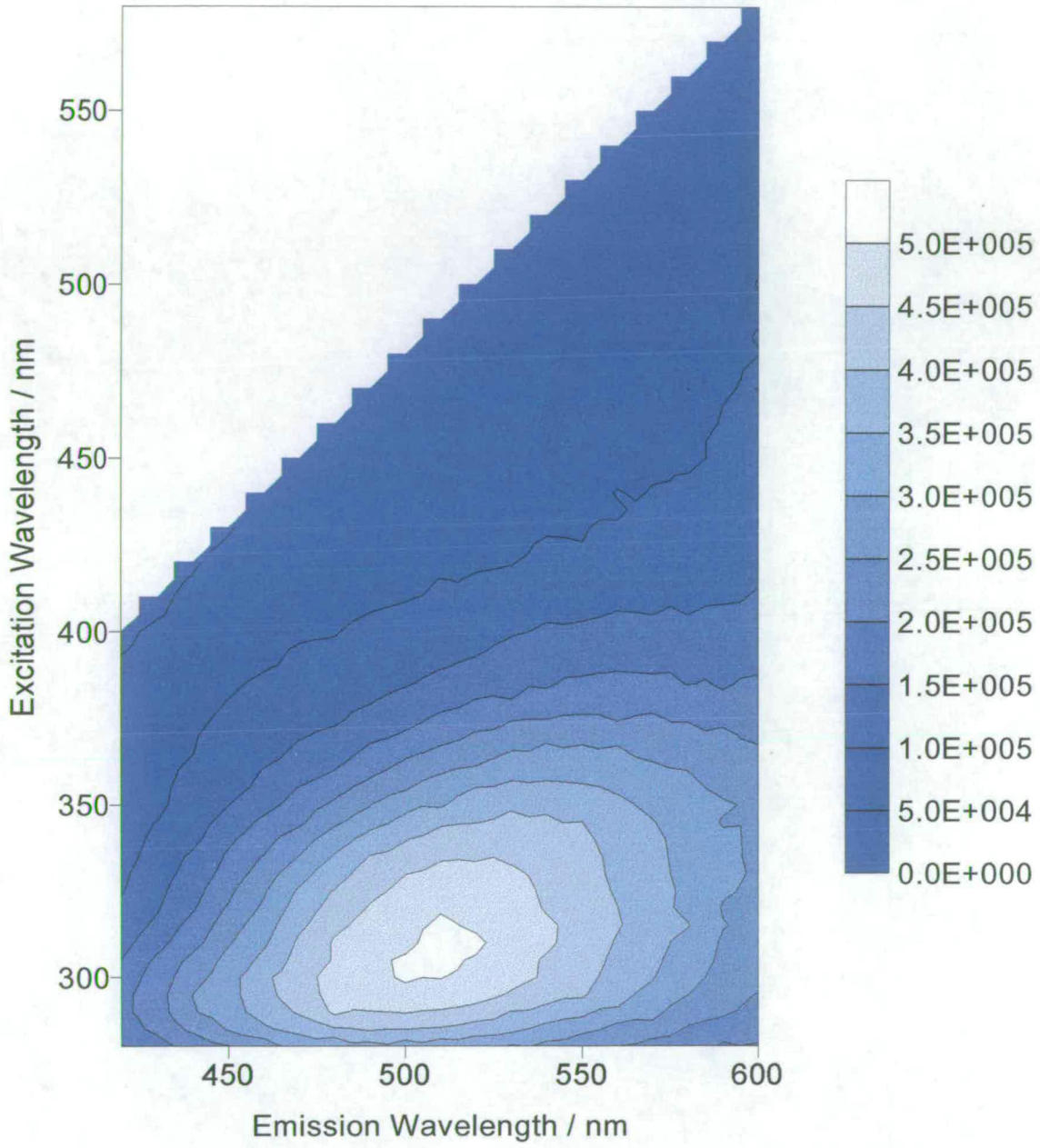

Figure 6.13: Phosphorescence EEM of a bright band of a sample of coral from Laing Island, PNG, recorded with a 20ms delay. The contours are plotted between 0 and 5 x 10^5 at 5 x 10^4 cps intervals.

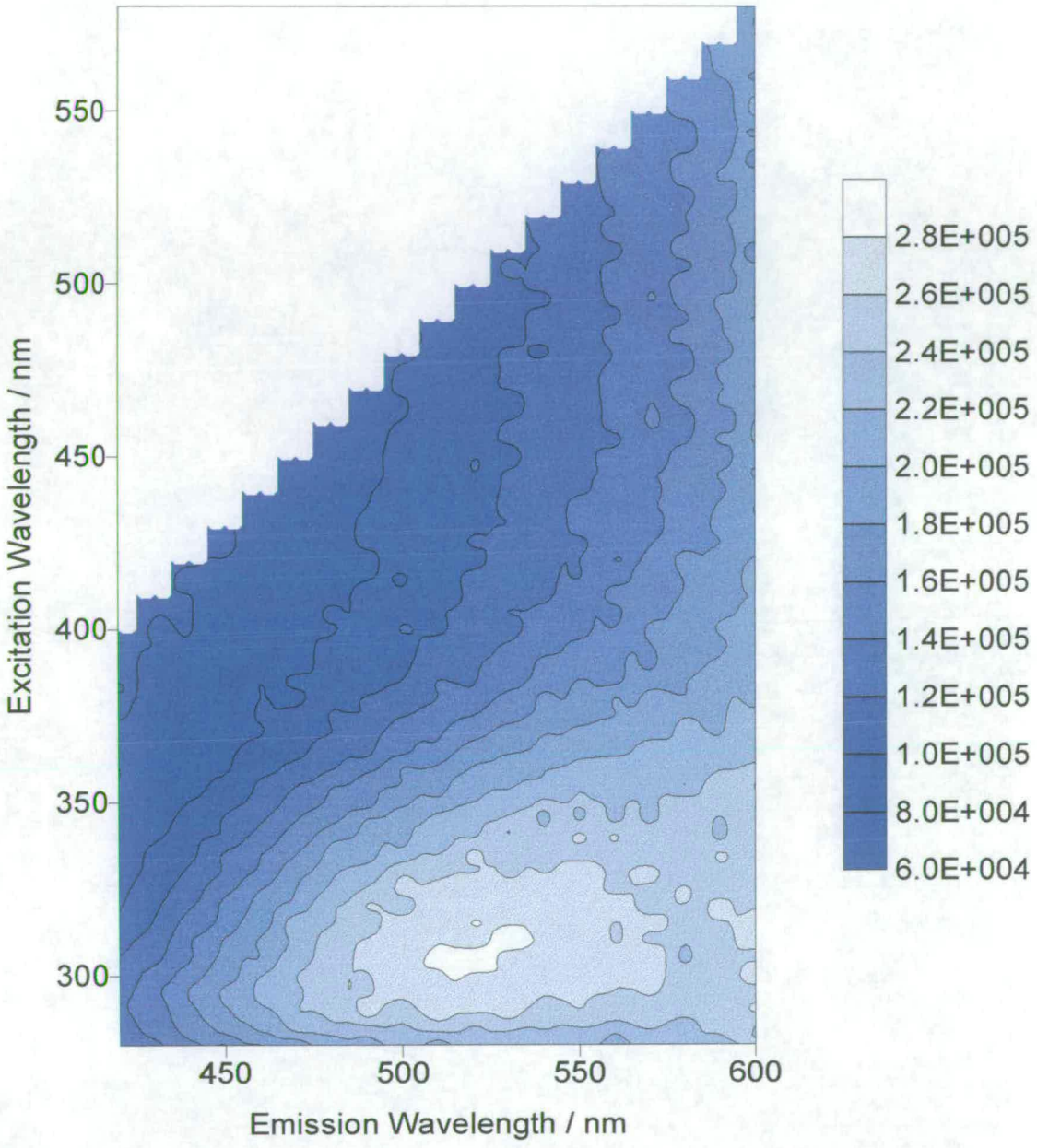

Figure 6.14: Phosphorescence EEM of a bright band of solid coral from Laing Island, PNG, recorded with a 100ms delay. The contours are plotted between 6 x 10^4 and 2.8 x 10^5 at 2 x 10^4 cps intervals.

6.6.2 Dull Band EEMs

Figure 6.15 shows the phosphorescence EEM of an adjacent dull band with a 20ms delay. In contrast to the bright band EEM, the peak intensity is greatly reduced from 5×10^5 cps to 2.8×10^5 cps. The maximum intensity peak occurs at 280/500nm. The EEM has a different shape to that of the corresponding bright band, with no visible shoulder between 300-350/500nm. Consequently, the dull band phosphorescence may be due to different phosphorophores than the bright band phosphorescence. The tryptophan peak at 280/450nm is also much more prominent. The corresponding dull band luminescence EEM (described in Chapter Five) has a peak intensity at 370/470nm. Again, the phosphorescence emission occurs at lower energy (longer wavelength) than the corresponding luminescence emission.

Figure 6.16 shows the dull band phosphorescence EEM recorded with a 100ms delay. The overall intensity is reduced, and the peak intensity emission occurs at 280/500-550nm. Again, the shoulder at 280/450nm is more predominant than in the equivalent bright band EEM (Figure 6.14).

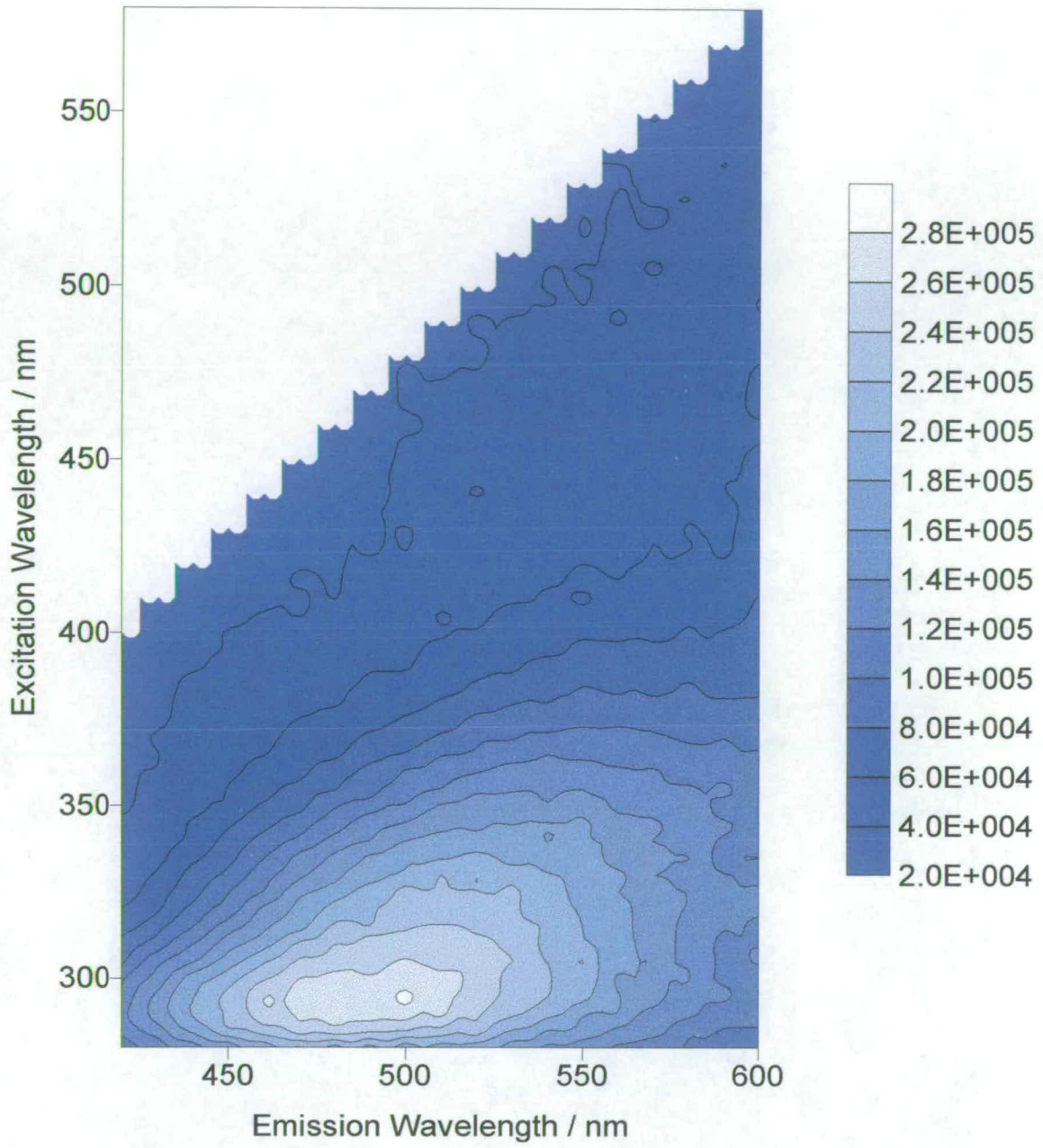

Figure 6.15: Phosphorescence EEM of a dull band of solid coral from Laing Island, PNG, recorded a 20ms delay. The contours are plotted between 2 x 10^4 and 2.8 x 10^5 at 2 x 10^4 cps intervals.

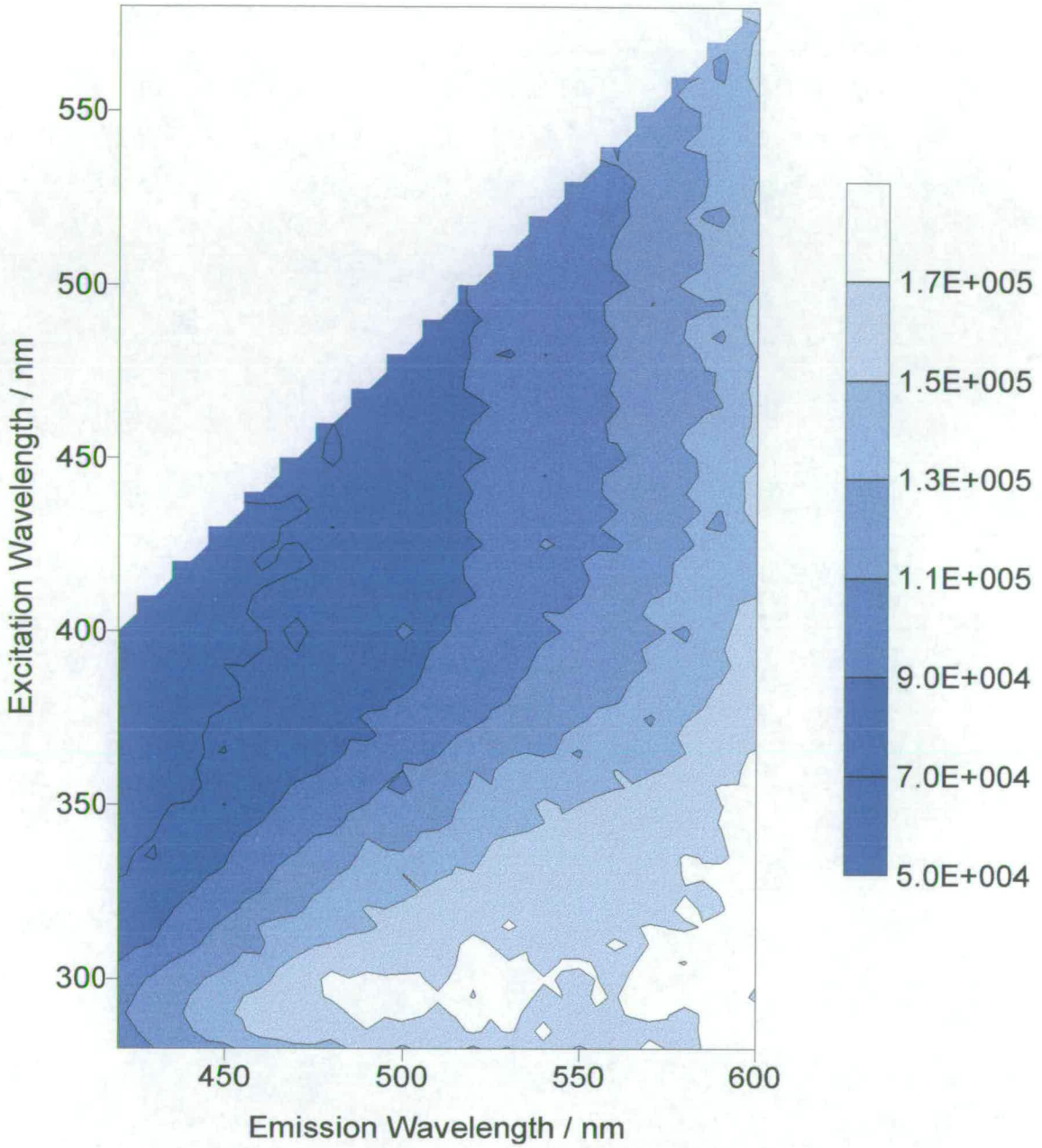

Figure 6.16: Phosphorescence EEM of a dull band of solid coral from Laing Island, PNG, recorded with a 100ms delay. The contours are plotted between 5 x 10^4 and 1.7 x 10^5 at 2 x 10^4 cps intervals.

6.6.3 Ratio EEMs

By dividing the bright band EEM, recorded with a 20ms delay, by the adjacent dull band EEM with the same time delay, a ratio EEM can be constructed. This shows the relative emission intensity across the wavelength range. The resultant EEM is shown in Figure 6.17.

The intensity ratio is greater than 1 across the entire wavelength range, implying that the bright band is more intense than the dull band at all wavelength combinations studied. The peak ratio of 2.2 corresponds to excitation/emission wavelength combinations between 340-370/450-600nm. At these wavelengths, the bright bands are more than twice as intense as the neighbouring dull bands. This is in agreement with previous estimates of the ratio of bright:dull band phosphorescence detailed earlier in the chapter.

Figure 6.18 shows the ratio EEM for neighbouring bright and dull bands recorded with a 100ms delay. With an increased delay time, the ratio of bright:dull band intensity is reduced. Figure 6.18 has a maximum ratio of 1.70 at 310-350/480-520nm. The ratio is above 1.0 across the entire wavelength range, as the bright bands are consistently more intense than the dull bands at all wavelength combinations. The maximum intensity ratio shifts to shorter excitation wavelengths with the increase in delay time. This is consistent with the observation that there is a different set of phosphorophores emitting at 100ms delay compared to 20ms delay.

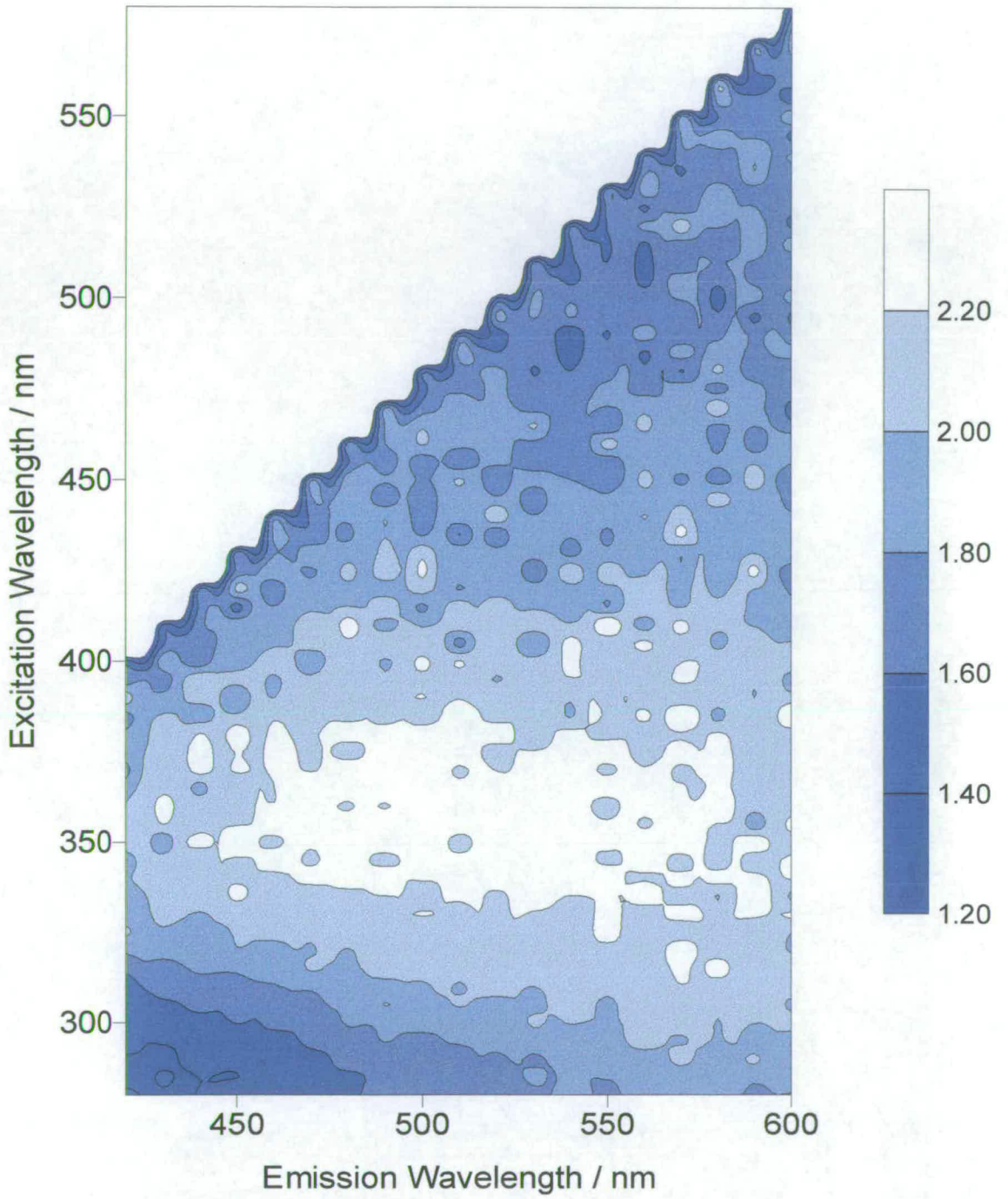

Figure 6.17: Ratio EEM constructed by dividing the bright band EEM by the adjacent dull band and recorded with a 20ms delay. The contours are plotted between 1.2 and 2.2 at 0.2 unit intervals.

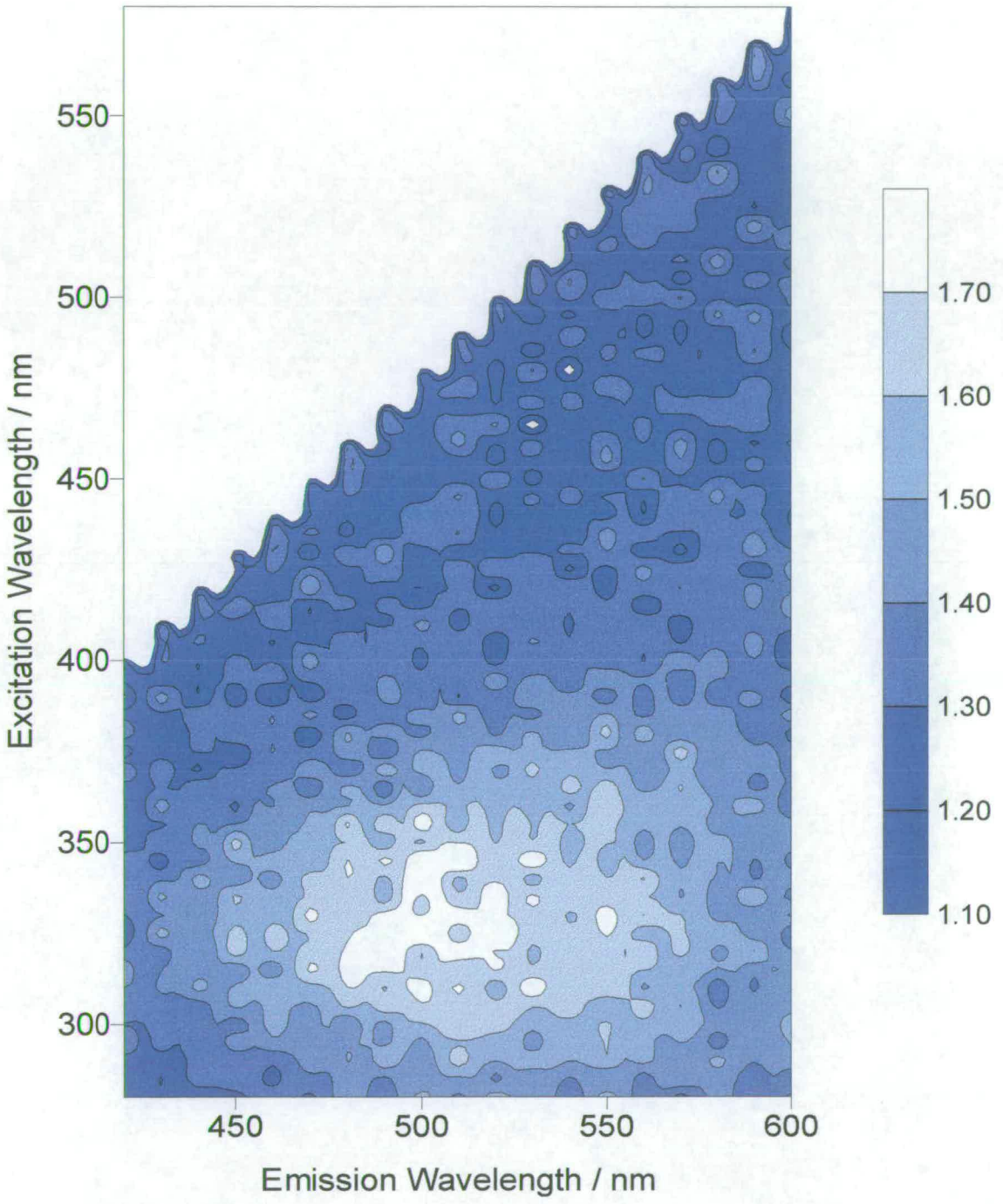

Figure 6.18: Ratio EEM for adjacent bright and dull bands of coral from Laing Island, Papua New Guinea, recorded with a 100ms delay. The contours are plotted between 1.10 and 1.7 at 0.1 unit intervals.

6.6.4 Subtraction EEMs

The subtraction EEMs were constructed for 20ms and 100ms delay times by subtracting the dull band EEM from the adjacent bright band EEM. Figure 6.19 shows the subtraction EEM constructed from the component EEMs with a delay of 20ms between the closing of the excitation shutter and the opening of the emission shutter. Figure 6.20 shows the subtraction EEM constructed from the component EEMs with a delay of 100ms between the closing of the excitation shutter and the opening of the emission shutter.

Both subtraction EEMs show similar features. The area of maximum absolute intensity difference between the phosphorescence of the bright and dull bands occurs in the region 300-350/480-550nm. This corresponds to the regions of peak intensity highlighted in the bright and dull band EEMs (Figures 6.13 – 6.16).

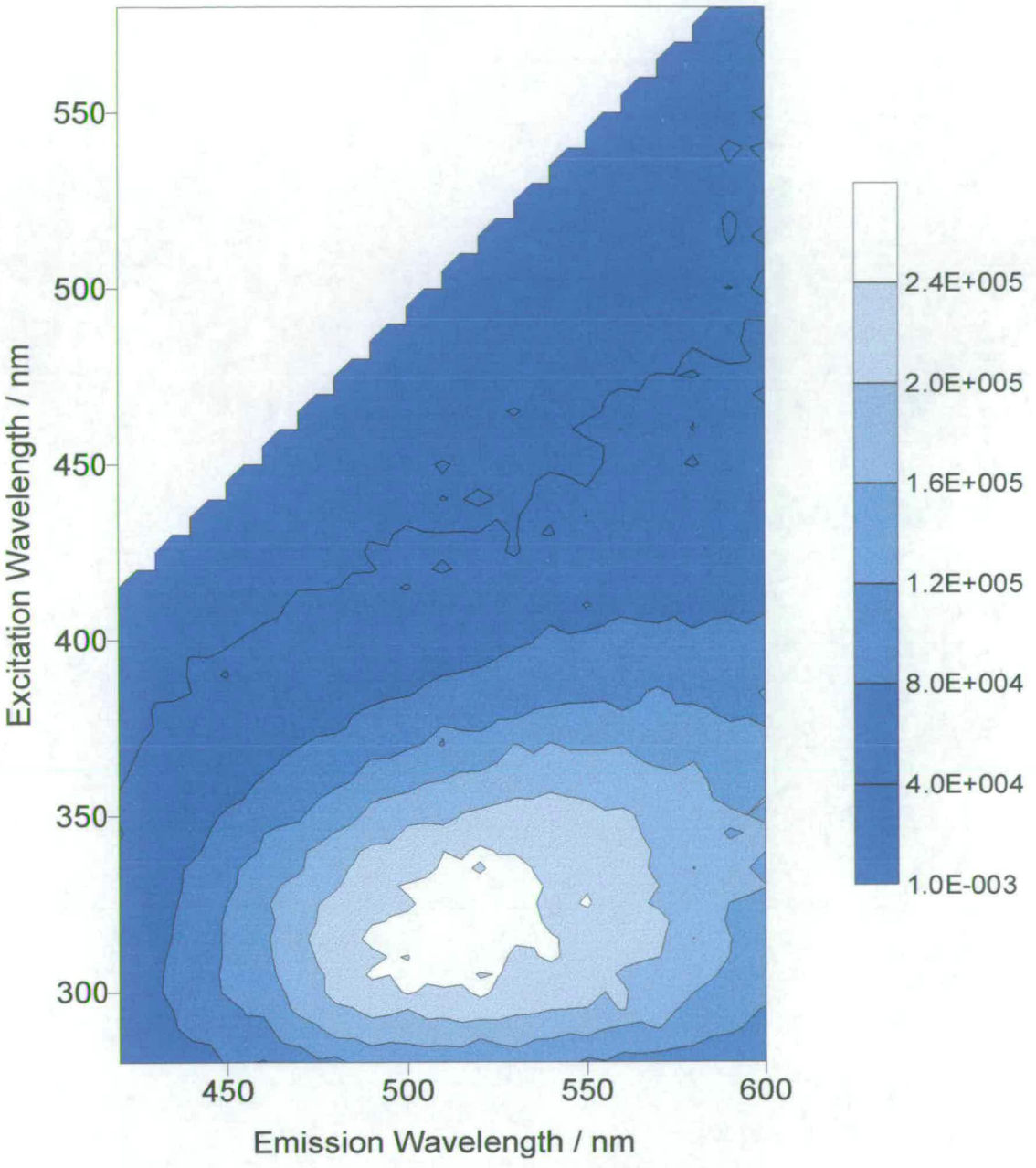

Figure 6.19: Subtraction EEM constructed by subtracting the dull band EEM from the adjacent bright band EEM, both recorded with a 20ms delay. The contours are plotted between 1.0 x 10^3 and 2.4 x 10^5 at intervals of 4.0 x 10^4cps.

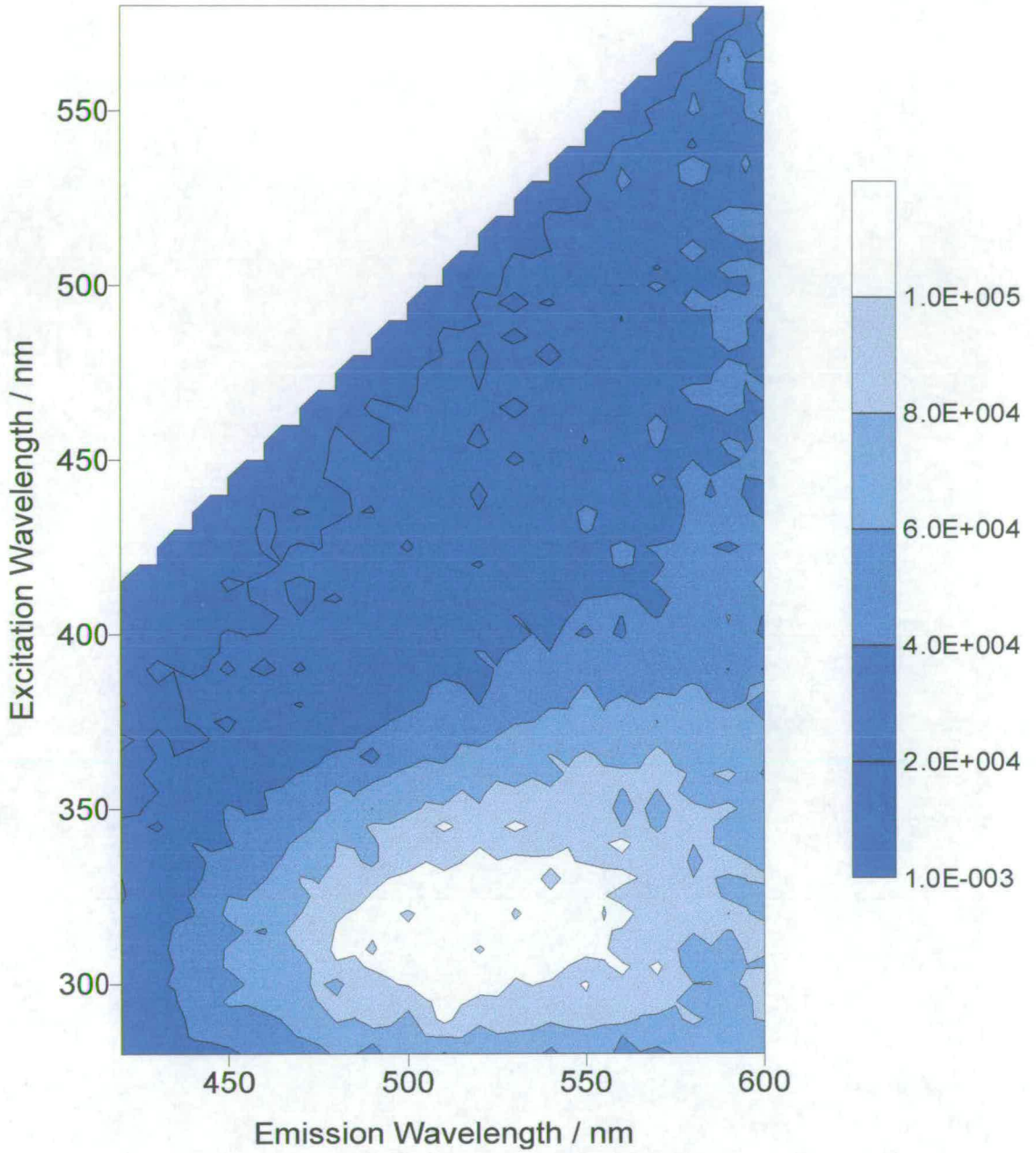

Figure 6.20: Subtraction EEM constructed by subtracting the dull band EEM from the adjacent bright band EEM, both recorded with a 100ms delay. The contours are plotted between 1.0×10^3 and 1.0×10^5 at intervals of 2.0×10^4 cps.

6.6.5 A comparison of luminescence and phosphorescence EEMs

The peak phosphorescence emission intensity is shifted to longer wavelength than the peak luminescence emission intensity. This would be expected since phosphorescence is due to a lower energy transition than fluorescence.

The peak phosphorescence excitation intensity is shifted to shorter wavelengths than the peak luminescence excitation intensity. This indicates that there are different species giving rise to the maximum phosphorescence and fluorescence emission and is therefore consistent with the postulate that the peak luminescence emission is mainly due to fluorescence.

The maximum ratio of bright:dull band intensity is observed at similar emission wavelengths in both the phosphorescence and luminescence EEMs. This also corresponds to the region of maximum intensity in the bright and dull band phosphorescence EEMs. This implies that phosphorescence may be the dominant contributor to luminescent banding.

The phosphorescence of the bright band is more intense than that of the dull band across the entire excitation/emission wavelength range studied. The luminescence of the bright band is only more intense at longer emission wavelengths. The luminescence signal is a combination of high intensity background fluorescence and relatively low intensity phosphorescence. If banding is due predominantly to a variation in phosphorescence intensity, then we expect to observe banding in the total luminescence signal at wavelengths where the variation in phosphorescence intensity is greater than the variation in background fluorescence intensity. This will occur at longer emission wavelengths where the intensity of background fluorescence is reduced relative to phosphorescence. The phosphorescence ratio EEM shows a clearly defined maximum region at 350/450-570nm. This is not apparent in the luminescence ratio EEM because it is obscured by the high background fluorescence intensity which reaches a maximum in this excitation region.

6.7 Conclusions

Until this study, it was thought that phosphorescence was only observed in fossil corals. However, this study proves that modern coral skeletons are phosphorescent and provides an insight to the value of phosphorescence as an indicator of the banding pattern. All samples studied are phosphorescent, and the bright bands are consistently more phosphorescent than the dull bands. For samples from Laing Island, PNG, the bright bands are twice as phosphorescent as the dull bands, despite only a concurrent 20% increase in luminescence intensity. Long-lived phosphorescence accounts for around 8% of the total luminescence of the system in the bright bands and 4% in the dull bands. It is likely that the contribution of phosphorescence to the total luminescence is underestimated as the recorded emission is limited by the temporal resolution of the shutter system.

The phosphorescence signal is made up from a number of component emitting species. The phosphorescing species identified have lifetimes between 0.05 and 1s, in comparison with estimated fluorescence lifetimes of 10ns. As would be expected, the maximum phosphorescence emission intensity occurs at longer wavelengths than the maximum luminescence emission intensity. There is a distinct emission at 280/450nm that can be attributed to phosphorescence from the direct excitation of tryptophan. This phosphorescence accounts for the vast majority of observed luminescence at 280/450nm. The peak intensity at 360/470nm identified in luminescence EEMs is not observed in phosphorescence EEMs, and hence can be attributed largely to fluorescence emission.

Luminescence scans of the banding pattern are subject to a varying background signal, which is particularly intense at 360/450nm and is attributed to fluorescence emission. In contrast, the phosphorescence scans show no background variation along the coral core. The phosphorescence is therefore a much better indicator of the

observed banding pattern, and may allow quantitative comparison of banding with variations in other environmental conditions.

6.8 Bibliography

Klein, R., Loya, Y., Gvirtzman, G., Isdale, P.J., and Susic, M., 1990. Seasonal rainfall in the Sinai Desert during the late quaternary inferred from fluorescent bands in fossil corals. Nature, 345: pp. 145-147.

7 Chapter Seven: Observations on Luminescent Banding and Skeletal Structure

7.1 Introduction

Luminescent bands are considered to result from the incorporation of terrestrial humic materials into coral skeletons. These humic materials are believed to be carried to the marine environment by terrestrial run-off (Boto and Isdale, 1985; Susic *et al.,* 1991). A correlation was identified between the timing of bright luminescent bands and peak river run-off in corals from the Great Barrier Reef (Isdale, 1984), Papua New Guinea (Scoffin *et al.,* 1989) and Florida (Smith *et al.,* 1989). However, the correlation was not found in corals from Thailand and Taiwan (Scoffin *et al.,* 1992; Fang and Chou, 1992). Luminescent bands have also been reported in corals far removed from land or any source of freshwater (Susic *et al.,* 1991; Tudhope *et al.,* 1996). Previously in this investigation (Chapters Four and Five) the luminescence characteristics of corals from Oman have been described. Despite not being subject to terrestrial run-off, these corals exhibit similar properties to those from Laing Island, which are regularly exposed to freshwater laden with organic matter. This suggests that the concentration of terrestrial humic material is not the only factor that controls luminescent banding.

Since luminescent banding cannot be exclusively attributed to the uptake of terrestrial humic material, it is important to consider what other factors are contributing to the observation of the banding pattern. It has been suggested that marine humic materials may contribute to luminescence banding (Tudhope *et al,* 1996). However, it is also possible that variations in skeletal structure could play a

role. This chapter studies the structural characteristics of coral skeletons and their relationship to the banding pattern, using three approaches:

1) annual density bands and their relationship to luminescent banding;
2) confocal fluorescence microscopy of bright and dull bands;
3) scanning electron microscopy of bright and dull bands.

Although the structure of coral skeletons is well documented, the relationship between the skeletal architecture and the luminescent banding pattern has never been studied. Coral has a very rugose and heterogenous surface, with deep pores that run through the coral matrix. It is reasonable to assume that the porous nature of the skeleton will affect the observed luminescence, since light entering and leaving the skeleton bounces off the surface of the coral and within the pores themselves.

7.2 Density and luminescent banding

Coral skeletons exhibit annual density variations (Knutson *et al.,* 1972). Barnes and Lough (1996) have proposed that as corals grow, they initially lay down a "scaffold" of skeleton, which may then be thickened throughout the depth of the tissue layer. Consequently, the width of the density bands may depend on the tissue thickness in individual corals, the health of the corals and the environment in which they are growing. Scoffin *et al.* (1989) found that bright luminescent bands coincided with regions of low-density skeleton in corals from PNG and Indonesia. Klein *et al.* (1990) found a similar relationship for corals from the Red Sea. However, Isdale (1984) found that in inshore reefs of the GBR, bright bands coincided with regions of high-density skeleton. It would seem then that the relationship between density and

luminescence is a complicated one. This section studies the luminescent banding pattern in corals that are not subject to terrestrial input, and its relationship to the density banding pattern.

7.2.1 Luminescent banding in reefs far removed from terrestrial run-off

All corals from the reefs studied (Chapter Three, Table 3-1) exhibited broad and regularly repeating luminescent banding. This includes corals from Ashmore, Myrmidon, 13-050 and Lagoon Reefs in the Great Barrier Reef, and Wadi Ayn in Oman.

Reefs that lie closer to the coast (13-050 and Lagoon reefs) showed several thin and especially bright subseasonal luminescent bands imposed on top of this broad, regular pattern. This suggests that these corals may have been affected by short-lived events influenced by the adjacent coast. Myrmidon and Ashmore Reefs are the only GBR reefs studied that showed no evidence of intense luminescent bands. Ashmore Reef lies 176 km offshore from Papua New Guinea (PNG). Myrmidon Reef lies 110 km offshore and is situated on a peninsula sticking out >10km from the shelf edge. It is highly unlikely that these two reefs are influenced by coastal run-off. Samples from these two reefs and from Oman can then be studied as terrestrially impact-free corals and hence the banding pattern can be studied in relation to other factors, such as annual variations in density.

7.2.2 Luminescent banding and density in reefs far removed from terrestrial run-off

In slices of coral from Myrmidon and Ashmore Reefs on the GBR and in slices of corals collected at Wadi Ayn, regions of bright luminescence coincided with low-density bands. In the Oman slice (Figure 7.1), high-density peaks on a densitometer trace coincided with darker regions on the X-radiograph positive image.

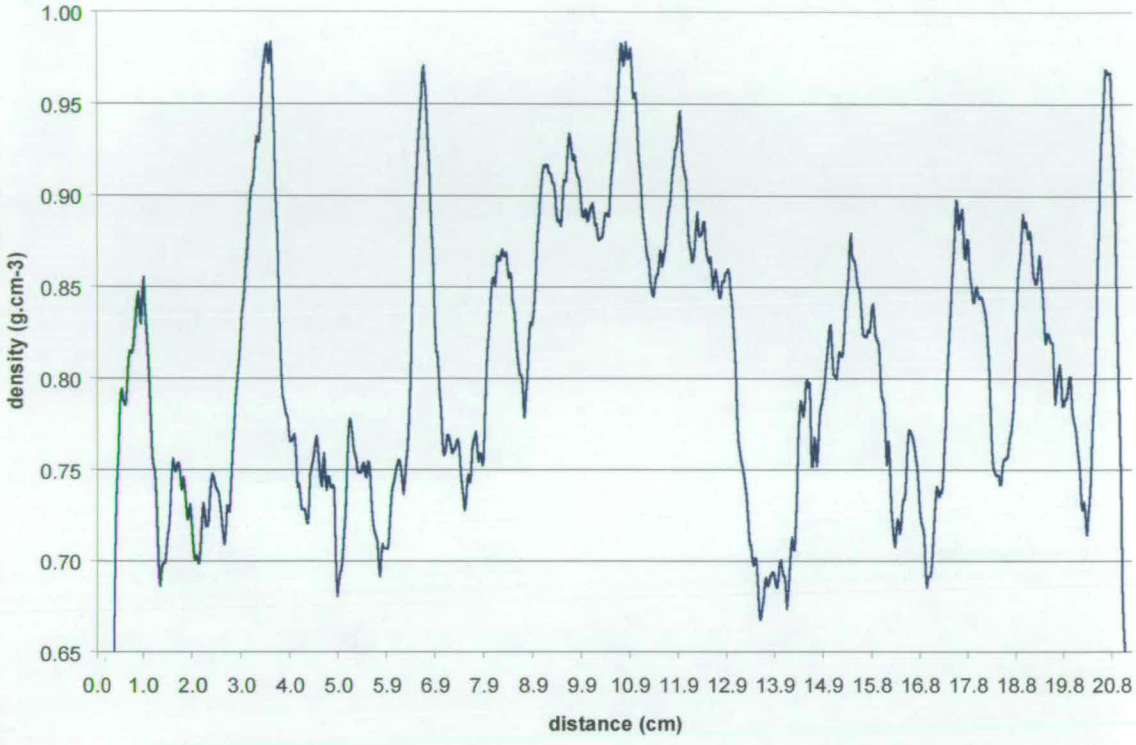

Figure 7.1: Densitometer trace along a slice of Oman coral (above) and X-radiograph of the same slice (bottom) overlaid with acetate of the luminescent banding pattern.

The top graph shows the variation in density along an Oman coral slice, as recorded by the densitometer. The growing edge of the coral is on the left-hand side of the

image and, since the coral was cored in August 1995 (Chapter Three, Table 3-1), the nearest high-density band to the growing edge was laid down in the summer of 1994. The slice dates back to 1976. It can be seen that the high-density peaks are laid down annually. The bottom image shows an X-radiograph positive image of the same slice, with regions of low density appearing lighter in the scan. Overlaid is the acetate-traced luminescent banding pattern, as determined by visual observation under uv illumination, with bright bands denoted as blank spaces between dashed lines. There is good overlap between the regions of low density and bright luminescence. This relationship was also found for all samples from Myrmidon and Ashmore Reefs. These observations are at least consistent with the hypothesis that skeletal density exerts some control over luminescence. However, since luminescence banding and density banding are both predominantly seasonal, a coincidence (rather than cause and effect) is still possible.

7.3 Confocal Fluorescence Microscopy

All work was carried out on samples of coral from Laing Island, Papua New Guinea. The samples had been freshly sliced, washed in deionised water, dried and stored in glass dishes to limit external contamination. Figure 7.2 shows an image of a bright band region of coral when illuminated at 488nm using the confocal fluorescence microscope at x10 magnification. The emission detection is limited by the equipment to wavelengths greater than 510nm. At 488/510nm, the ratio of bright to dull band luminescence intensity is approximately 1.10 i.e. the bright bands are 10% more intense than the dull band (Chapter Four, Figure 4.5). The 488nm light is focused on to the spot and the image is collected as a series of planes through the coral sample. These planes are collated to give a three-dimensional image. Figure 7.2 consists of 60 individual image planes, covering a total thickness of approximately 250 μm. The image has been coloured to highlight regions of high and low intensity. The white

regions show the highest intensity emission and the dark purple regions the lowest intensity emission.

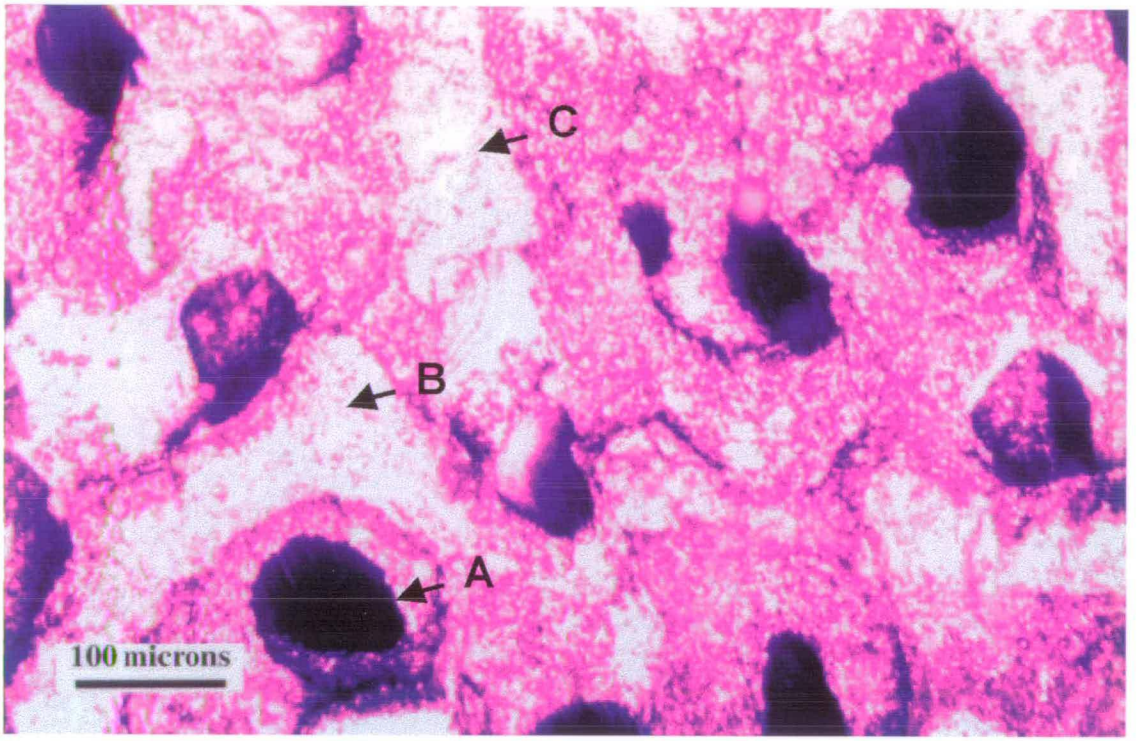

Figure 7.2: Confocal fluorescence micrograph of a bright band region of coral from Laing Island, Papua New Guinea. The image was recorded at x10 magnification, exciting at 488nm and detecting emission at wavelengths greater than 510nm. Point A marks a pore space, point B marks a cut surface and point C marks the walls of a pore space. The light regions correspond to high intensity emission and the dark regions correspond to low intensity emission.

The image shows the very porous nature of the coral skeleton, with pores running both parallel and perpendicular to the cut axis. The pores running perpendicular to the cut axis appear dark. The regions of most intense emission are found on the cut

surfaces and from the walls of pores that run parallel to the cut axis. In comparison, the confocal fluorescence micrograph image of a dull band region of coral from the same sample is shown in Figure 7.3.

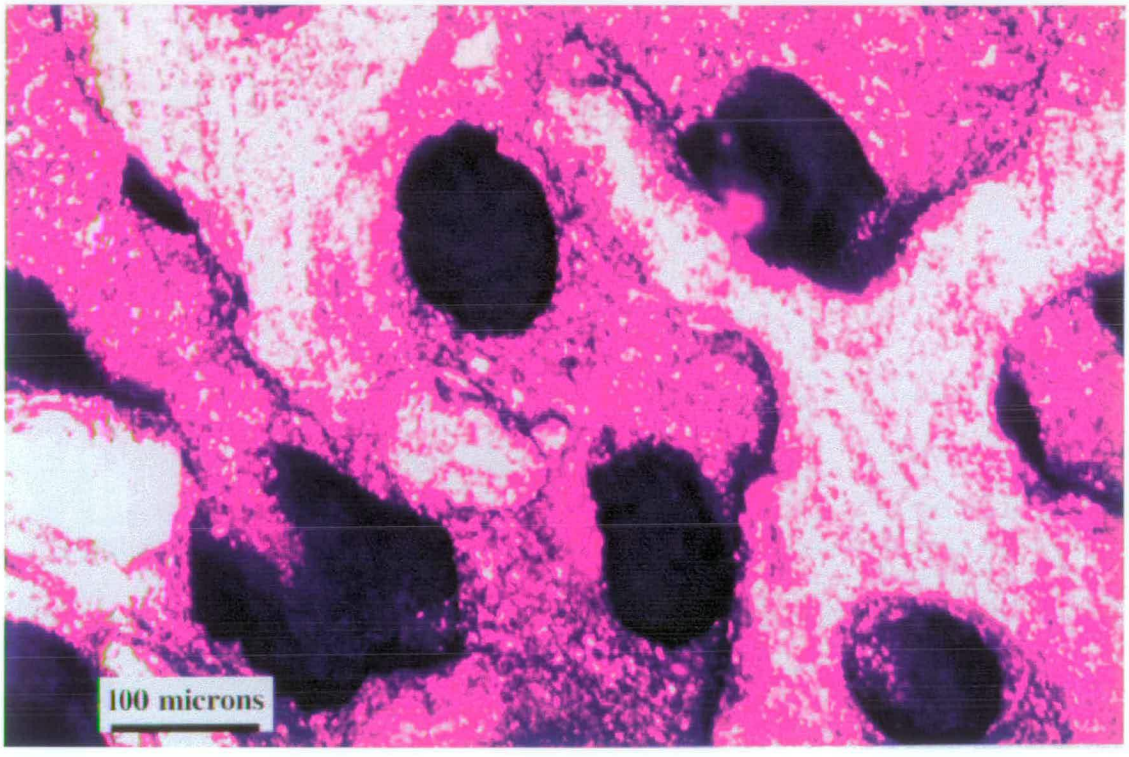

Figure 7.3: Confocal fluorescence micrograph of a dull band region of coral from Laing Island, Papua New Guinea. The image was recorded at x10 magnification, exciting at 488nm and detecting emission at wavelengths greater than 510nm. The light regions correspond to high intensity emission and the dark regions correspond to low intensity emission.

The image consists of 60 individual planar scans, covering a total thickness of approximately 250 μm. This image shows reduced overall intensity compared to

Figure 7.2. This would be expected since all other measurements have shown that dull bands exhibit less intense emission than neighbouring bright bands at 488/510nm (Chapter Four, Figure 4.5). This relationship was observed in all other comparative images of dull and bright bands. Figure 7.4 shows another pair of images of bright and dull band regions of the same coral sample. The bright band regions of the skeletons studied show an increased fluorescence intensity at 488/510nm. This corresponds to the regions of increased relative intensity in the bright bands as identified in Chapter Four, Figure 4.5 and Chapter Five, Figure 5.14. The technique used in this investigation should correctly be termed luminescence microscopy, since the images captured here will also show some phosphorescence emission. The excitation beam is continuous and hence all the luminescence (fluorescence + phosphorescence) will be collected from the sample. This may account for the marked difference in intensity at such long excitation and emission wavelengths, which would not be expected if fluorescence alone were being detected.

It is difficult to compare the architectural differences between the images using this technique, but superficial inspection suggests that the bright band images have a more rugose and grainy structure. To gain a greater insight into the structural differences between the bright and dull bands, the same samples were studied using a scanning electron microscope.

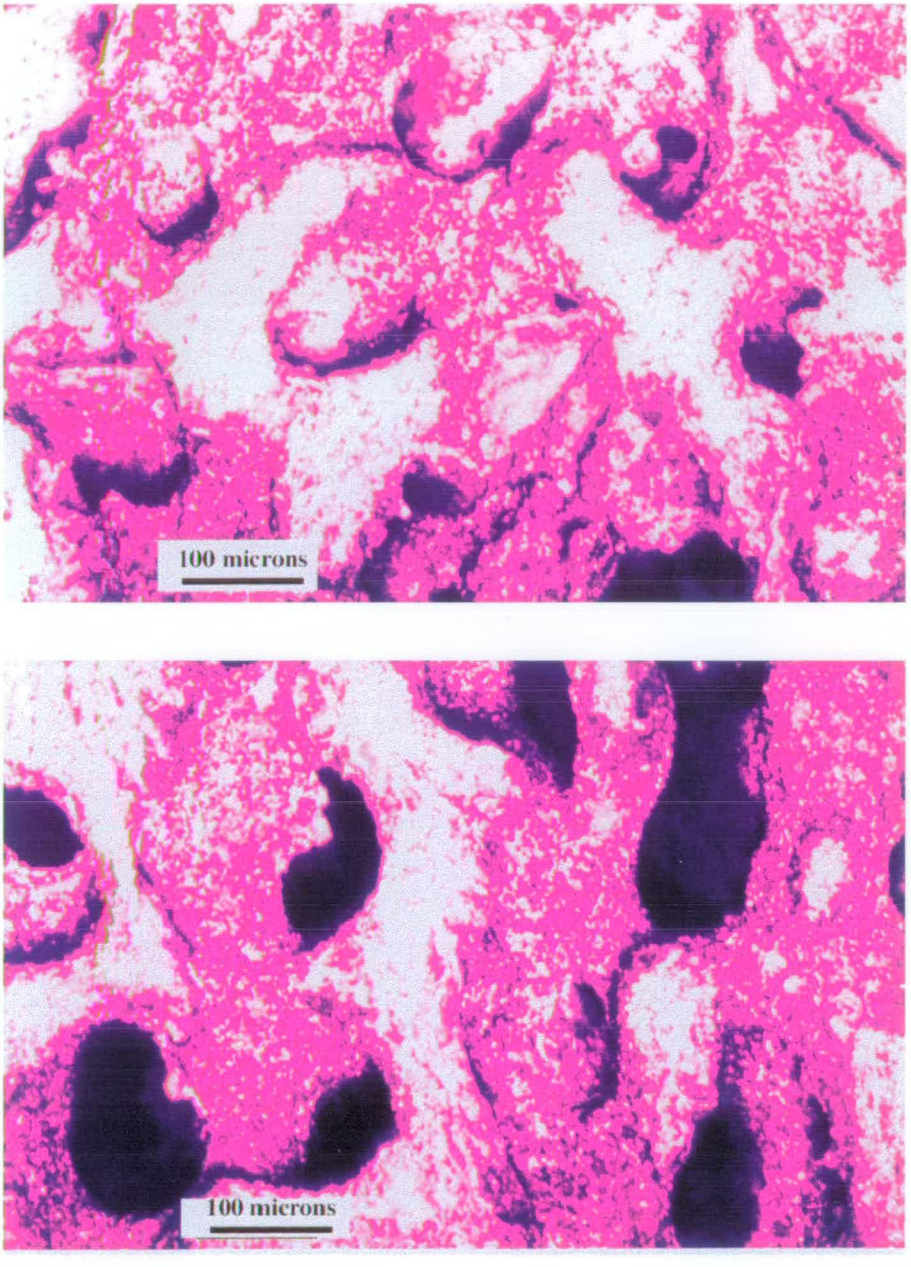

Figure 7.4: Confocal fluorescence micrograph of bright (top image) and dull (bottom image) bands of coral from Laing Island, Papua New Guinea. The images were recorded at x10 magnification, exciting at 488nm and detecting emission at wavelengths greater than 510nm. The light regions correspond to high intensity emission and the dark regions correspond to low intensity emission.

7.4 Scanning Electron Microscopy

Once the sample had been analysed using the confocal fluorescence microscope, it was spray coated in gold and mounted in the scanning electron microscope. Figure 7.5 shows a scanning electron micrograph image of a bright band region of coral from Laing Island. The region studied covers some of the same area as that shown in Figure 7.2 (which is reproduced here), so the images can be directly compared. The magnification is x 92. The scanning electron micrograph of the dull band region is shown in Figure 7.6. Again, this corresponds to the same region as the image shown in Figure 7.3.

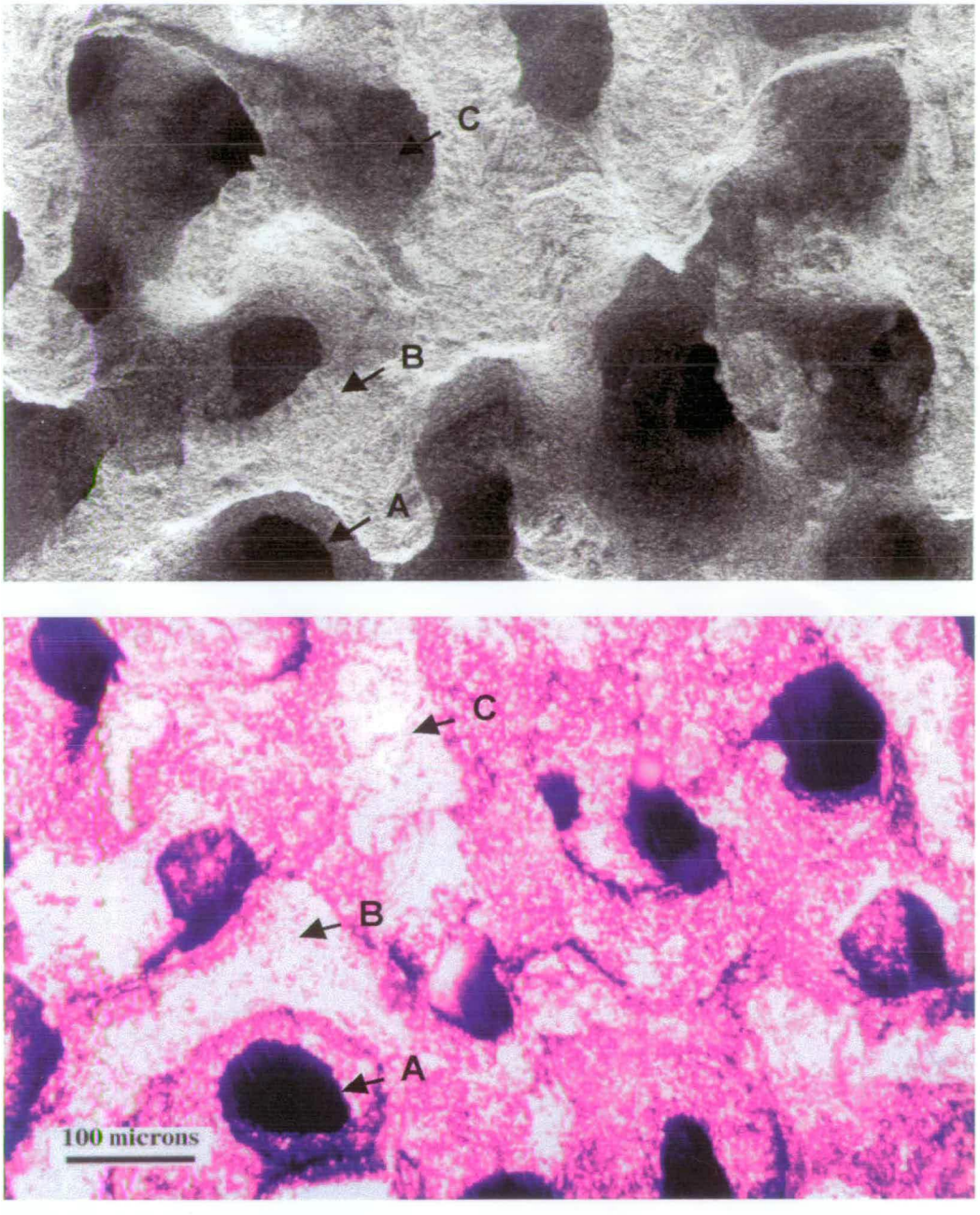

Figure 7.5: The upper image shows the scanning electron micrograph of a bright band region of coral from Laing Island, Papua New Guinea. The magnification is x 92. The lower image shows the confocal luminescence micrograph image of the same region (Figure 7.2) for comparison. Point A marks a pore space, point B marks a cut surface and point C marks the walls of a pore space.

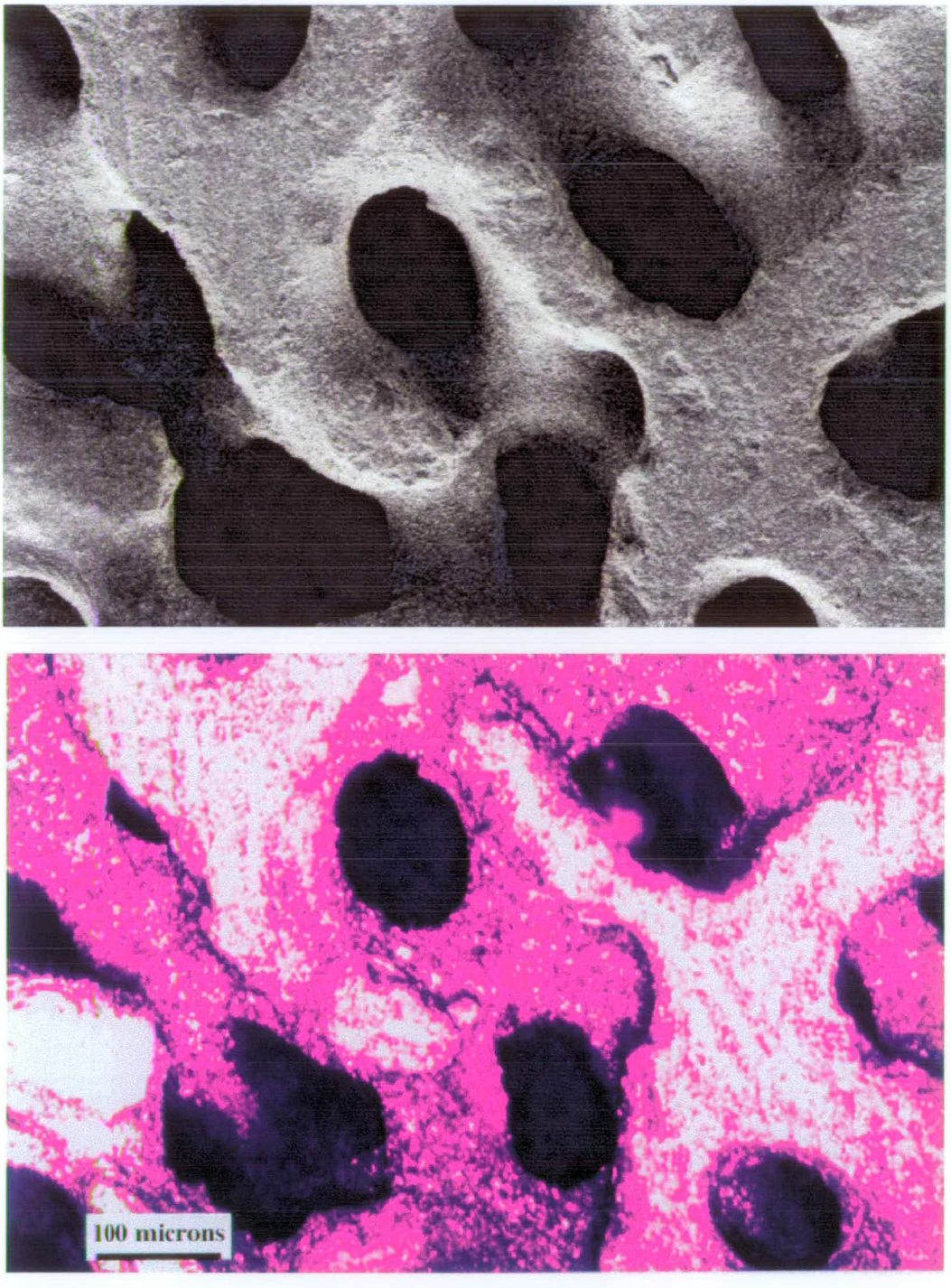

Figure 7.6: The upper image shows the scanning electron micrograph of a dull band region of coral from Laing Island, Papua New Guinea. The magnification is x 92. The lower image shows the confocal luminescence micrograph image of the same region (Figure 7.3) for comparison.

There are two notable differences between the structure of the bright and dull bands when studied using the scanning electron microscope. Firstly, the dull band has a more robust skeleton, i.e. the skeletal elements appear to be more tightly packed together. Secondly, the bright bands have a more granular texture in the walls of pores. These differences are observed for all comparative images of dull and bright bands. The bright regions in the luminescence micrographs correspond to cut surfaces or walls of pore spaces. Luminescence does not appear to emanate from the interior of pores. Figure 7.7 shows scanning electron micrographs of adjacent bright and dull band regions from another sample of coral from Laing Island, Papua New Guinea. These images correspond to the same regions shown in Figure 7.4.

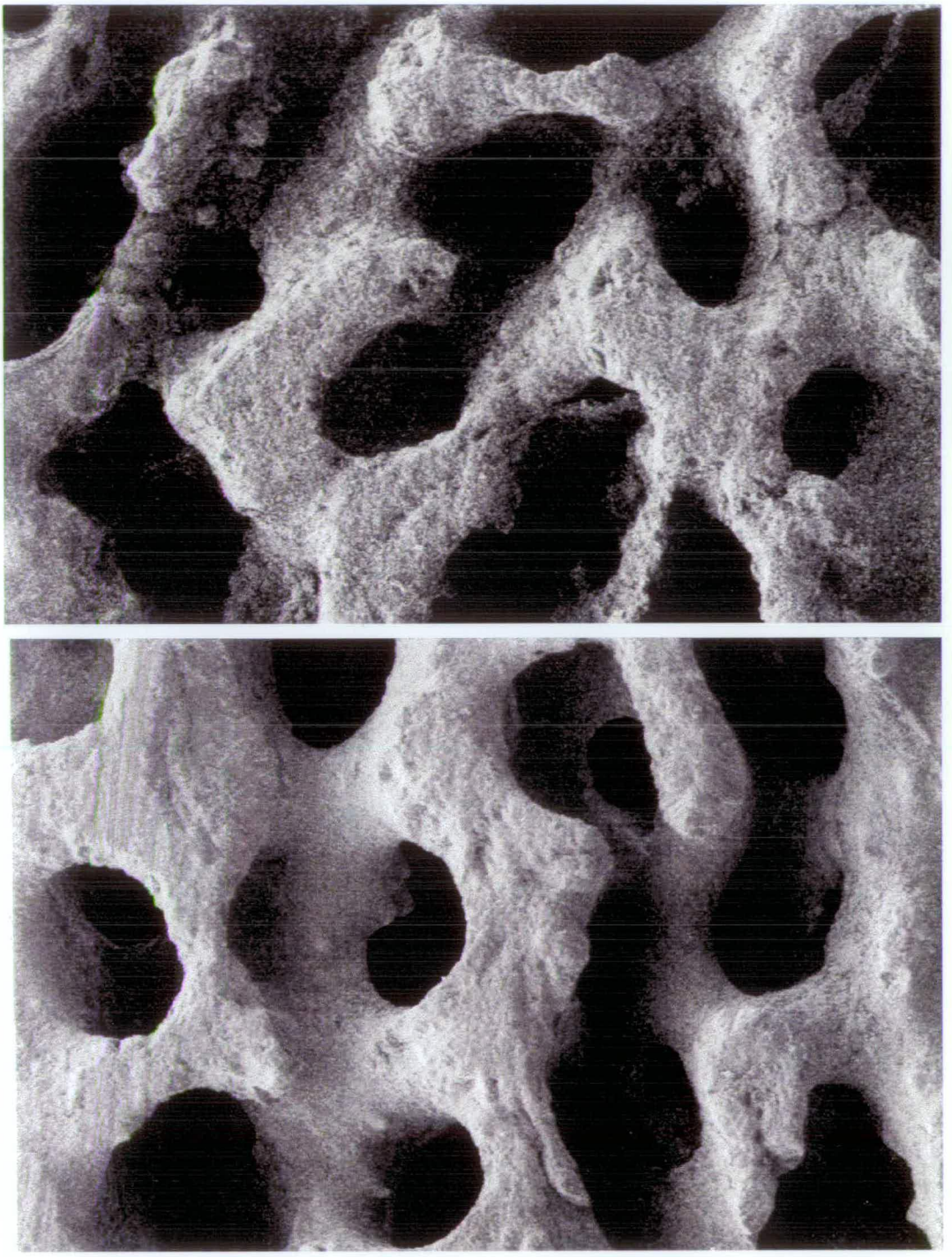

Figure 7.7: Scanning electron micrographs of bright (top image) and dull (bottom) band regions of a sample of coral from Laing Island, Papua New Guinea. The magnification is x 92.

7.5 Conclusions

Luminescent bands are found in GBR corals that grow more than 20km from the shore, contrary to initial findings by Isdale (1984). The samples from Ashmore and Myrmidon reefs both exhibit luminescent banding and lie far offshore from the North Queensland coast. Since luminescent banding is observed in corals that are not affected by terrestrial run-off (such as those from Oman, Ashmore and Myrmidon reefs), it can be assumed that other environmental factors may lead to the observation of luminescent banding. In these corals, the regions of bright luminescence coincide with regions of low density skeleton, as identified by X-radiography. It is possible that the density may act as a controlling factor in the observation of banding in offshore corals, but the evidence presented here is not conclusive. However, how do we explain Isdale's observation that in inshore reefs of the GBR, the bright bands coincided with regions of high density? The implication of this observation, combined with the occurrence of bright luminescence in low density corals that are far removed from terrestrial run-off, is that either the density banding or the luminescence banding occurs during different seasons, according to distance from the coast. To help resolve this issue, the timing of density and luminescent band deposition should be carefully monitored at offshore and inshore reef sites. It is possible that the uptake of terrestrial humics into the skeleton distorts the background luminescence which has been identified in the offshore samples, or that the offshore bands are a record of marine humic levels, that may vary on a different time period to the terrestrial humics.

Confocal fluorescence microscopy can be used to identify bright and dull regions of the skeleton, since the bright bands are more intensely fluorescent at 488/510nm. This corresponds with earlier findings in this thesis (Chapters Four and Five) which suggest that the bright bands are relatively more intense at these long excitation and emission wavelengths. From the scanning electron microscopy investigation, it can be said that the bright bands exhibit a more rugose and grainy structure than the dull

bands. The sample studied was from Laing Island, a reef that is affected by terrestrial run-off. Consequently, the results suggest there may be differences between the skeletal architecture of the bands that could affect the luminescence properties. The information presented here suggests that there is a relationship between luminescence and the structure of the coral skeleton, but further work is required to elucidate exactly how the two interrelate.

7.6 Bibliography

Barnes, D.J., and Lough, J.M., 1996. Coral skeletons: storage and recovery of environmental information. Global Change Biology, 2: pp.569-582

Boto, K., and Isdale, P., 1985. Fluorescent bands in massive corals result from terrestrial fulvic acid inputs to the nearshore zone. Nature, 315: pp. 396 - 397

Fang, L.S., and Chou, Y.C., 1992. Concentration of fulvic acid in the growth bands of hermatypic corals in relation to local precipitation. Coral Reefs, 11: pp. 187 – 191

Isdale, P., 1984. Fluorescent bands in massive corals record centuries of coastal rainfall. Nature, 310: pp.578-579

Klein, R., Loya, Y., Gvirtzman, G., Isdale, P., and Susic, M., 1990. Seasonal rainfall in the Sinai desert during the late quaternary inferred from fluorescent bands in fossil corals. Nature, 345: pp.145-147

Knutson, D.W., Buddemeier, R.W., and Smith, S.V., 1972. Coral chronometers: seasonal growth bands in reef corals. Science, 177: pp.270-272

Scoffin, T.P., Tudhope, A.W., and Brown, B.E., 1989. Fluorescent and skeletal banding in *Porites lutea* from Papua New Guinea and Indonesia. Coral Reefs, 7: pp.169-178.

Scoffin, T.P., Tudhope, A.W., Brown, B.E., Chansang, H., and Cheeney, R.F., 1992. Patterns and possible environmental controls of skeletogenesis in *Porites lutea*, South Thailand. Coral Reefs, 11: pp. 1 – 11

Smith, T.J., Hudson, J.H., Robblee, M.B., Powell, G.V.N., and Isdale, P., 1989. Freshwater flow from the Everglades to Florida Bay. Bulletin of Marine Science, 44: pp. 274-282

Susic, M., Boto, K., and Isdale P., 1991. Fluorescent humic acid bands in coral skeletons originate from terrestrial run-off. Marine Chemistry, 33: pp.91-104

Tudhope, A.W., Lea, D.W., Shimmield, G.B., Chilcott, C.P., and Head, S., 1996. Monsoon climate and Arabian Sea coastal upwelling recorded in massive corals from southern Oman. Palaois, 11: pp.347-361

Chapter Eight: Conclusions

This work has elucidated the photophysical processes that are responsible for the appearance of bright and dull bands in coral skeletons. The "fluorescence" banding pattern that is observed when coral skeletons are illuminated under uv light is actually due to a combination of fluorescence and phosphorescence, and should correctly be termed **luminescent banding**.

Several objectives have been achieved as the work has progressed. The luminescence characteristics of coral skeletons have been reproducibly recorded directly from intact coral samples using excitation-emission-matrix spectroscopy. Spatial resolution of the variations in luminescence and phosphorescence has been achieved using optical fibre probes for excitation and emission beam delivery. The banding pattern can be reproducibly recorded along the length of a coral core. The luminescence has been temporally resolved in order to study the role of long-lived phosphorescence to the observed banding pattern.

The luminescence of coral is composed of emission from many individual species which can be represented as a three-dimensional contour plot, or EEM. The EEMs of all samples showed the same macroscopic features. Six component peaks have been identified that are present in all the samples studied. These peaks are characteristic of the presence of protein-type luminophores (short excitation and emission wavelengths) and humic-type luminophores (longer excitation and emission wavelengths). Comparative studies between the luminescence of bright and dull bands have successfully characterised the spectral differences between the regions. The percentage difference in luminescence intensity between bright and dull bands is relatively small at all wavelength combinations. For example, samples from Laing Island, which show very distinct banding, only exhibit a maximum of 25% increase in intensity in the bright bands compared to the neighbouring dull bands. The bright

bands show enhanced intensity at long emission wavelengths (greater than 450nm), which may be due to increased electronic energy transfer, an increased concentration of low energy luminophores or increased phosphorescence emission (or most likely a combination of these factors). The intensity of the dull band regions of the skeleton, or regions of background luminescence, is not constant along the length of a coral core, but shows a gradual increase or decrease as the scan progresses. This suggests that this emisson is varying with factors that are not subject to seasonal variation.

Samples were studied from three locations, Laing Island and Madang Lagoon, Papua New Guinea, and Wadi Ayn in Oman. Samples from Oman that are not subject to terrestrial run-off show the same component species as those from Laing Island and Madang Lagoon that are regularly inundated by terrestrial run-off. Samples from Oman and Laing Island also show the same relative bright:dull band intensity across the excitation and emission wavelength ranges studied. This implies that both are subject to similar conditions that affect the appearance of the banding pattern. It therefore seems unlikely that the impact of terrestrial run-off is the major controlling factor in the laying down of the bright and dull bands. Preliminary studies have shown that there may be a relationship between skeletal architecture and luminescence banding in corals that are not subject to terrestrial run-off. Samples free from terrestrial run-off on the Great Barrier Reef, and those from Oman show a correlation between regions of low density skeleton and increased luminescence. Confocal luminescence and scanning electron microscopy have shown that bright bands have a less robust skeletal architecture.

This study proves that modern coral skeletons are phosphorescent. The maximum intensity of phosphorescence is at longer emission wavelengths than the corresponding luminescence emission. This is expected since phosphorescence is due to a lower energy transition than fluorescence. The phosphorescence accounts for only a small proportion of the total luminescence, around 10%, but it is a very accurate indicator of the banding pattern. Bright bands are consistently more

phosphorescent than dull bands, and in samples from Laing Island, Papua New Guinea, the bright bands exhibit twice the phosphorescence intensity of the dull bands. This can be compared to only a 20% increase in luminescence. The phosphorescence emission, unlike luminescence, is not subject to any background variation in intensity. Comparison of phosphorescence and luminescence measurements suggests that the background variation observed in luminescence scans is composed largely of fluorescence. The maximum intensity peak in the luminescence EEMs consists mainly of background fluorescence and contributes little to the banding pattern. The intensity of background fluorescence is dependent on the excitation and emission wavelength and therefore it is important to choose the correct wavelength combination in order to be able to resolve the banding pattern when measuring total luminescence. Since the phosphorescence is not subject to a wavelength-dependent background variation, it is much better as a quantitative indicator of the banding pattern than luminescence.

The nature and significance of luminescent banding in reef corals is not a simple correlation between terrestrial run-off and bright band deposition, since corals that are not subject to terrestrial run-off exhibit similar features and characteristic band intensity ratios as those that are regularly exposed to terrestrial run-off. Other factors affect the appearance of the banding pattern, including, for example, skeletal architecture. Previous studies of the luminescence of solid coral have been unable to determine the major differences between the bright and dull bands, since the luminescence intensity is wavelength dependent and subject to background variation. Phosphorescence provides a new way of studying the banding pattern that is not subject to background variation in the regions of the spectrum where luminescent banding is observed.

From the results presented here, it can be seen that phosphorescence is a powerful tool that will enable quantitative comparisons to be made between the banding pattern and other environmental variations and may serve to unravel the

environmental records stored in coral skeletons. Extending the phosphorescence analysis to include longer coral cores from other locations will allow the direct comparison of phosphorescence intensity with skeletal variations such as stable oxygen isotope ratios and trace element analysis, and environmental variations such as rainfall, light intensity and salinity. Although the environmental records stored in coral skeletons have yet to be fully understood, phosphorescence gives us a reliable and accurate record of the visibly observed banding pattern.